Tropical cyclone analysis using microwave satellite imagery

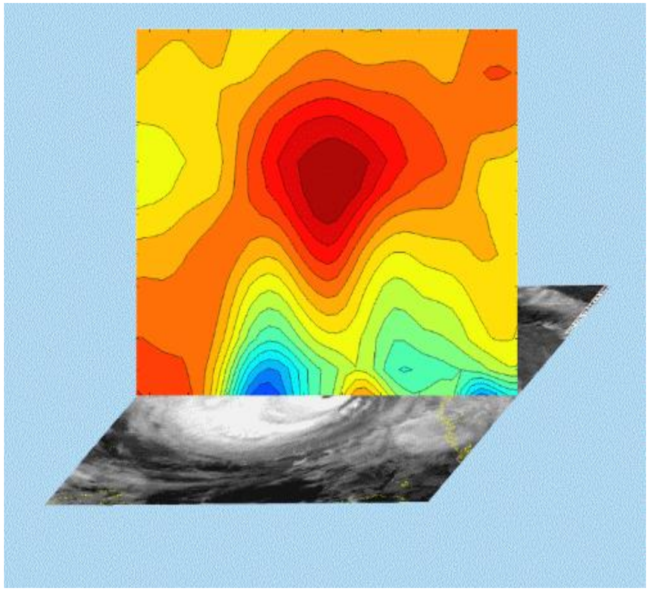

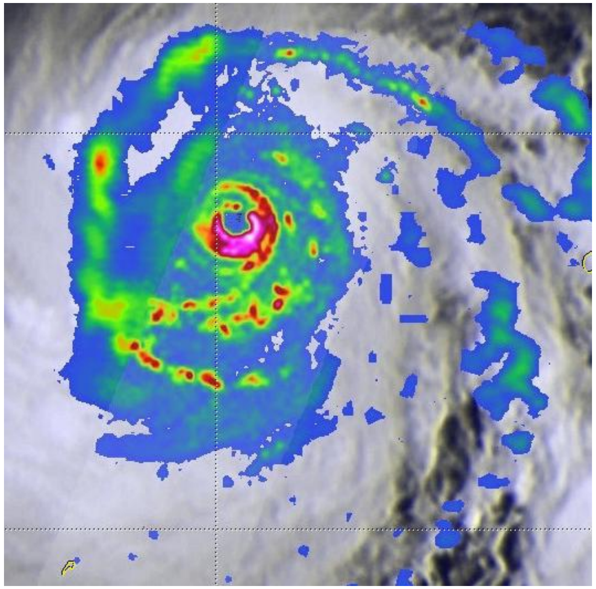

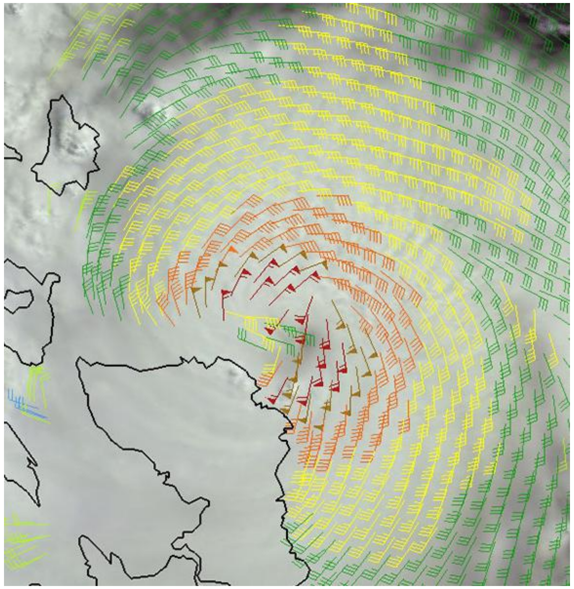

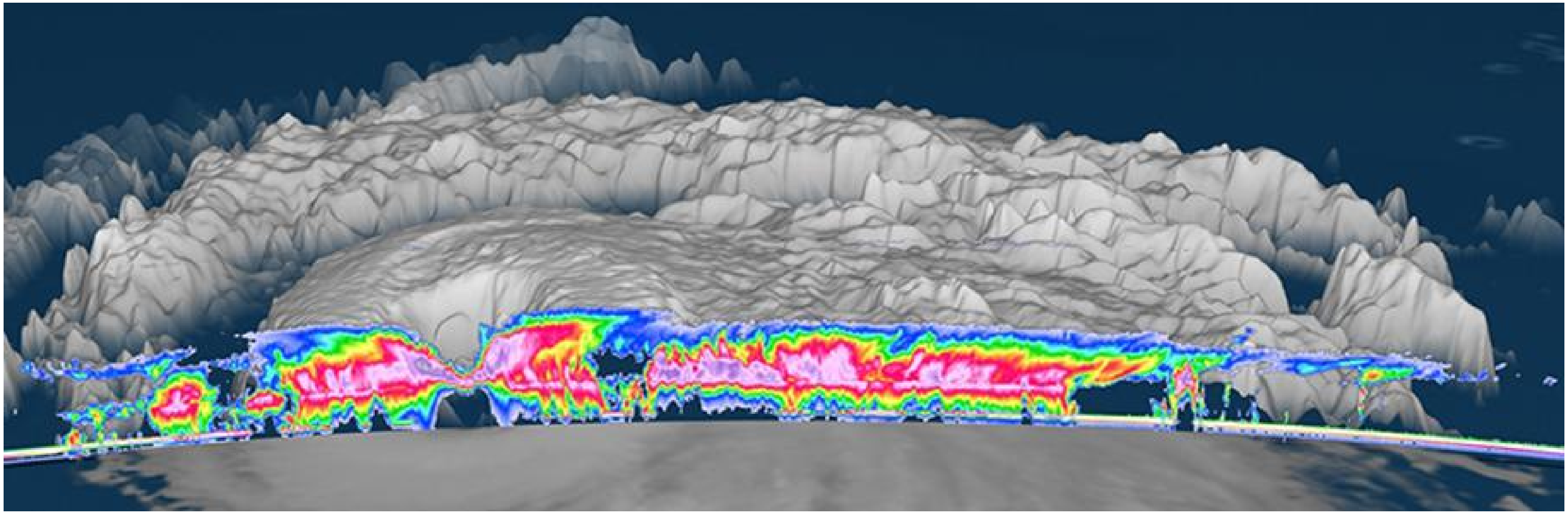

Outline

- Introduction to microwave remote sensing
- Passive microwave detection data application
  - Application of microwave imager data in typhoon monitoring
  - Application of microwave sounder data in typhoon monitoring
- Active microwave detection data application
  - Wind field scatterometer data application
  - Rain radar data application

Why microwave is used to detect tropical cyclones?

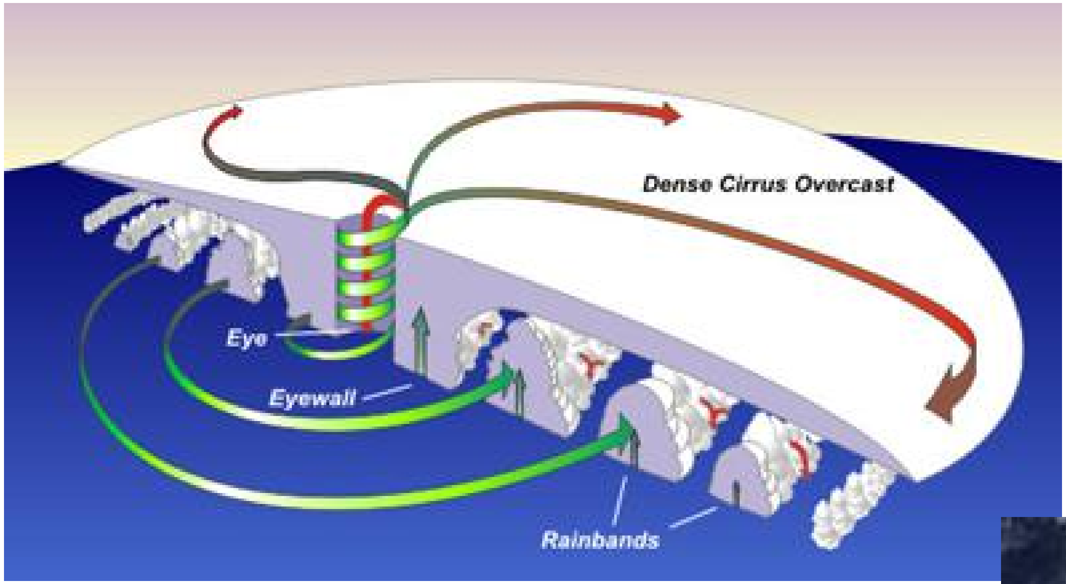

Schematic diagram and satellite observation of tropical cyclone cloud and rain

Reason: Due to the dense cirrus clouds covering the tropical cyclone, visible and infrared instruments cannot detect the internal thermal , cloud and rain structures of TC.

The microwave has high transmission characteristics, which can reveal the spiral structure of the dense cloud area of the typhoon, and can be used to identify the warm center position of typhoon. Microwave is divided into passive microwave and active microwave detection.

Measuring Electromagnetic Energy

- Passive Instruments:
  - Receive radiation from the earth-atmosphere system
  - Measure solar radiation reflected by earth/atmosphere targets
  - Measure emitted and scattered infrared radiation
  - Measure microwave radiation from emission and scattering
- Active Instruments:
  - Emit pulses of radiation, usually at microwave frequencies
  - Measure radiation returned to the sensor
  - Examples
    - Surface-based and airborne radars
    - Satellite scatterometers

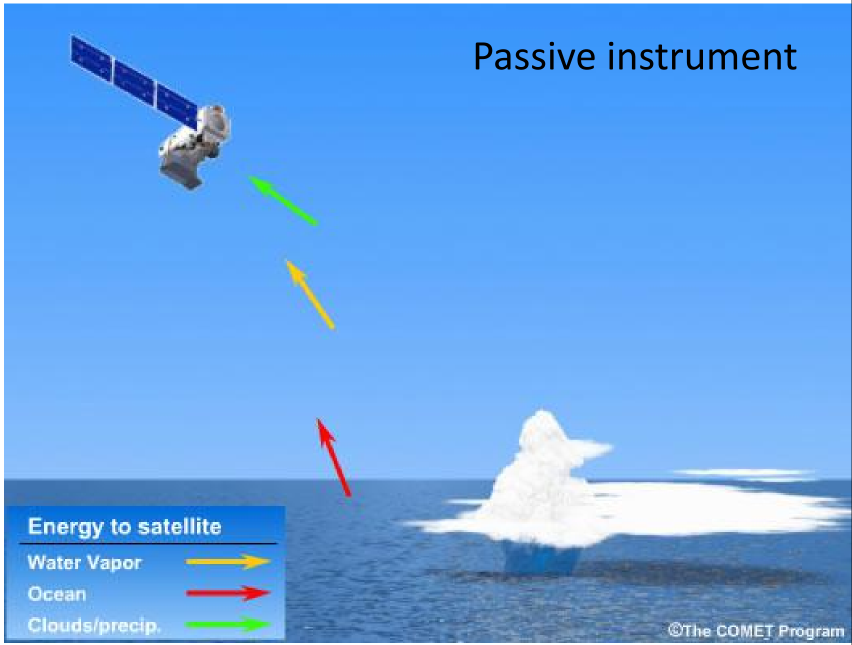

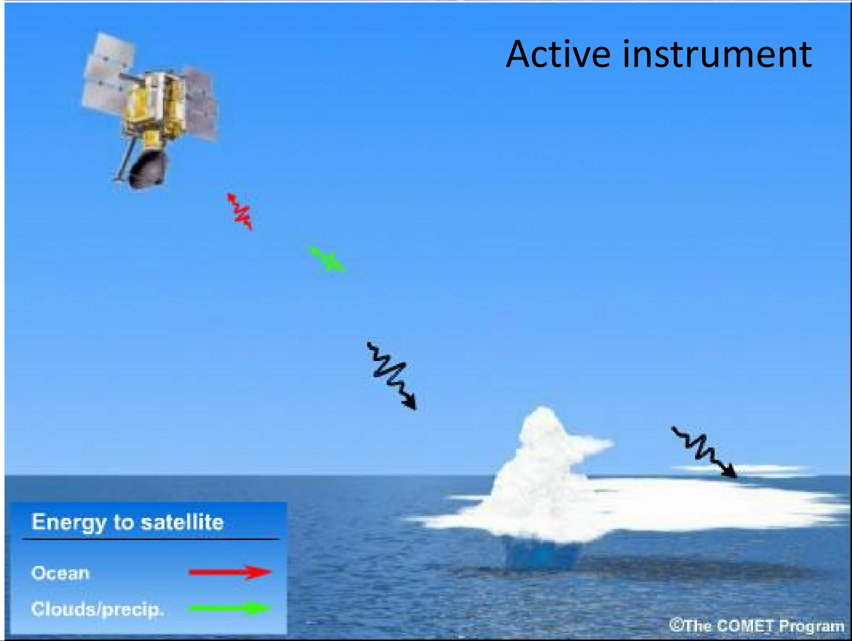

Passive Microwave Sensor

Passive sensors (FY-3,SSM/I, SSMIS, TMI, AMSU, AMSR2, etc.) measure emitted microwave energy from 19 to 200 GHZ

Emissivities are directly related to brightness temperatures (T_b)

- scattering effects by ice
- emission by light precipitation
- emission/absorption by cloud liquid water and rain droplets

Microwave window channel T_b can be used to quantify these emissivities

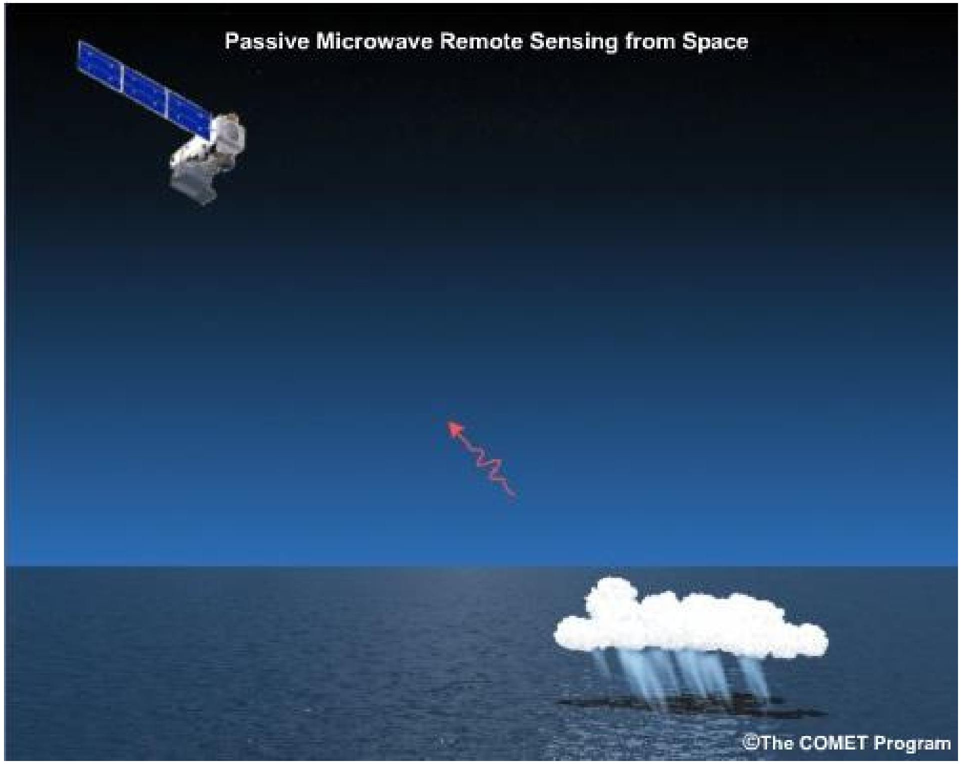

Based on different detection targets, passive on-board microwave instruments can be divided into two categories:

- one is a microwave imager that targets atmospheric cloud rain and surface features. The detection channel is located in the atmospheric window or the weak water vapor absorption zone ,mainly affected by the absorption and scattering of water vapor, liquid water and ice crystals in the atmosphere.
- The other is a microwave sounder that targets the vertical distribution of atmospheric temperature and humidity. The detection channel is located near the strong absorption band of oxygen and water vapor. The selected channels are located at different positions of the absorption band, and the detected weights are different in height, and the atmospheric temperature and wet profile can be detected.

Microwave Transmittance

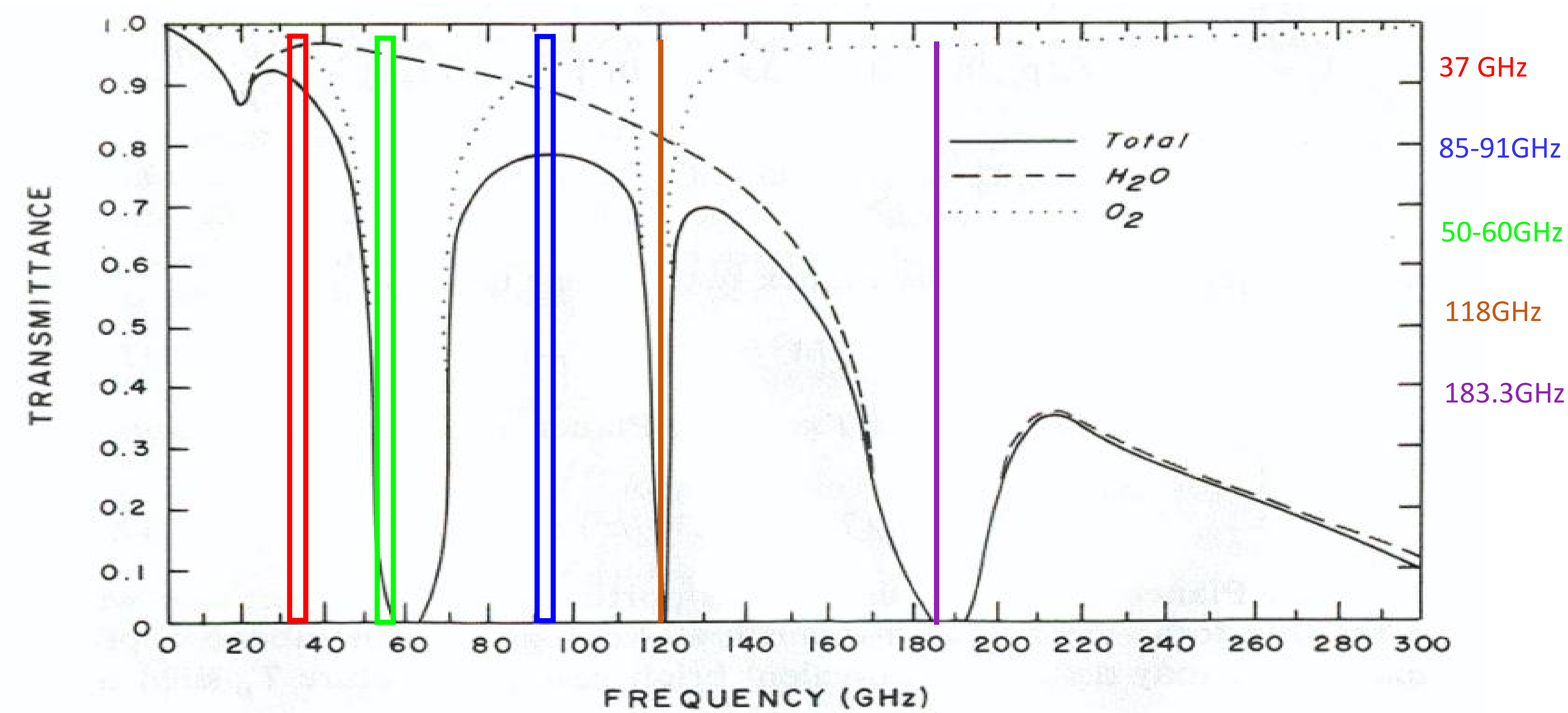

Current/Operational Microwave Imagers and Sounders/Platforms

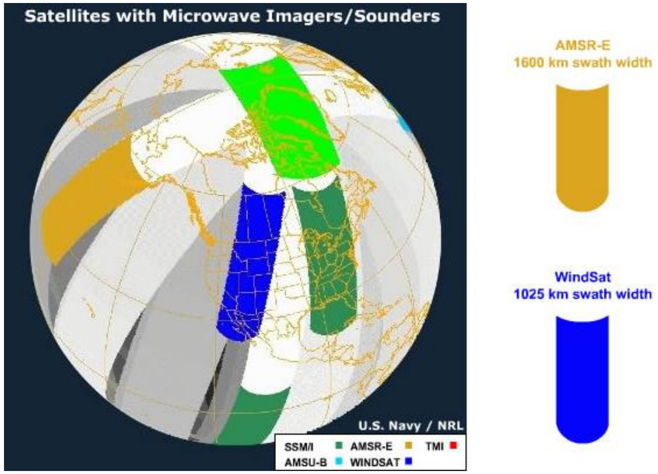

Microwave imager

- SSM/I – 1 DMSP satellite (F-15)
- SSMIS – 3 DMSP satellites (F-16, F-17, F-18)
- TMI and PR – TRMM – NASA/Japan
- MWRI—FY-3

Microwave sounder

- AMSU-A/B – 6 satellites (NOAA 15, 16, 18, 19) and European MetOP-A/B
- MWTS/MWHS— FY-3

Microwave Imager

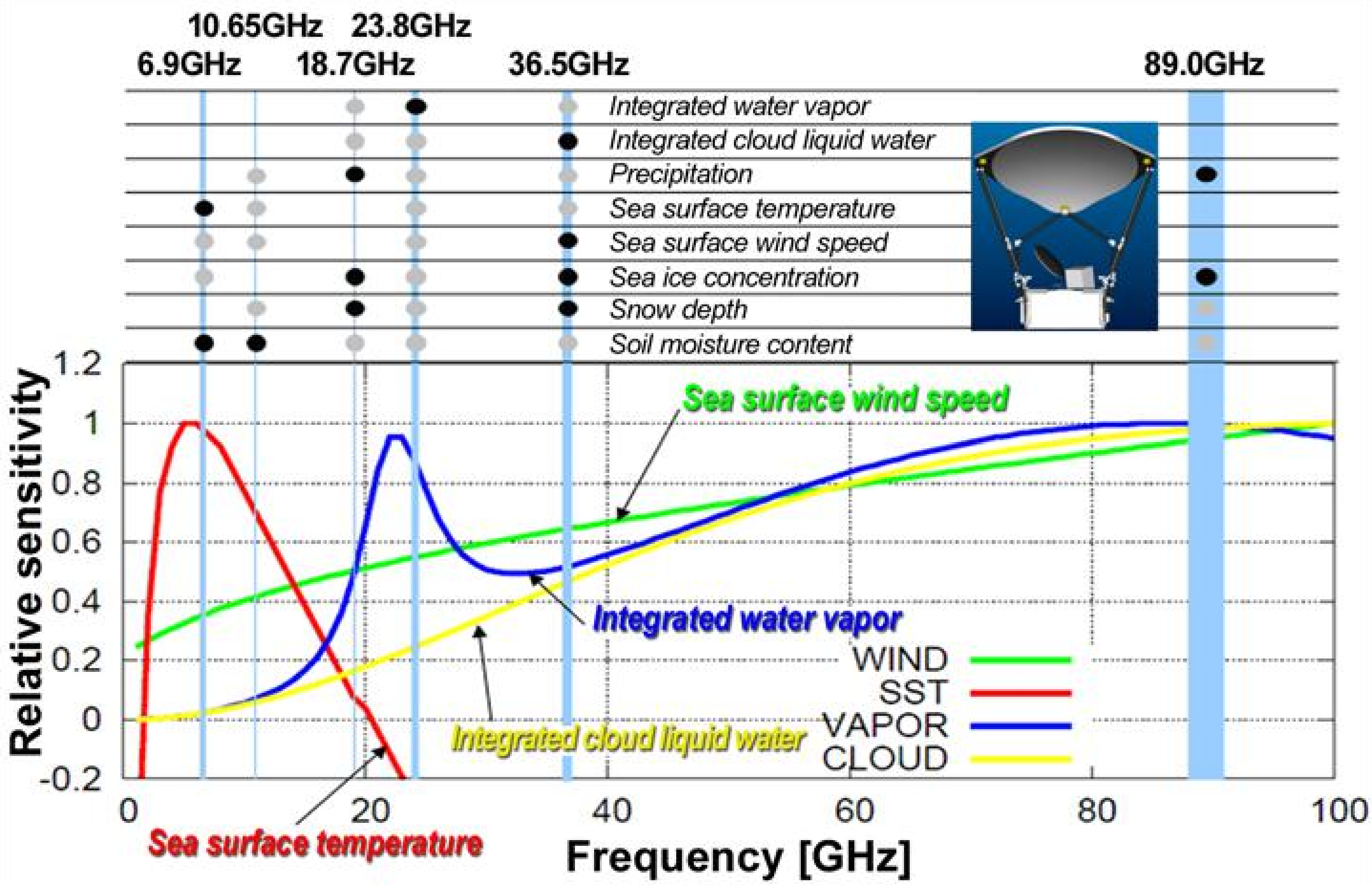

Typical Products:

Atmosphere: atmospheric precipitable water, precipitation

Land Surface: LST, soil moisture, snow water equivalent

Ocean Surface: SST

Microwave Imager

MicroWave Radiation Imager

MWRI/FY-3

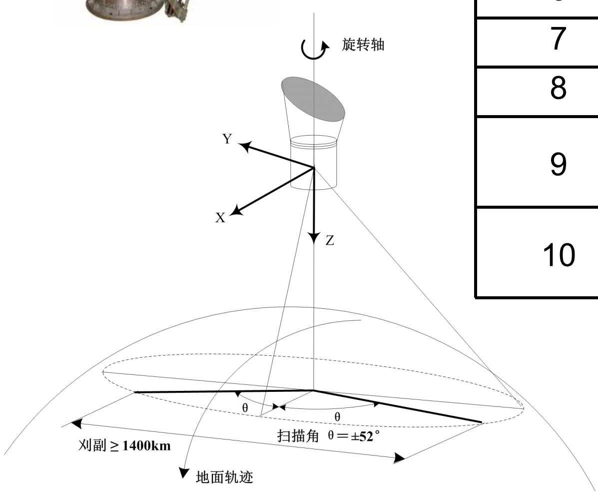

MWRI Instrument Specification

Channel No.	Central Freq.	Bandpass （MHz）	NEΔT	Dynamic Range (K)	Beam Efficiency	Nadir Resolution
1	10.65V	180 10%	0.6K	3-340	90%	51km 85km
2	10.65H	180 10%	0.6K	3-340	90%	51km 85km
3	18.7V	200 10%	1.0K	3-340	90%	30km 50km
4	18.7H	200 10%	1.0K	3-340	90%	30km 50km
5	23.8V	400 10%	1.0K	3-340	90%	27km 45km
6	23.8H	400 10%	1.0K	3-340	90%	27km 45km
7	36.5V	900 10%	1.0K	3-340	90%	18km 30km
8	36.5H	900 10%	1.0K	3-340	90%	18km 30km
9	89V	双边带2300 2 10%	2.0K	3-340	90%	9km 15km
10	89H	双边带2300 2 10%	2.0K	3-340	90%	9km 15km

Key Characteristics of Microwave Radiation

Water surfaces (e.g, oceans) have low emissivity (~0.4-0.5) and appear "cold" at microwave frequencies.

Land surfaces have a much greater emissivity (~0.9).

Raindrops have high emissivity and are "warmer". They contrast against a "colder" ocean background.

Higher frequency (shorter wavelength) microwaves (~85 GHz) are scattered by ice particles in precipitating clouds, reducing radiation reaching the satellite (these regions also look "cold").

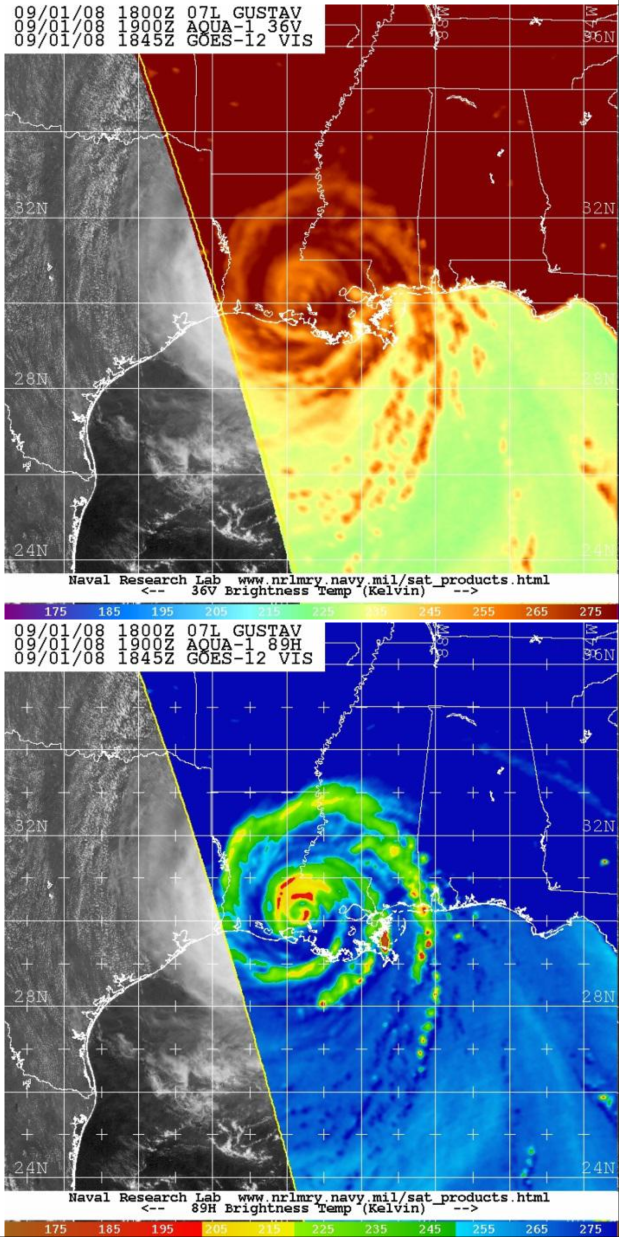

Sinlake from MWRI Map
（20080912）

10v

台风“森拉克”10v通道亮温

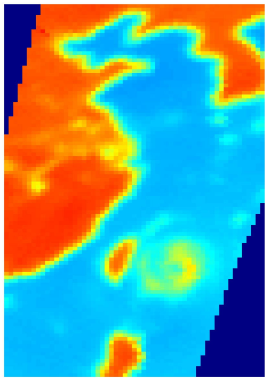

10h

台风“森拉克”10h通道亮温

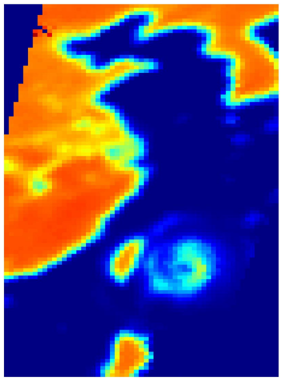

18v

台风“森拉克”18v通道亮温

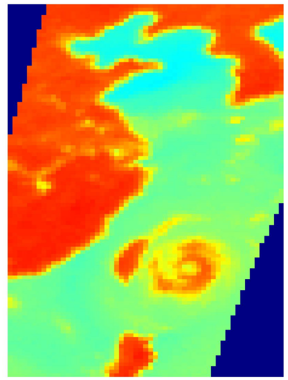

18h

台风“森拉克”18h通道亮温

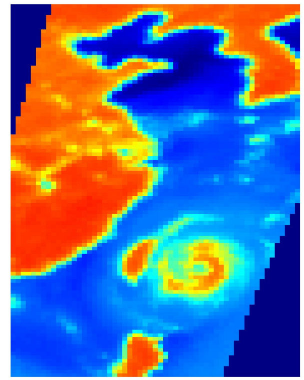

23v

台风“森拉克”23v通道亮温

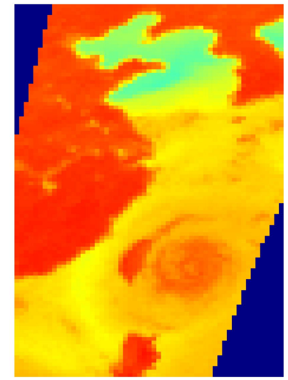

23h

台风“森拉克”23h通道亮温

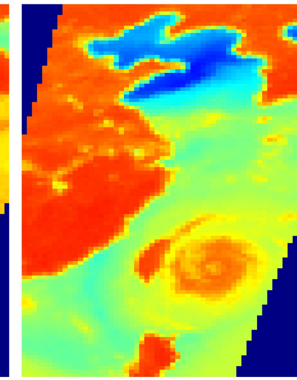

36v

台风“森拉克”36v通道亮温

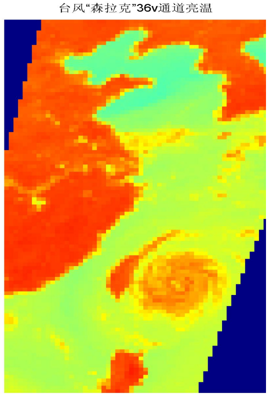

36h

台风“森拉克”36h通道亮温

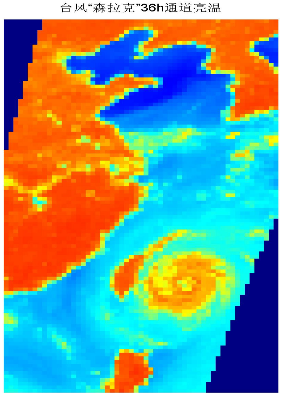

89v

台风“森拉克”89v通道亮温

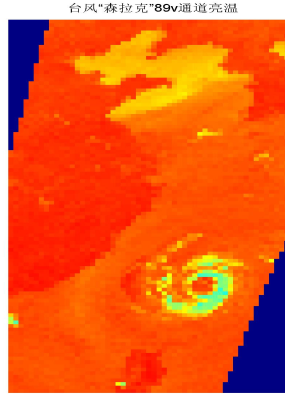

89h

台风“森拉克”89h通道亮温

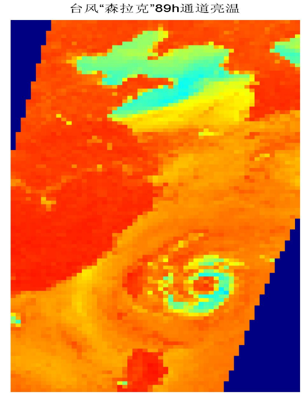

- **BT map of Sinlake from low freqency to high freqency**
- **Strong rainfall structure within Typhoon related highly with low frequency map (10 and 18 GHz)**
- **Typhoon 2D structure is more perfect and clearer at high frequency map (36 and 89 GHz)**

drop size in cloud increase the scattering signal in low frequency map

3D precipitation analysis

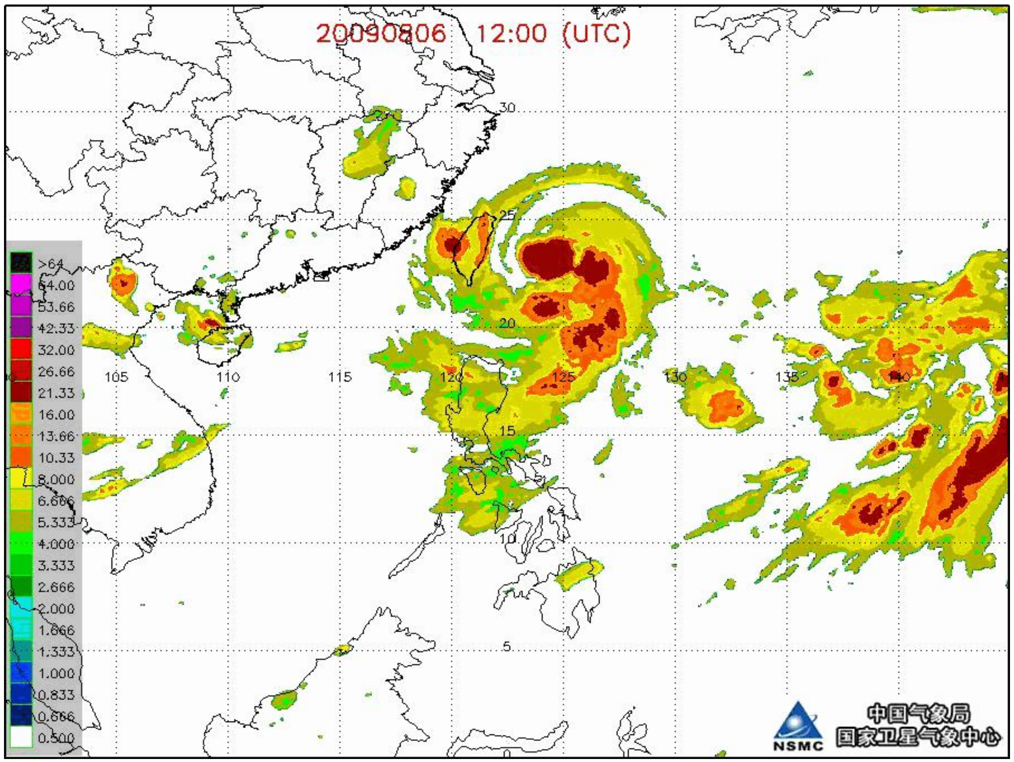

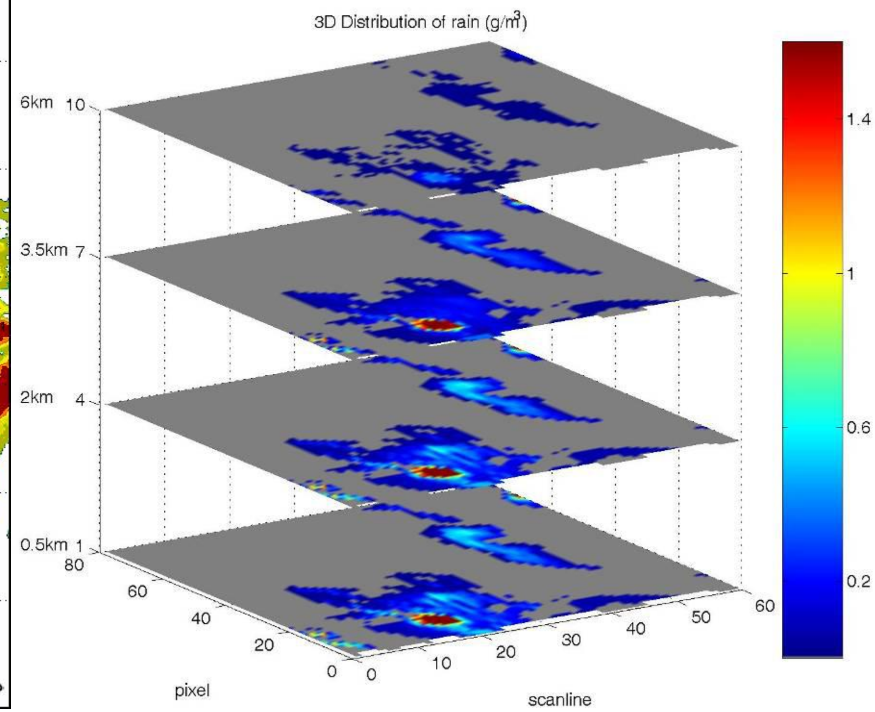

Microwave imager data analyze typhoon characteristics (FY-3 MWRI， EOS AMSER-E,TRMM TMI) 37 Vs 89 GHz

- 36–37 GHz is sensitive to raindrop particles, used to detect low-level cloud/raindrop distribution and circulation;
- 85–91GHz is sensitive to ice particles, used to detect deep convective cloud structures.
- High and low level circulation changes can by detected by combined use.

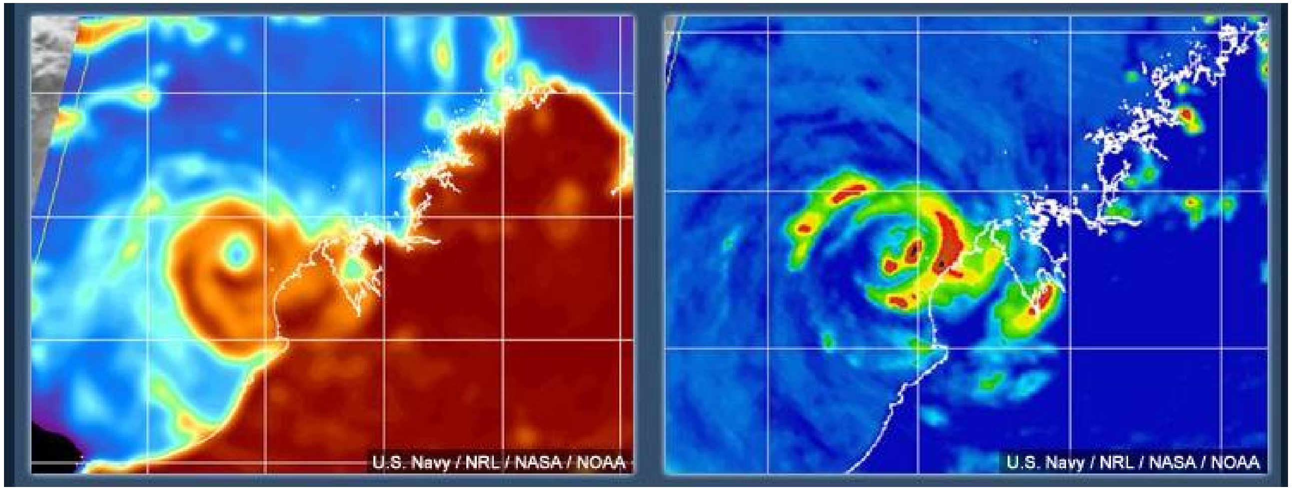

37GHz 85GHz

The application of Microwave image data

85-91-GHz images → primary signature is lowered T_b caused by ice scattering and cloud and rain droplets within deep convection and precipitating anvil clouds

36-37-GHz images → primary signature is elevated Tb because of minor emission from liquid hydrometeors near or below the freezing level

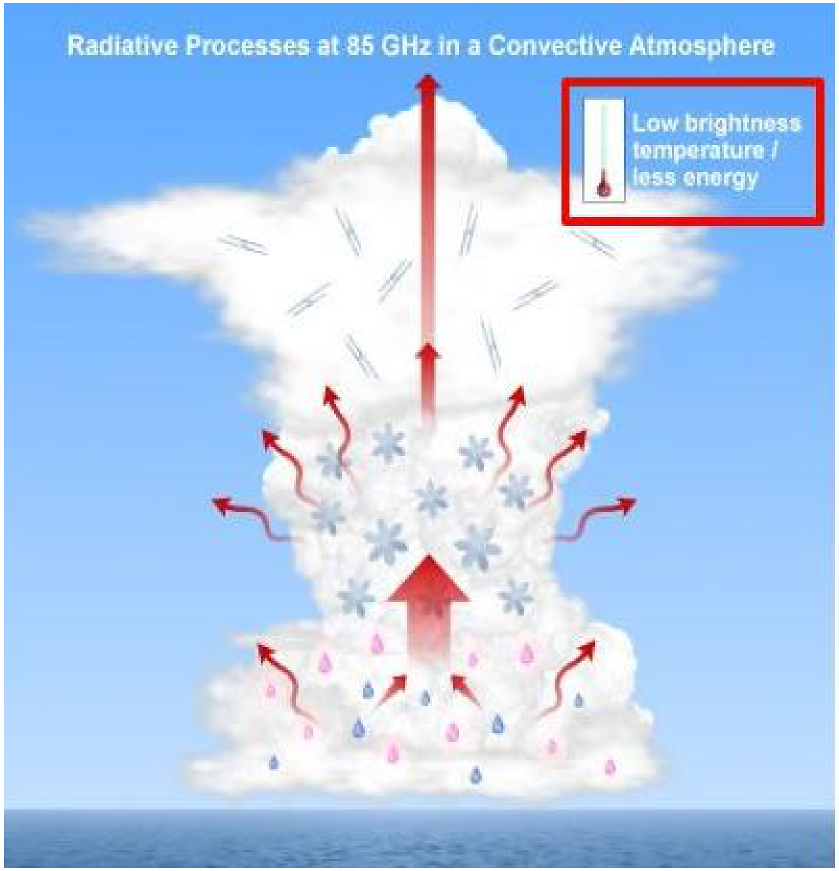

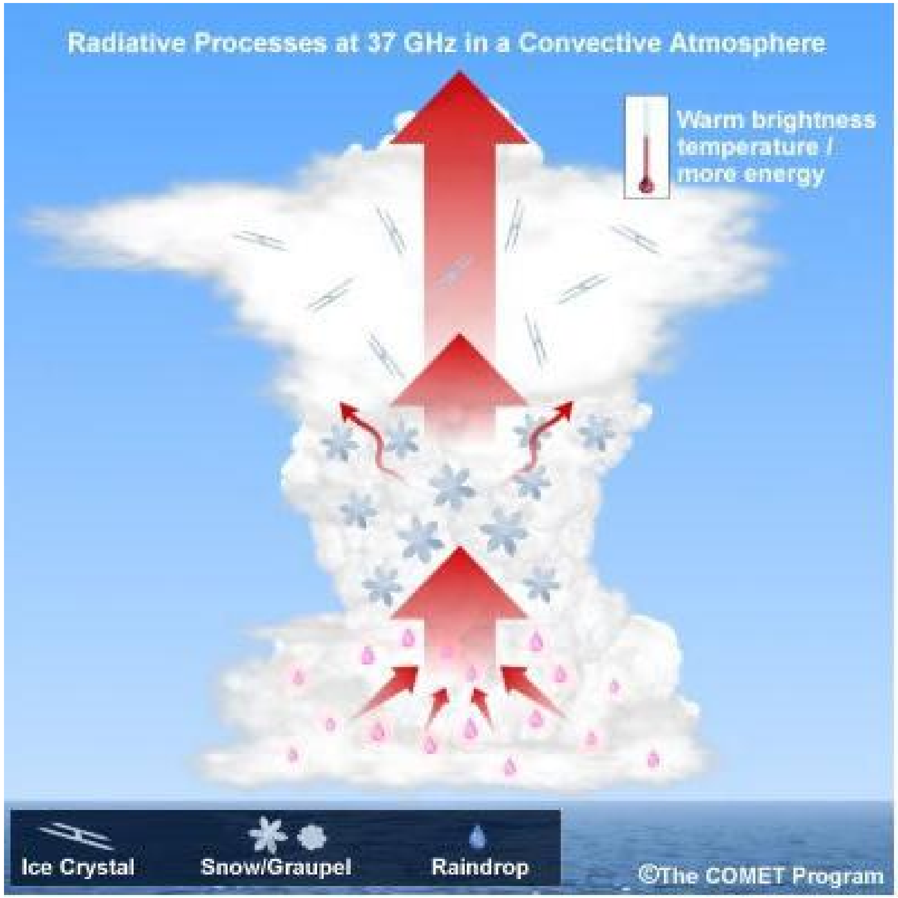

Typhoon positioning

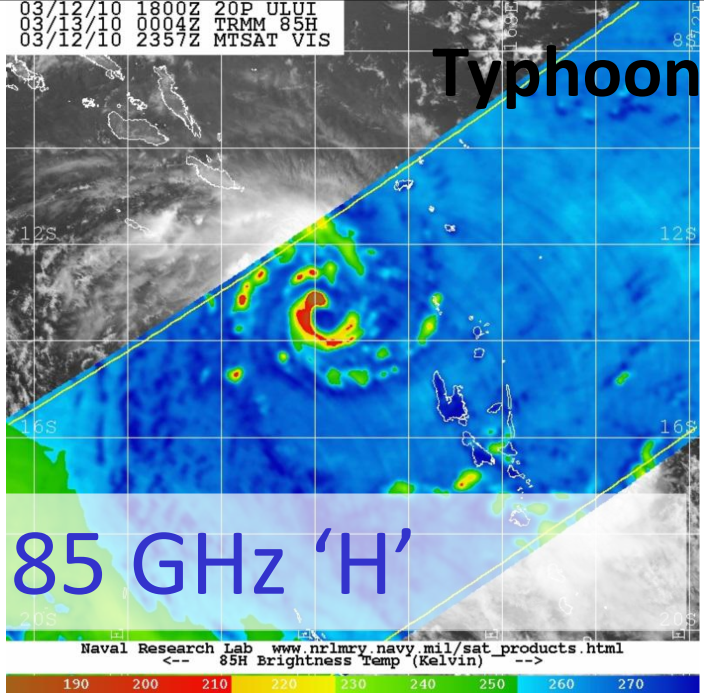

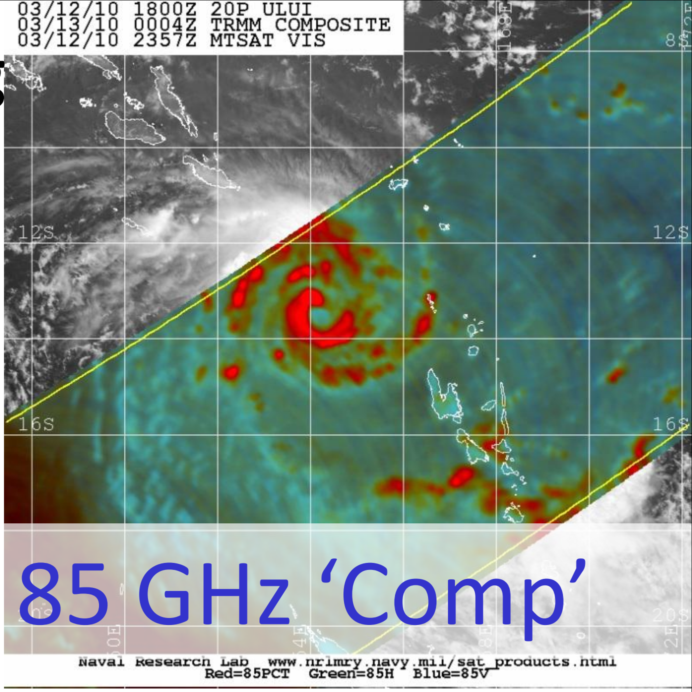

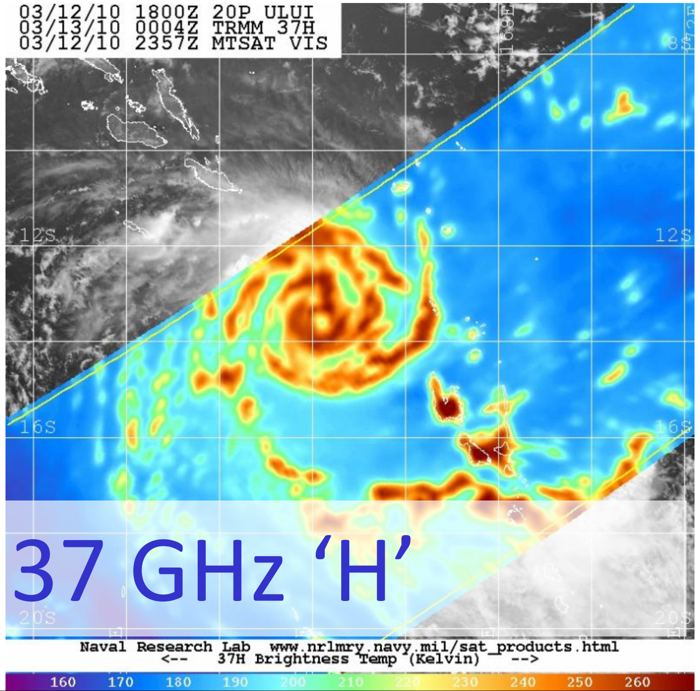

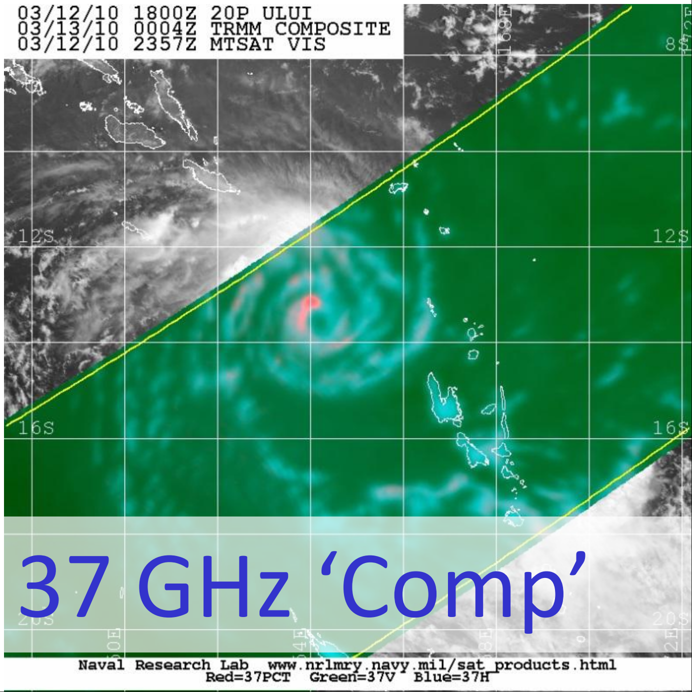

Typhoon Position

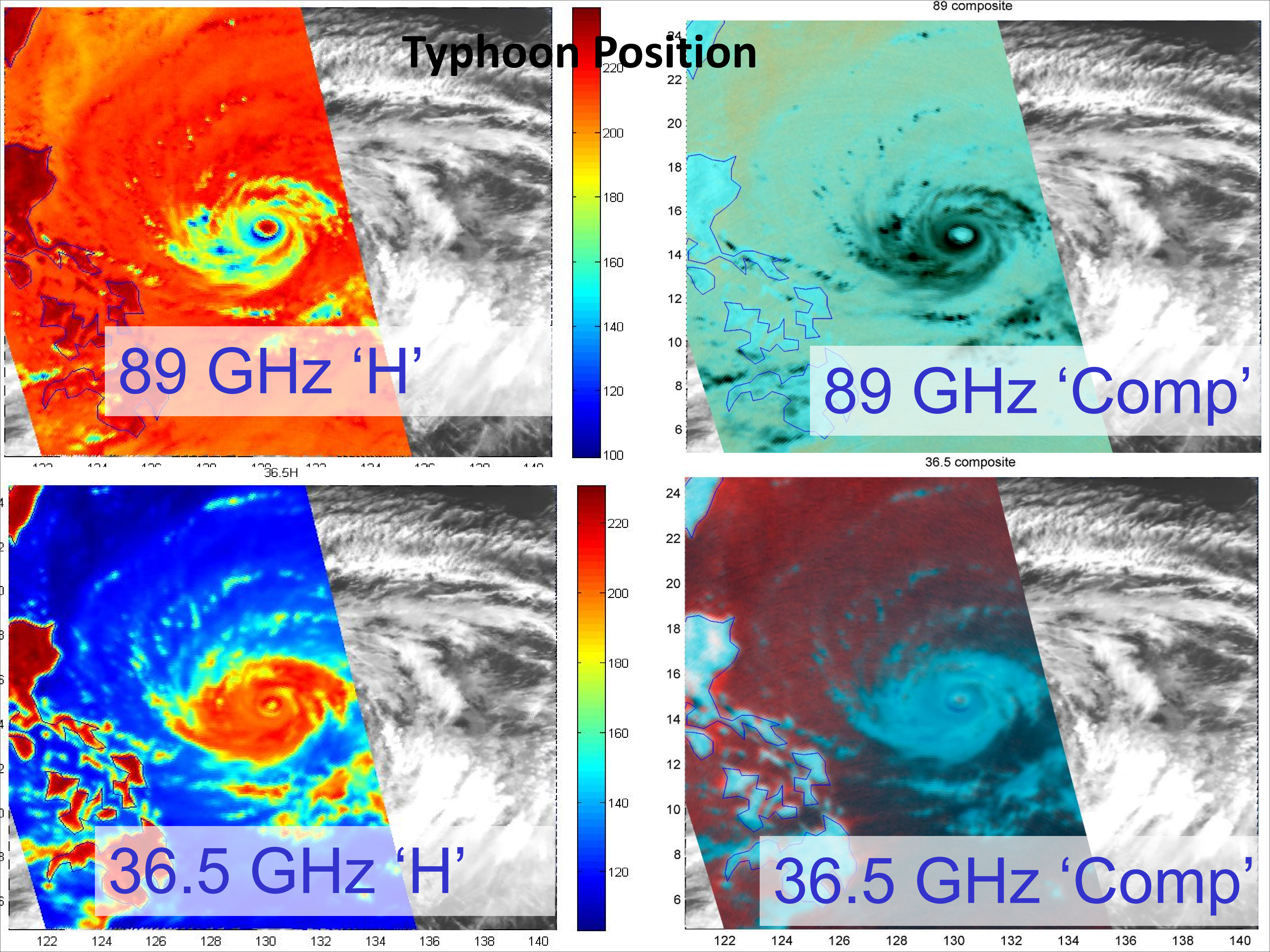

85-91GHZ Imagery Interpretation

- Imagery can penetrate through cirrus clouds and reveal internal storm structure
- Land appears warm relative to water surfaces
- Water surfaces and deep convection appear relatively cold (due to scattering from ice)
- Low-level moist air masses act to warm brightness temperatures over water surfaces
- Imagery is better at locating tropical cyclone centers than conventional visible and infrared
- Imagery is able to distinguish deep convection, but can not always see low-level circulations associated primarily with low-level clouds

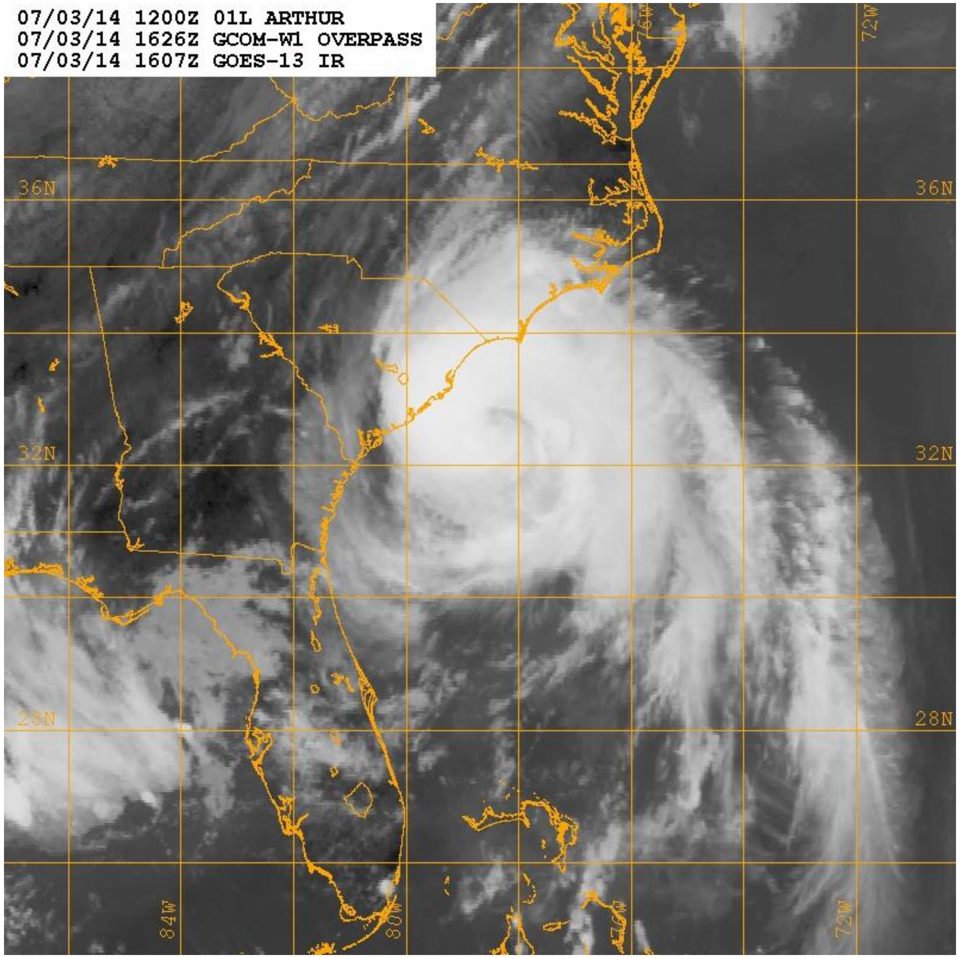

36-37GHZ Imagery Interpretation

Precipitating clouds and land-surface appear warm against a relatively cold ocean background

Cold features: sea surface only

Imagery highlights low-level cloud features and storm structure

Imagery identifies cirrus-covered eyes and gives a ‘true’ low-level center instead of a mid/upper-level center (as in 85-91 GHz imagery

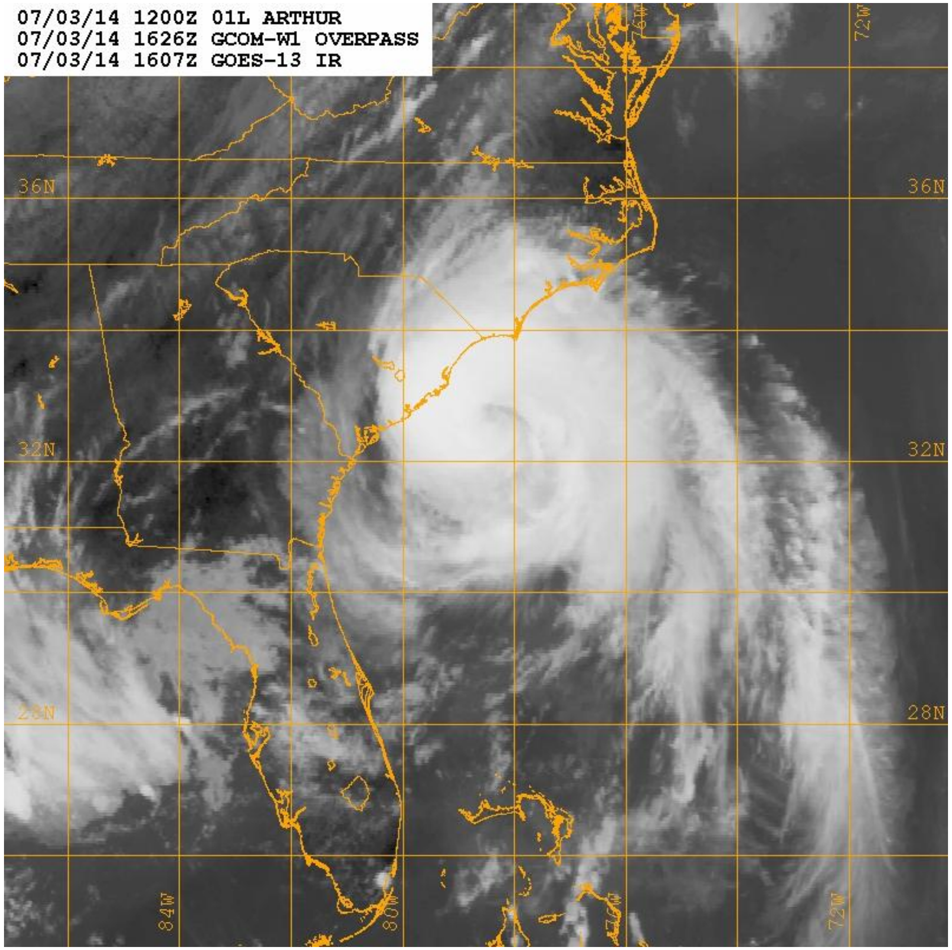

Single Frequency Interpretation

Ocean region appear **Cool** in 89H

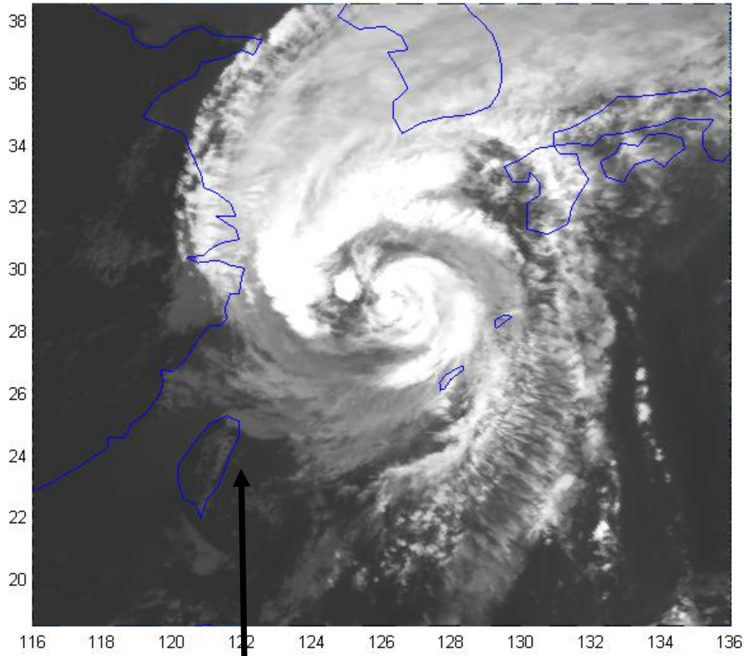

Ocean region appear **Cold** in 36.5V

ocean

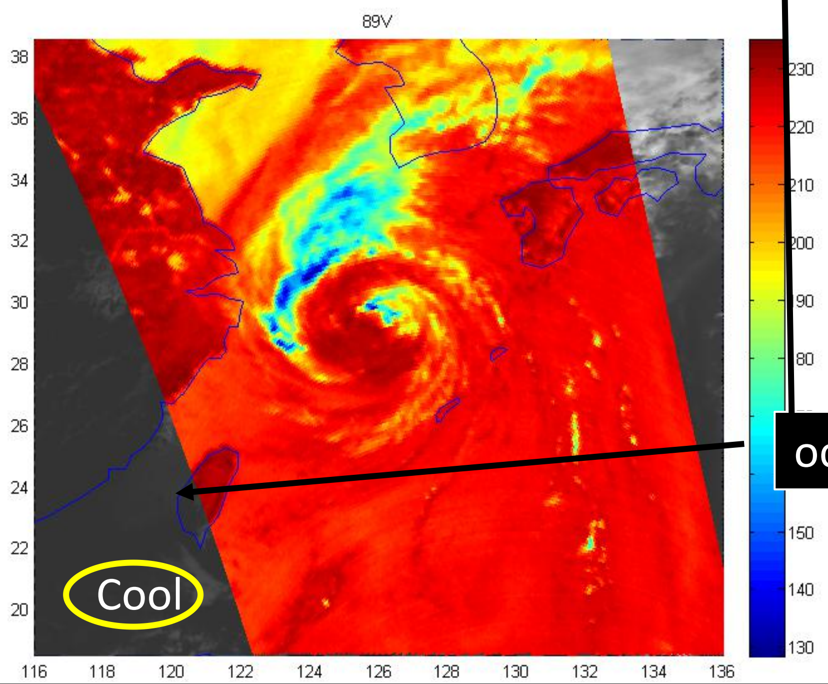

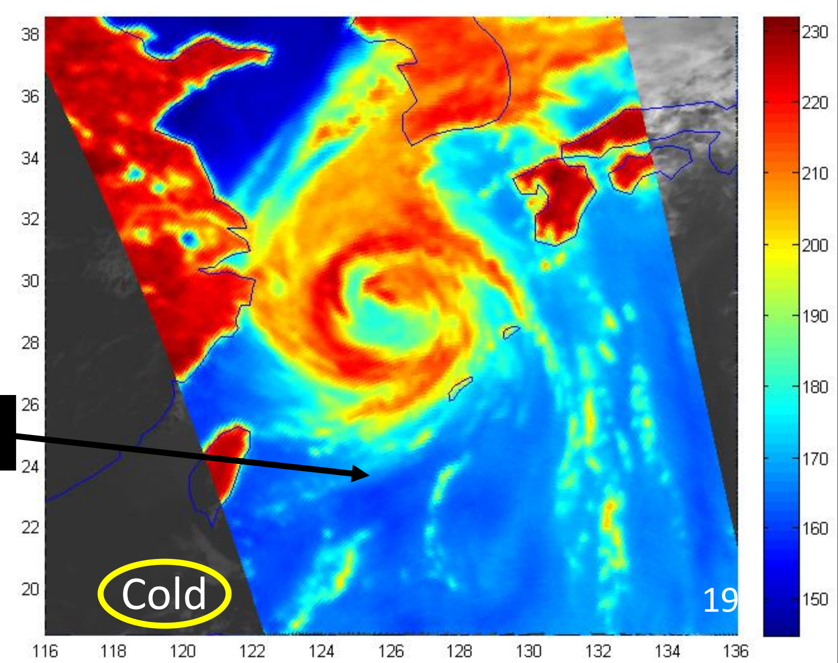

Single Frequency Interpretation

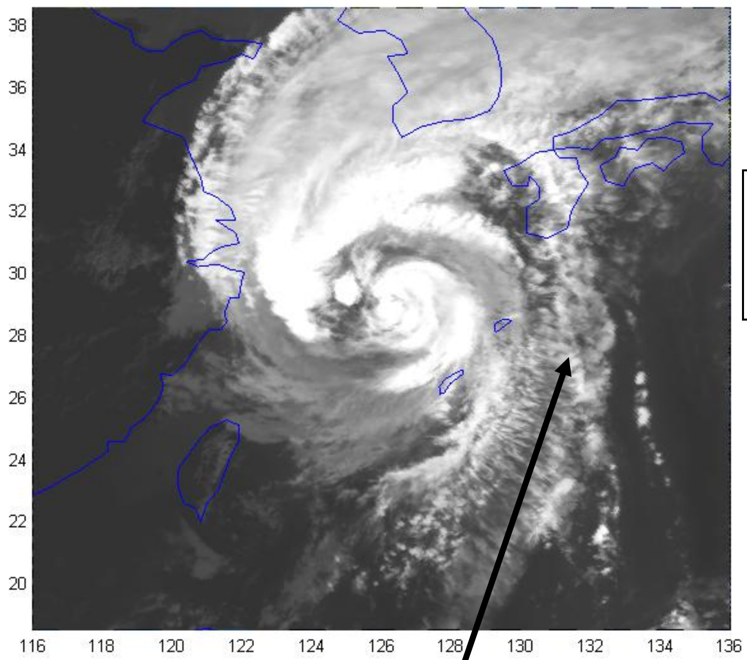

Rain appears Warm in 89H

Rain appears Cool in 36.5H

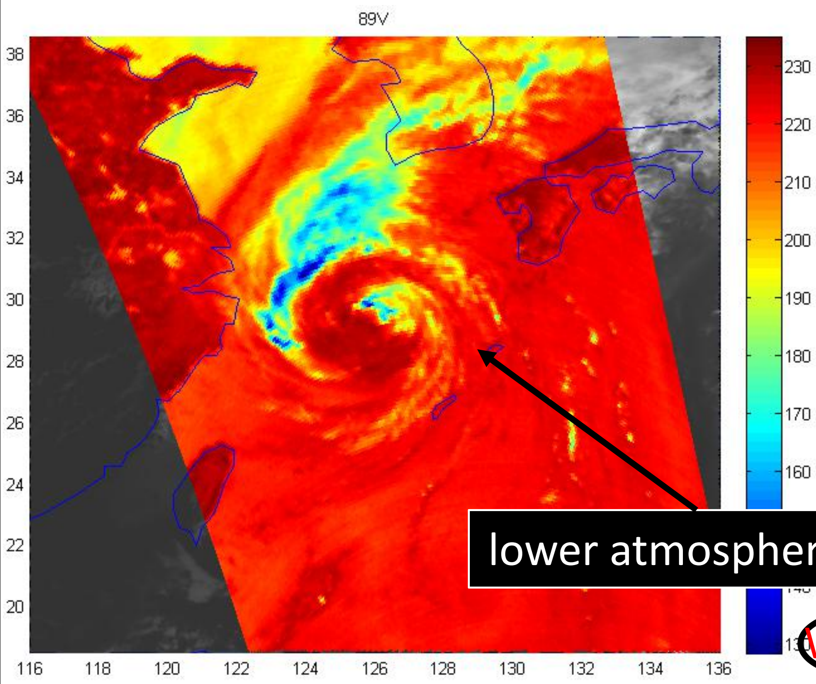

lower atmosphere rain/cloud water

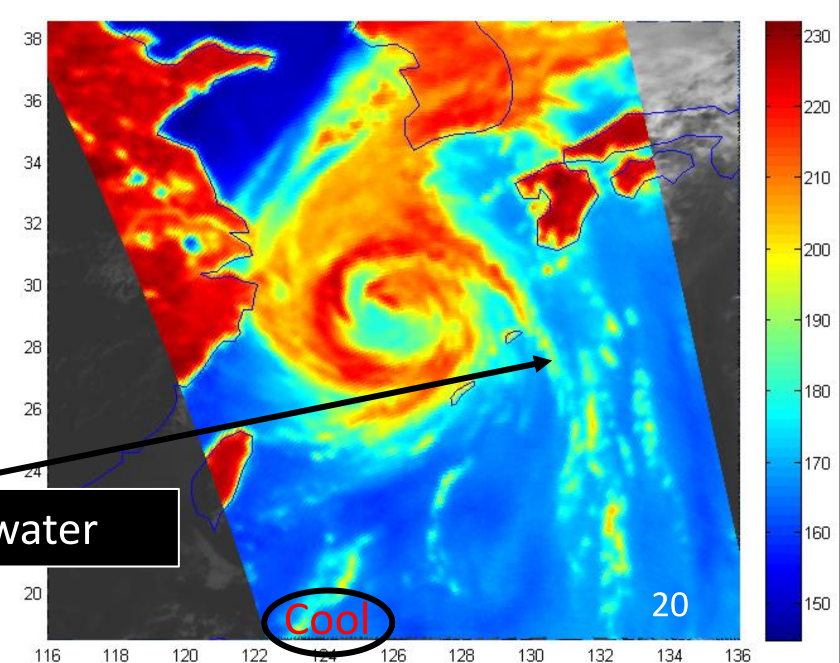

Single Frequency Interpretation

Ice appears <u>Cool</u> to <u>Cold</u> in 85H; rain is <u>Warm</u>

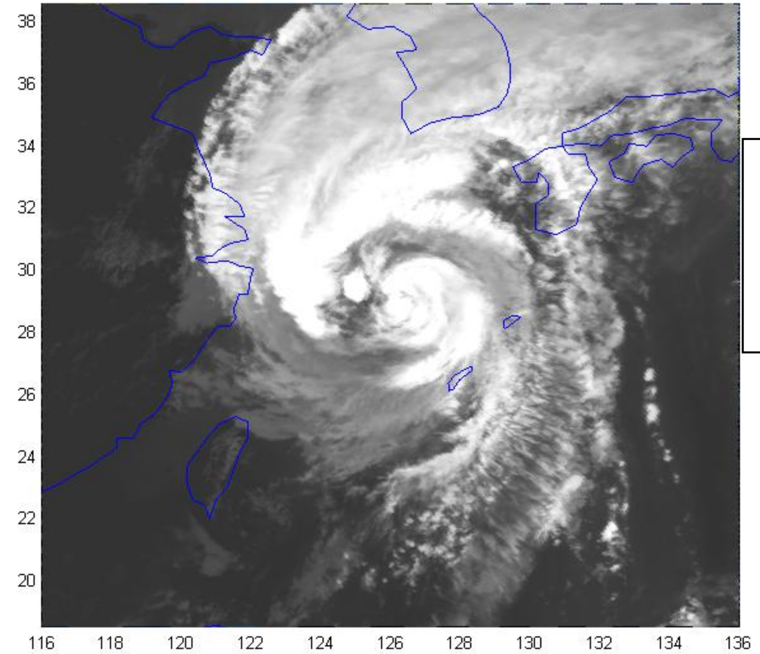

Rain appears <u>Cool</u> in 37V (<u>less cold</u> over water Dense ice looks <u>Warm</u>

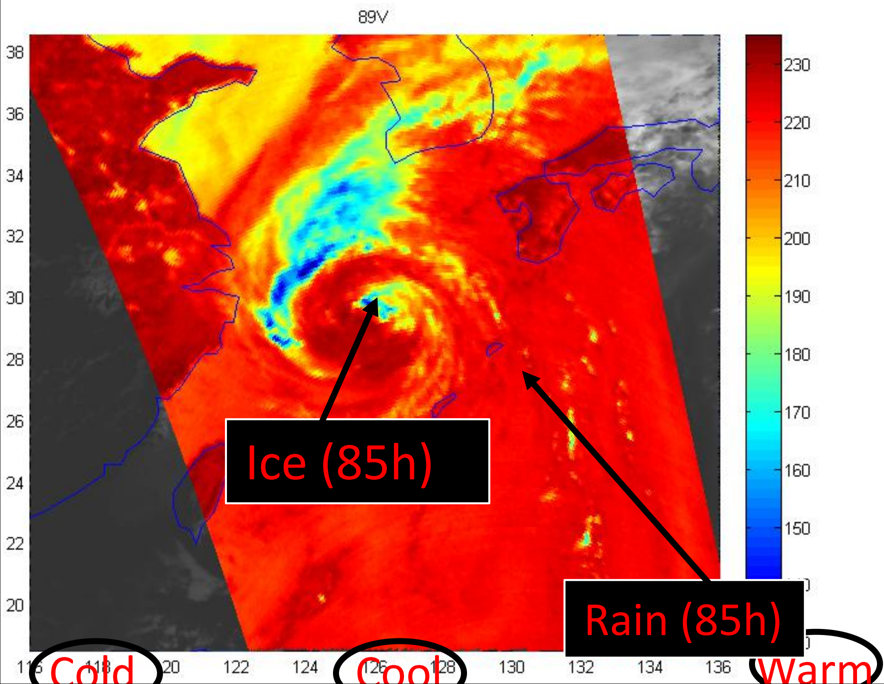

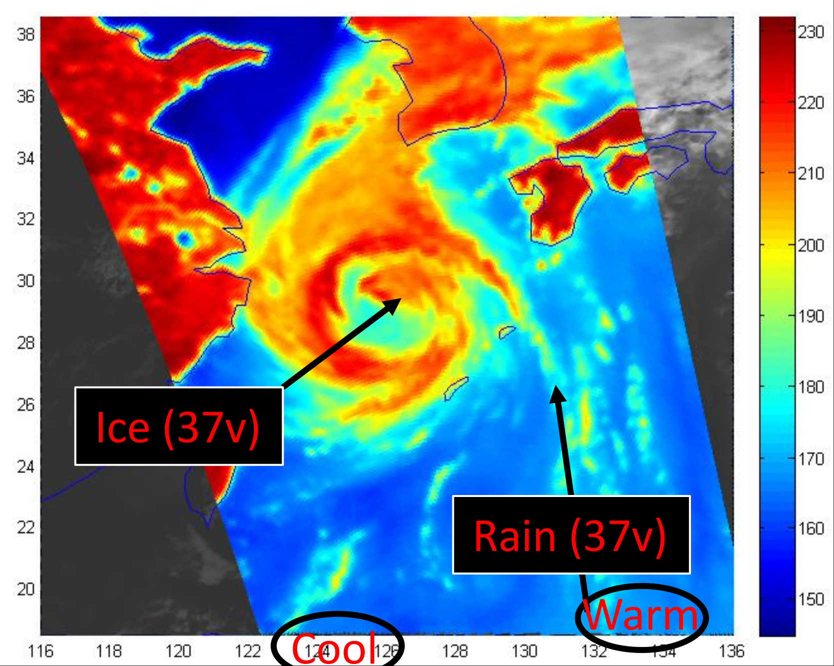

Advantages of Using 85-GHz and 37-GHz Imagery for TC Analysis

- In a sense, “sees” through clouds
- Identification of circulation center (critical step in initiating TC advisories)
- Acquire positioning of TCs in difficult situations (especially in early stages of development and at night)
- View of convective rain bands is more directly related to intensification of the TC
- Monitoring structural changes such as eyewall formation and eyewall replacement cycles

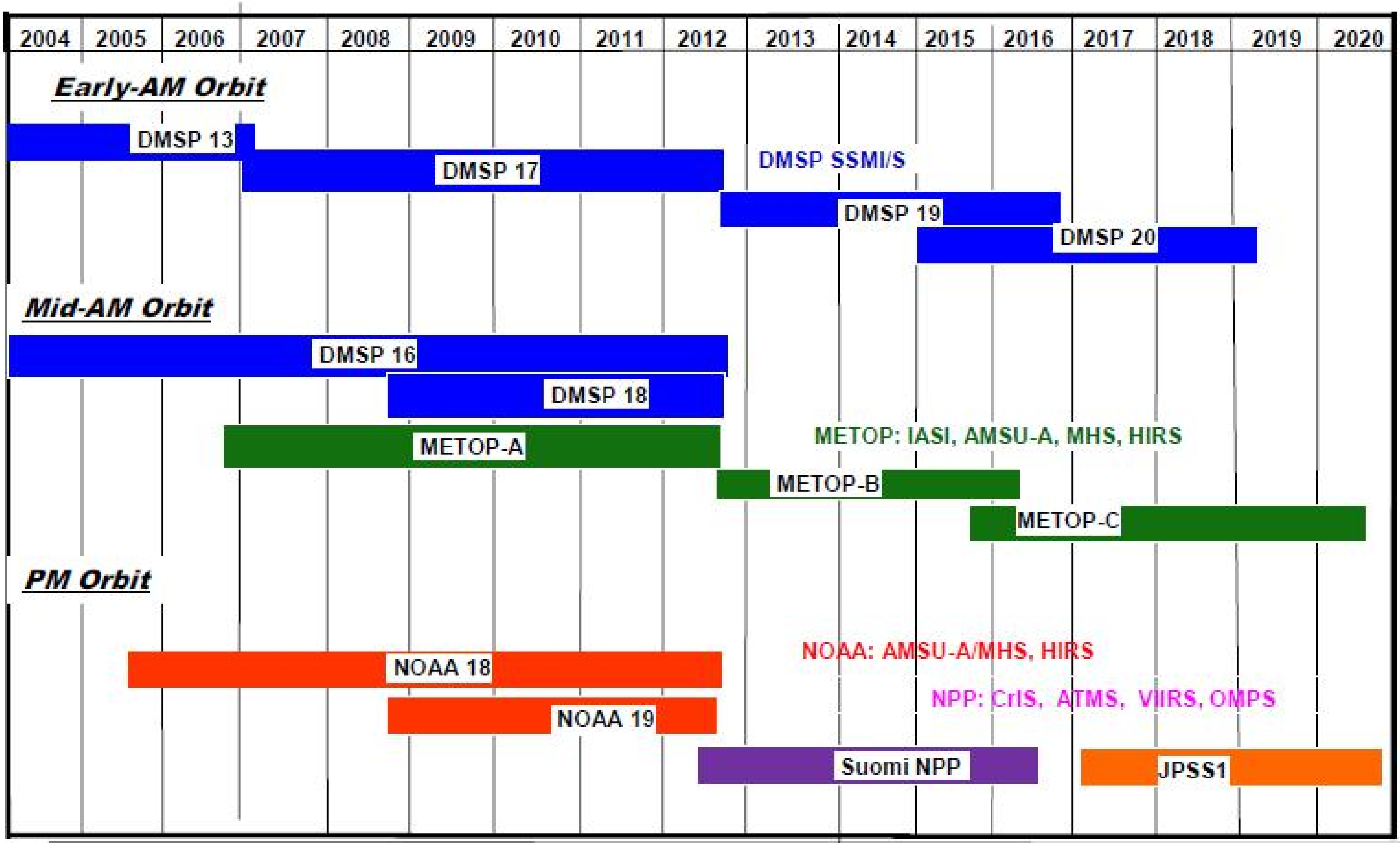

2004
2005
2006
2007
2008
2009
2010
2011
2012
2013
2014
2015
2016
2017
2018
2019
2020
Early-AM Orbit
DMSP 13
DMSP 17
DMSP SSMI/S
DMSP 19
DMSP 20
Mid-AM Orbit
DMSP 16
DMSP 18
METOP-A
METOP: IASI, AMSU-A, MHS, HIRS
METOP-B
METOP-C
PM Orbit
NOAA: AMSU-A/MHS, HIRS
NOAA 18
NPP: CrIS, ATMS, VIIRS, OMPS
NOAA 19
Suomi NPP
JPSS1

Eye Size Bias Correction: Account for Eyewall Slope

Vertical Cross Section of Tb Anomalies for Typhoon Lekima

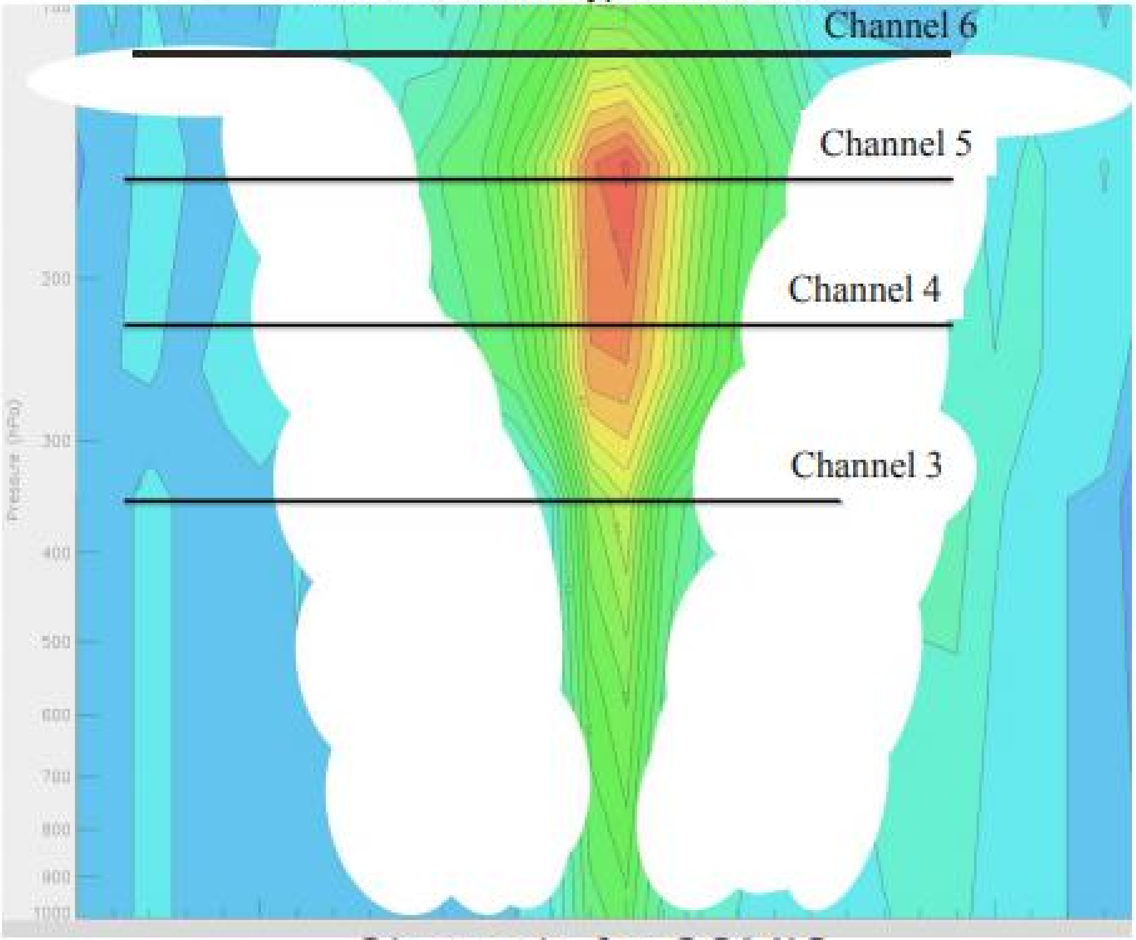

Channels for SSMIS

Eye size bias correction for each channel accounts for Eyewall slope.

Currently 45 degree eyewall slope is assumed however recent research suggests eyewall slope may change with TC eye size

Smaller eye = steeper slope

Parallax Error in Center Fixing

Satellite derived position error exists, potentially up to 20 km from actual position

Occurs due to conical viewing angle and/or viewing geometry of the satellite

Higher parallax error in 89-GHz images since scattering hydrometeors produce a signature much higher in the eyewall at 89 GHz than at 36.5 GHz

37 Vs 85 GHz – Parallax

- 37 GHz 5 km or less
- 85 GHz - 10-20 km

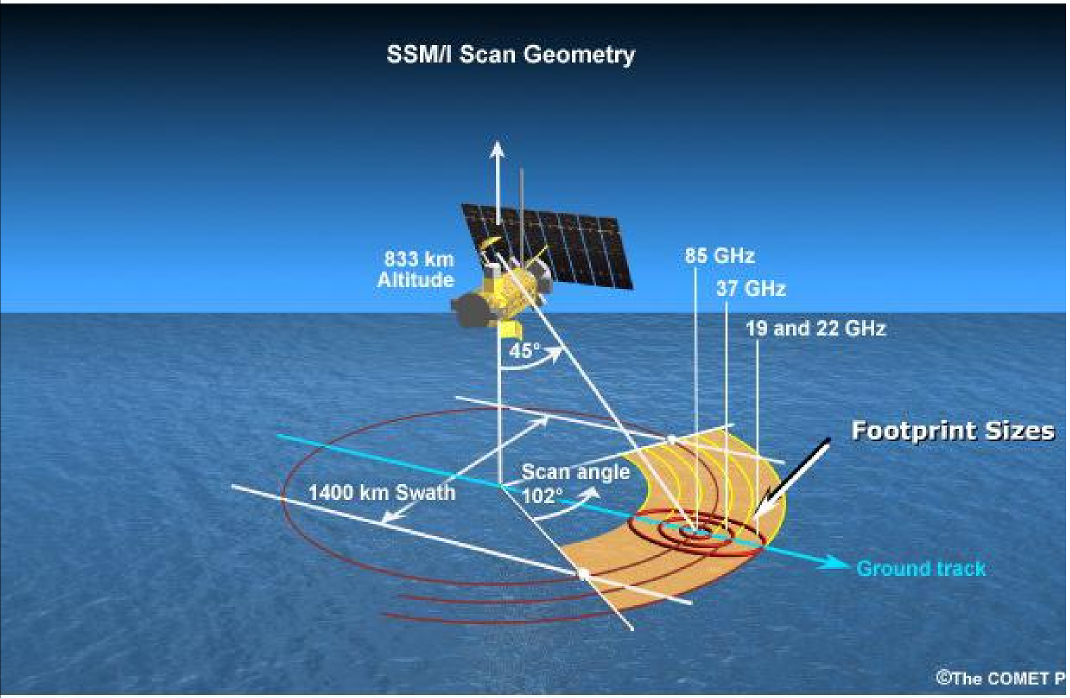

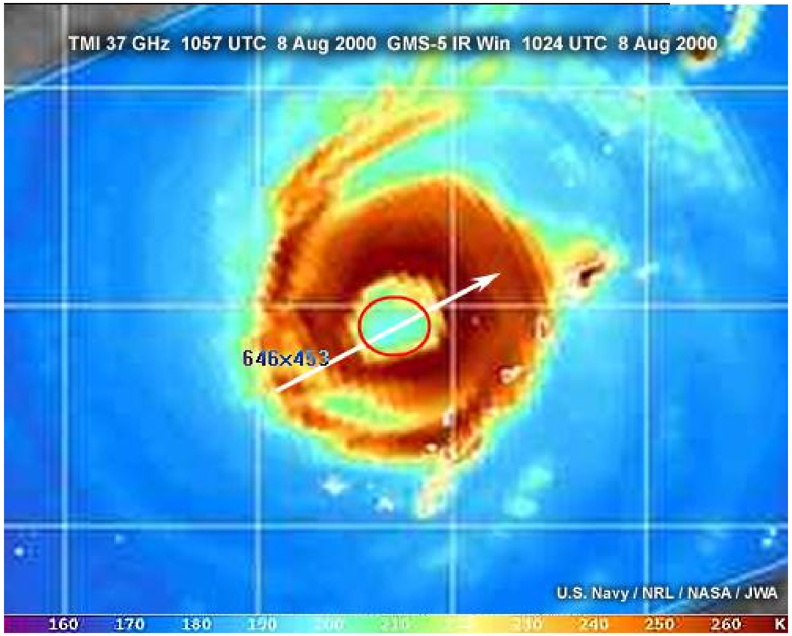

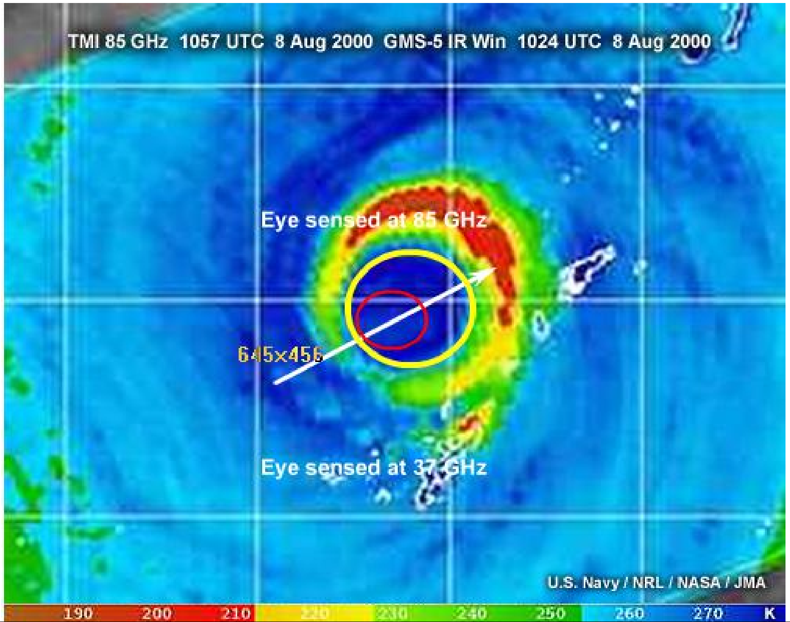

85-GHz Parallax

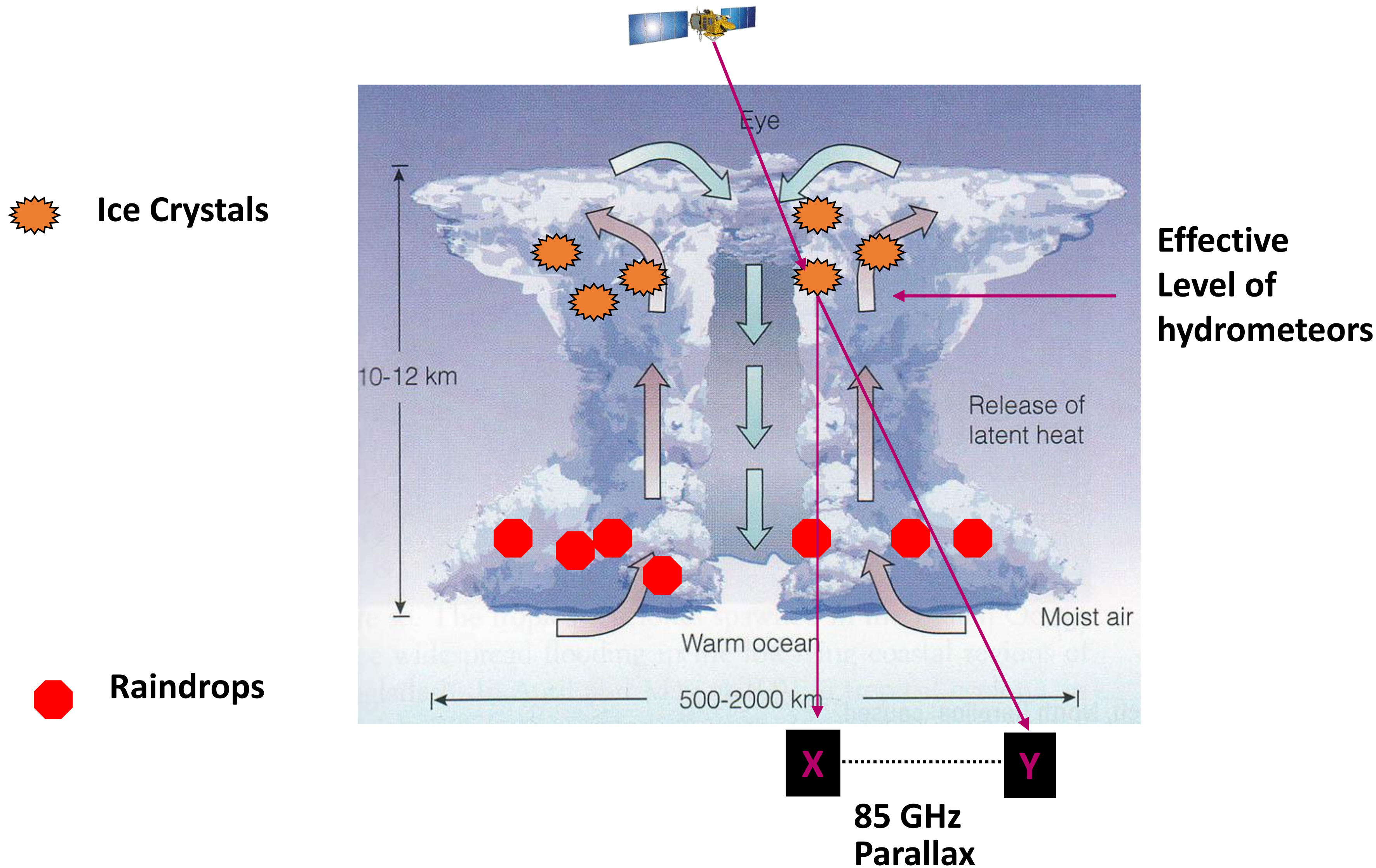

Parallax viewing effect has an effect on the positioning of the centers of tropical cyclones. At 85 GHz the satellite views a feature composed of ice crystals high in the cloud system, apparently above point X. **But because of the conical viewing angle or viewing geometry**, the satellite-derived position is displaced to point Y.

37-GHz Parallax

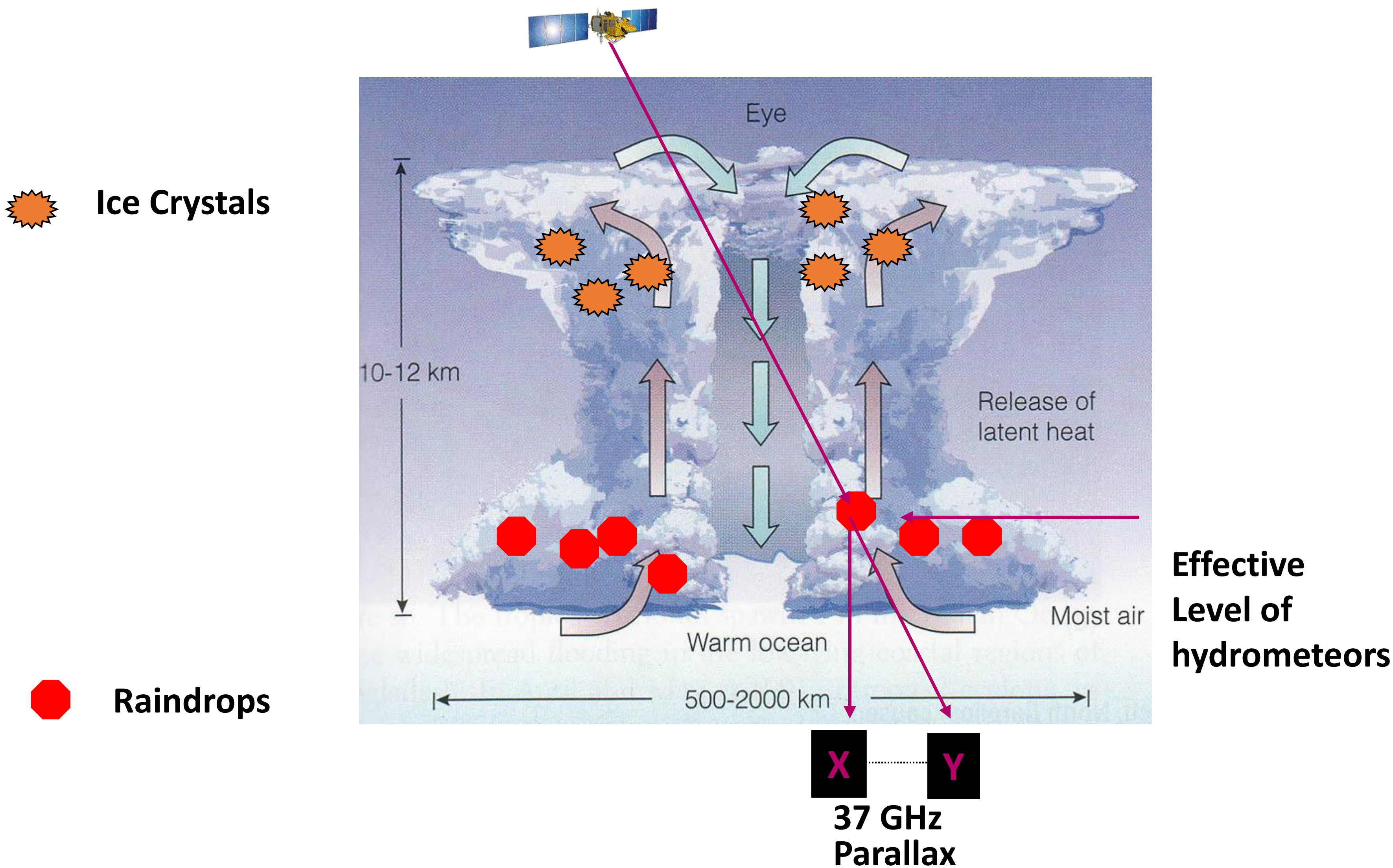

But at 37 GHz the rain feature sensed is much lower in the cloud as we have mentioned. The displacement due to viewing geometry still occurs, but the displacement is less.

Positioning for typhoon of CDO type

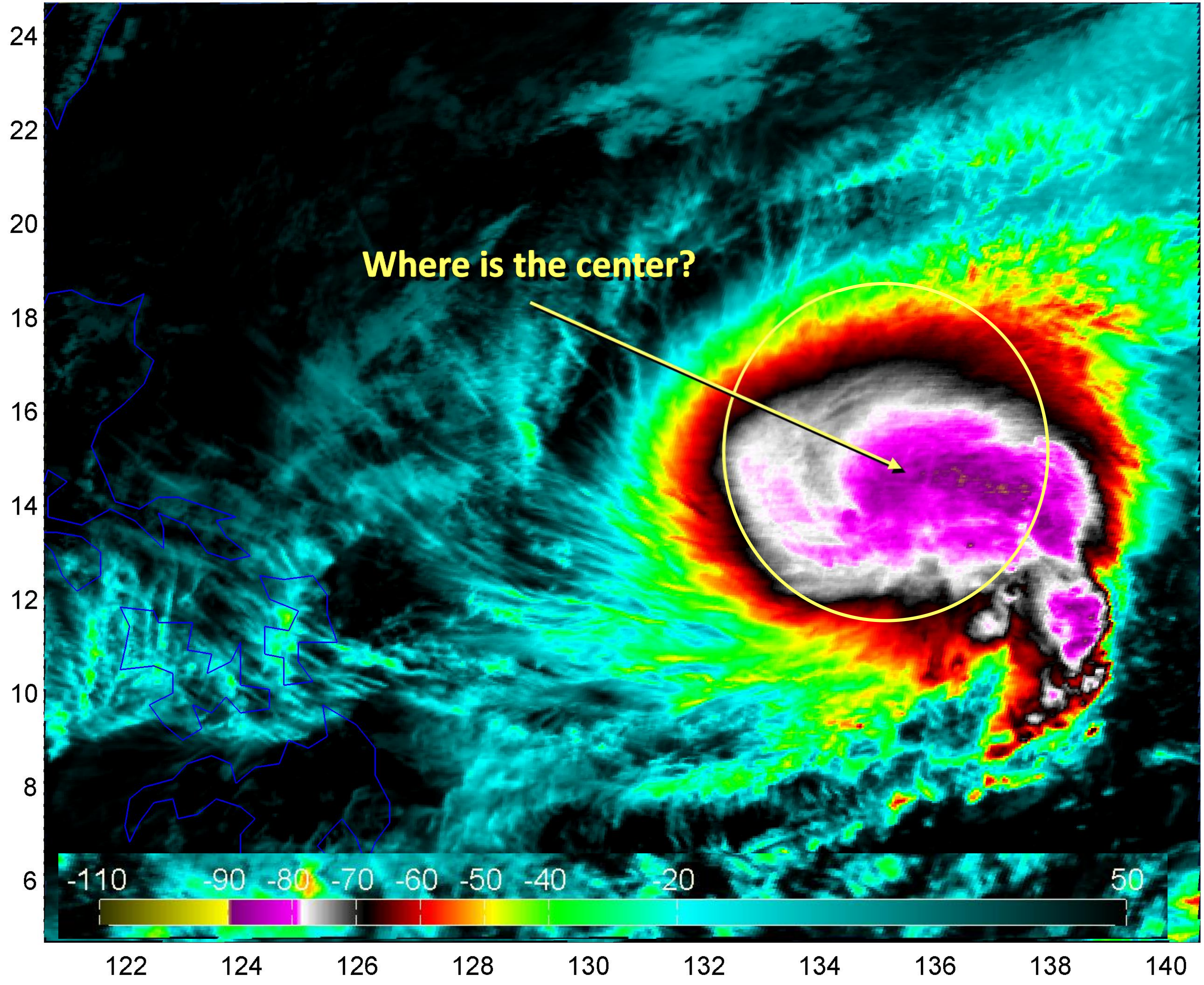

FY4 AGRI IR ch12 (11μm)

Positioning for typhoon of CDO type

FY3D MWRI 89H

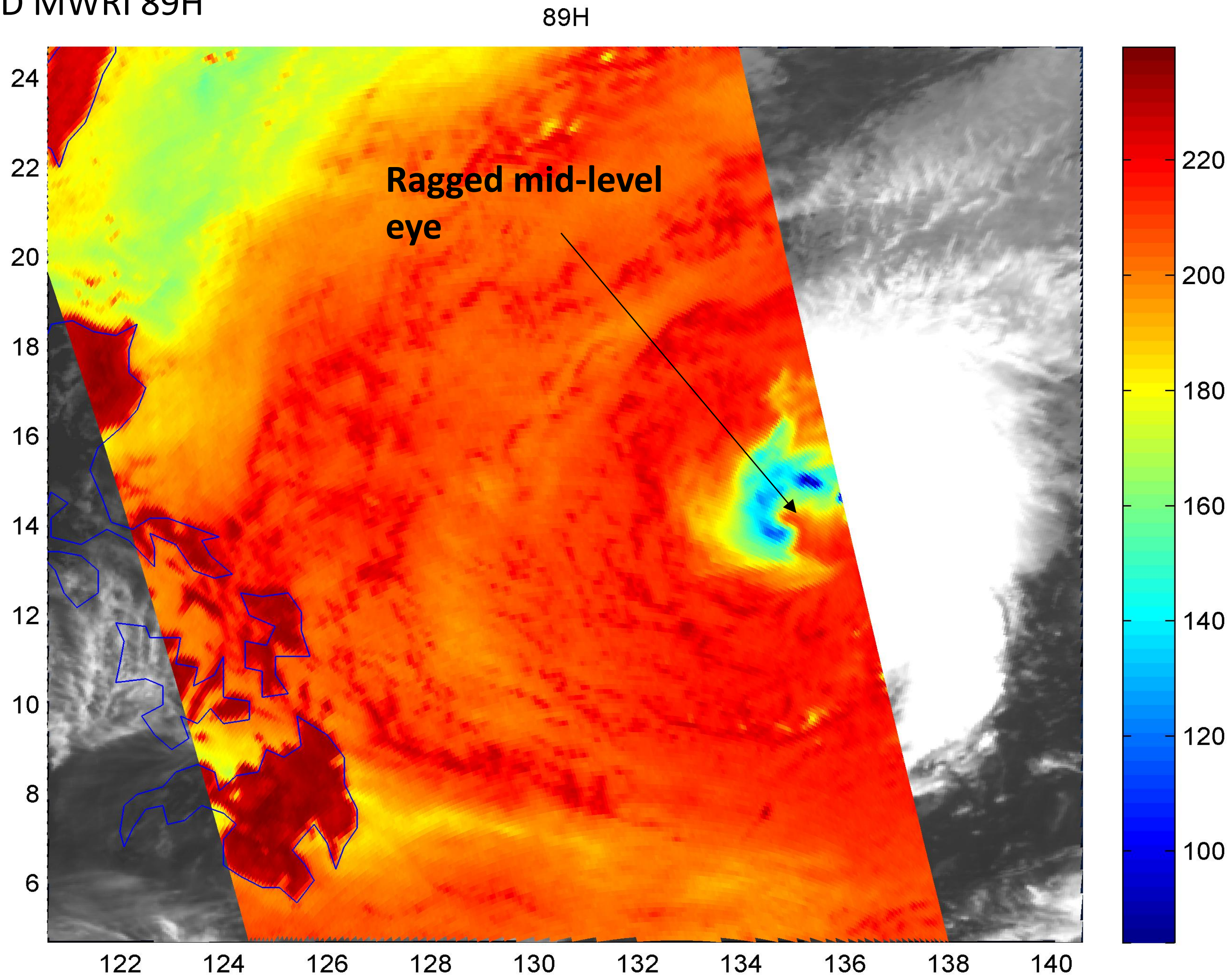

Positioning for typhoon of CDO type

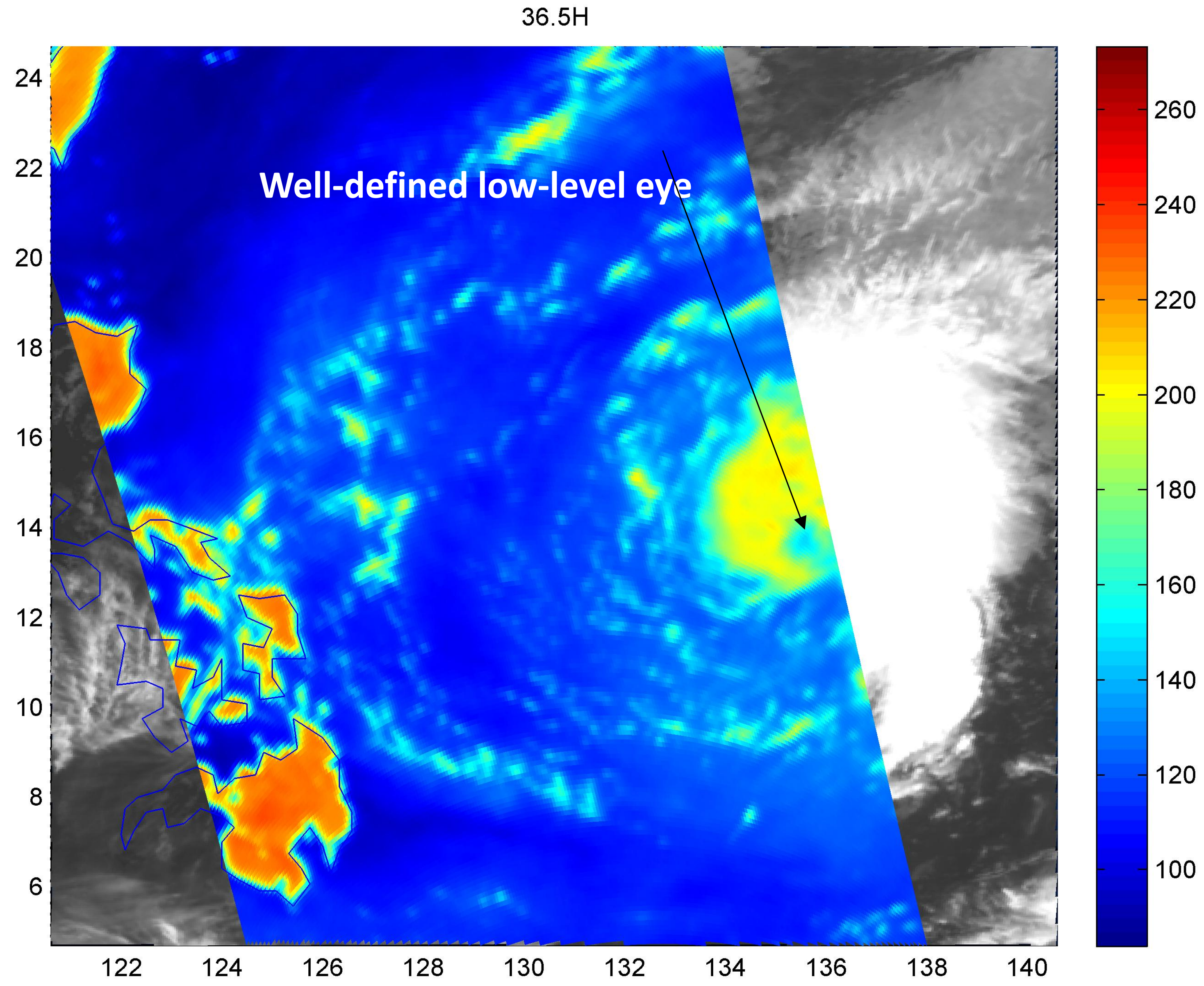

Positioning for typhoon of CDO type

Eye feature visible on both 36.5-GHZ composite

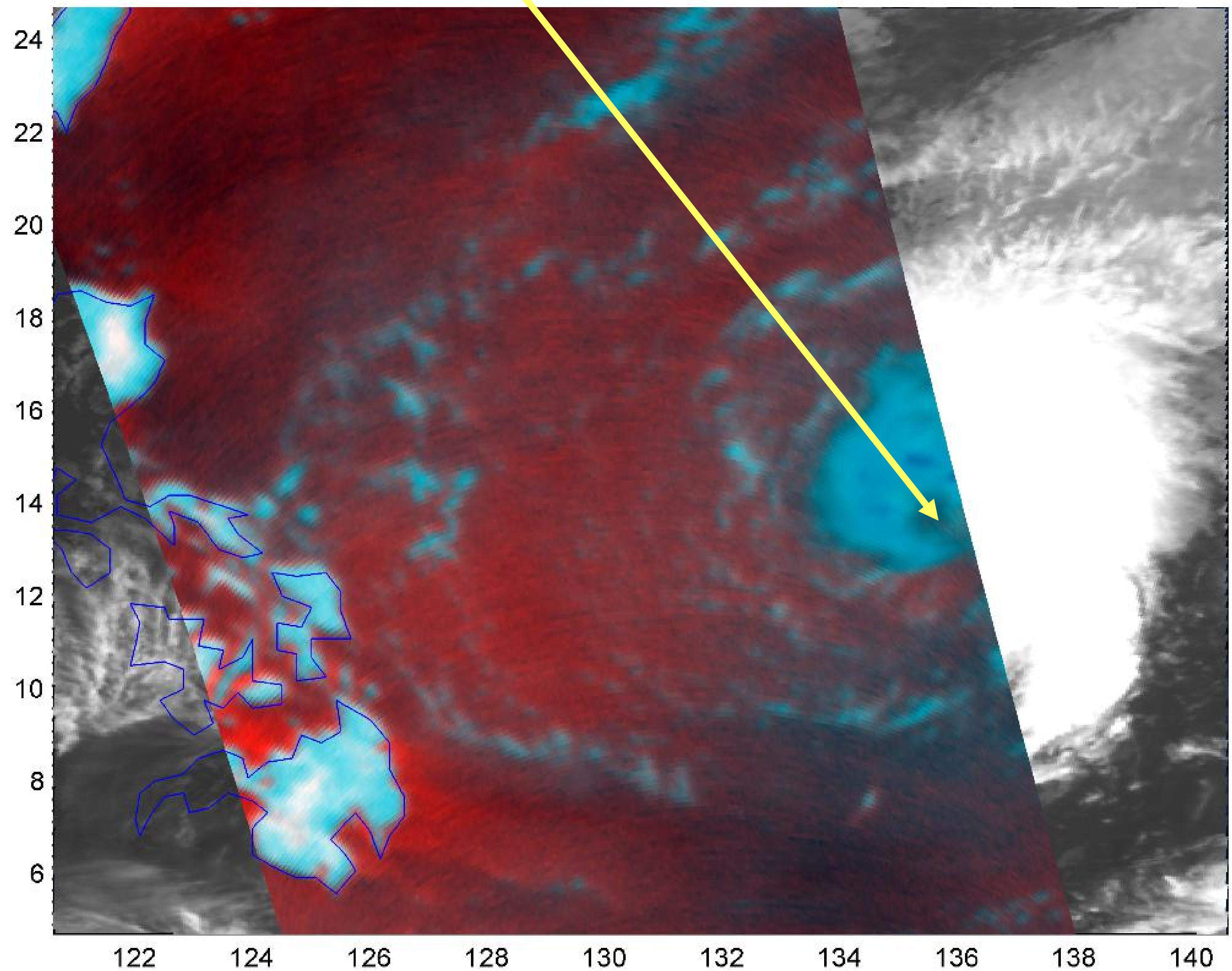

Positioning for CDO typhoon

Compared to the IR images, the circulations of typhoon can be shown clearly in microwave image

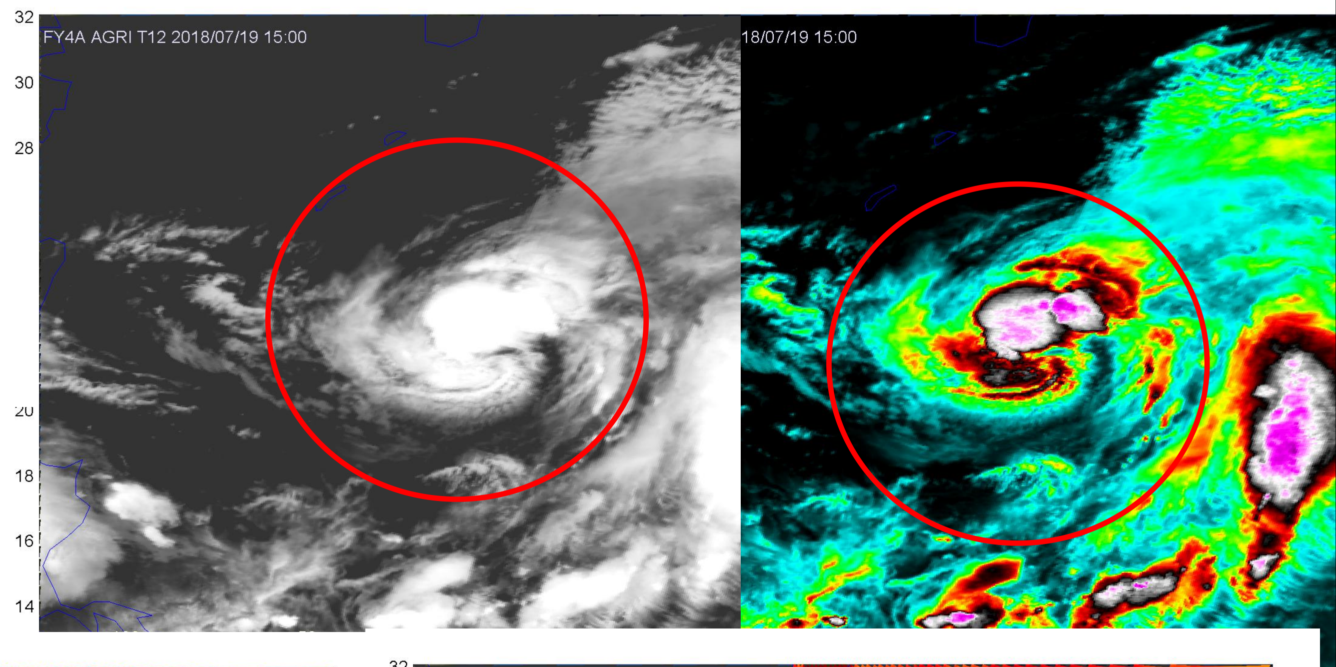

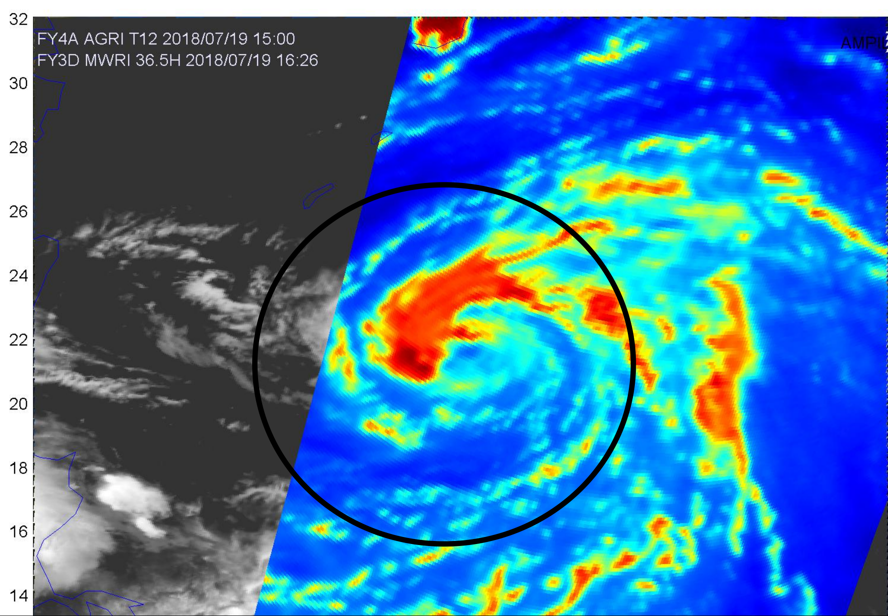

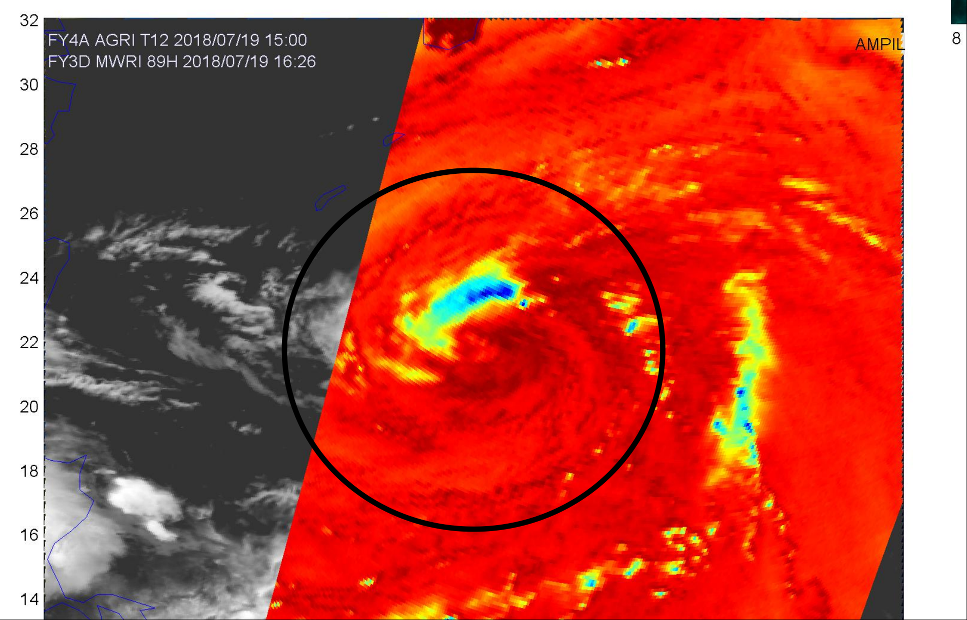

Positioning for weak typhoon
Look for eye in low level

Compared to the enhanced IR figure, the 36 GHz or 89 GHz can show the eye circulation very clear.

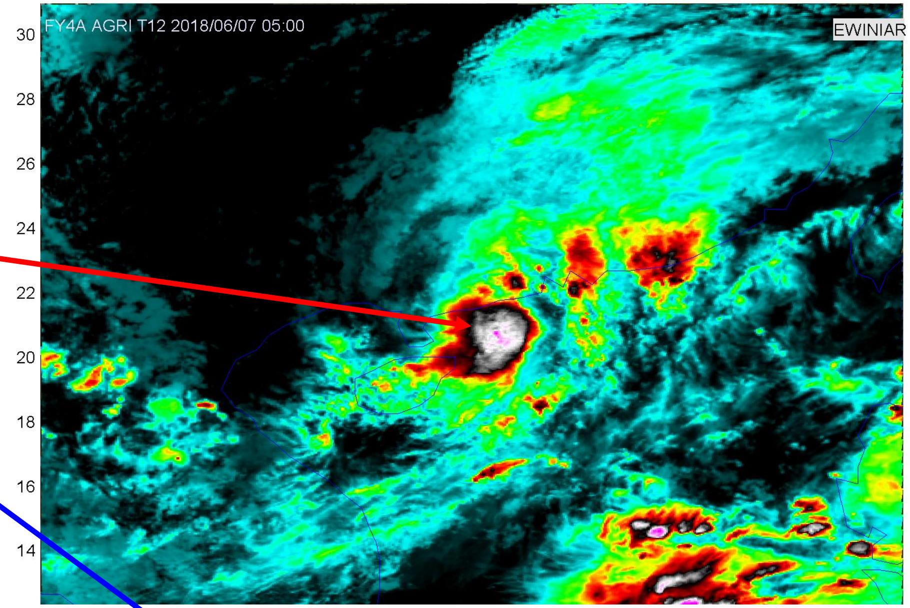

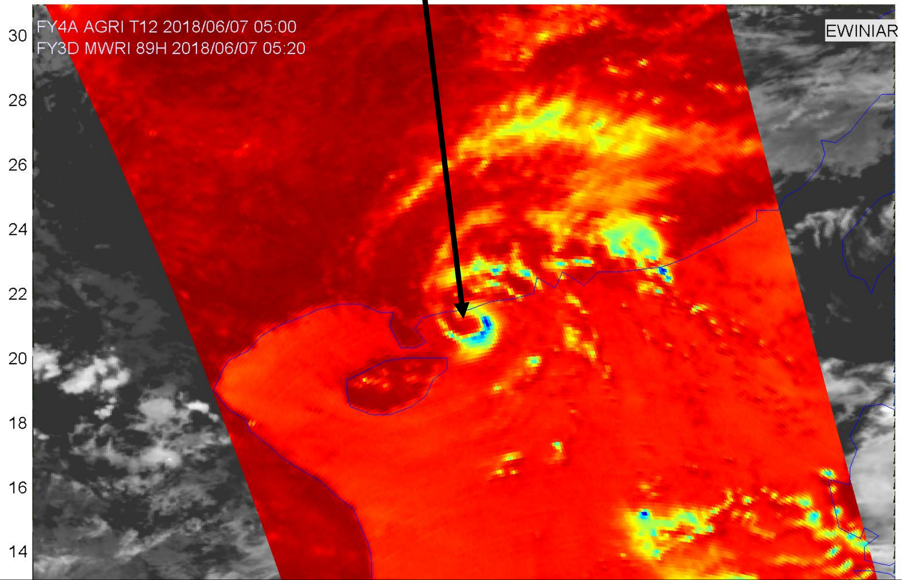

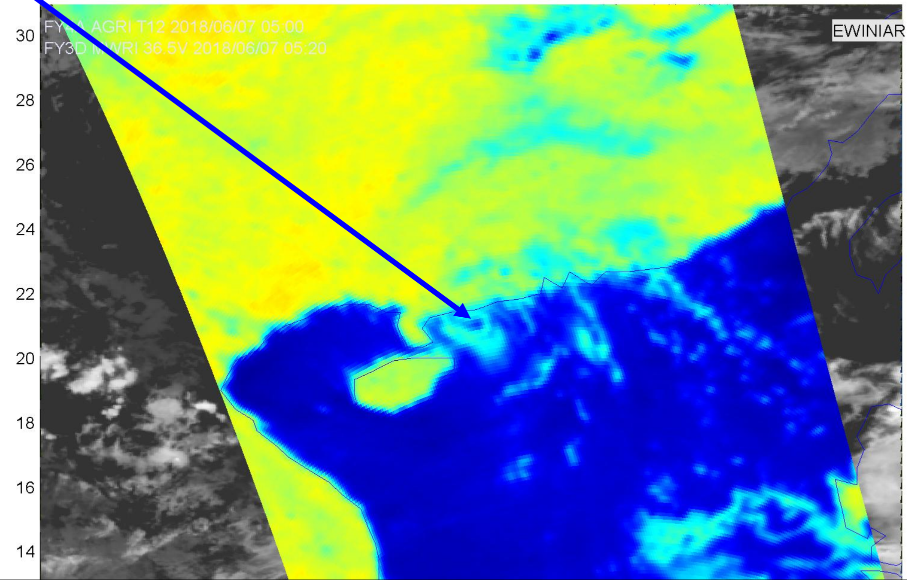

Positioning for weak typhoon

Look for convective free darker areas

Compared to the IR images, the circulations of typhoon can be shown clearly in microwave image

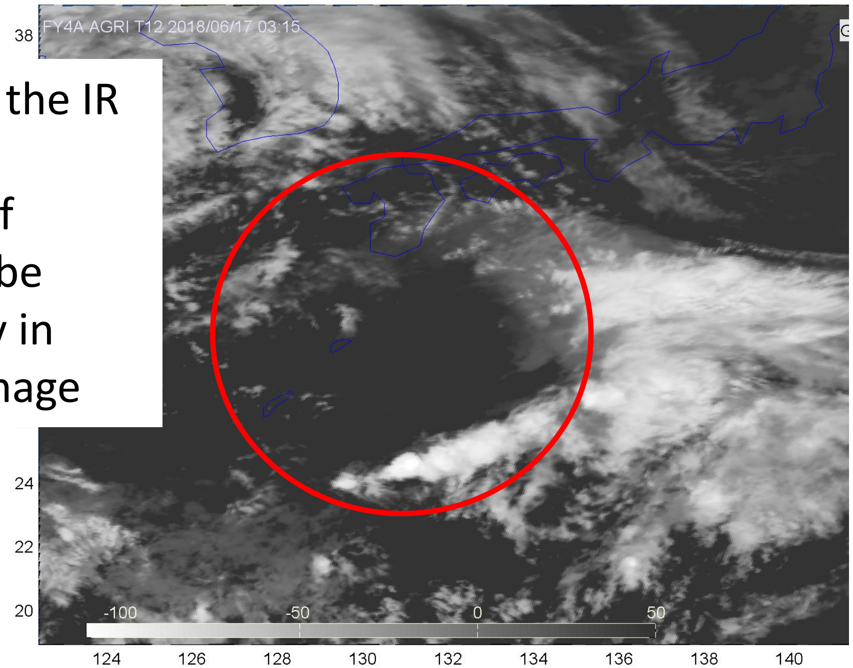

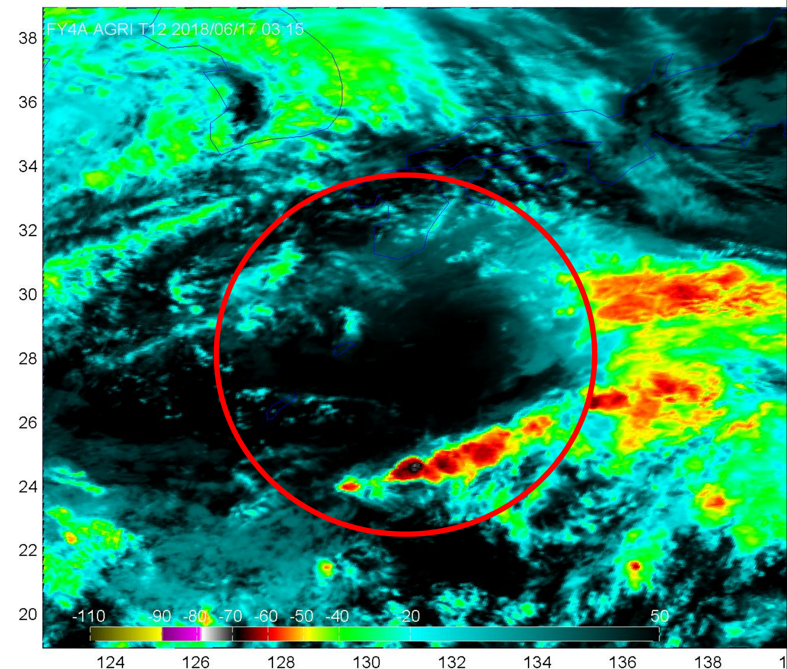

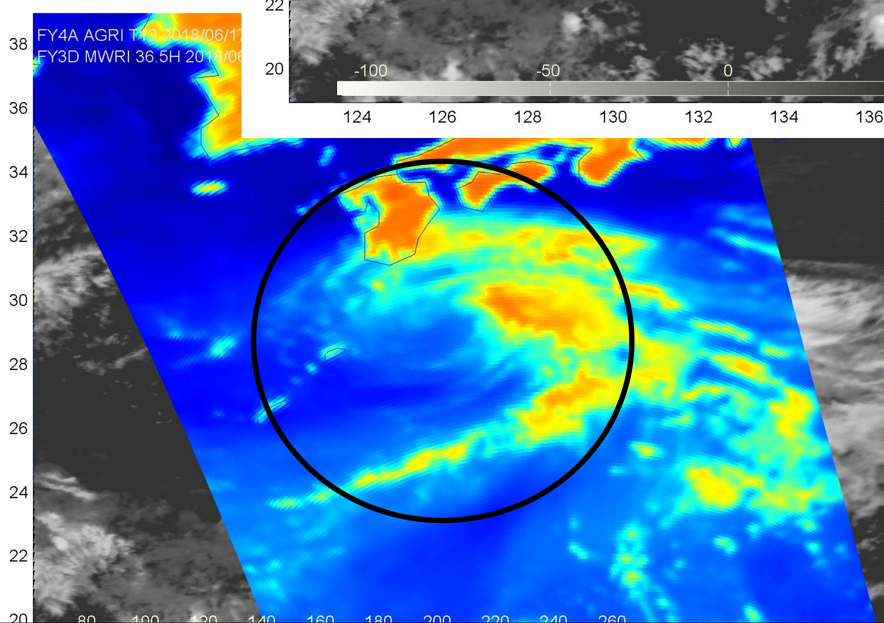

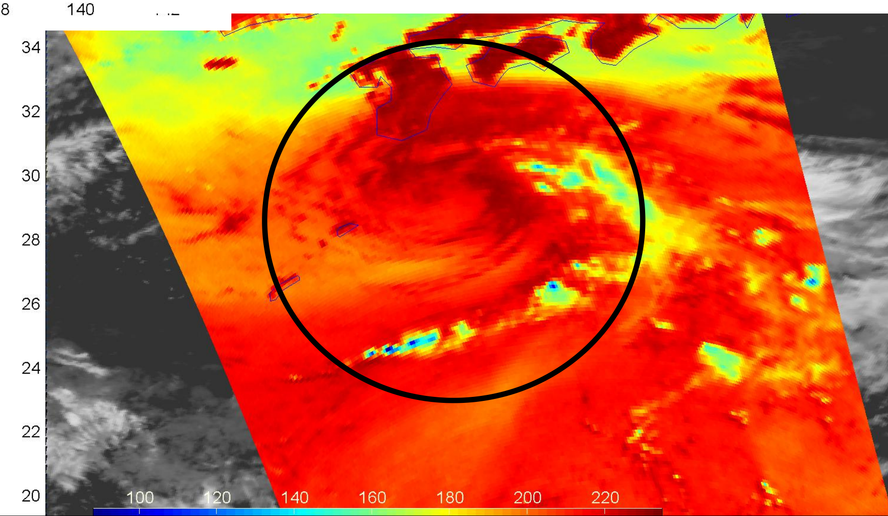

Positioning for weak typhoon
Look for low level circulation

Compared to the IR images, the circulations of typhoon can be shown clearly in microwave image

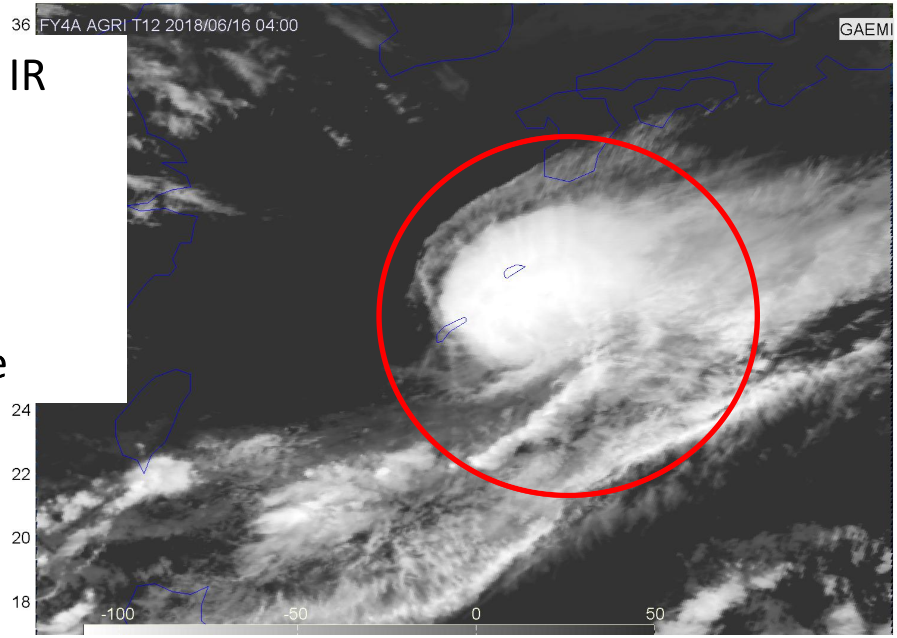

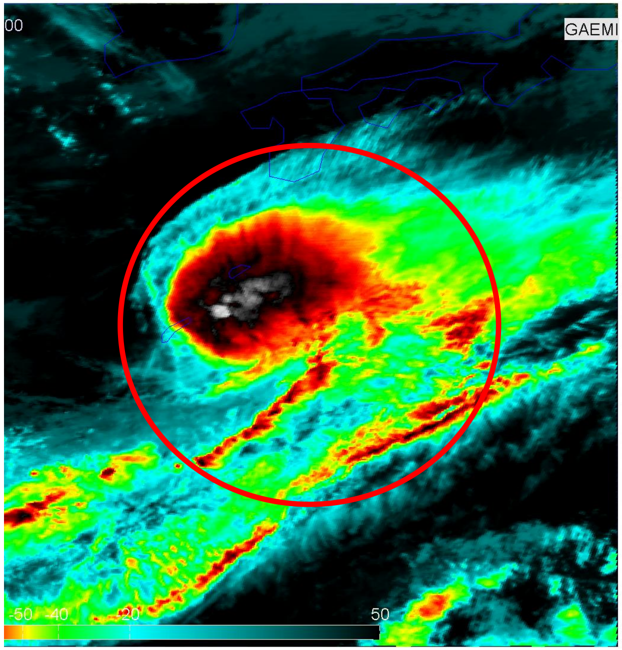

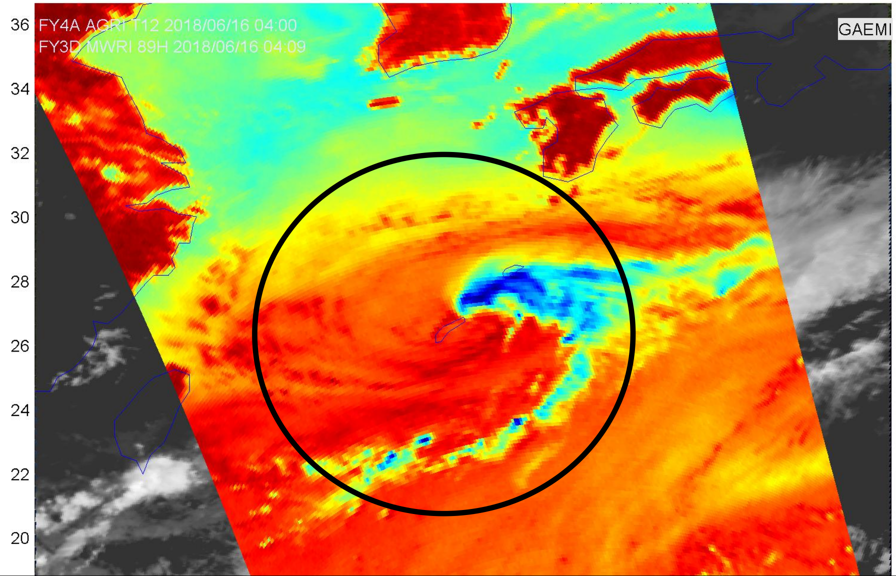

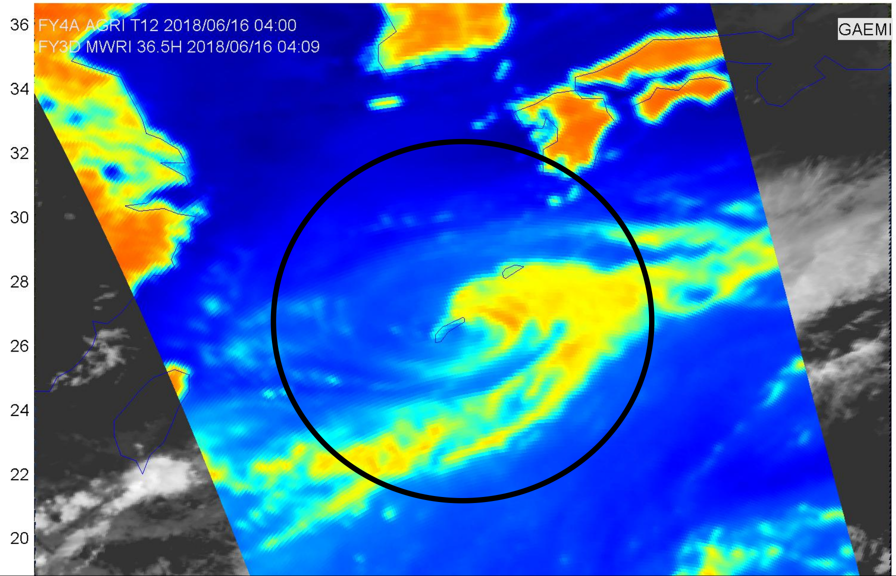

Positioning for weak typhoon
Look for low level circulation

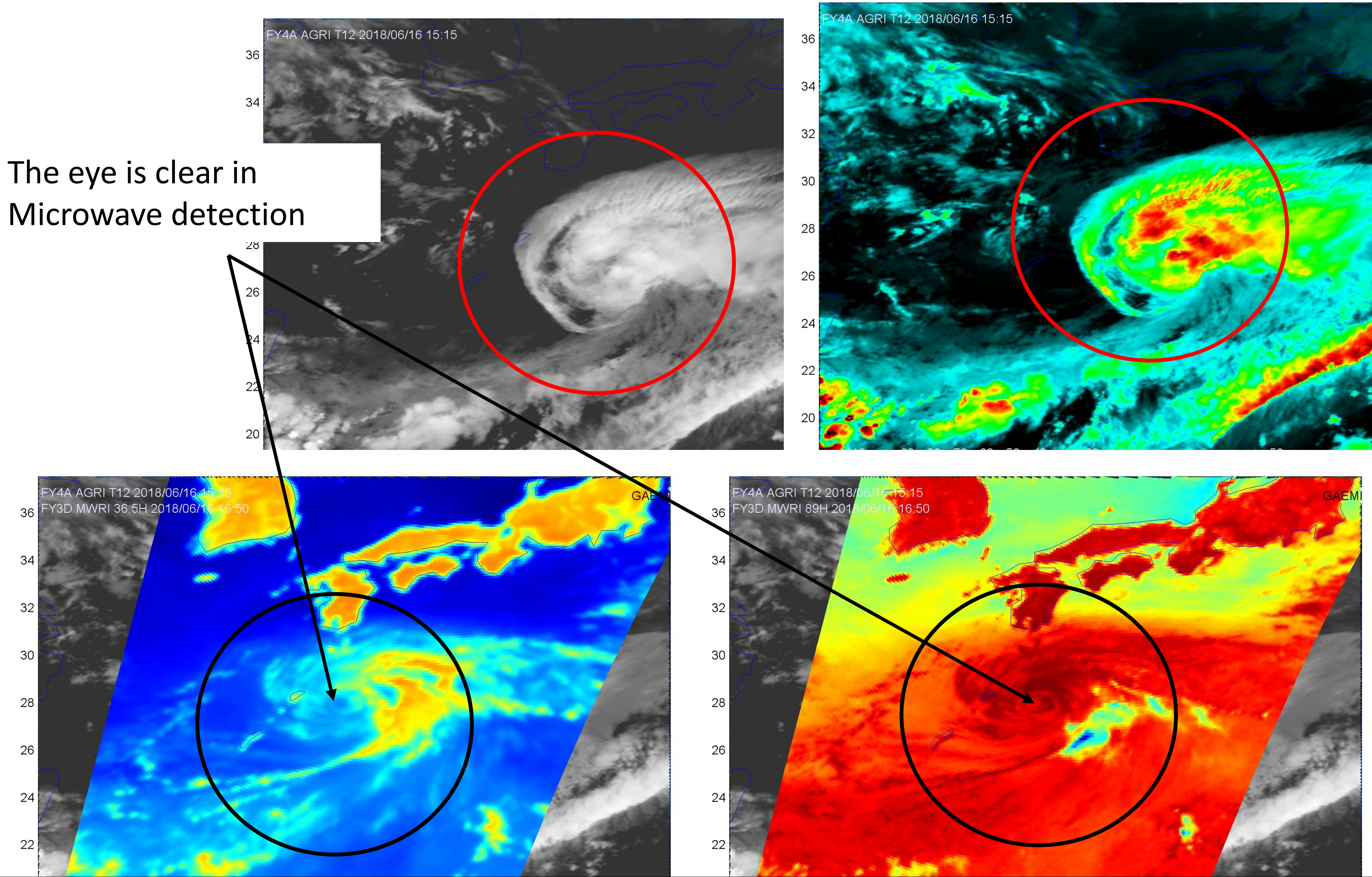

Differences of Position of typhoon between IR and MW

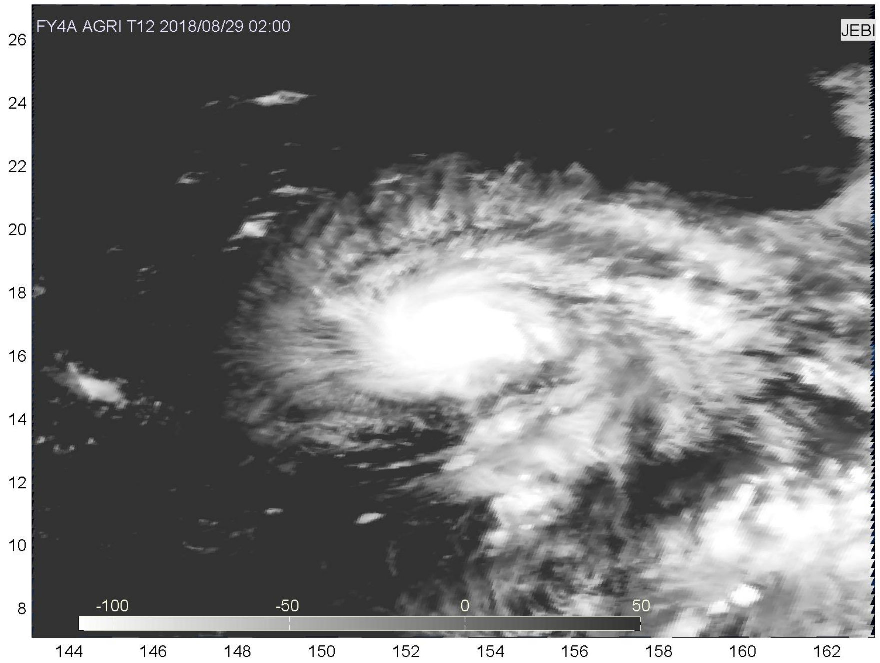

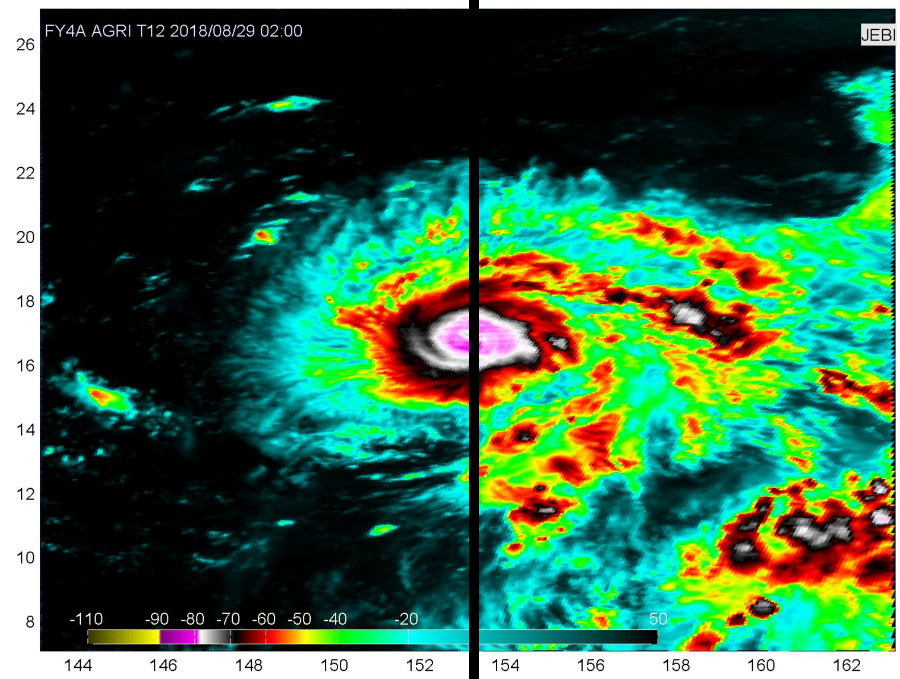

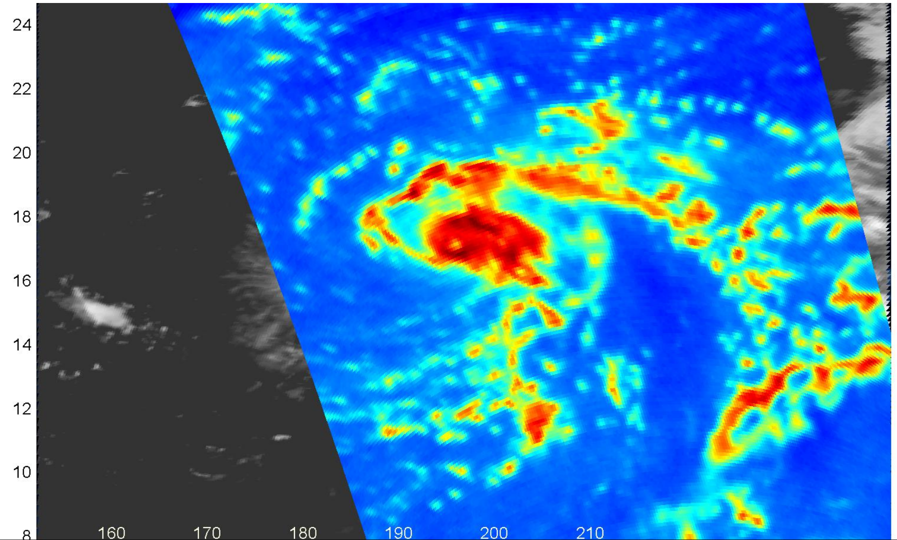

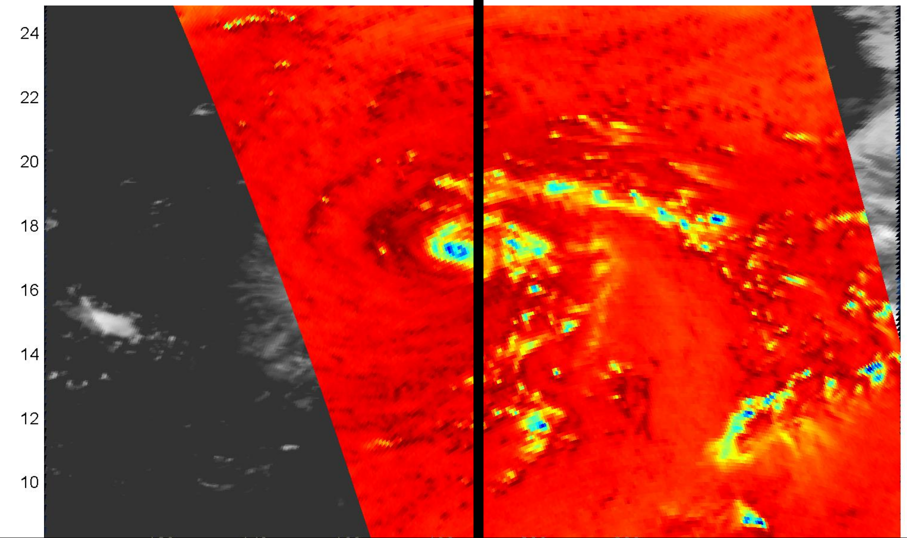

Differences of Position of typhoon between IR and MW

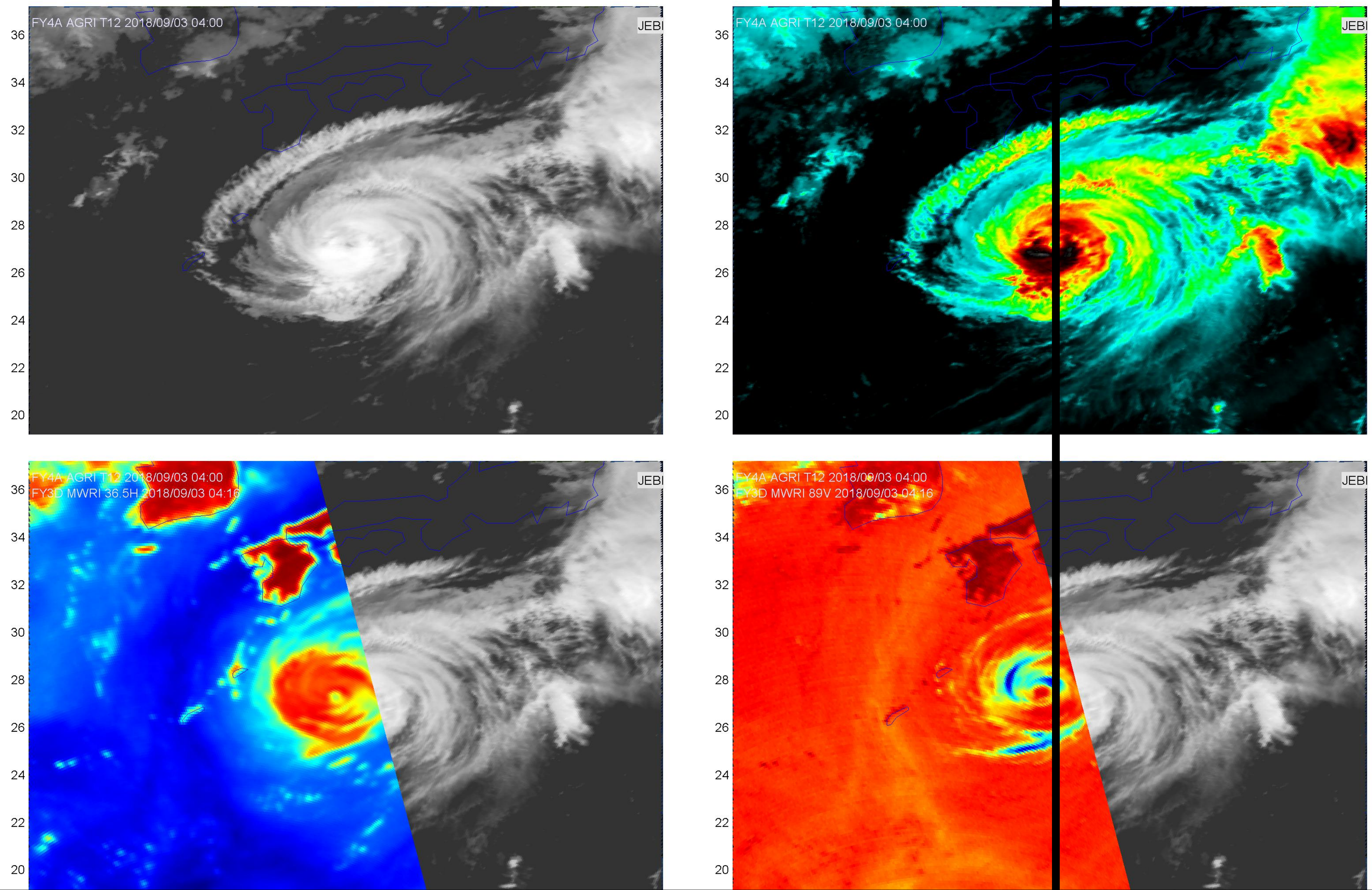

Morphed Integrated Microwave Imagery at CIMSS (MIMIC)

Aqua AMSR-E

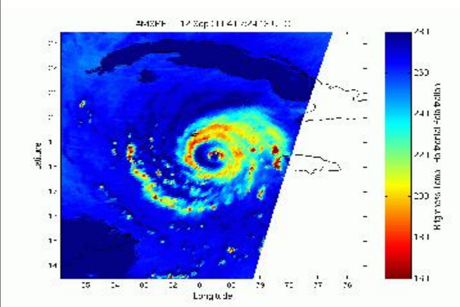

TRMM TMI

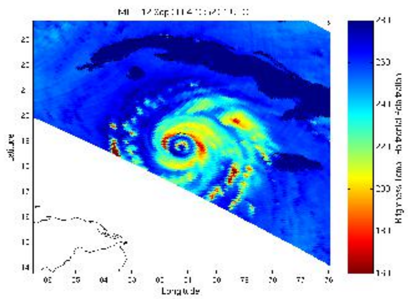

Five polar-orbiting satellites are used: DMSP-13/14/15， SSM/I (85 GHz channel)，TRMM TMI (89 GHz channel)，Aqua AMSR-E (85 GHz (A) channel)

DMSP-15 SSM/I

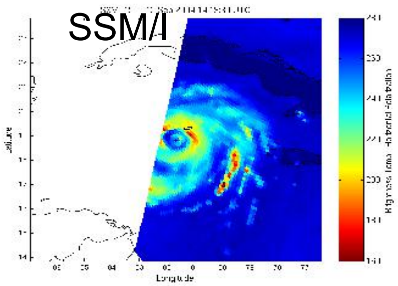

DMSP-13 SSM/I

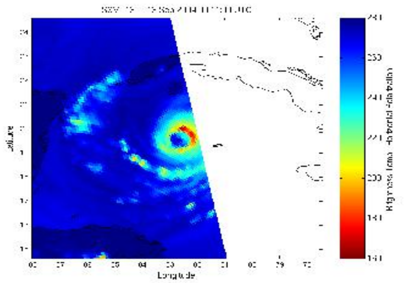

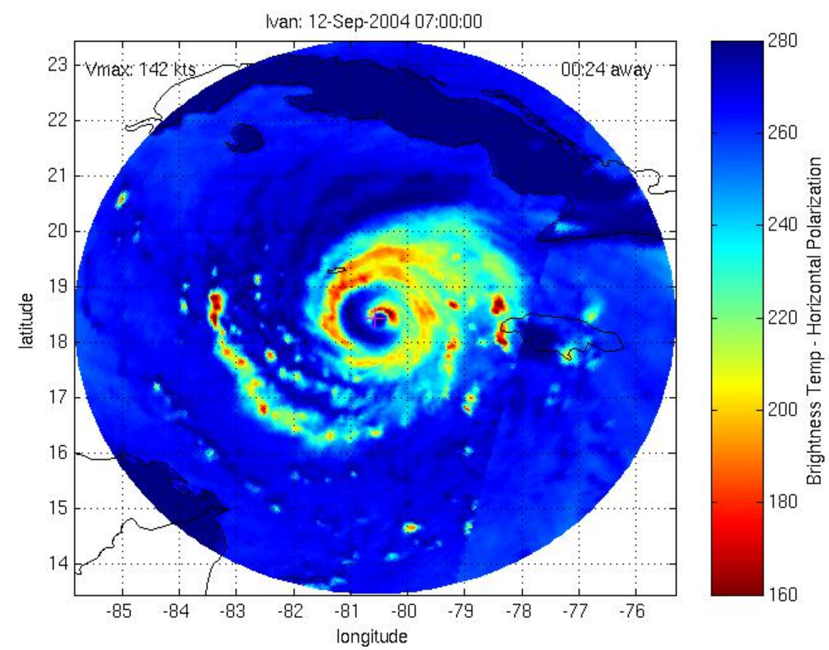

The observation interval is from 30 minutes to 25 hours. But a 15-minute interval simulation image can be obtained by integrated evolution techniques.

Microwave Imager Intensity Algorithm Based on SSMIS

Ritchie etal, 2014

$$SSMIS\_Vmax = 0.7*p\_anom + 2.0*max\_grad + 0.4*archer\_score + 37$$

- ✓ p_anom：SSMIS derived mean sea level pressure (MSLP) anomaly,
- ✓ max_grad：the maximum Tb gradient determined within 120km of the TC centre
- ✓ archer_score：the intensity score determined by ARCHER

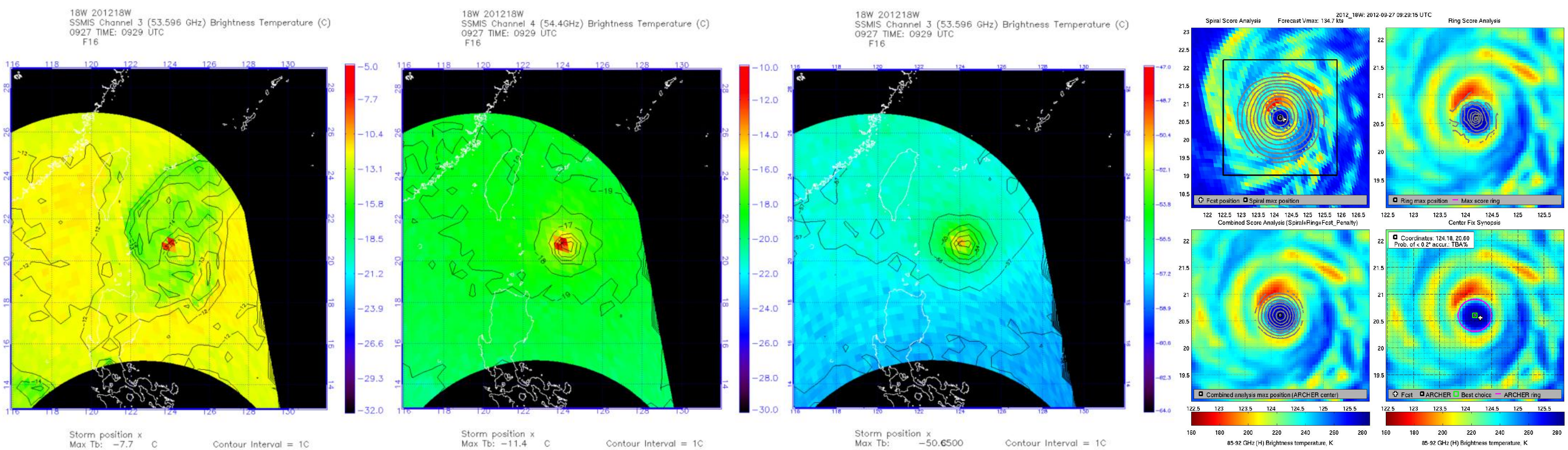

SSMIS channels 3, 4 and 5 show the TC warm core anomaly and ARCHER panel based on SSMIS 91GHz

JMA Objective Intensity Algorithm based on TRMM/TMI Brightness Temperature Distribution

- ✓ Cluster Analysis is performed for 19, 37 and 85 GHz Imagery
- ✓ Clusters are located either within a radial distance from the TC center or within quadrants aligned with the TC motion vector
- ✓ Regression analysis of the Tb associated with these clusters is then performed
- ✓ Some subjective re-classifying of the clusters is still

- ✓ JMA introduced this method in 2014 and further refinements of the method are expected.
- ✓ In future, it may be expanded to AMSR2 or GPM data

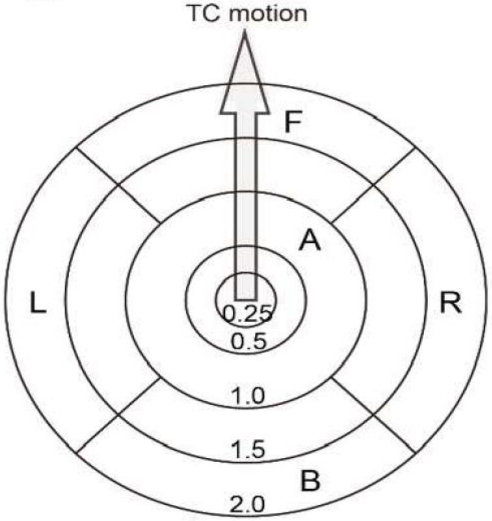

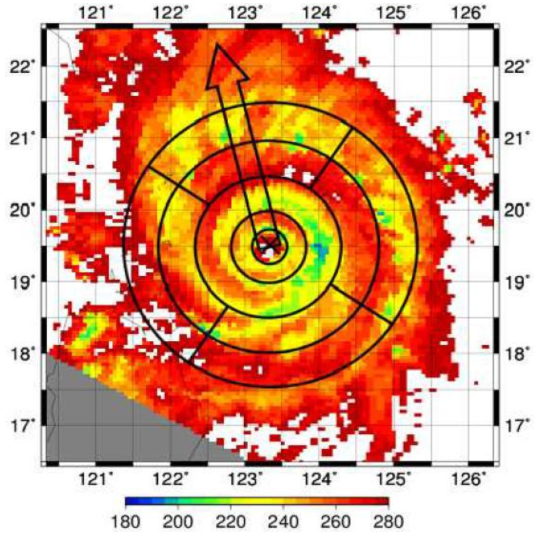

CIMSS SATellite CONsensus Method （SATCON）

- Members: CIMSS ADT, CIRA and CIMSS AMSU and CIMSS SSMIS algorithms
- Weighting each member according to the past statistical performance
- In future, S-NPP ATMS sounder

$$\text{SATCON} = \frac{W_1W_2\,(W_1+W_2)E_3 + W_1W_3\,(W_1+W_3)E_2 + W_3W_2\,(W_3+W_2)E_1}{W_1W_2\,(W_1+W_2) + W_1W_3\,(W_1+W_3) + W_3W_2\,(W_3+W_2)}$$

W_n = weight of method n E_n = estimate of method n

Final SATCON = 0.25*P-W_MSW + 0.75*SATCON_MSW

CIMSS SATCON Web

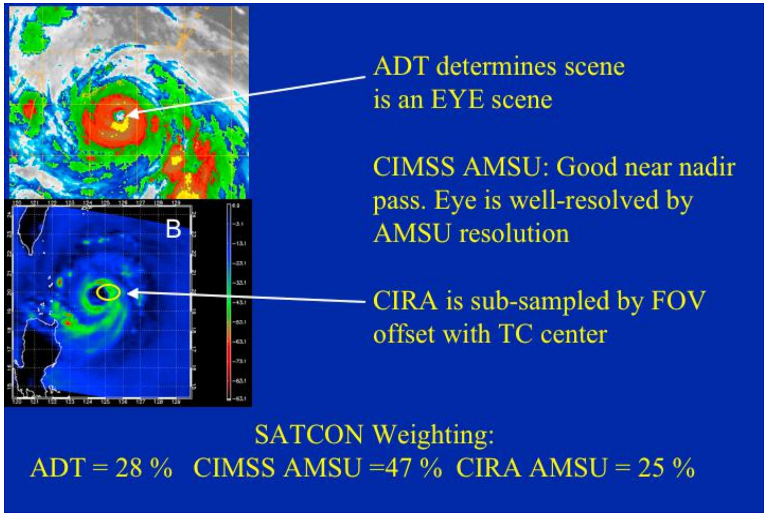

Summary for the MW imagery applications

- Improve position estimates for Dvorak intensity estimates
  - Helps locate center when obscured by clouds
  - Incorrect center location can yield incorrect intensity estimates, especially when using embedded center or shear pattern
- Monitoring internal TC structure
  - Eye formation
  - Eyewall replacement cycle

Atmospheric Sounder

Spectral continuity, higher spectral resolution, higher NEΔT

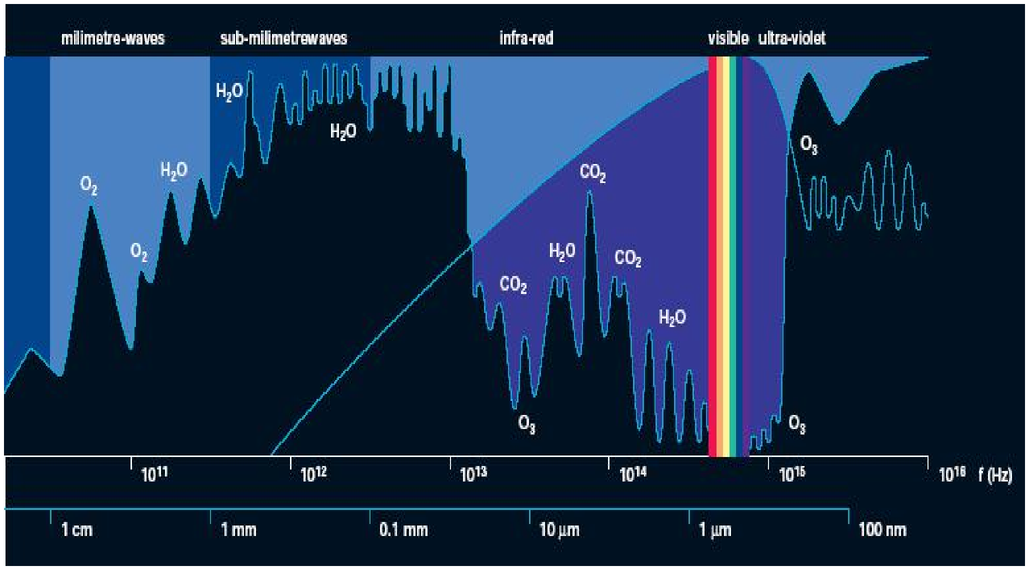

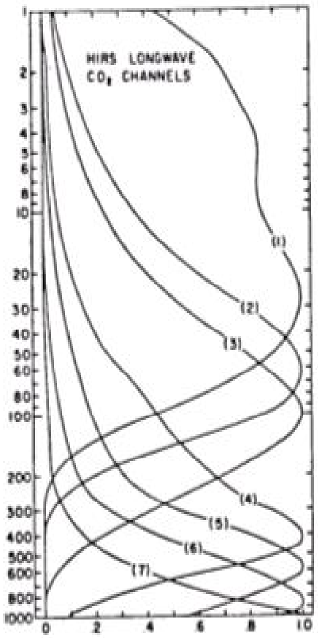

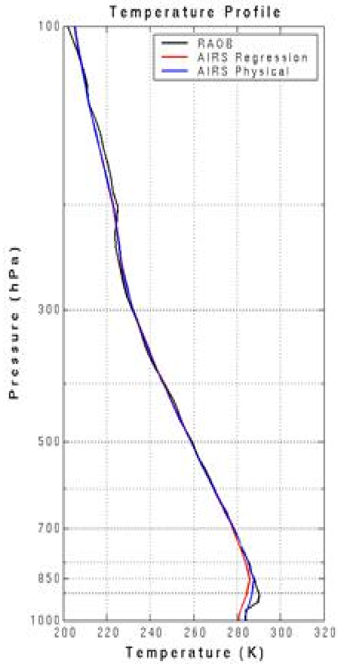

Spectrum → **Weighting Function** → **Atmospheric Profile**

Typical Products:

- Temperature Profile, Moisture Profile, Ozone amount
- Atmospheric Instabilities

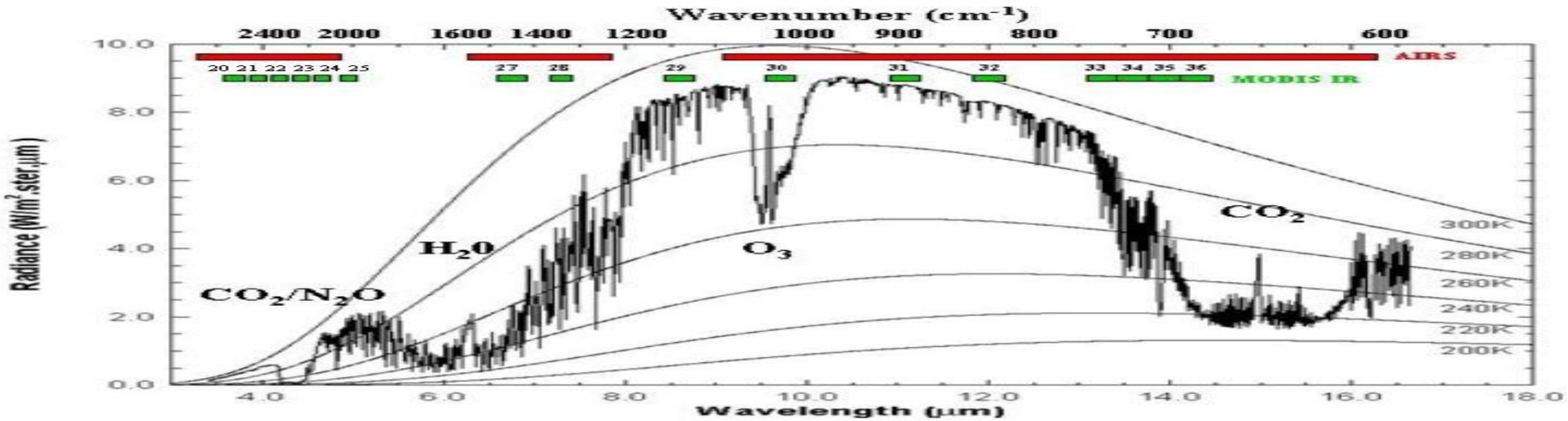

$$I(\tau,\mu) = I(\tau_1,\mu)e^{-(\tau_1-\tau)/\mu} + \int_{\tau}^{\tau_1} B[T(\tau')]e^{-(\tau'-\tau)/\mu}\frac{d\tau'}{\mu}$$

Infra-red: Sounding for clear sky

CO_2 for Temperature

H_2O for Moisture

MW: Sounding for cloudy sky

O_2 for Temperature

H_2O for Moisture

Atmospheric Sounder

红外分光计

Infrared Atmospheric Sounder

IRAS/FY-3

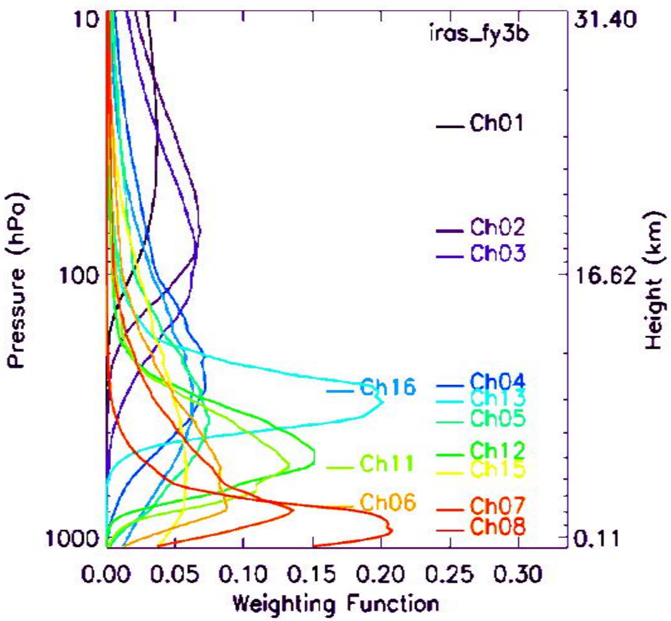

TABLE II
FY3B/IRAS CHANNEL CHARACTERISTICS

Channel (HIRS channel)	Central Wavenumber (cm^{-1})	Central Wavelengh (μm)	Half Power Bandwidth (cm^{-1})	Absorbing Gas	NEΔN ($mW/m^2.sr.cm^{-1}$)	EnergyPeakAltitude (hPa)
1 (1)	669	14.95	3	CO_2	4.00	30
2 (2)	680	14.71	10	CO_2	0.80	60
3 (3)	690	14.49	12	CO_2	0.60	100
4 (4)	703	14.22	16	CO_2	0.35	400
5 (5)	716	13.97	16	CO_2	0.32	600
6 (6)	733	13.84	16	CO_2/H_2O	0.36	800
7 (7)	749	13.35	16	CO_2/H_2O	0.30	900
8 (10)	802	12.47	30	Window	0.20	Surface
9 (8)	900	11.11	35	Window	0.15	Surface
10 (9)	1030	9.71	25	O_3	0.20	25
11	1345	7.43	50	H_2O	0.23	800
12 (11)	1365	7.33	40	H_2O	0.30	700
13 (12)	1533	6.52	55	H_2O	0.30	500
14 (13)	2188	4.57	23	N_2O	0.009	1000
15 (14)	2210	4.52	23	N_2O	0.007	950
16 (15)	2235	4.47	23	CO_2/N_2O	0.007	700
17 (16)	2245	4.45	23	CO_2/N_2O	0.007	400
18 (17)	2388	4.19	25	CO_2	0.007	700
19 (18)	2515	3.98	35	Window	0.007	Surface
20 (19)	2660	3.76	100	Window	0.003	Surface
21(20)	14500	0.69	1000	Window	0.10%A	Cloud
22	11299	0.885	385	Window	0.10%A	Surface
23	10638	0.94	550	H_2O	0.10%A	Surface
24	10638	0.94	200	H_2O	0.10%A	Surface
25	8065	1.24	650	H_2O	0.10%A	Surface
26	6098	1.64	450	H_2O	0.10%A	Surface

Atmospheric Sounder

微波温度计

MicroWave Temperature Sounder

MWTS/FY-3

Parameter	Specification
Scan Angle	±49.5°
Pixels Per Scan Line	90
Quantization	13 bits

15

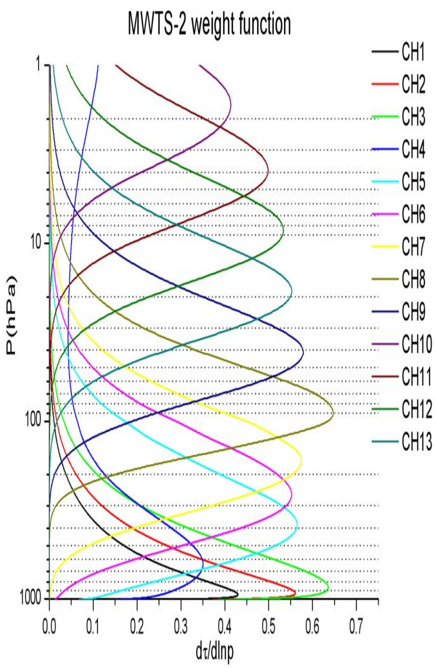

Ch No.	Central Frequency （GHz）	3dB Bandwidth （MHz）	NEΔT （K）	Main Beam Eff.	Dynamic Range （K）	Cal. Acc. （K）	Purpose
1	50. 3	180	1. 20	>90%	3～340	1. 5	Surface Emiss.
2	51. 76	400	0. 75	>90%	3～340	1. 5	Atmospheric Temperature Profile
3	52. 8	400	0. 75	>90%	3～340	1. 5	
4	53. 596	400	0. 75	>90%	3～340	1. 5	
5	54. 40	400	0. 75	>90%	3～340	1. 5	
6	54. 94	400	0. 75	>90%	3～340	1. 5	
7	55. 50	330	0. 75	>90%	3～340	1. 5	
8	57. 290344(fo)	330	0. 75	>90%	3～340	1. 5	
9	fo±0. 217	78	1. 20	>90%	3～340	1. 5	
10	fo±0. 3222±0. 048	36	1. 20	>90%	3～340	1. 5	
11	fo±0. 3222±0. 022	16	1. 70	>90%	3～340	1. 5	
12	fo±0. 3222±0. 010	8	2. 40	>90%	3～340	1. 5	
13	fo±0. 3222±0. 0045	3	3. 60	>90%	3～340	1. 5	

Atmospheric Sounder

微波湿度计

MicroWave Humidity Sounder

MWHS/FY-3

Parameter	Specification
Scan Angle	±53.35°
Pixels Per Scan Line	98
Quantization	14 bits

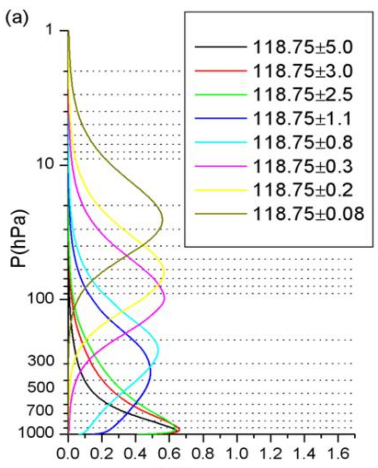

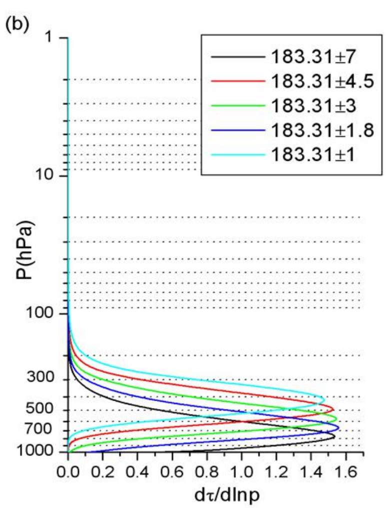

Ch No.	Central Frequency (GHz)	Polarization	Band width (MHz)	Freq. Stability (MHz)	Dynamic Range (K)	NE ΔT (K)	Cal. Acc. (K)	Main Beam Width	Main Beam Eff.	Purpose
1	89.0	V	1500	50	3—340	1.0	1.3	2.0°	>92%	Surface and Precipitation
2	118.75±0.08	H	20	30	3—340	3.6	2.0	2.0°	>92%	Atmospheric Temperature Profile
3	118.75±0.2	H	100	30	3—340	2.0	2.0	2.0°	>92%	
4	118.75±0.3	H	165	30	3—340	1.6	2.0	2.0°	>92%	
5	118.75±0.8	H	200	30	3—340	1.6	2.0	2.0°	>92%	
6	118.75±1.1	H	200	30	3—340	1.6	2.0	2.0°	>92%	
7	118.75±2.5	H	200	30	3—340	1.6	2.0	2.0°	>92%	
8	118.75±3.0	H	1000	30	3—340	1.0	2.0	2.0°	>92%	
9	118.75±5.0	H	2000	30	3—340	1.0	2.0	2.0°	>92%	
10	150.0	V	1500	50	3—340	1.0	1.3	1.1°	>95%	Surface and Precipitation
11	183.31±1	H	500	30	3—340	1.0	1.3	1.1°	>95%	Atmospheric Moisture Profile
12	183.31±1.8	H	700	30	3—340	1.0	1.3	1.1°	>95%	
13	183.31±3	H	1000	30	3—340	1.0	1.3	1.1°	>95%	
14	183.31±4.5	H	2000	30	3—340	1.0	1.3	1.1°	>95%	
15	183.31±7	H	2000	30	3—340	1.0	1.3	1.1°	>95%	

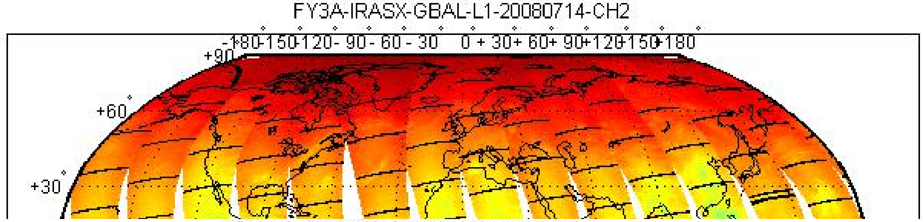

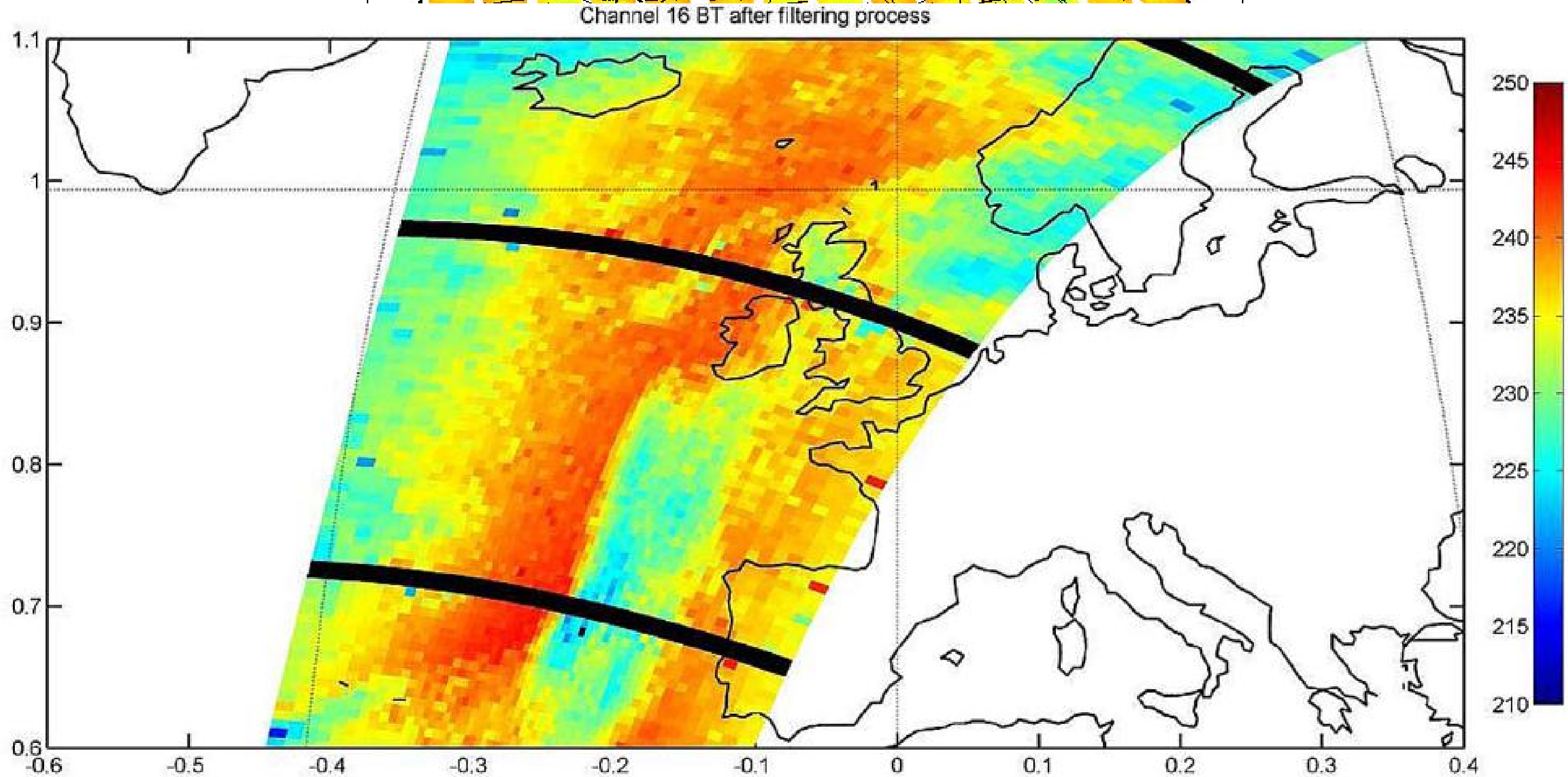

Global Mosaicing Image from Ascending Orbit of MWTS Ch. 1

Global Mosaicing Image from Ascending Orbit of MWHS Ch. 1

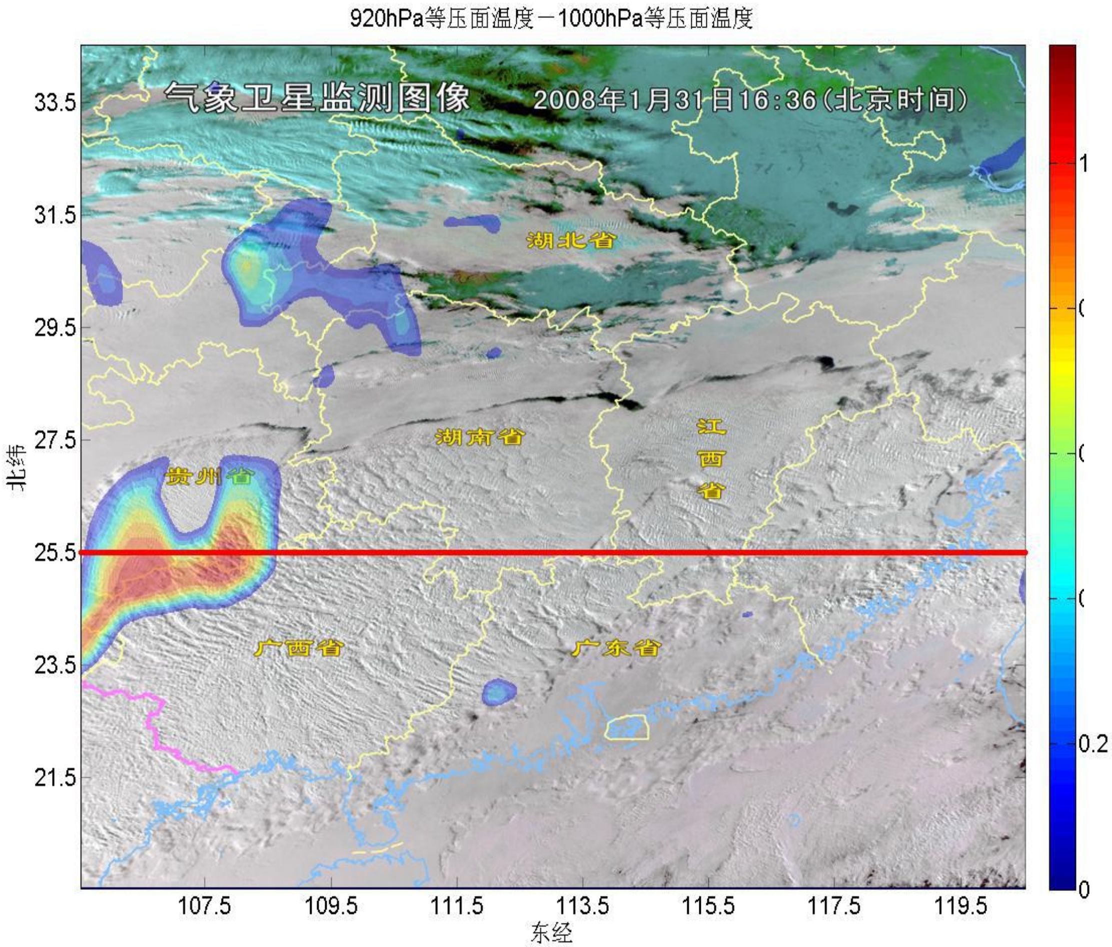

Temperature inversion layer (31 Jan,2008)

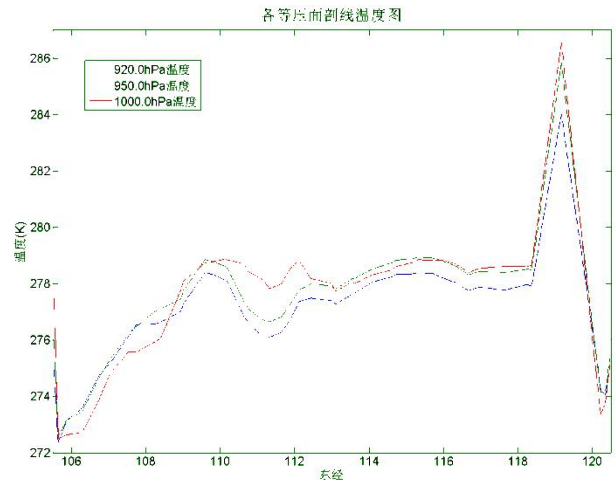

Temperature in 3 layers along the red track

Radiometric characteristics of the AMSU-A

Channel Number	Frequency (GHz)	Polarization (at nadir)	Number of Bands	Instrument Sensitivity NEDT (K)	Primary Function
1	23.8	vertical	1	0.30	Water Vapor Burden
2	31.4	vertical	1	0.30	Water Vapor Burden
3	50.3	vertical	1	0.40	Water Vapor Burden
4	52.8	vertical	1	0.25	Water Vapor Burden
5	53.596 ± 0.115	horizontal	2	0.25	Tropospheric Temperature
6	54.4	horizontal	1	0.25	Tropospheric Temperature
7	54.94	vertical	1	0.25	Tropospheric Temperature
8	55.5	horizontal	1	0.25	Tropospheric Temperature
9	57.290	horizontal	1	0.25	Stratospheric Temperature
10	57.290 ± 0.217	horizontal	2	0.40	Stratospheric Temperature
11	57.290 ± 0.3222 ± 0.048	horizontal	4	0.40	Stratospheric Temperature
12	57.290 ± 0.3222 ± 0.022	horizontal	4	0.60	Stratospheric Temperature
13	57.290 ± 0.3222 ± 0.010	horizontal	4	0.80	Stratospheric Temperature
14	57.290 ± 0.3222 ± 0.0045	horizontal	4	1.20	Stratospheric Temperature
15	89.0	vertical	1	0.50	Cloud Top/Snow

Radiometric characteristics of the AMSU-B

Channel Number	Frequency (GHz)	Polarization (at nadir)	Number of bands	Instrument Sensitivity NEDT (K)
16	89.9 ± 0.9	vertical	2	0.37
17	150 ± 0.9	vertical	2	0.84
18	183.31 ± 1.00	vertical	2	1.06
19	183.31 ± 3.00	vertical	2	0.70
20	183.31 ± 7.00	vertical	2	0.60

Microwave sounder used for typhoon positioning

Microwave sounder can not only detect vertical profiles of atmospheric temperature and humidity, but it also has the unique ability to penetrate through heavy cloud layers, except for precipitation clouds, and it can detect the inner structure of typhoons.

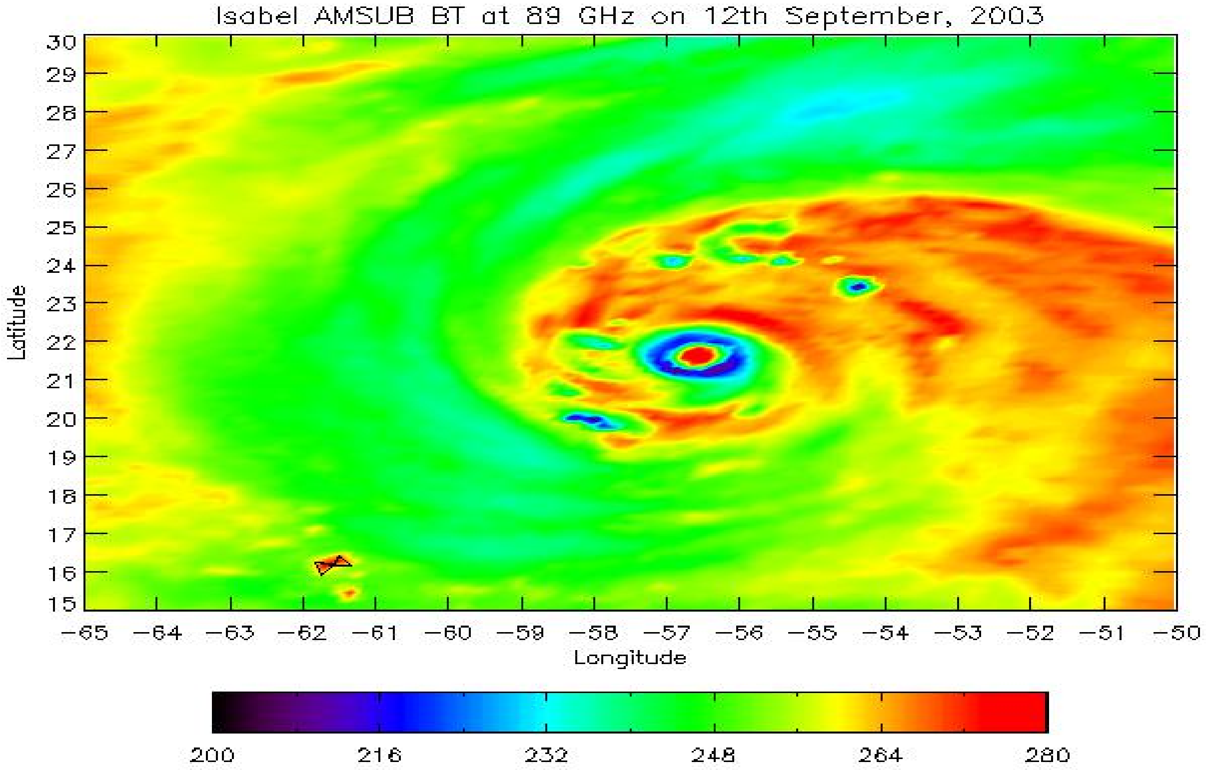

AMSU-B data estimate the center of weak tropical cyclones

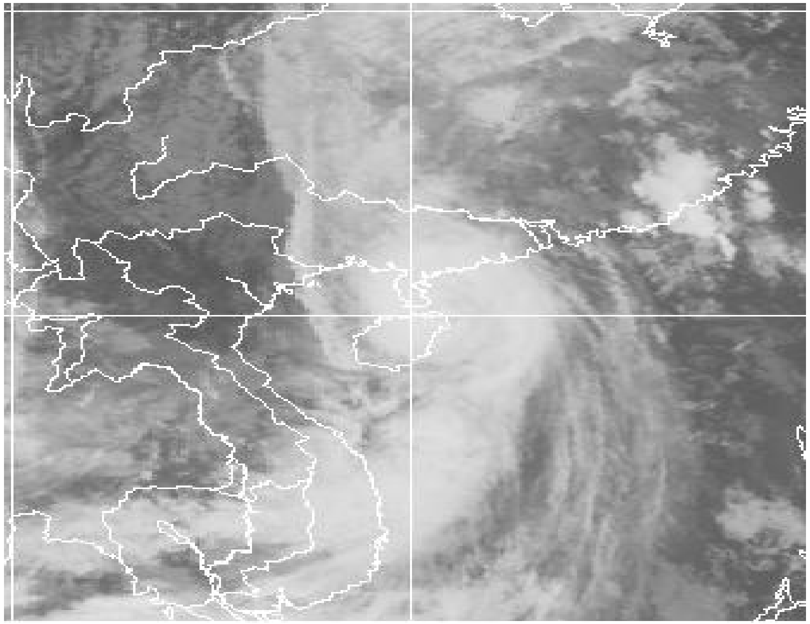

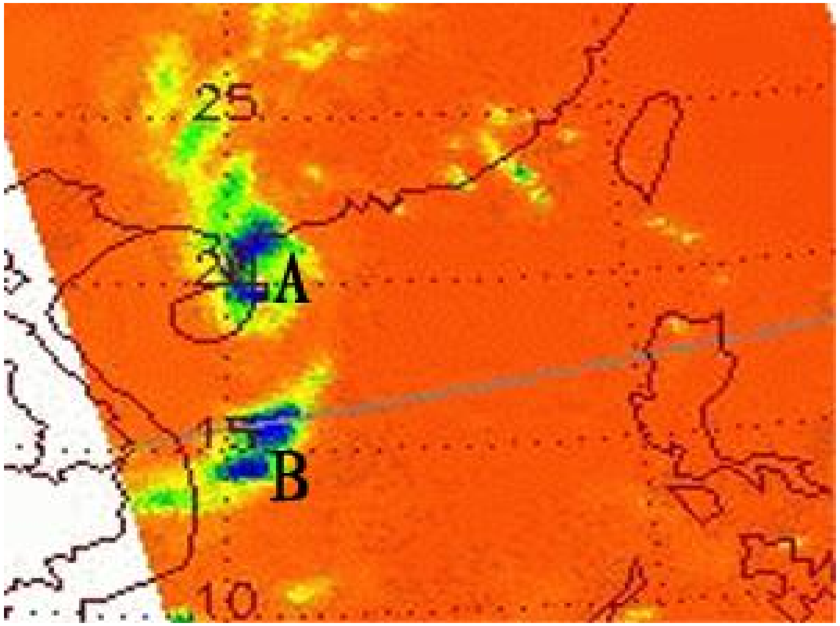

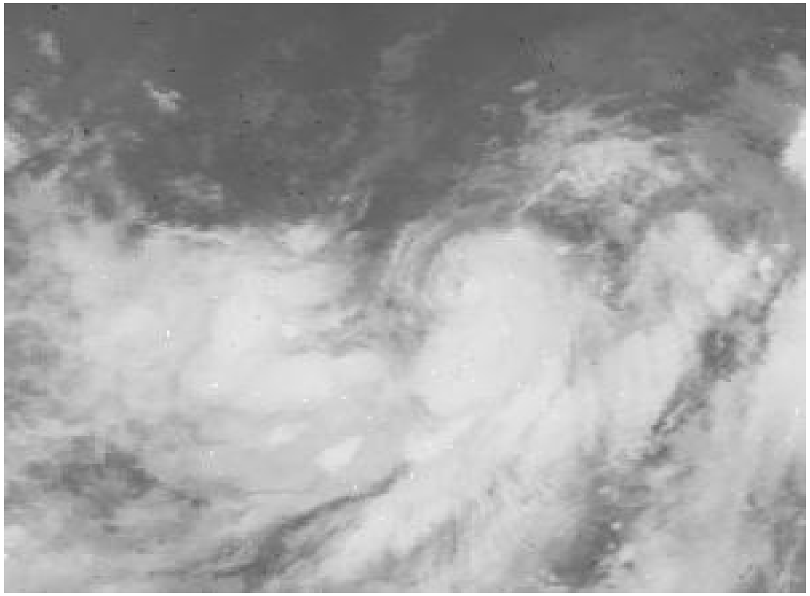

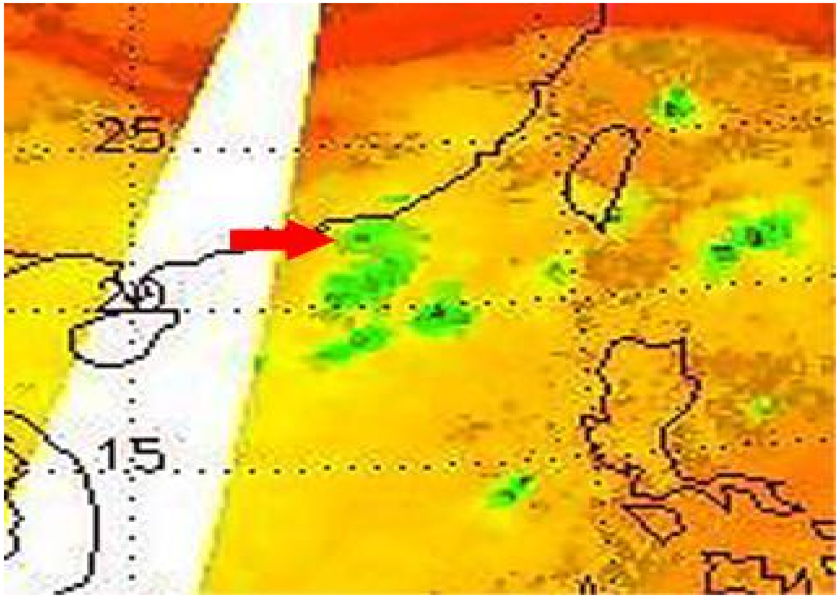

Precipitation Estimation

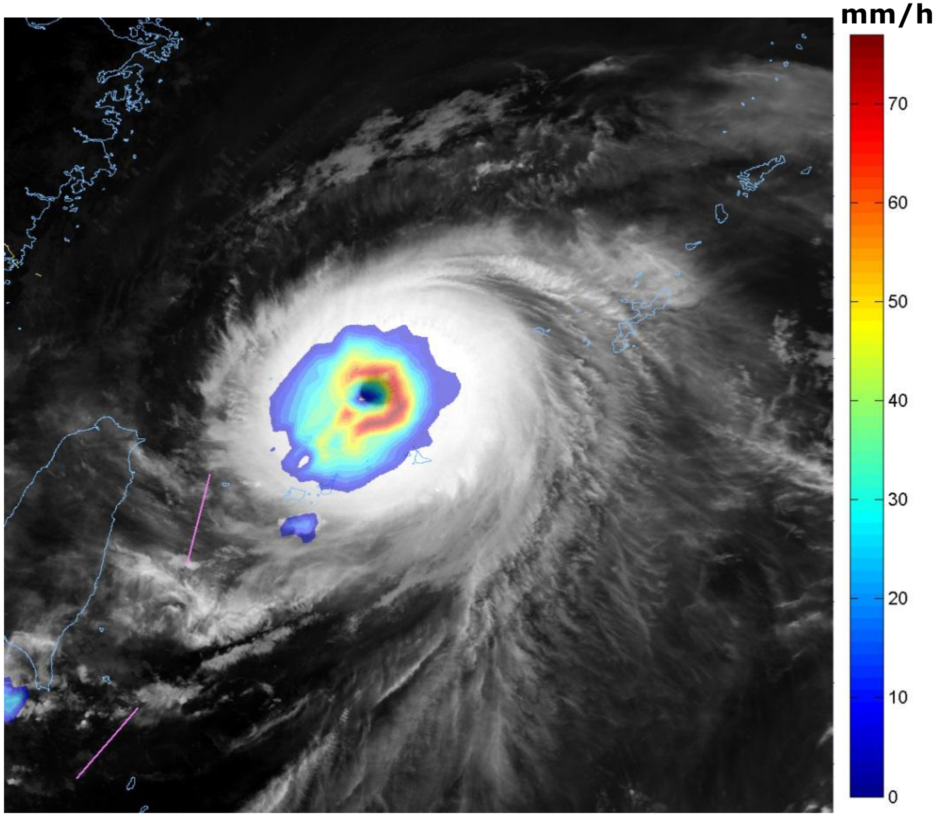

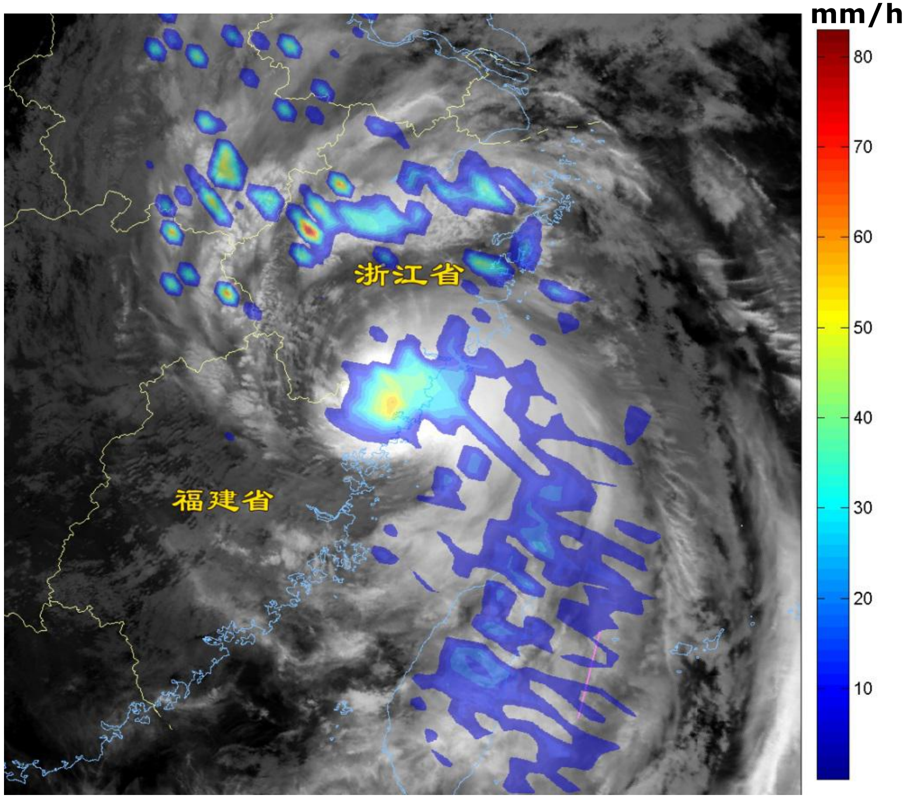

These two figures is the microwave precipitation estimation with background of infrared image. The left figure shows the symmetric typhoon circulation with regular precipitation distribution around the typhoon center, while the right image shows another typhoon with comma circulation and precipitation distribution.

Application of Microwave Thermometer Data in Analysis of Tropical Cyclone Heat Structure

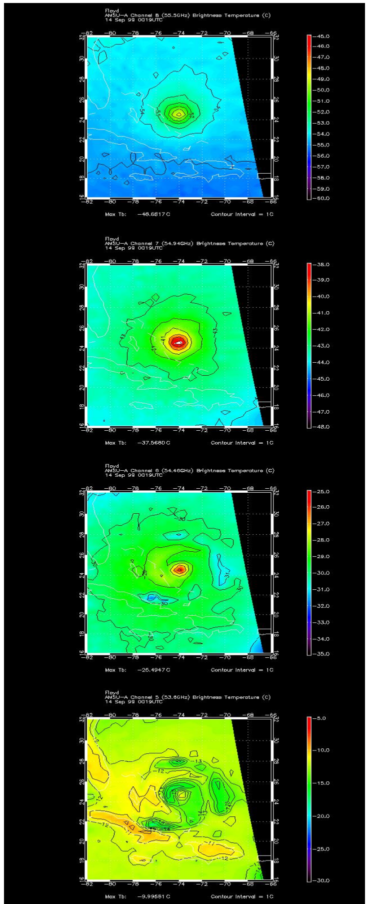

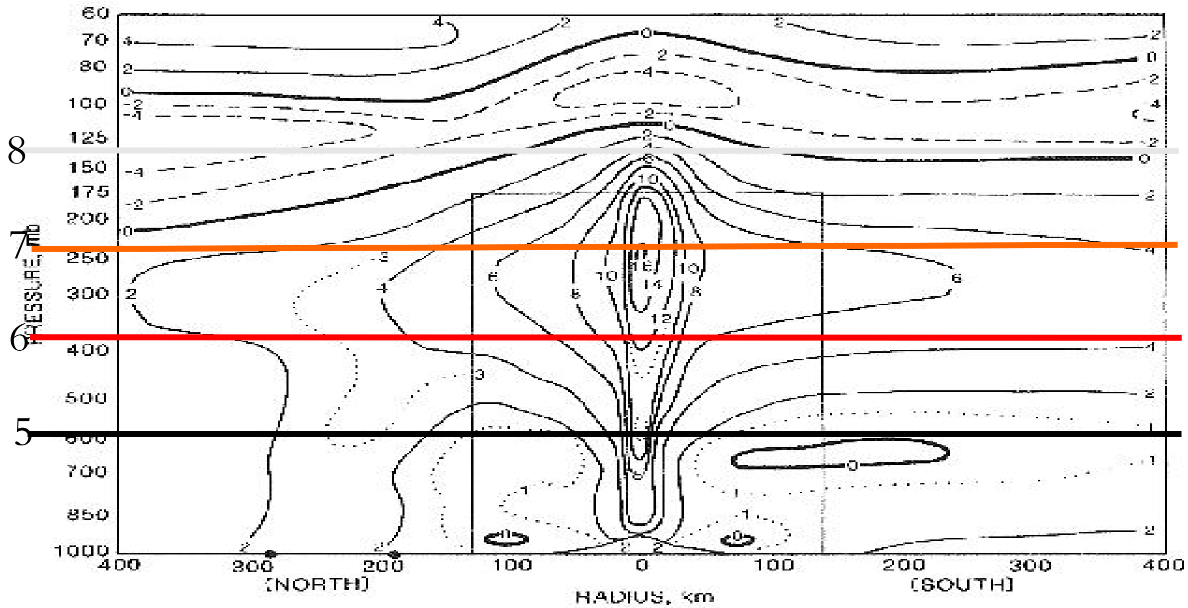

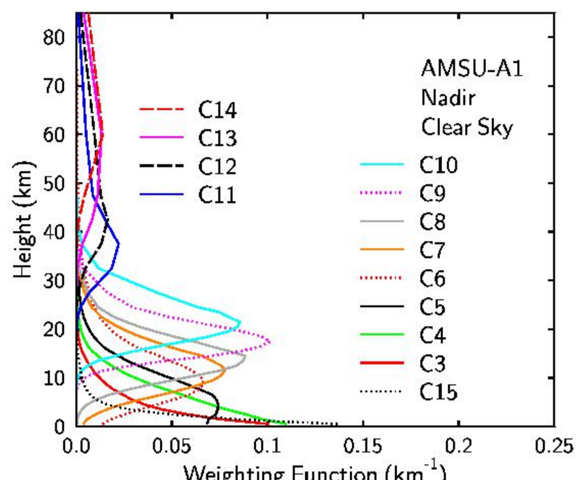

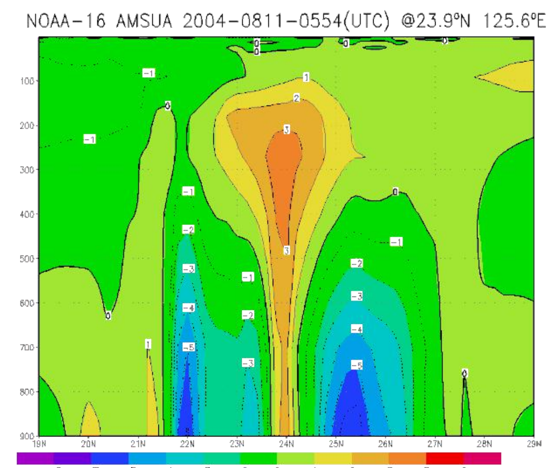

The correspondence between AMSU and typhoon cloud height

Simulation of the response of the thermal characteristics by AMSU tropospheric temperature channel (Andrew, 1992).

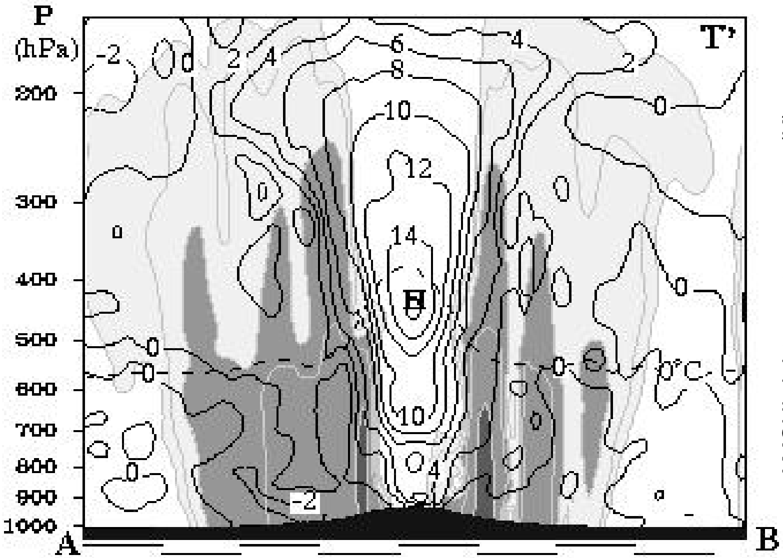

Temperature anomaly of hurricane simulated by MM5

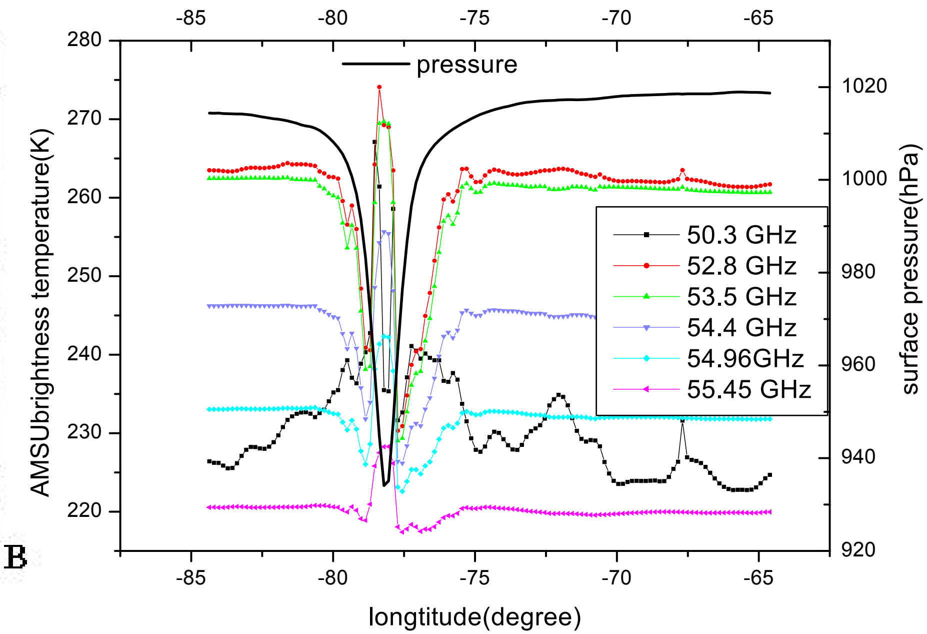

Response to Warming of Tropical Cyclone Center Simulated by AMSU-A

The simulation shows that the AMSU-A temperature channel on 50-60 GHz band has a significant radiation response to the upper center of the cyclone center, which can reveal the warm core structure of the cyclone upper layer.

Haurwrits (1935) proved by fluid mechanics that the measured tropical cyclone center pressure should be supported by a warm nuclear structure that extends the entire troposphere. AMSU-A observations can provide typhoon warm-heart monitoring and obtain typhoon intensity—the central lowest sea level pressure.

AMSU Response Analysis of Tropical Cyclone Cloud Rain Structure

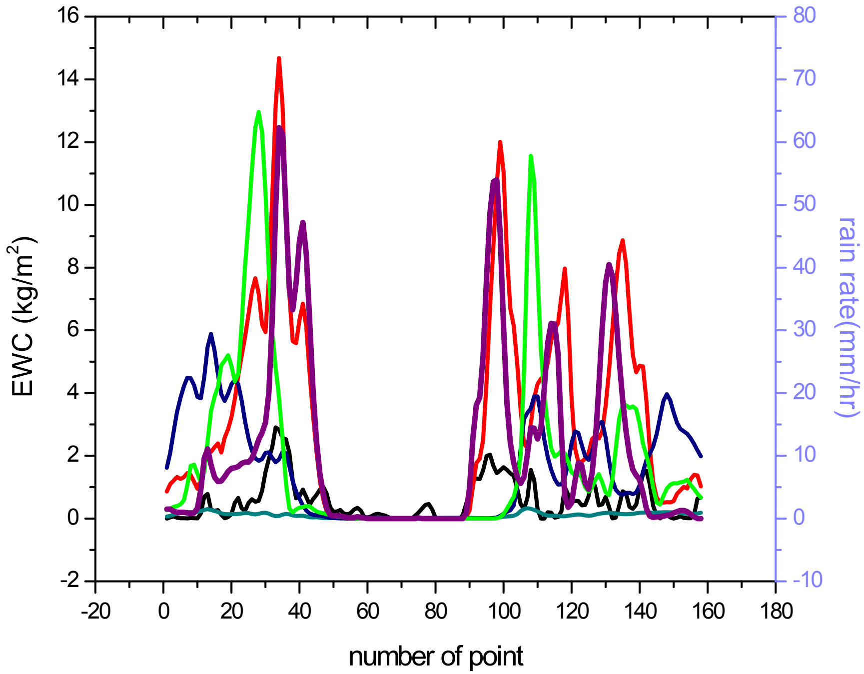

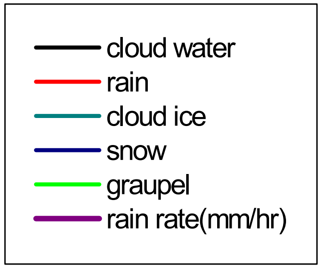

BOB Hurricane (1990) Cloud Rain Structure Profile (GCE Simulation)

Response of simulated AMSU to tropical cyclone BOB (1990) cloud rain structure

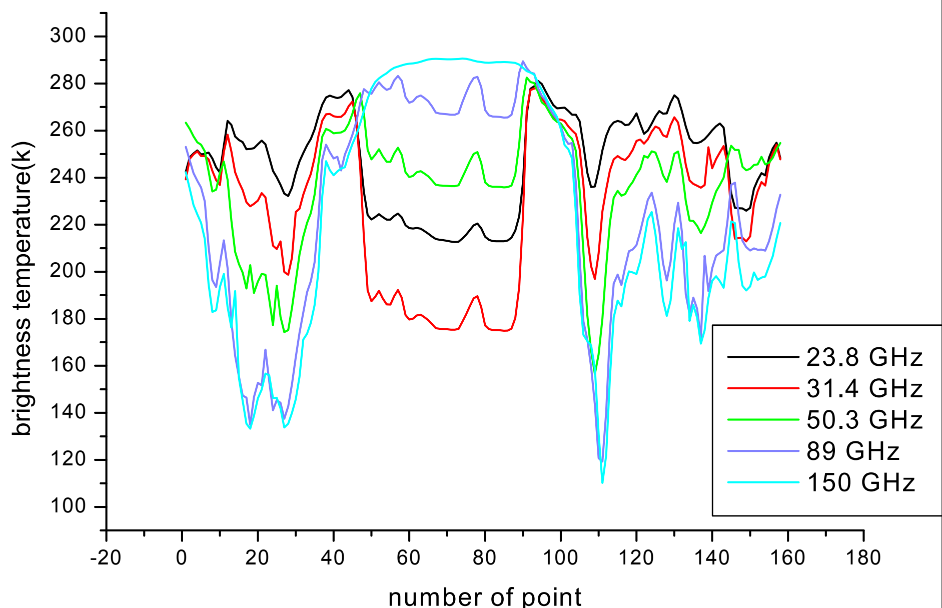

The simulation analysis shows that the water vapor and liquid cloud raindrops mainly contribute to the AMSU-A low-frequency channel radiation, and the large ice-phase particles are mainly scattered; for the AMSU-B high-frequency channel, the liquid cloud and the rain particles show weak scattering effect. The scattering effect of the ice phase cloud rain particles is significant.

Studies have shown that the maintenance and development of typhoons is mainly provided by the release of latent heat in the atmosphere. The disclosure of the typhoon cloud and rain structure contributes to the understanding of the development of tropical cyclones.

Case study: （Nuri，0812#）

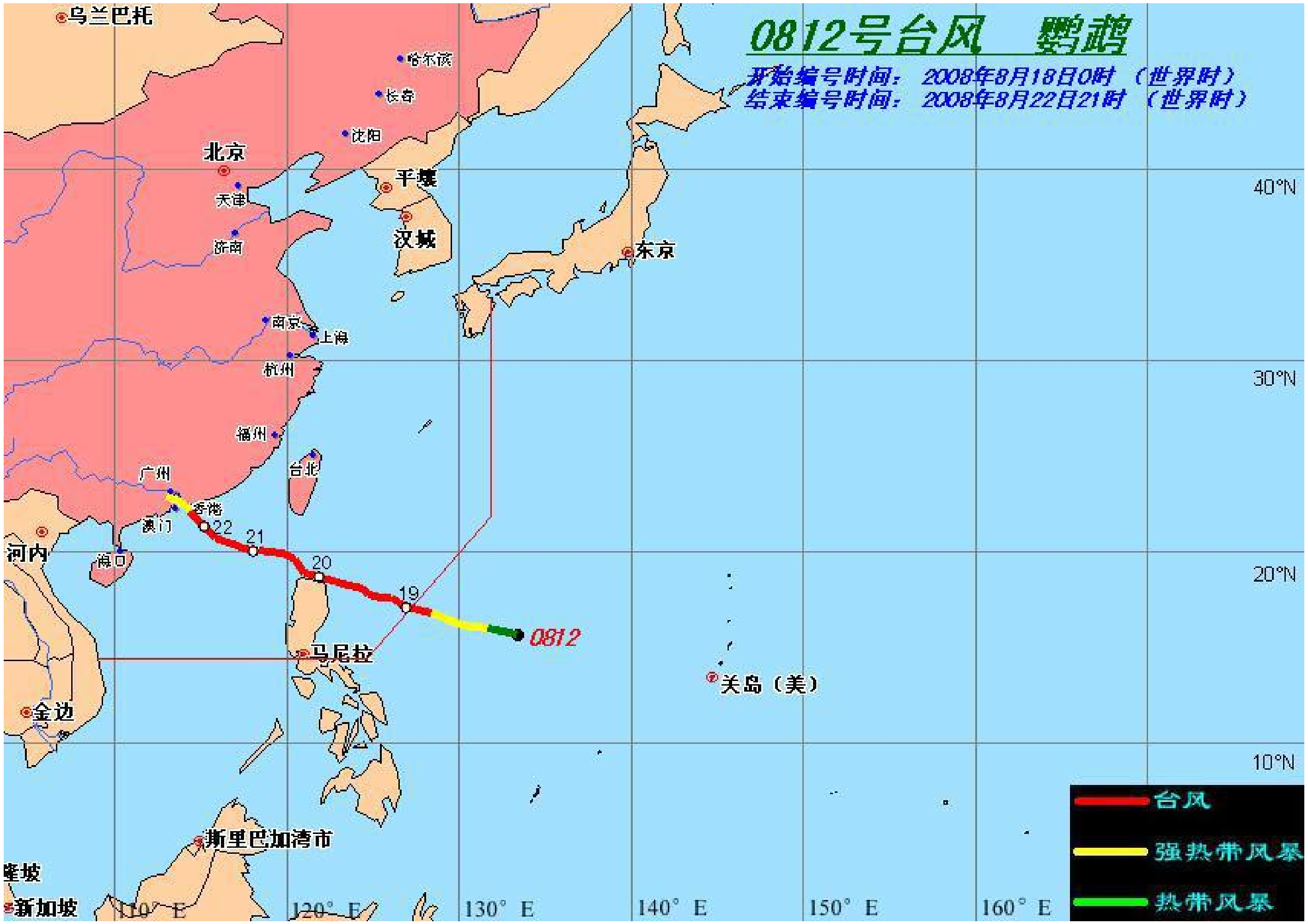

Nuri (0812) August, 20th, 2008, 05:16（UTC)

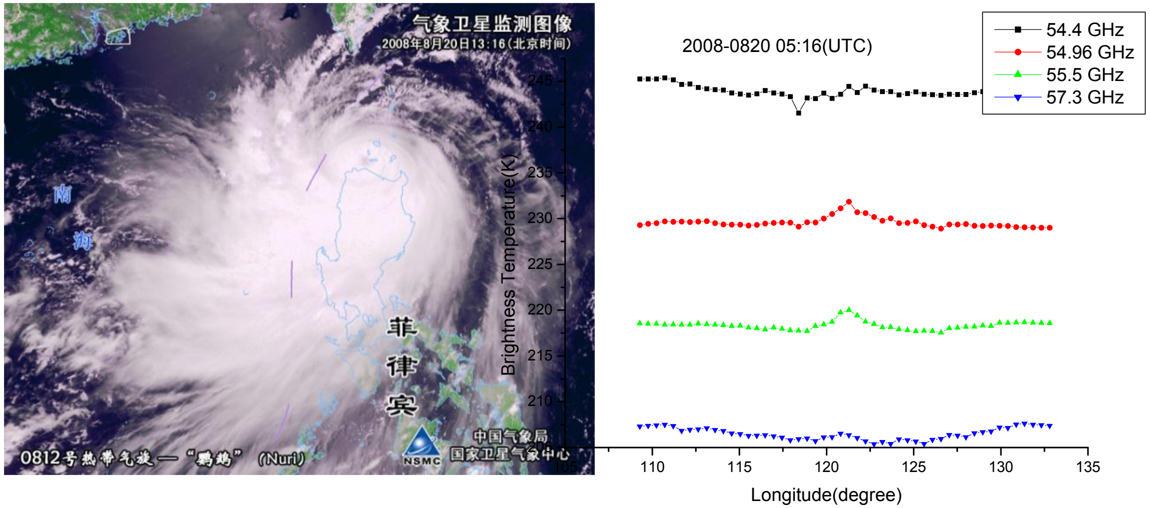

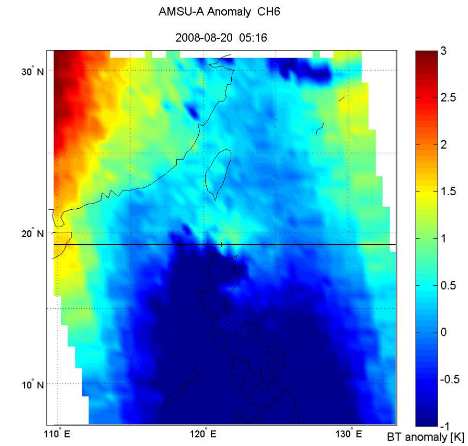

54.4GHz

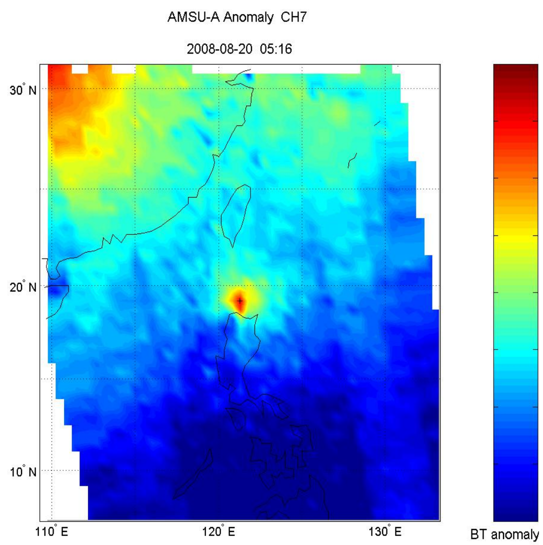

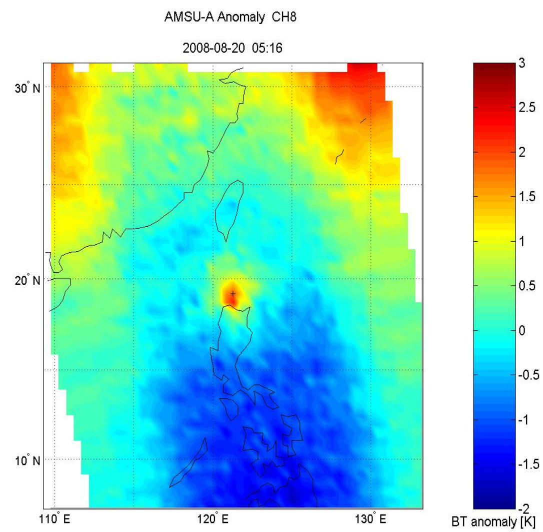

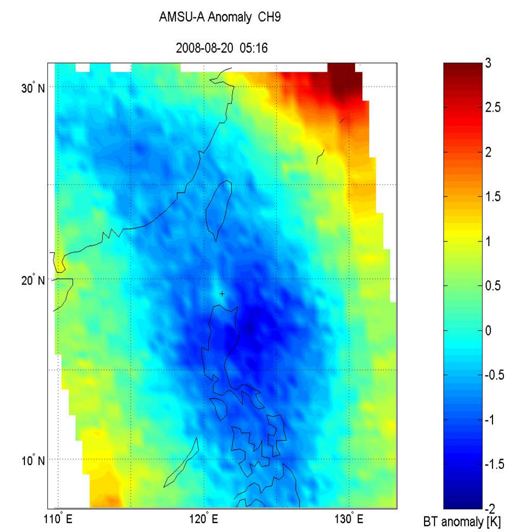

54.96GHz

55.5GHz

57.29 GHz

Nuri（0812） August 20, 2008 05:16 (UTC)

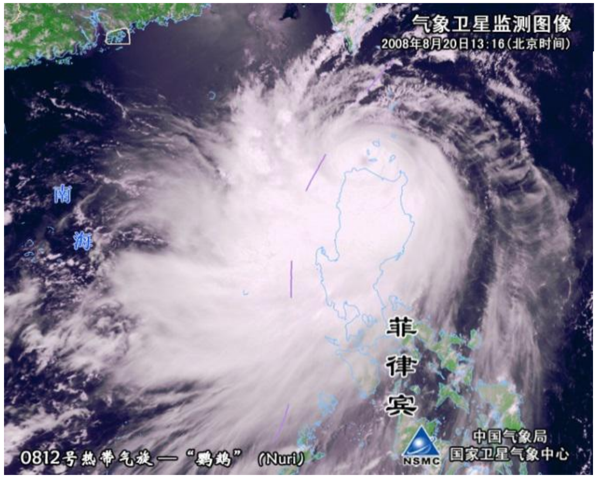

NOAA-18/AVHRR

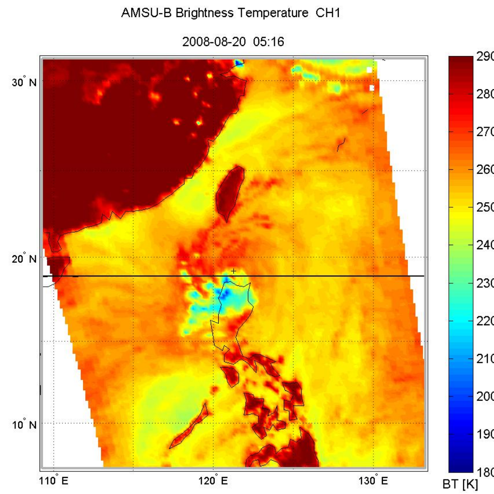

89GHz

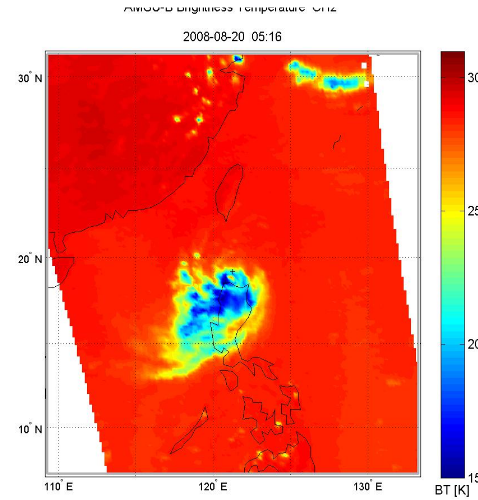

150GHz

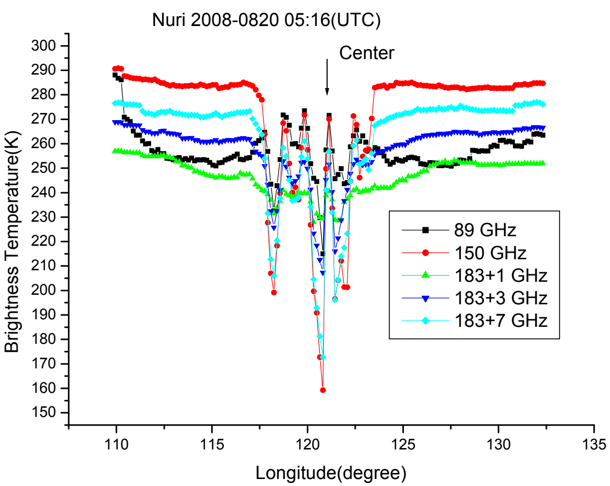

AMSU-B Bright temperature profile

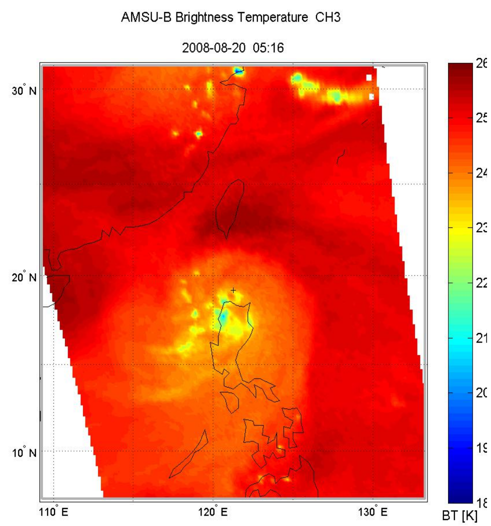

183.31±1 GHz

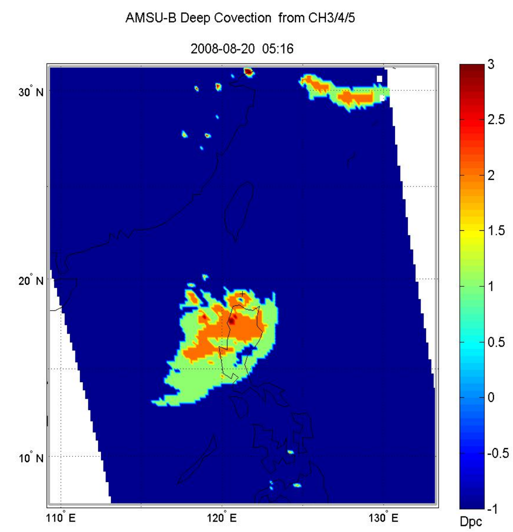

Convection distribution

Changes in the warming of the upper layer of Parrot (0812) from August 19 to August 21, 2008

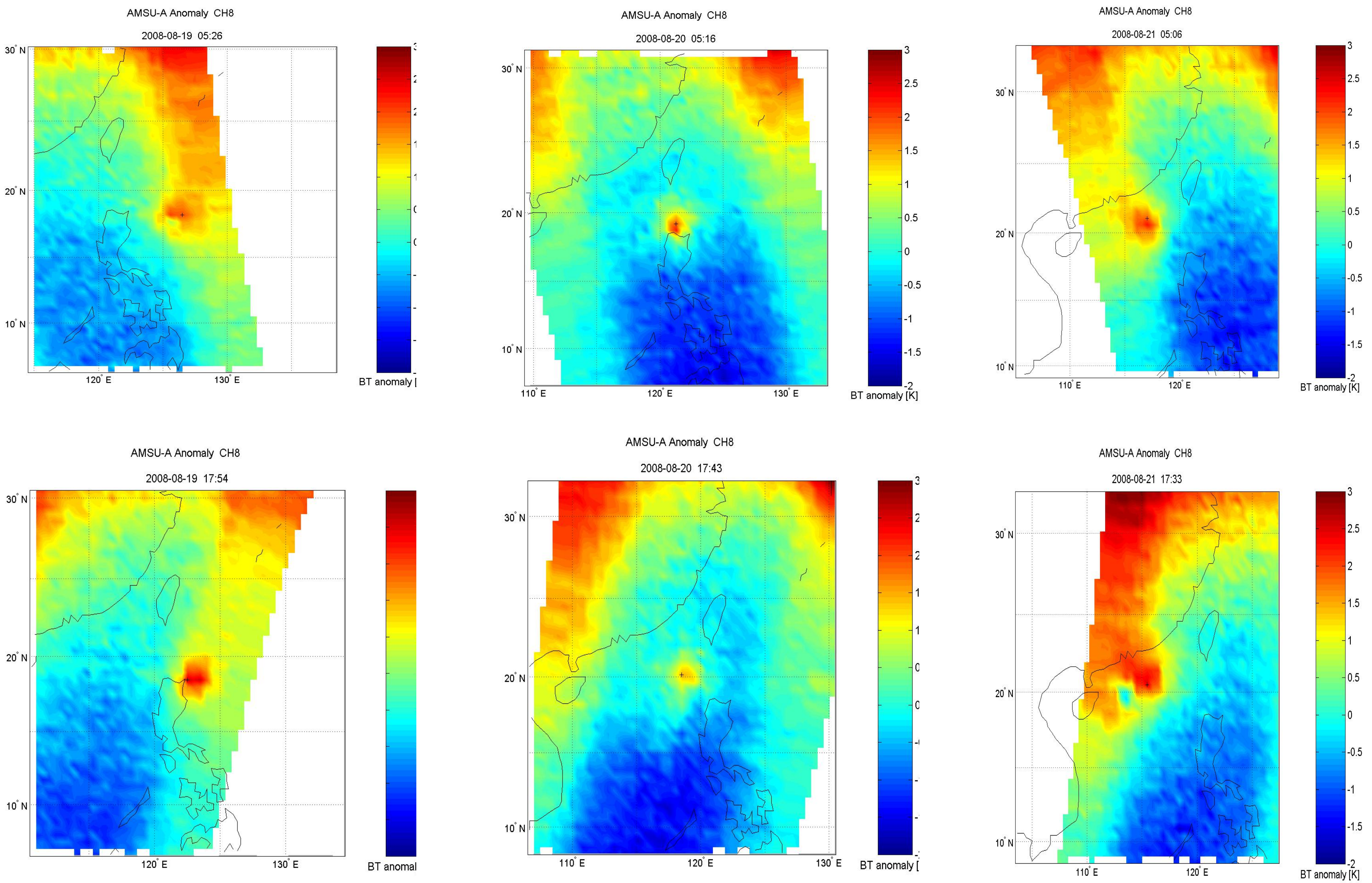

The analysis of the changes of typhoon upper warming, it can be seen that the typhoon is a process of strengthening-weakening-reinforcement.

Nuri (0812) Changes in cloud and rain structure from August 19 to 21, 2008

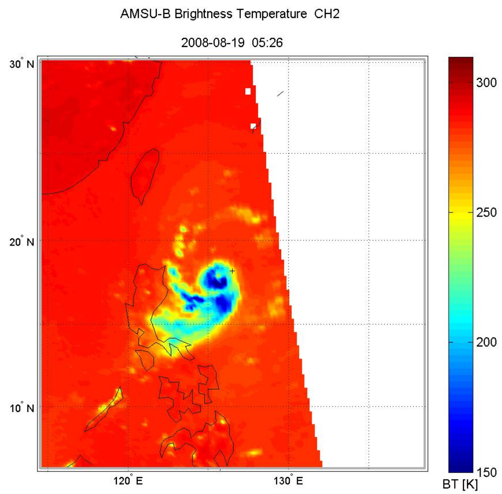

8月19日05：26

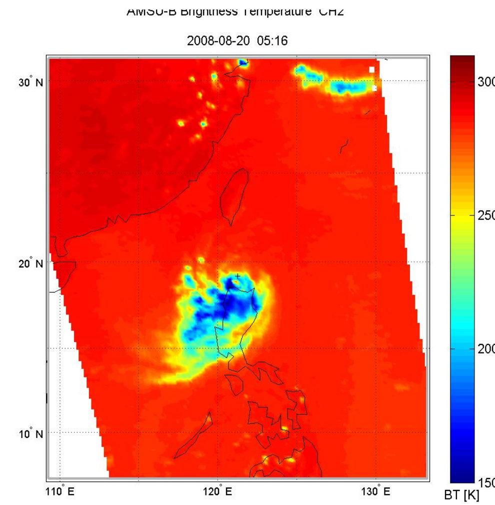

8月20日05：16

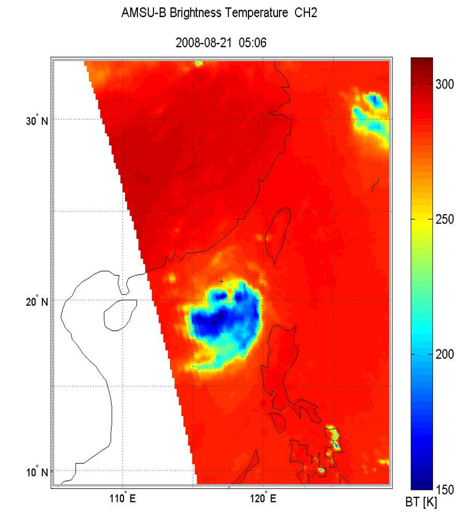

8月21日05：06

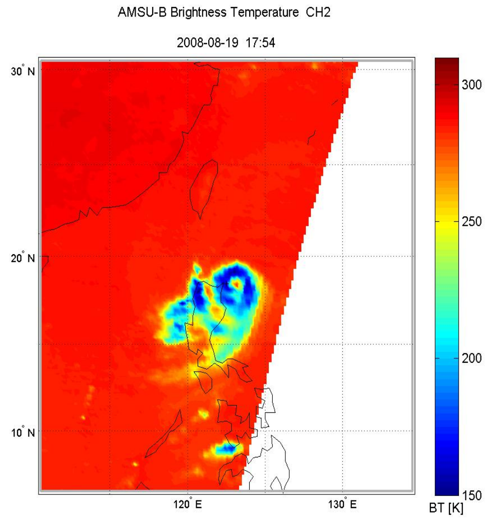

8月19日17：54

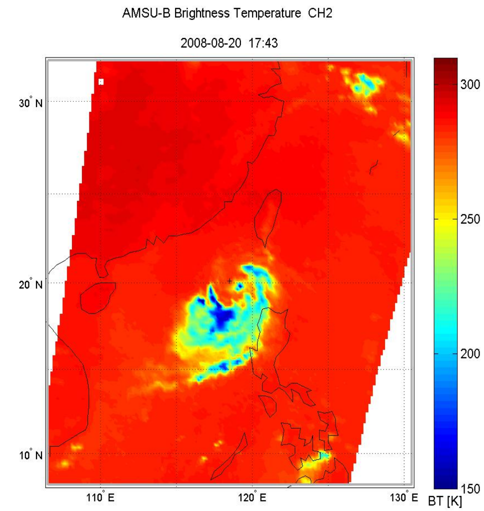

8月20日17：43

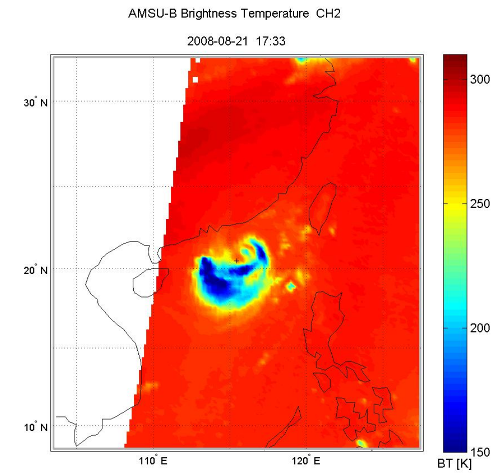

8月21日17：33

Case study:（Sinlaku，#0813）

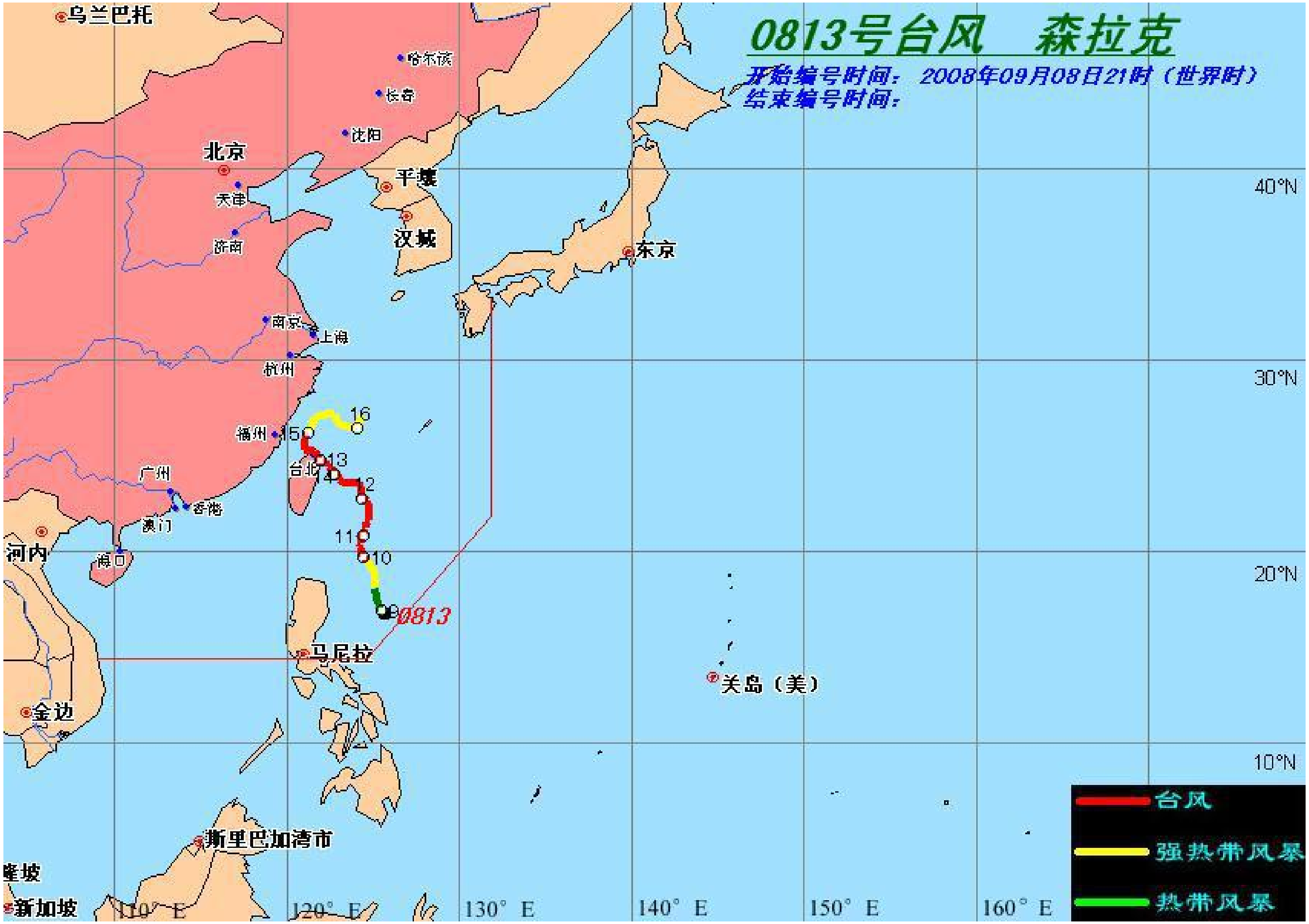

Sinlaku(0813) 2008-0910 17:25(UTC)

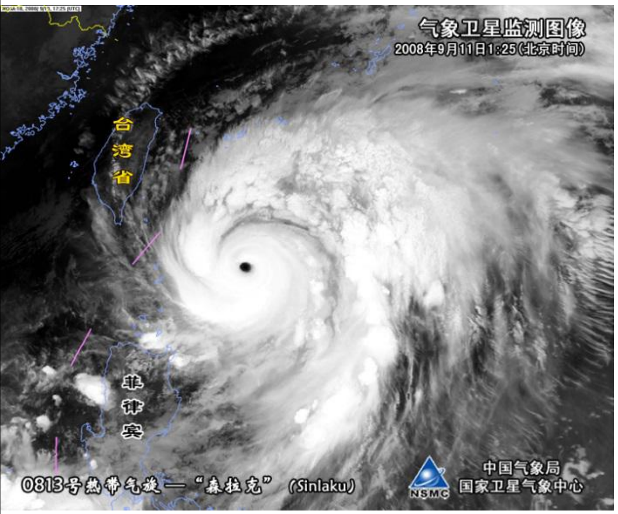

NOAA-18/AVHRR

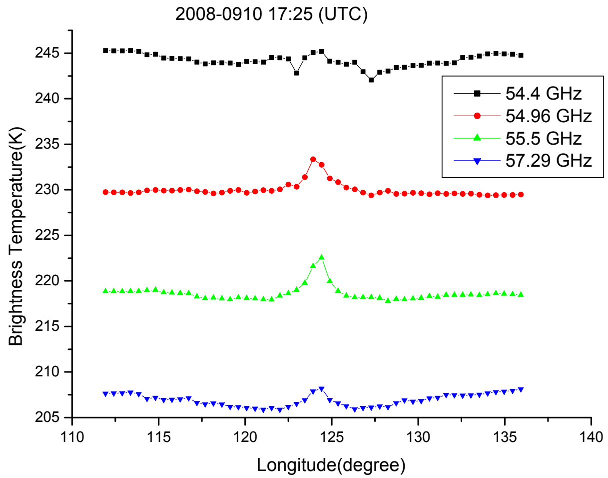

AMSU-A Brightness temperature profile

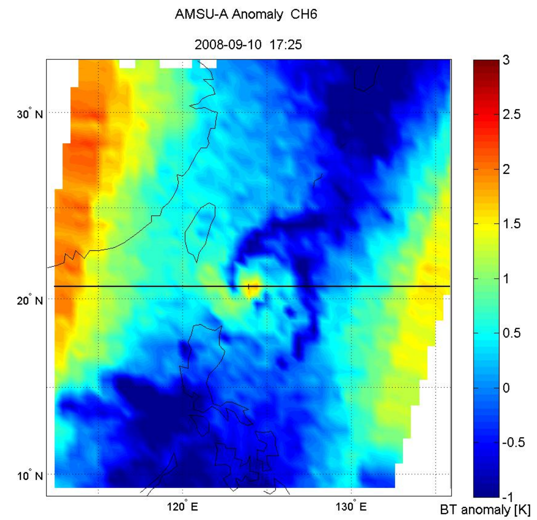

54.4GHz

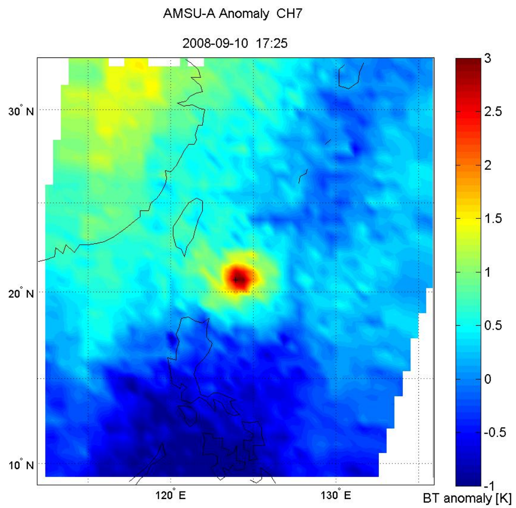

54.96GHz

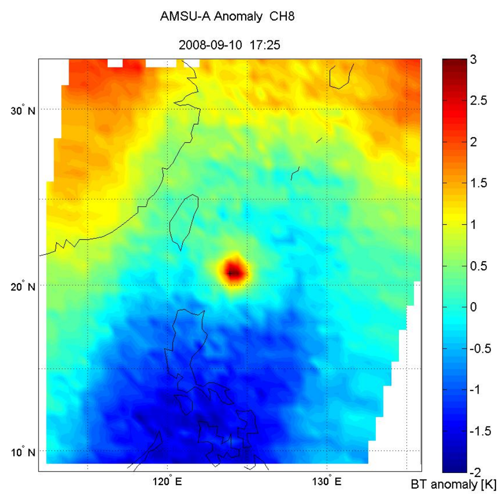

55.5GHz

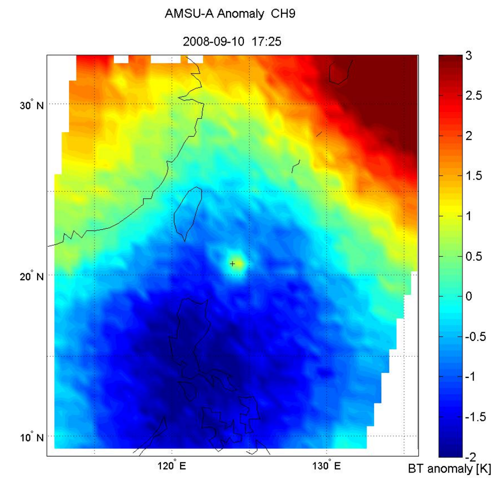

57.29 GHz

Sinlaku(0813) 2008-0910 17:25(UTC)

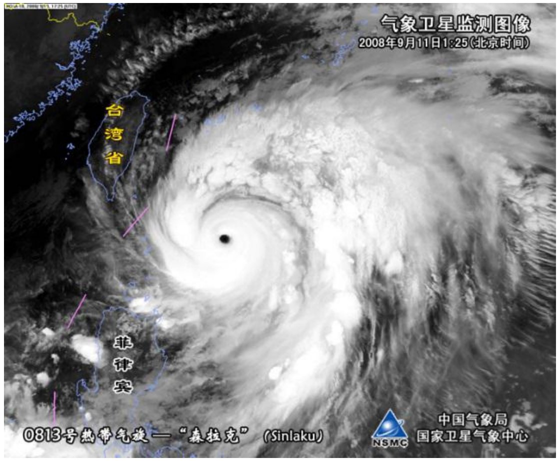

NOAA-18/AVHRR

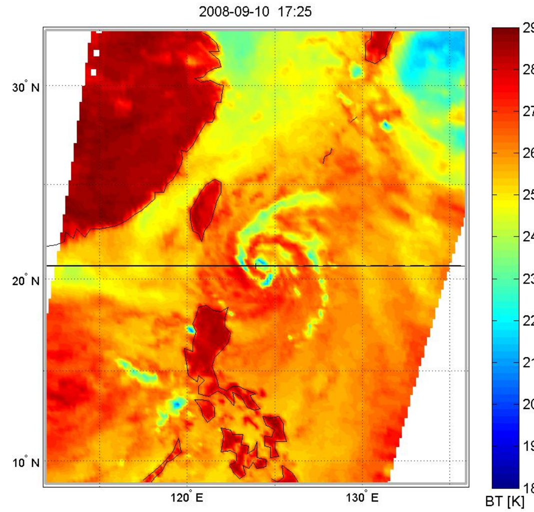

89GHz

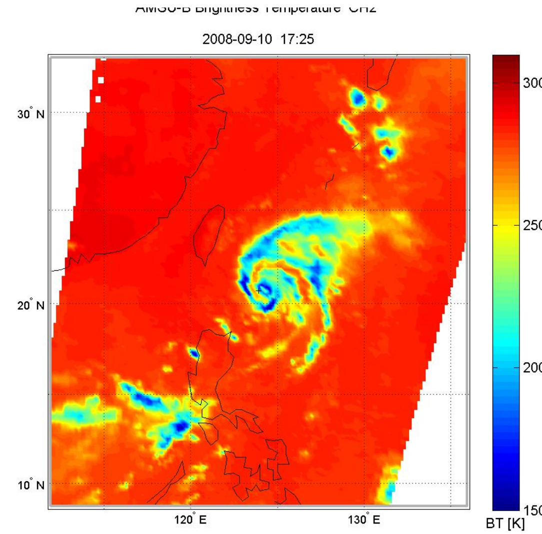

150GHz

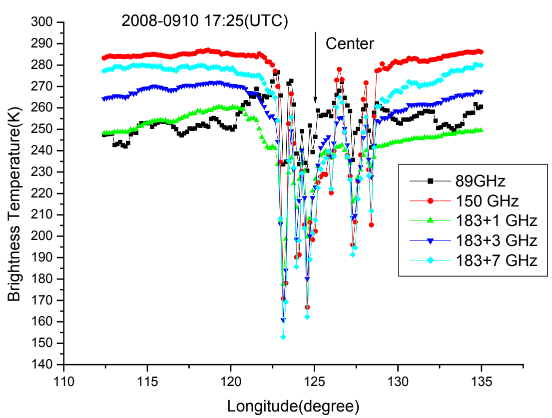

AMSU-B Brightness temperature profile

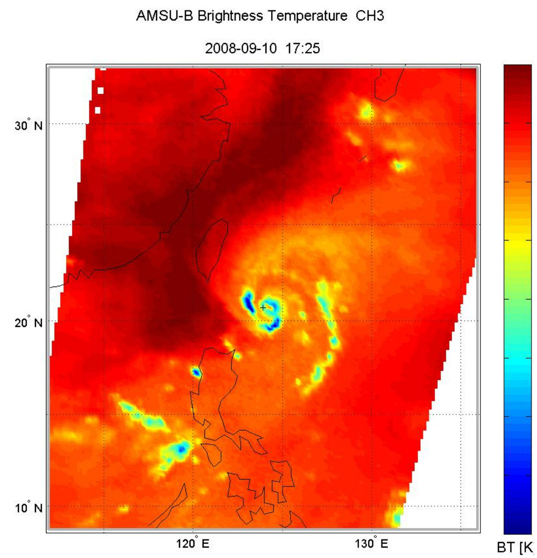

183.31±1 GHz

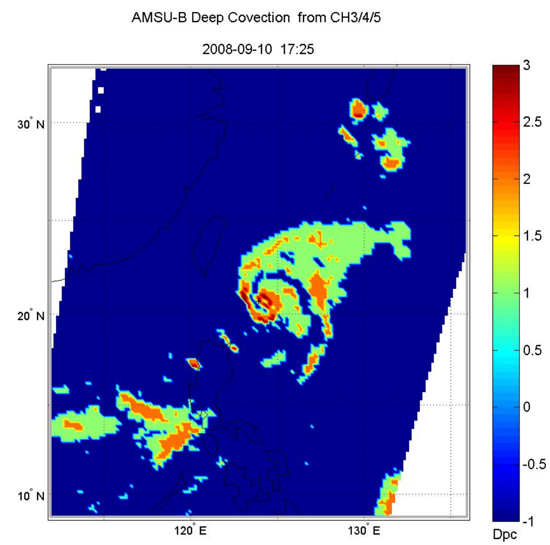

Distribution of convection

Sinlaku Warm heart structure development (September 08 - 13, 2008)

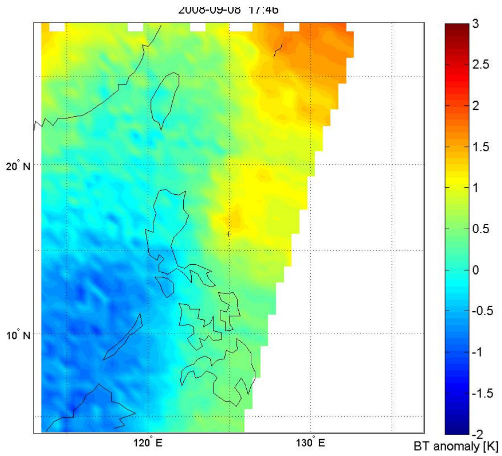

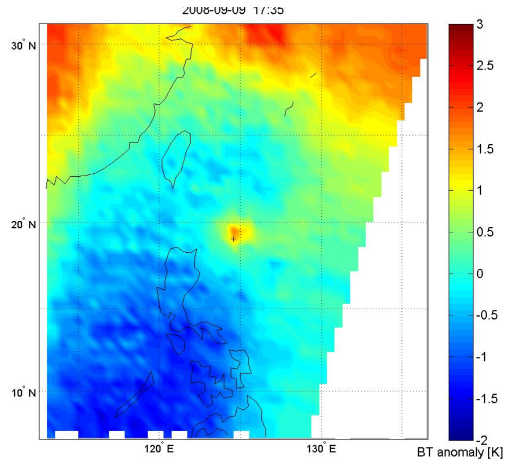

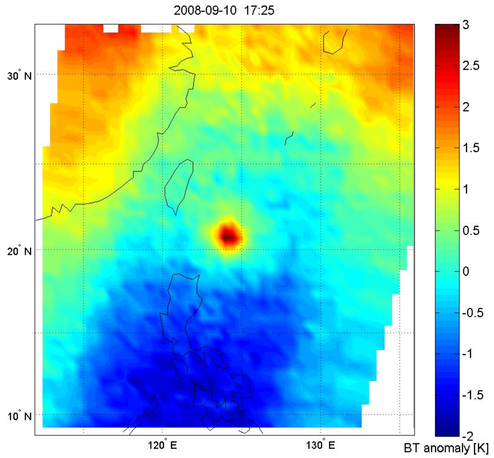

9月8日17：46　　9月9日17：35　　9月10日17：25

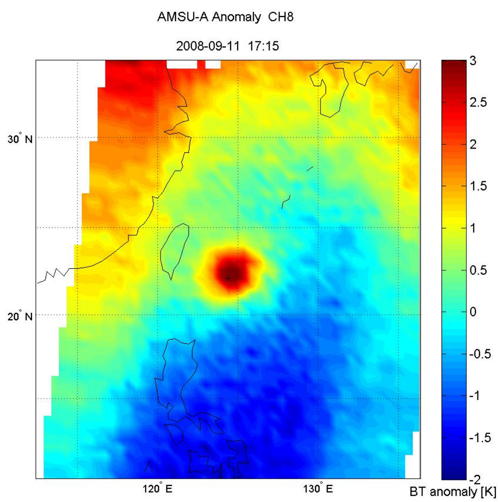

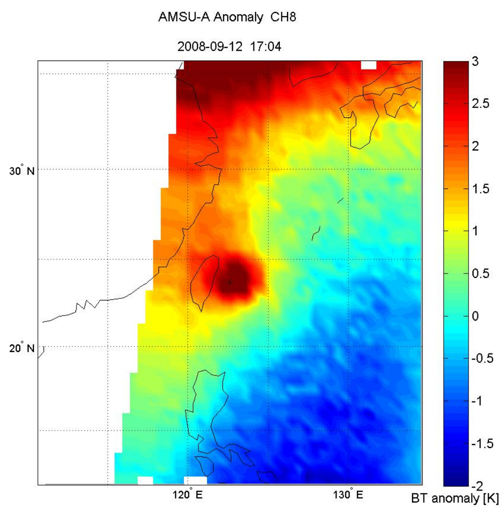

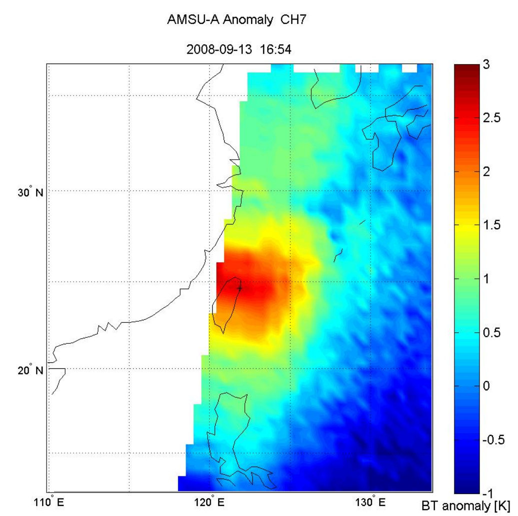

9月11日17：15　　9月12日17：04　　9月13日16：54

Sinlaku Cloud and Rain Structure Development (September 08-13, 2008)

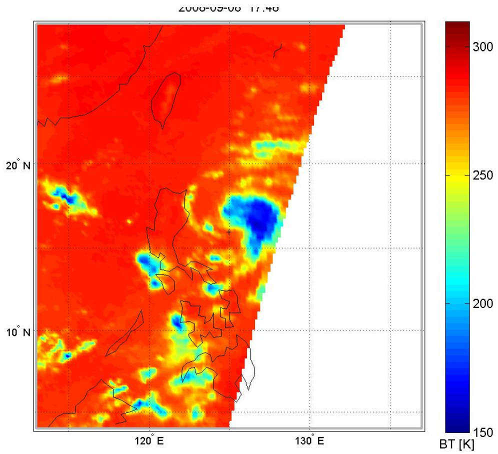

9月8日17：46

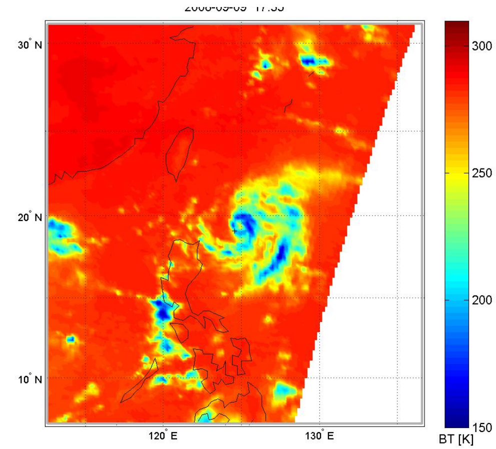

9月9日17：35

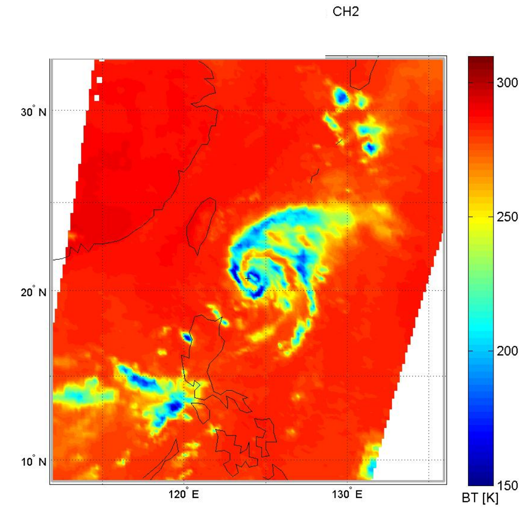

9月10日17：25

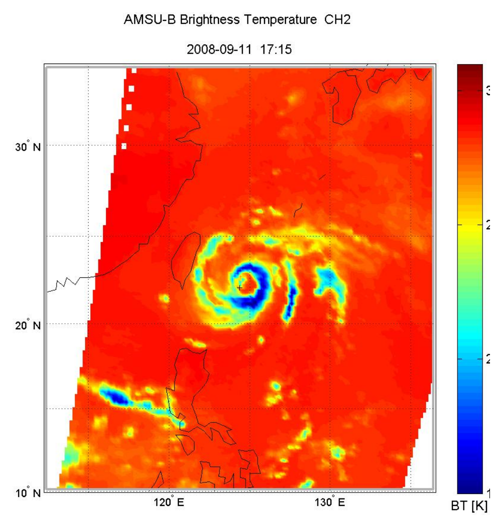

9月11日17：15

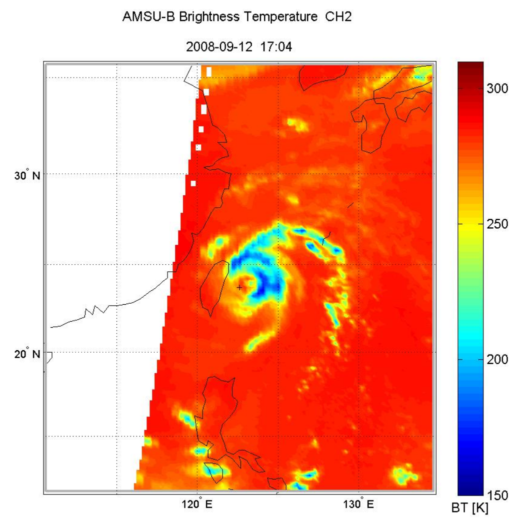

9月12日17：04

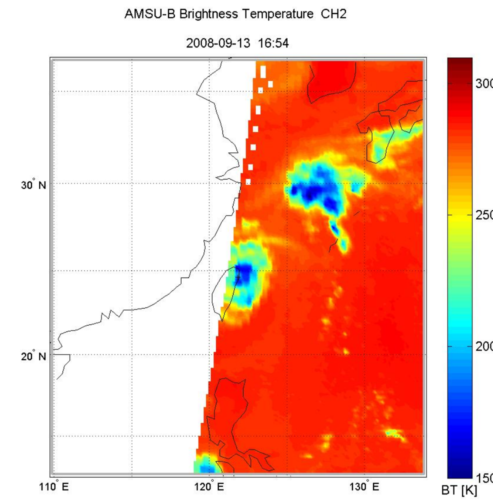

9月13日16：54

Case study:（ "Maria" ，#1808）

Typhoon warm heart structure evolution

201807051041

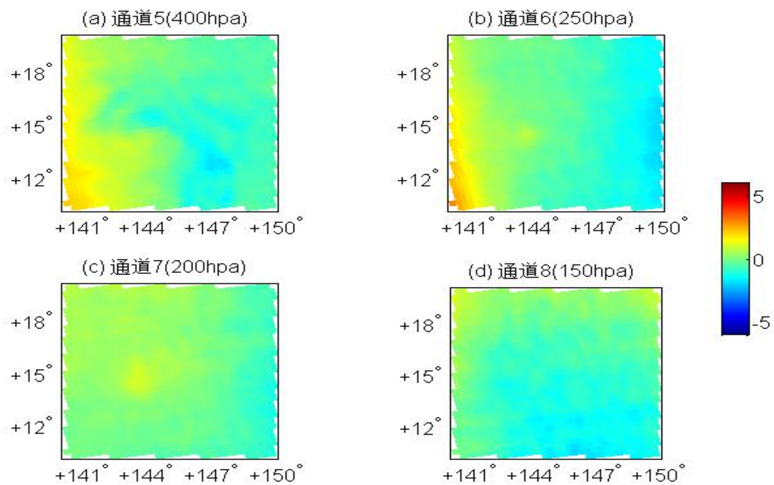

201807062212

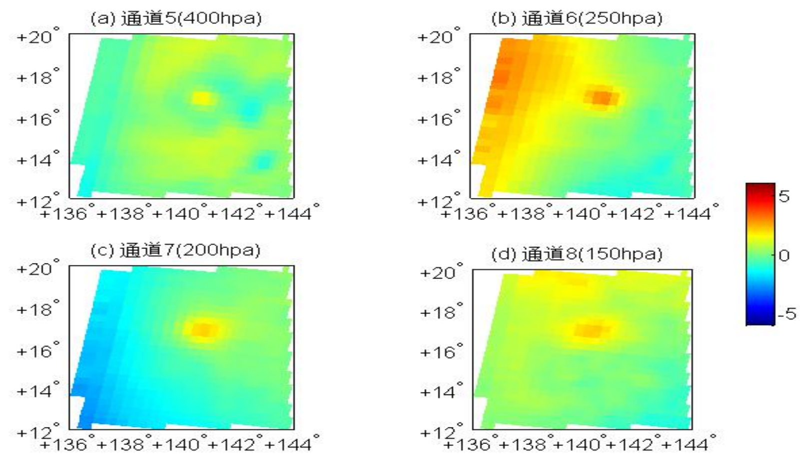

201807082315

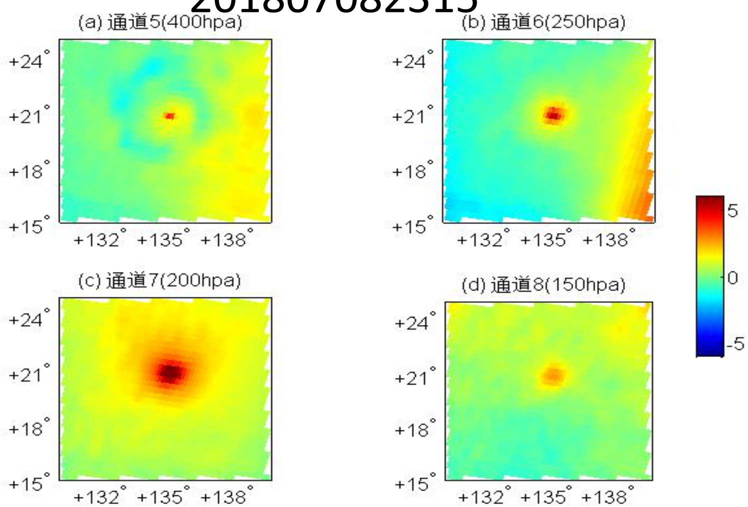

201807101218

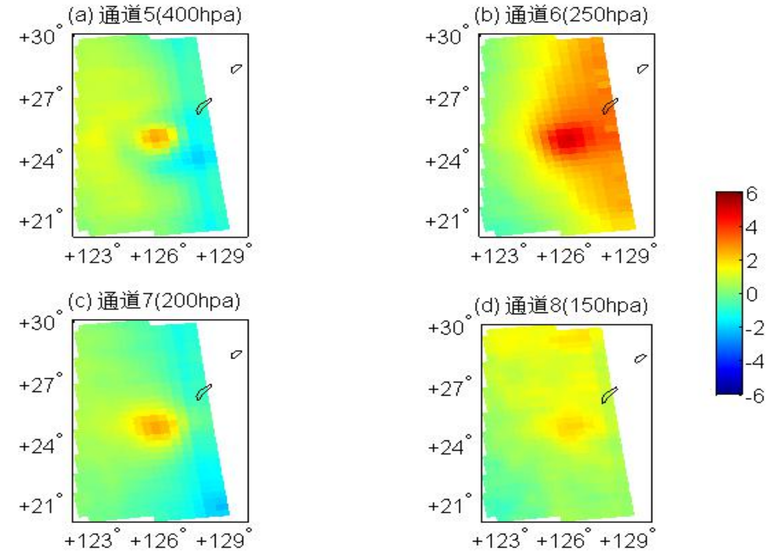

On July 5th, the warm heart of Maria Typhoon first appeared from 200hpa. On July 6th, the warm heart strengthened and became deep (the warm heart appeared in 400-150hpa). On July 8th, the warm heart was further strengthened, July On the 10th, the warm heart began to weaken, but it was still deep, indicating that the release of latent heat has not yet ended.

After the typhoon landed, the forecasters should pay attention to the impact of convective precipitation.

FY-3C / D microwave cloud water contents products

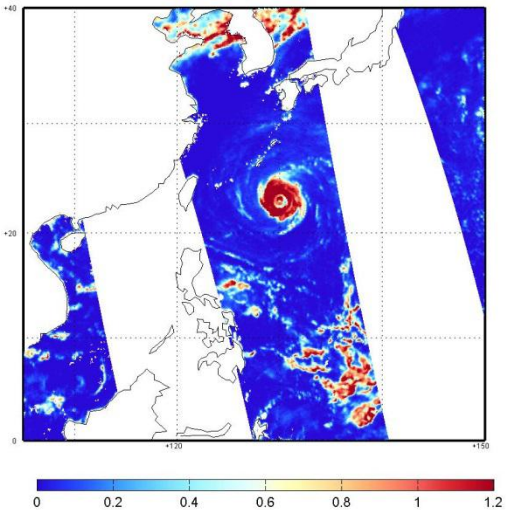

FY-3C 2018年7月9日22:00

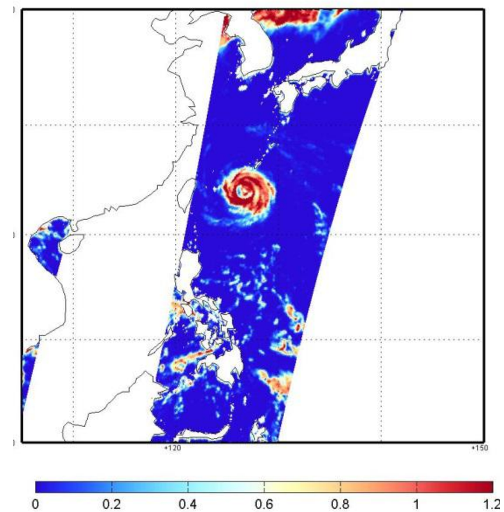

FY-3C 2018年7月10日 10:00

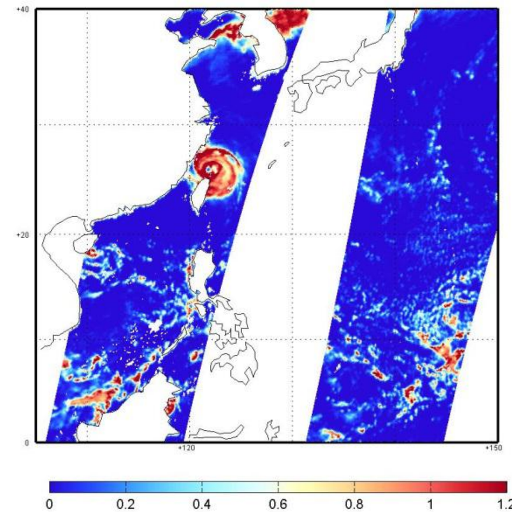

FY-3D 2018年7月11日 02:30

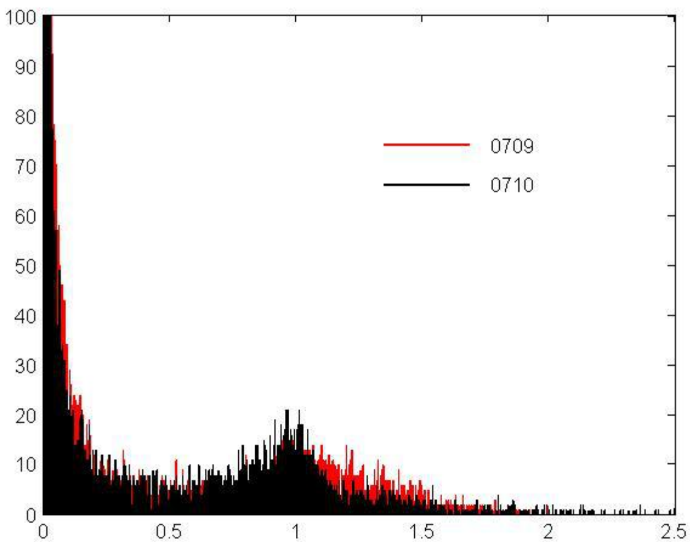

On July 11, the cloud water content inside the typhoon was significantly reduced, and the structure of the double-eye wall is still very obvious. 。

FY-3B/C/D continuously track and monitor the typhoon "Maria" precipitation

7.4~7.11: The strong precipitation belt gradually transitions from the wind eye wall to the peripheral spiral cloud belt

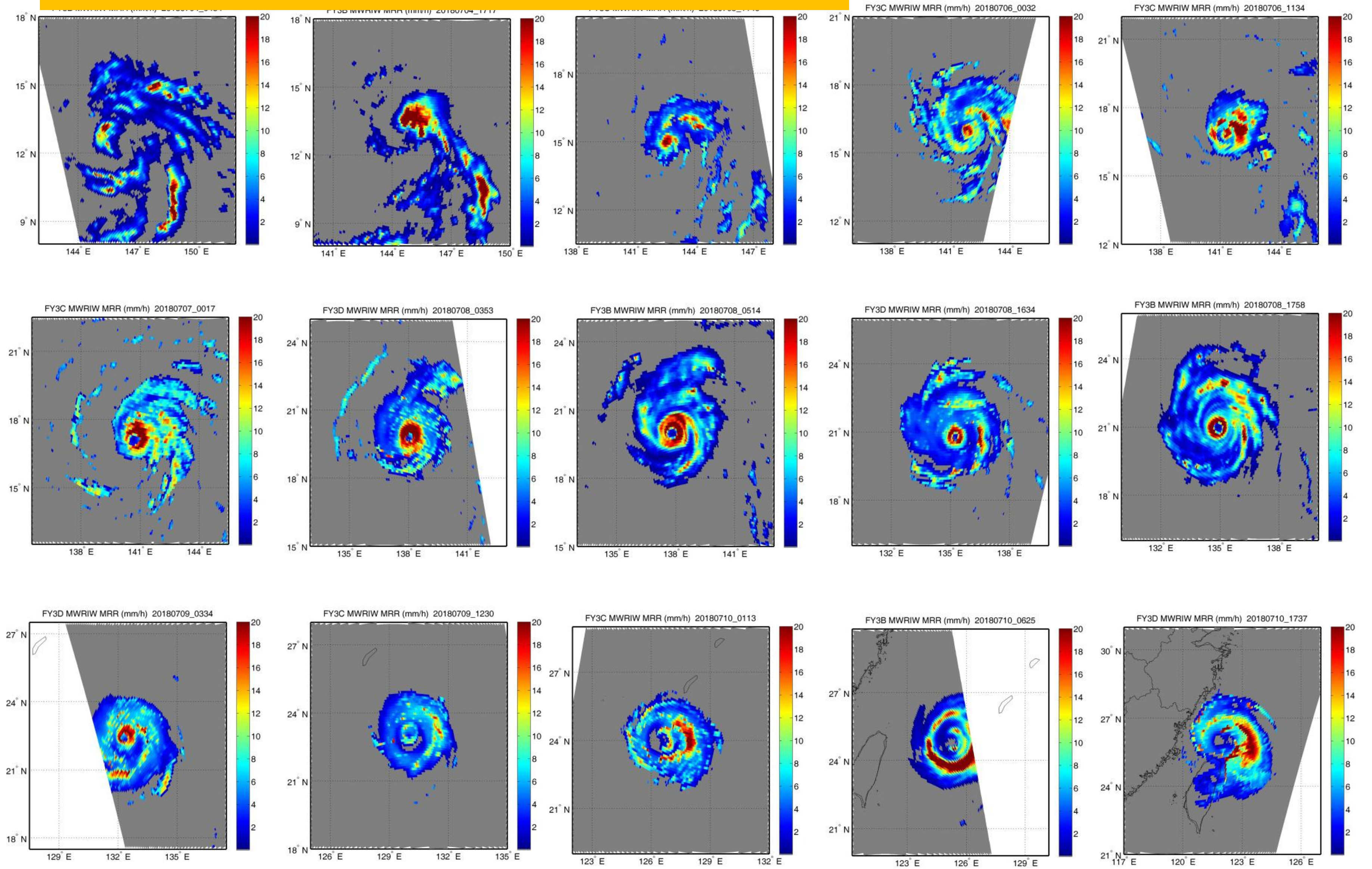

Average precipitation in the typhoon area

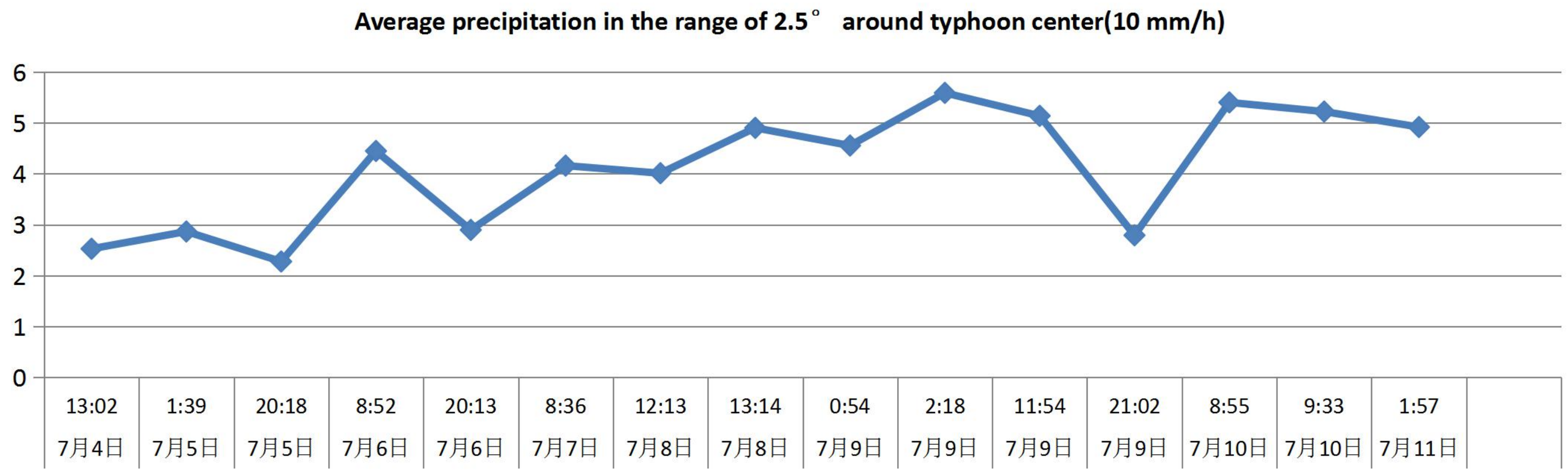

FY-3B/C/D continuously track and monitor the typhoon "Maria" precipitation

FY3 microwave water condensate profile

rain

Cloud ice

Ice

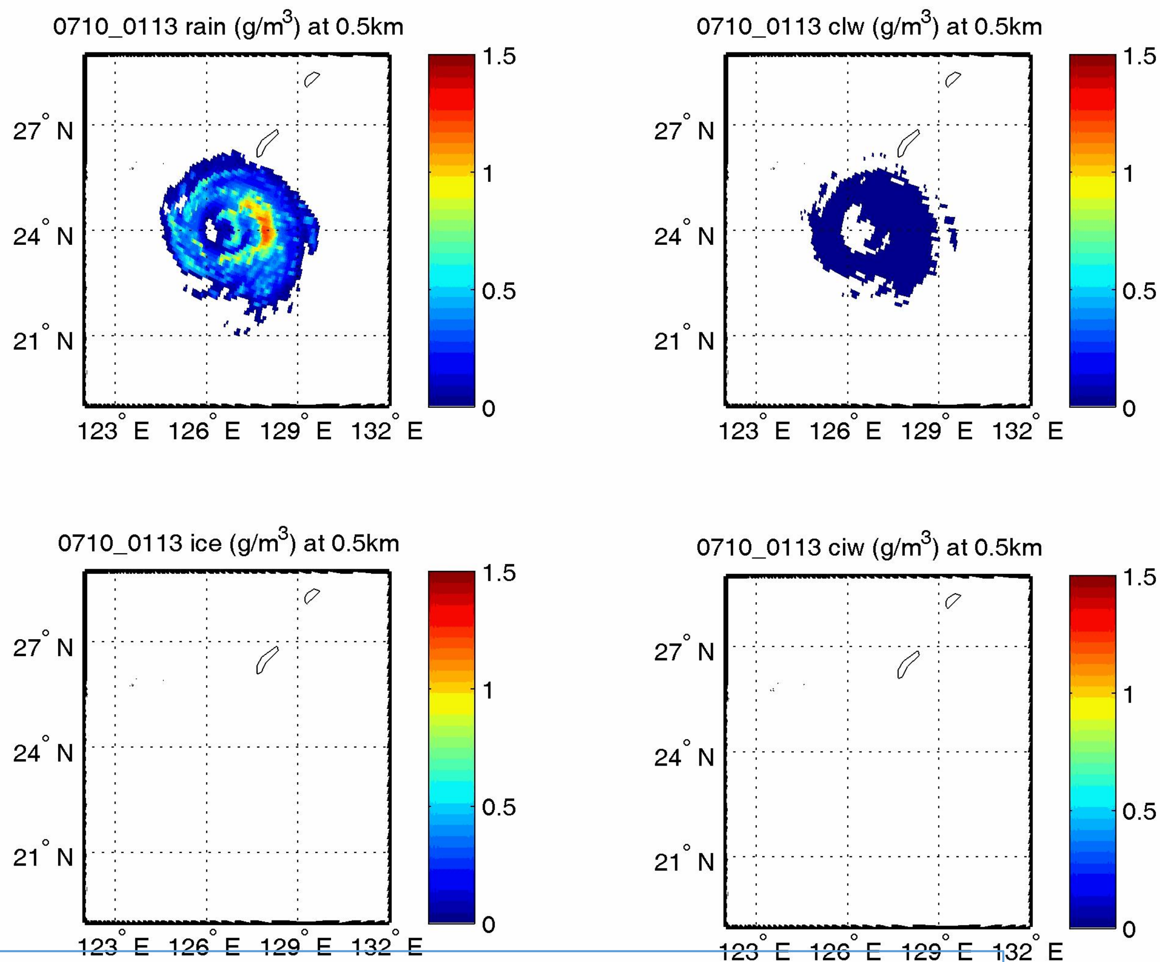

Precipitable ice particles (snow, sputum): 3-18 km (convection) the peak value is 8 km, up to 1.2g/m3

Rain particle rain: below 5 km, peak at 3.5 km

Cloud ice: 8-18 km

Microwave reveal typhoon structure

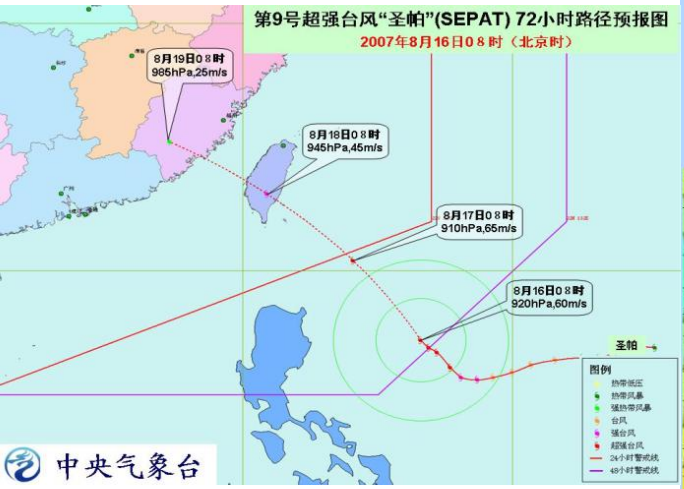

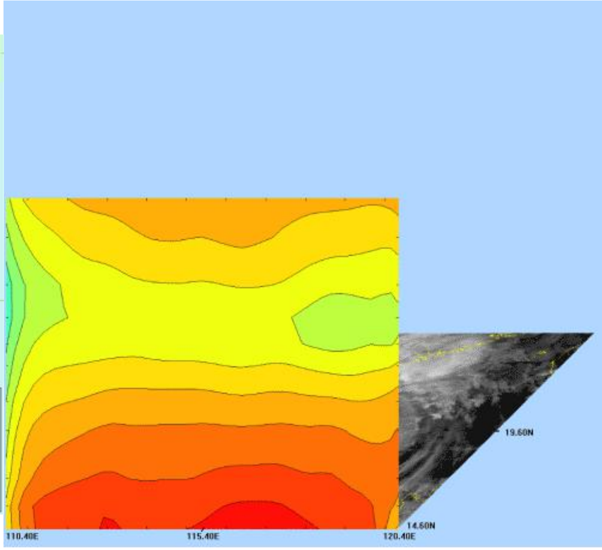

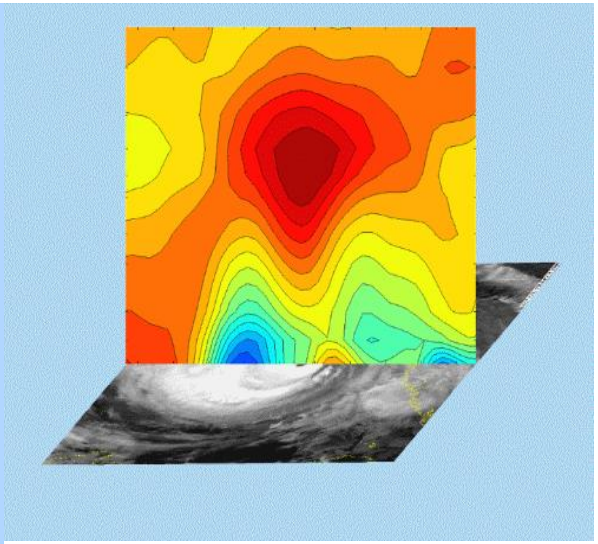

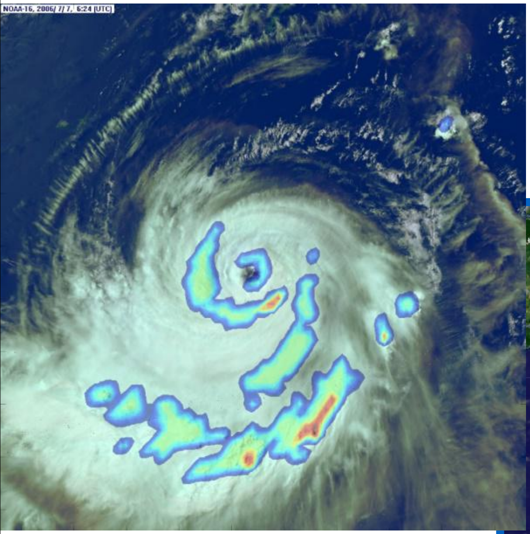

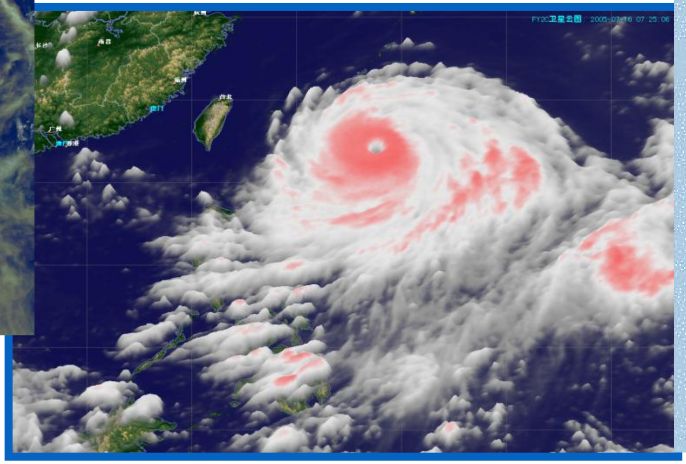

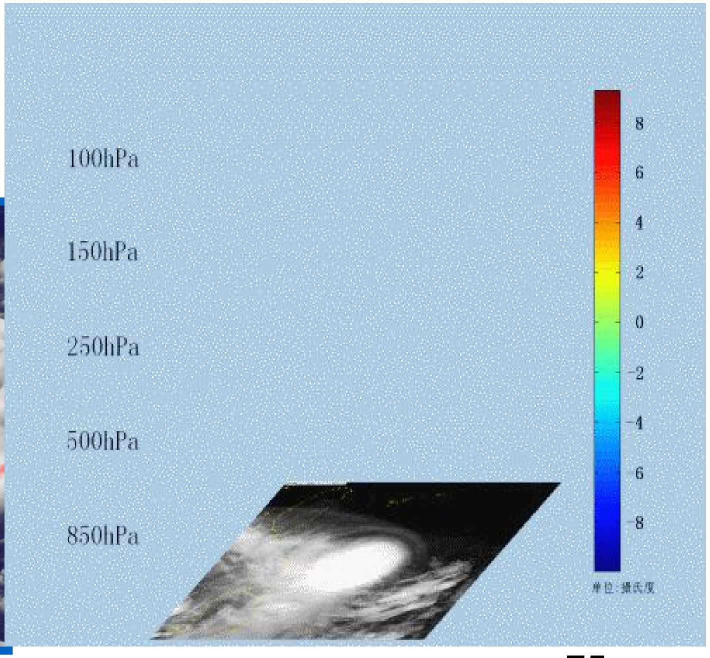

Comprehensive monitoring of typhoon using FY3D MWTS and FY4 AGRI

FY3D MWTS Temperature anomaly (K) distribution in different levels

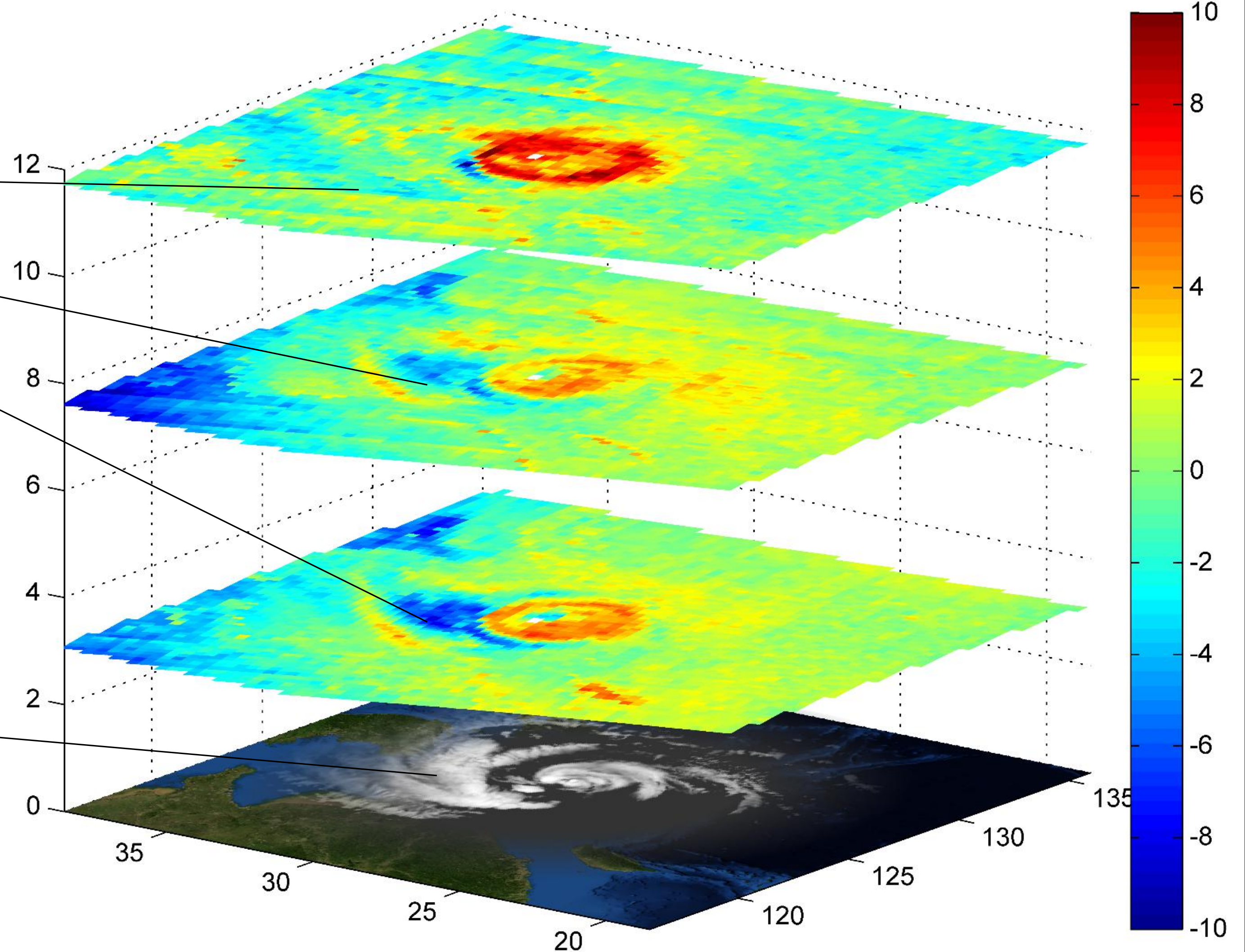

FY4 AGRI 12^{th} channel Brightness temperature

Comprehensive monitoring of typhoon using FY3D MWHS and FY4 AGRI

FY3D MWHS Humidity anomaly (%) in different levels

FY4 AGRI 12th channel Brightness temperature

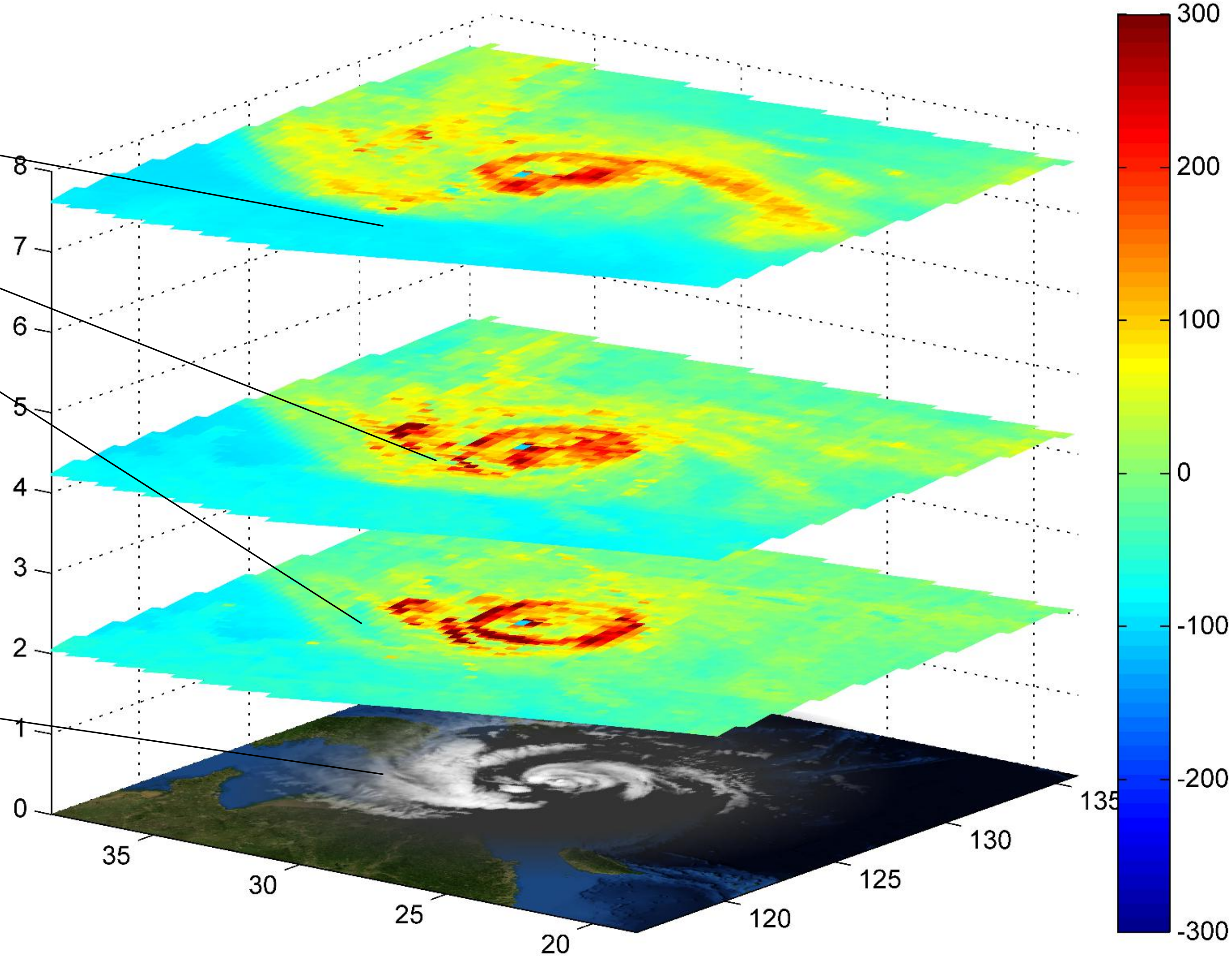

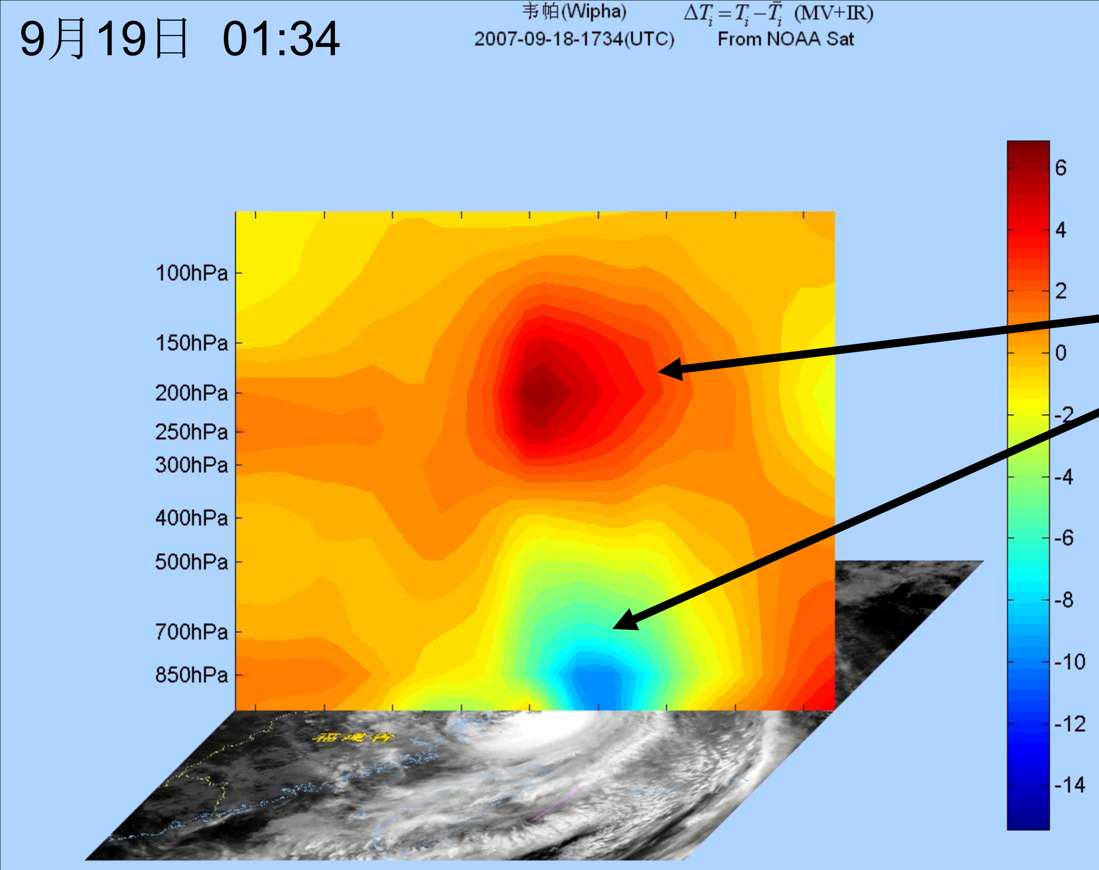

Typhoons Microwave depiction of warm core anomaly and rain rate

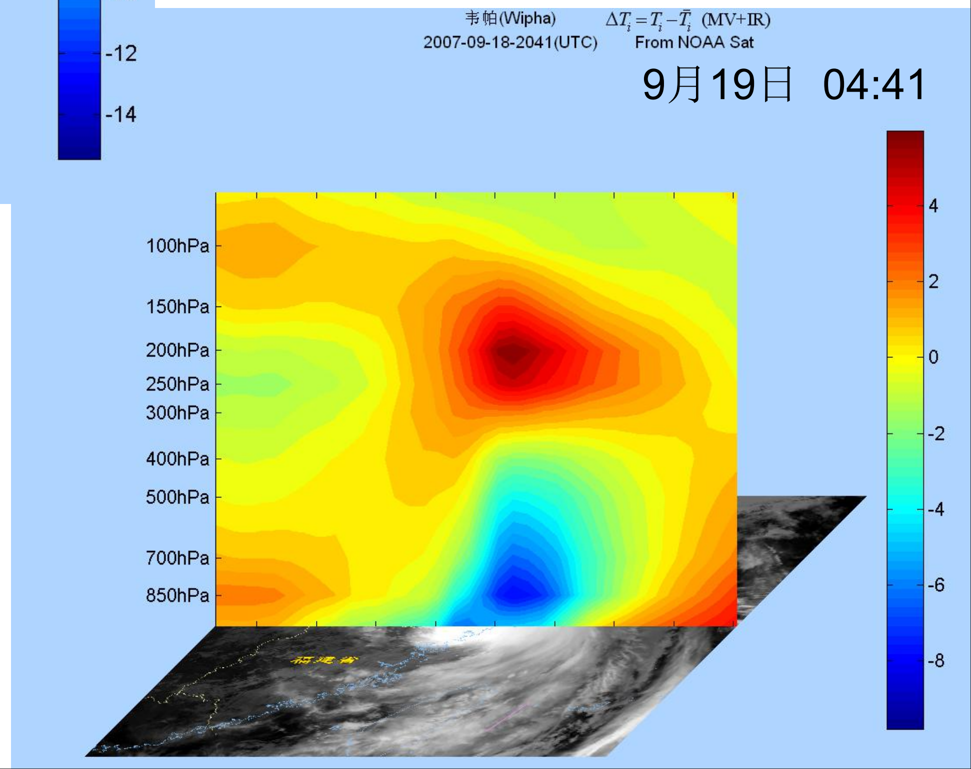

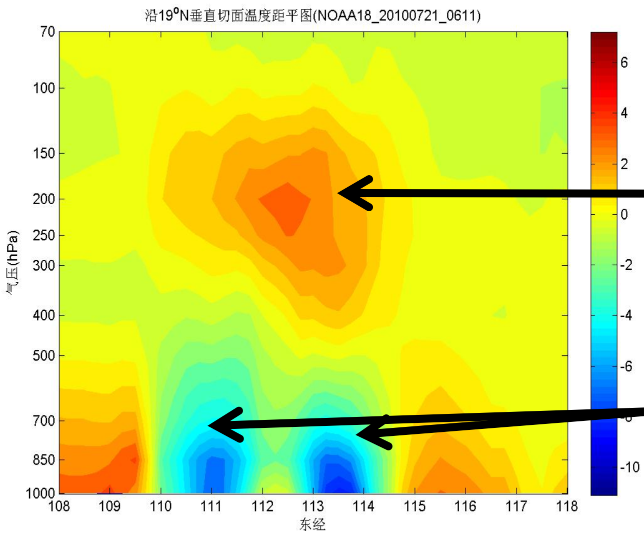

Warm center

Heavy railfall area

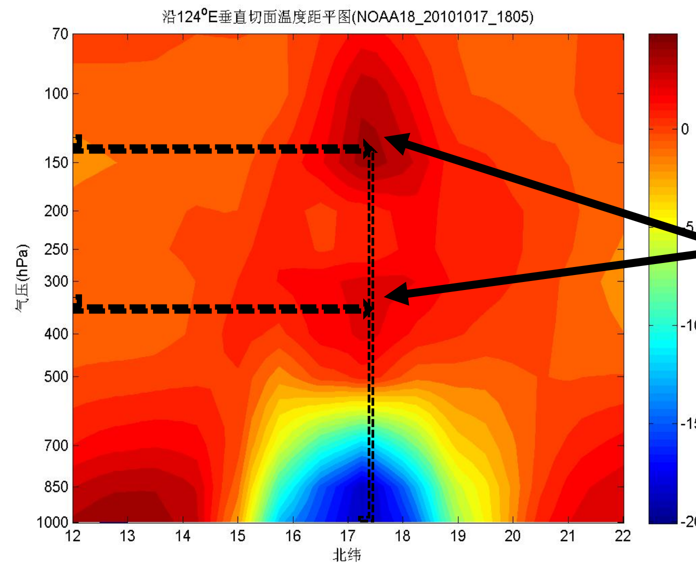

Double warm center

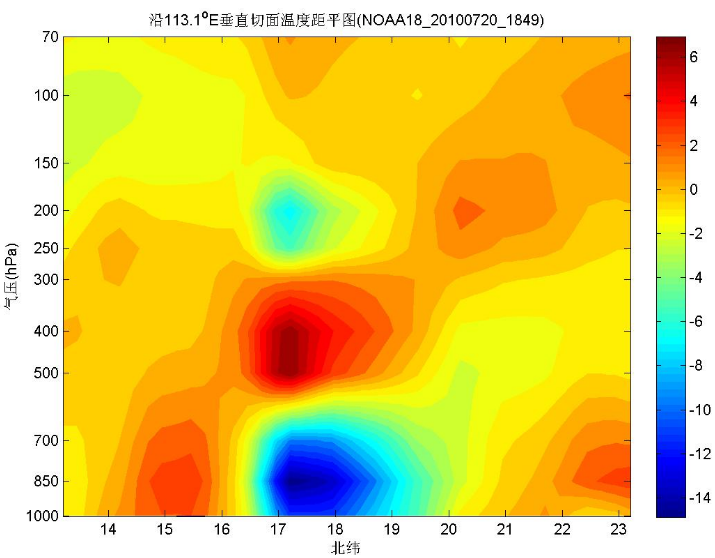

Inclining warm center

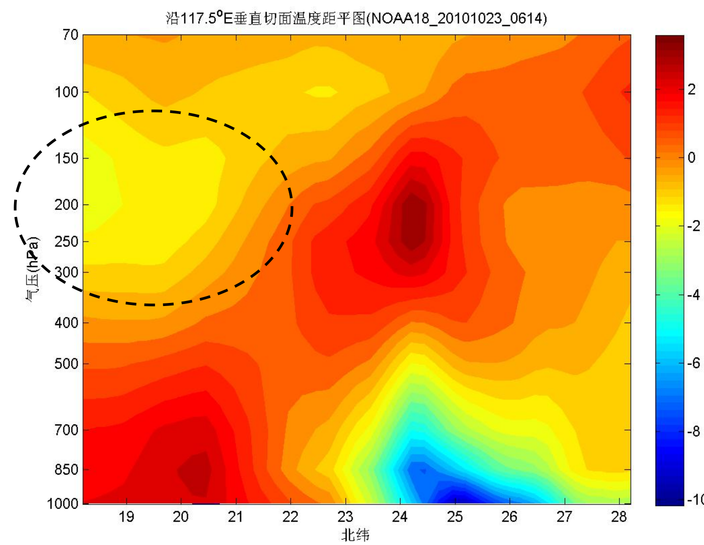

Cold air invading

Intensity Estimation of Typhoon by Microwave Temperature Sounder

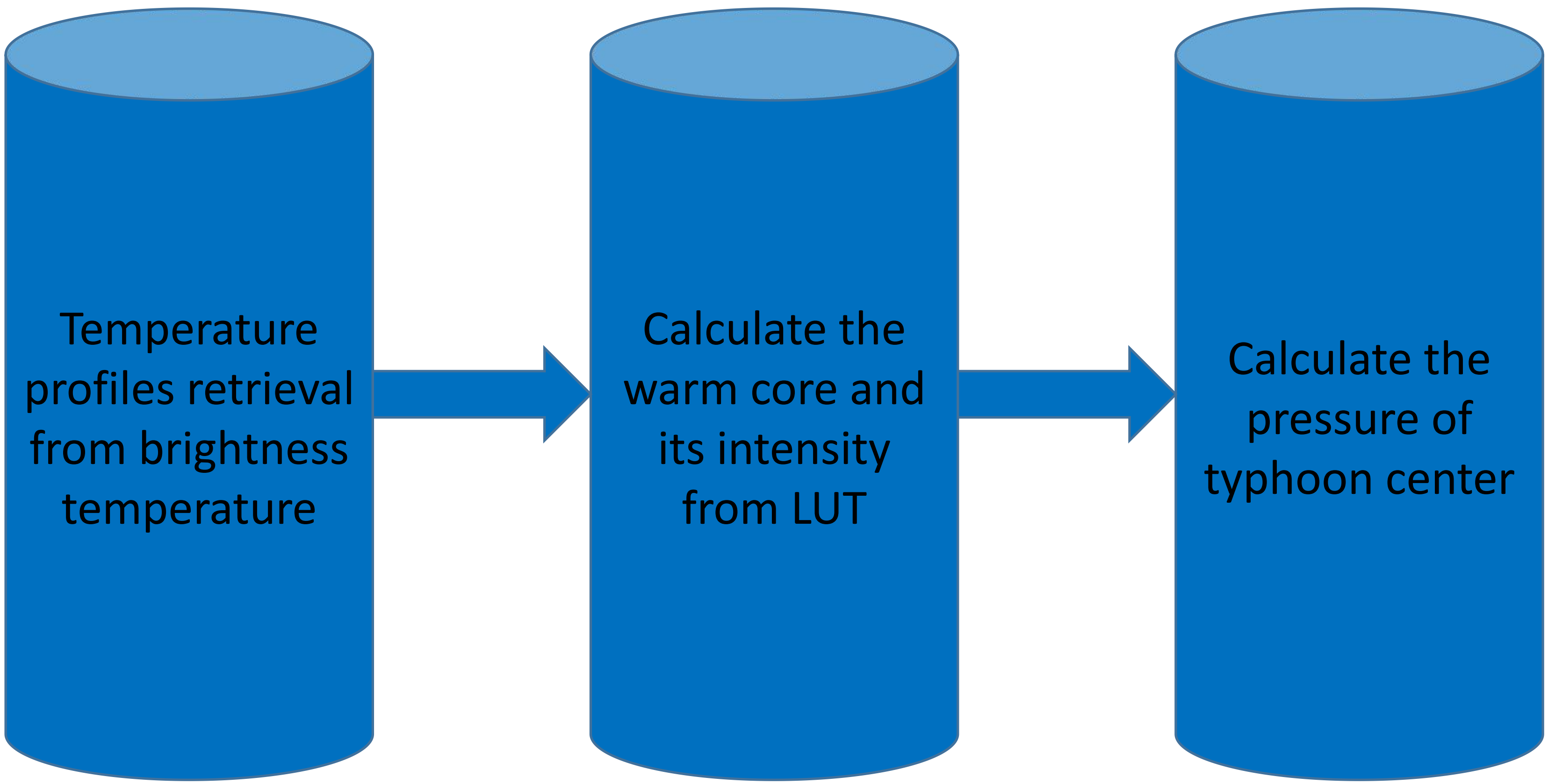

Intensity comparisons from estimation and best track of some typhoons in 2012

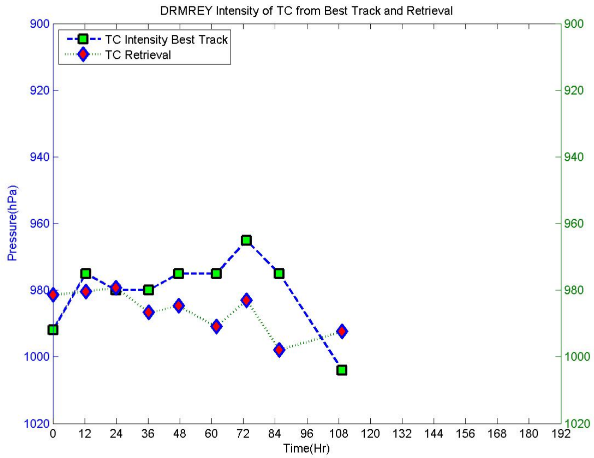

DRMREY(2012)

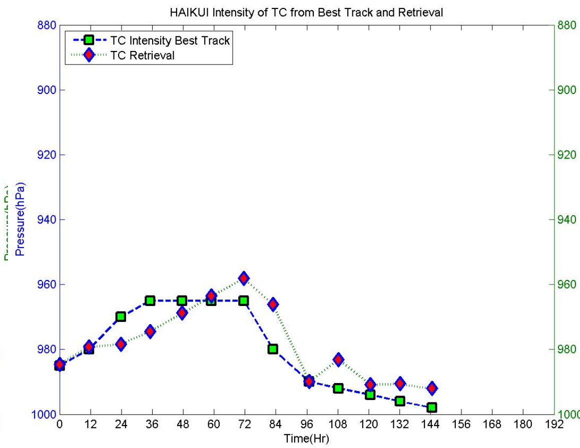

HAIKUI(2012)

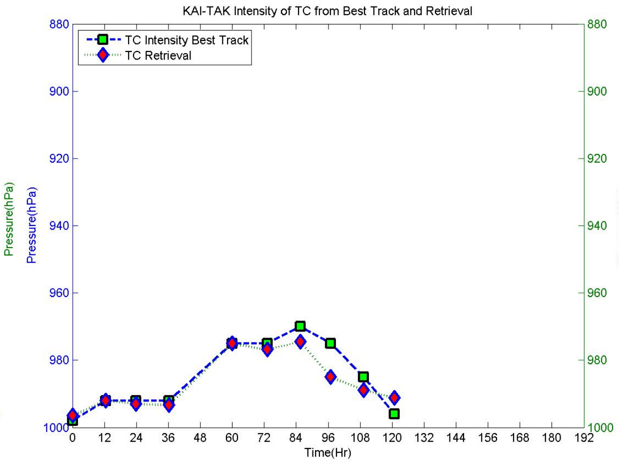

KAI-TAX(2012)

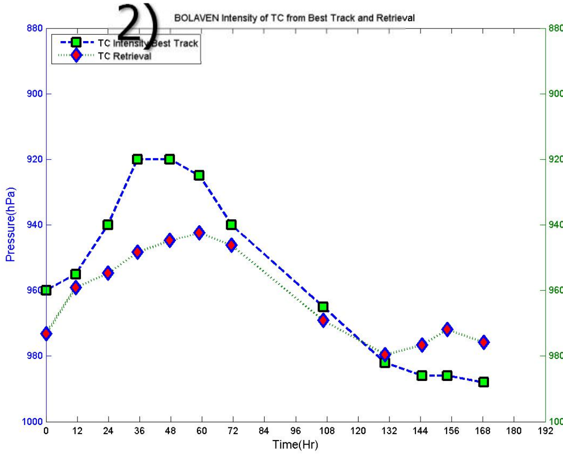

BOLAVEN(2012)

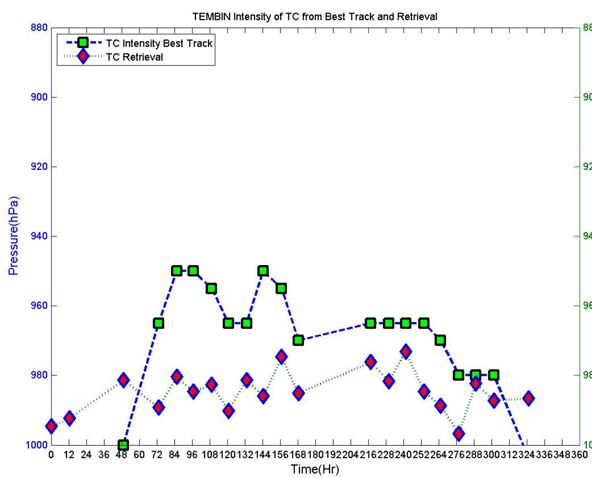

TEMBIN(2012)

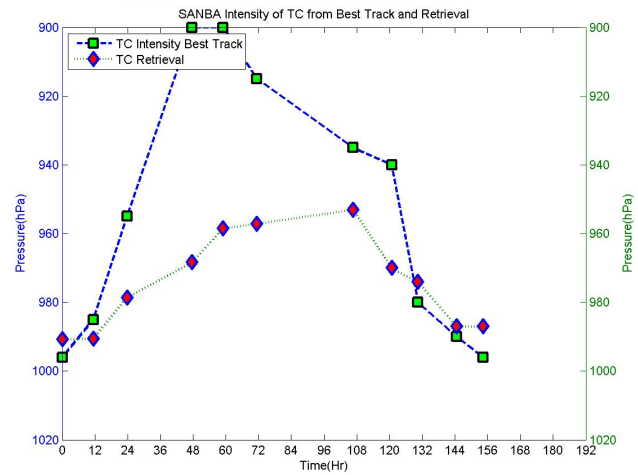

SANBA(2012)

MWHS Channel 1 with 15 km Resolution

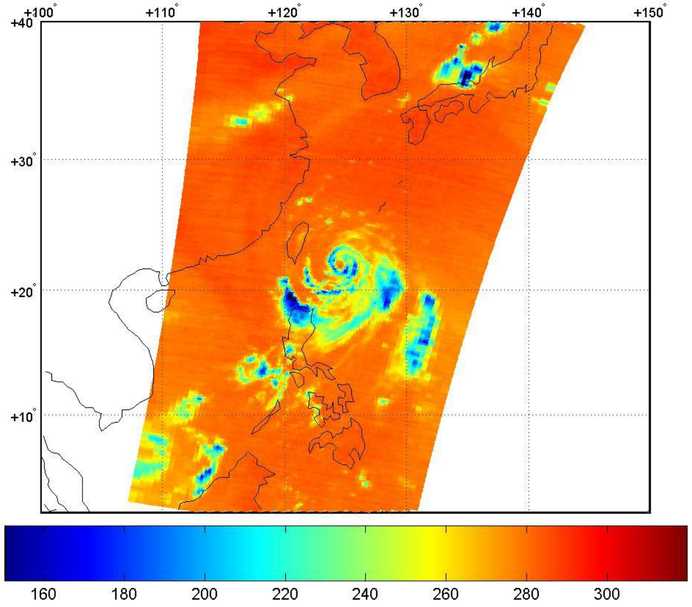

Water Vapor at 400hPa from MWHS

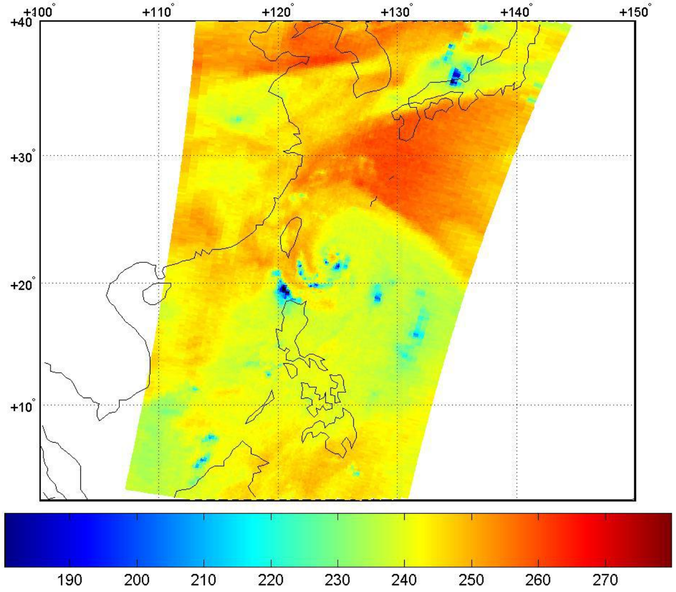

Water Vapor at 600hPa from MWHS

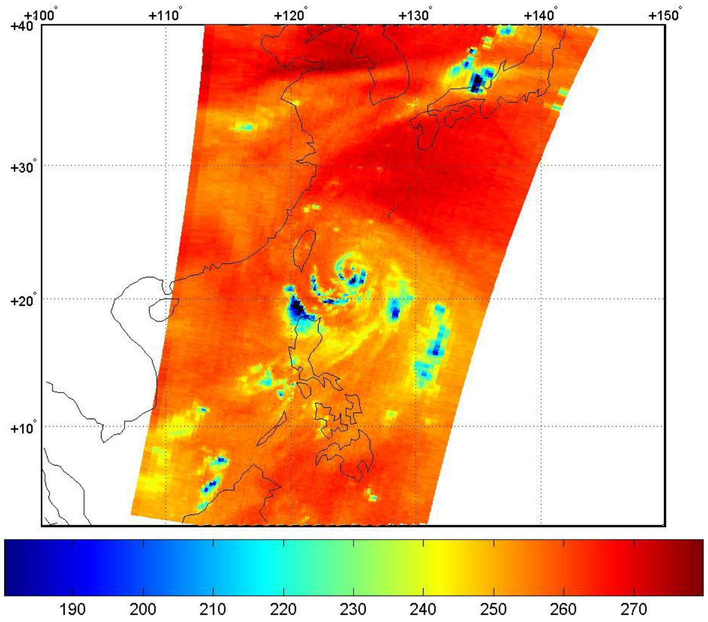

Water Vapor at 800hPa from MWHS

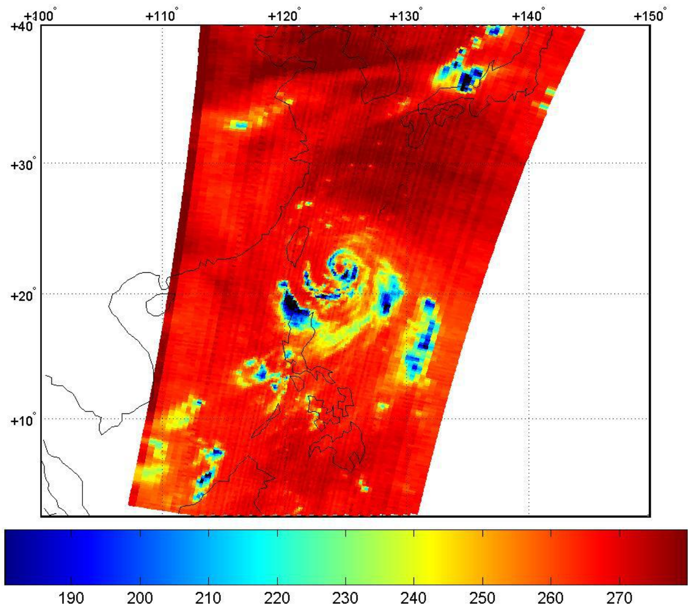

Water Vapor at 400HPa Variation within 24 Hours

subtropical high pressure

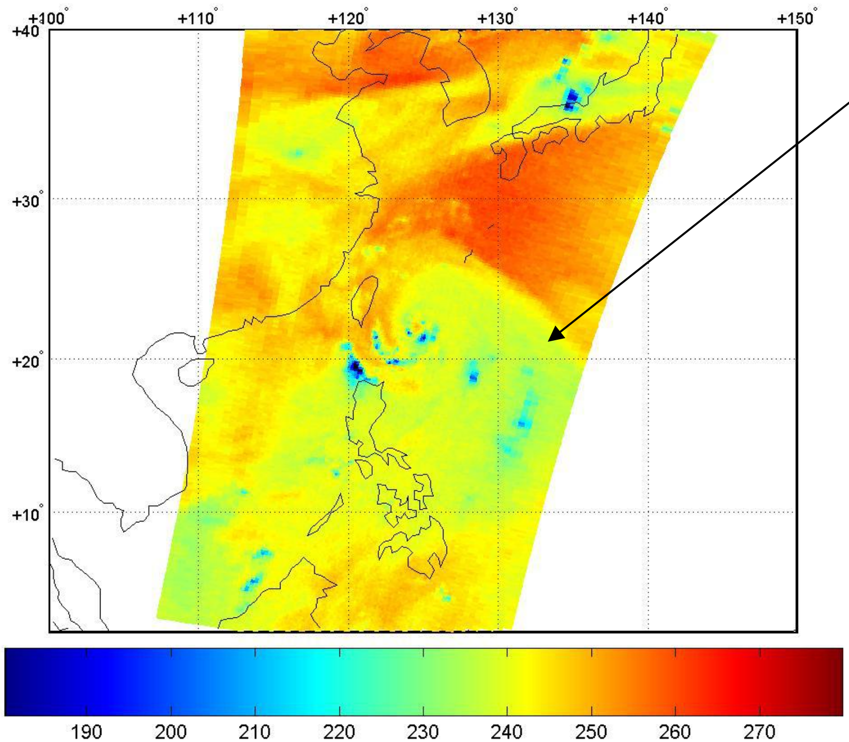

24 hours before

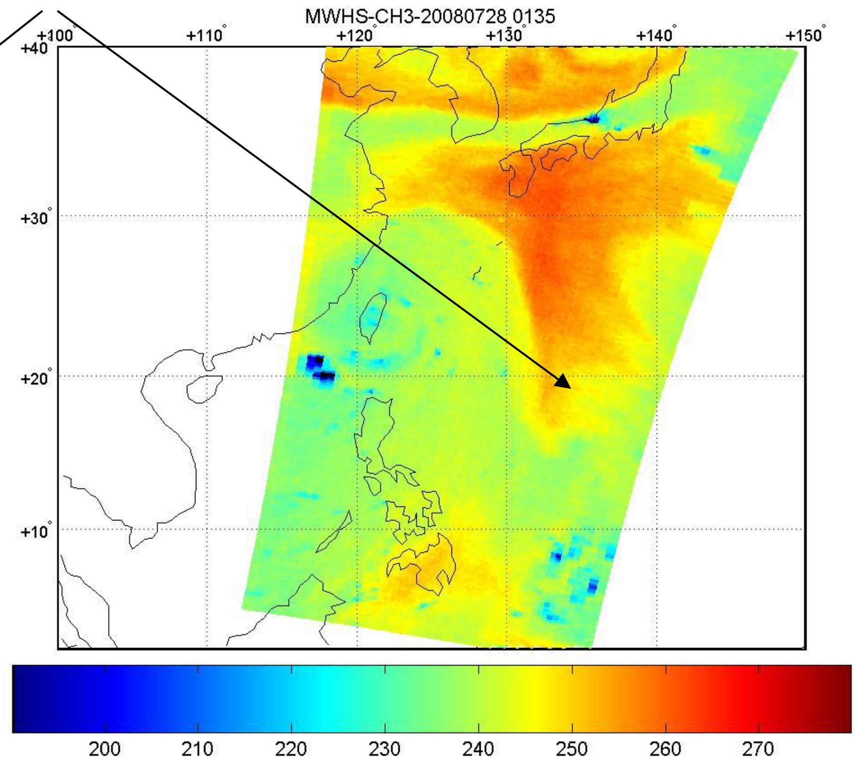

9:45 28 July, 2008

The shape of the subtropical high pressure has changed within 24 hours

The applications of Satellite Ocean Surface Vector Winds

Scatterometry Basics

- Scatterometer → active microwave imager
- Microwave energy sensitive to roughness of ocean surface generated by the surface winds
  - Small capillary-scale Bragg Waves
- By viewing the same patch of ocean from several angles, it is possible to derive wind speed and direction

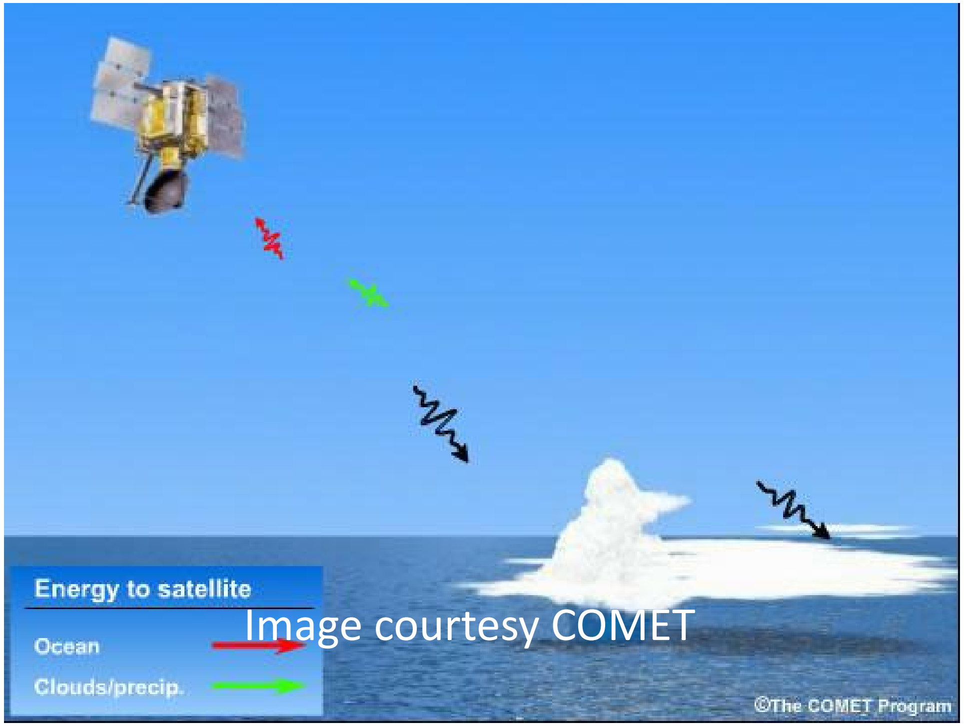

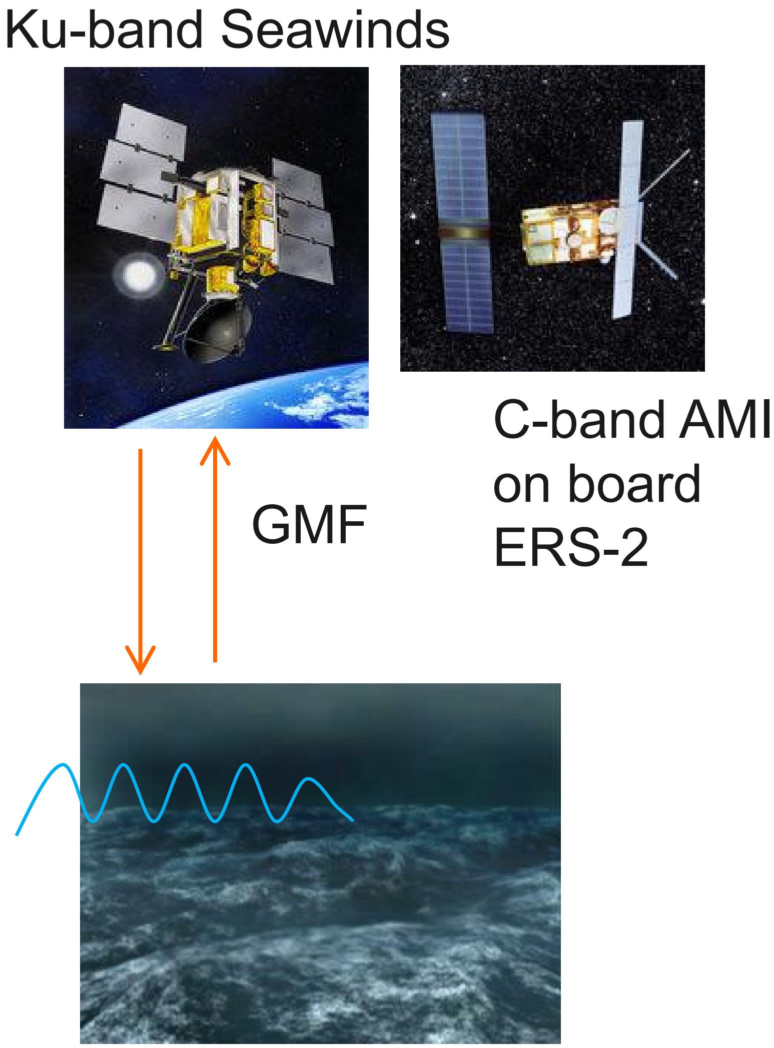

Scatterometer on
Polar-orbiting Satellites

- Measuring wind speeds and **wind directions** simultaneously
- Penetrate thick **Cloud and Precipitation**
- Continuous Observation
- Global Coverage

Instrument	Satellite	Operational Period	Frequency
SASS	Seasat	1978.6~1978.10	Ku
AMI/SCAT	ERS-1	1991.7~2000.3	C
AMI/SCAT	ERS-2	1995.4~2011.7	C
NSCAT	ADEOS-1	1996.8~1997.6	Ku
Seawinds	QuikSCAT	1999.7~2009.11	Ku
Seawinds	ADEOS-2	2002.12~2003.8	Ku
ASCAT	MetOp-A	2006.10~	C
ASCAT	MetOp-B	2012~	C
OSCAT	OceanSAT	2009~2014.2	Ku
RapidSCAT	ISS	2014~	Ku
HY-2	HY-2A	2011~	Ku

- Several generations of wind scatterometers have been flown in space by NASA, ESA, NASDA and National Satellite Ocean Application Service in China.
- A dual-frequency scatterometer (WIFIR) to be onboard FengYun-3E will be lauched in 2019.

Ocean Vector Surface Vector Winds Constellation

Current status and Outlook – NRT data access

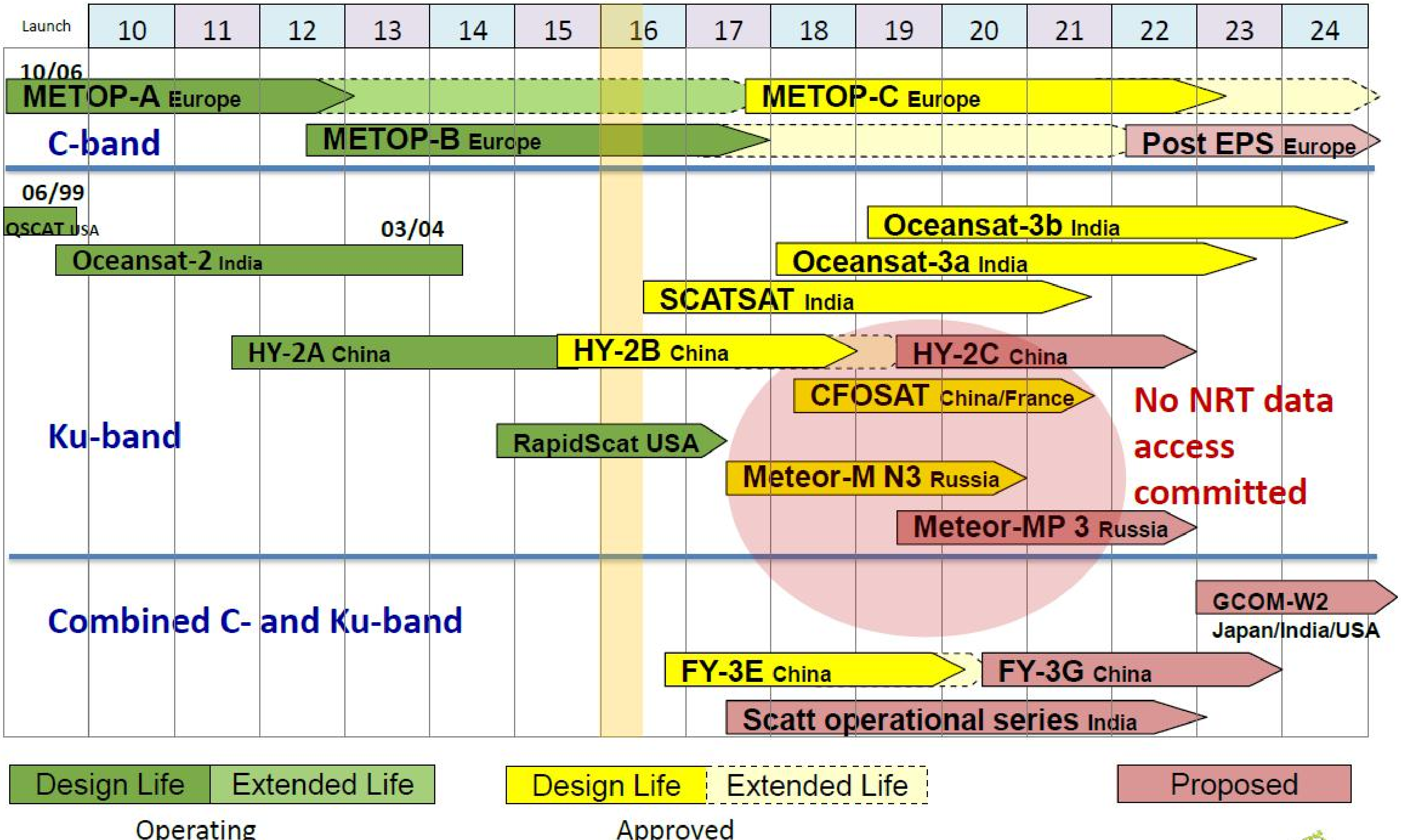

Advanced SCATterometer (ASCAT)

Sensor: Microwave radar
Spacecraft: MetOp-1, 2, 3
Launch: 2006, 2012, 2017
Heritage: ERS-1, 2

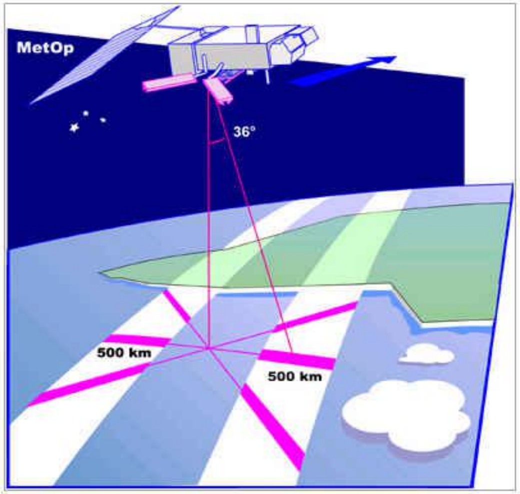

Channel: 5.25 GHz, C-band

Swath: Two 520-km swaths, with 700-km nadir gap

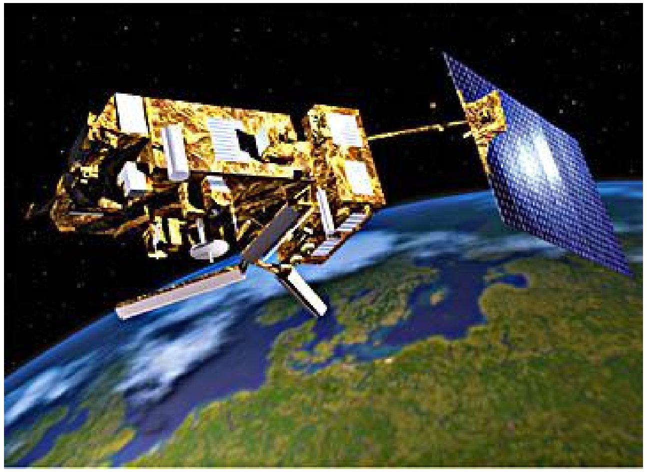

Enhancements for TC Applications:
((1)) Only long term operational scatterometer series
((2)) C-band, less rain contamination, larger footprint
((3)) 25- and 50-km wind vector products, good for winds up to gale force winds
((4)) Gap in swath center is a major drawback for coverage
((5)) 60% of QuikSCAT's coverage

NOAA processed data: http://manati.orbit.nesdis.noaa.gov/datasets/ASCATData.php

Distribution and accuracy of ASCAT wind

ASCAT wind speed global map

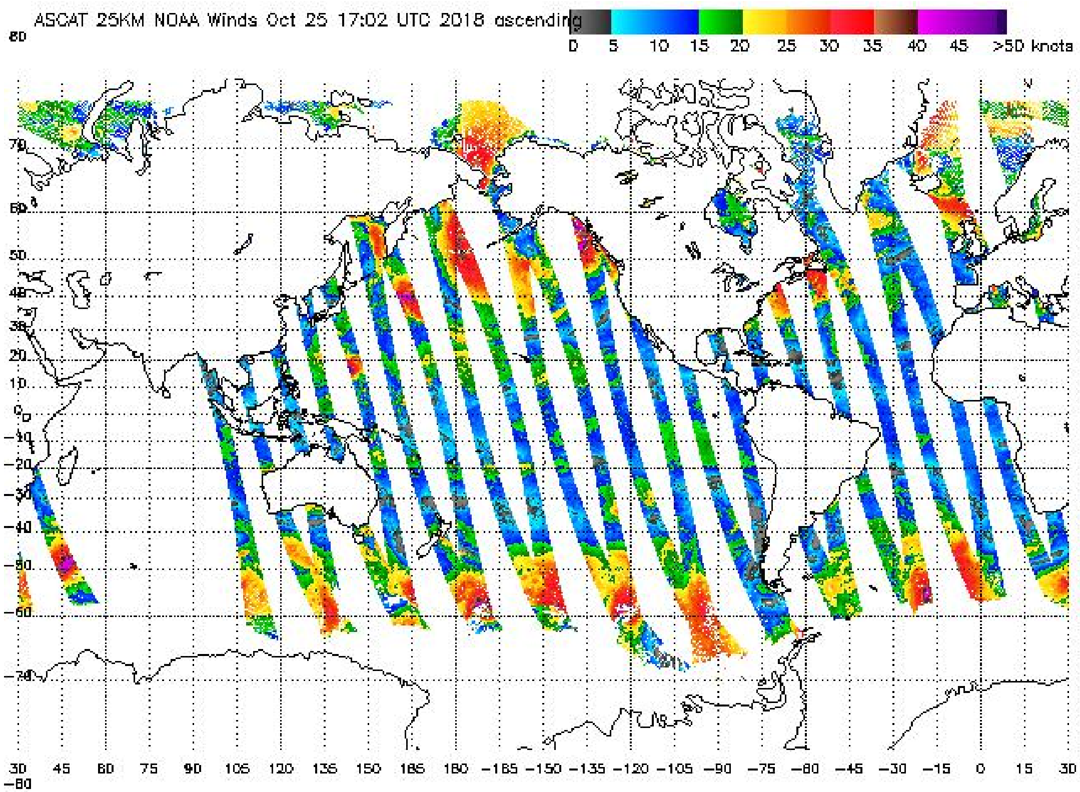

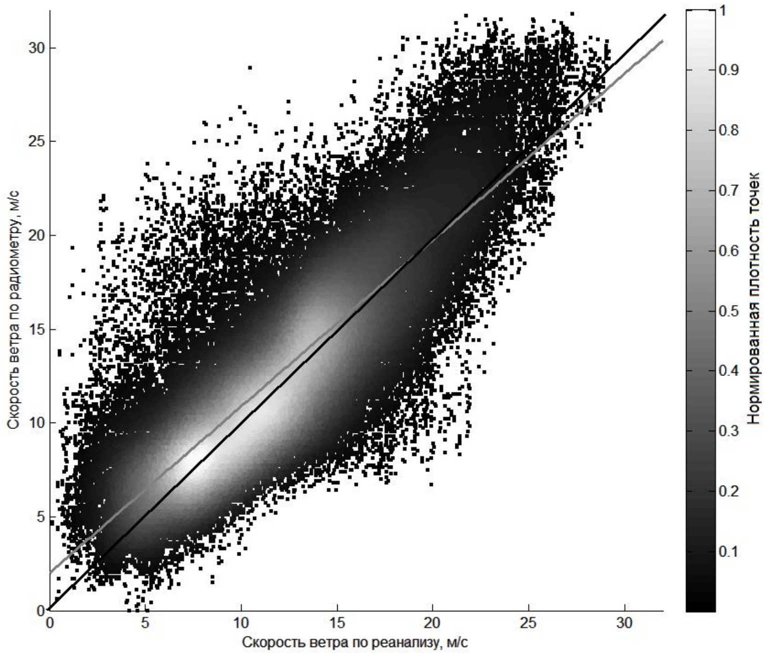

Comparison of ASCAT and reanalysis

Example of ASCAT Use

Analysis of weather systems

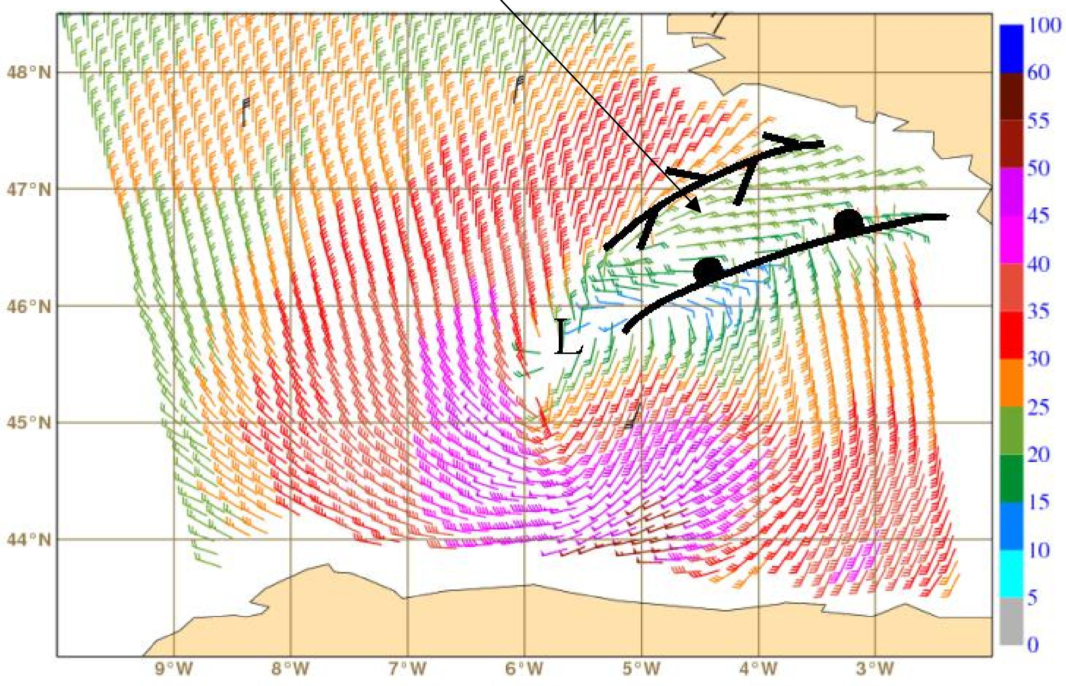

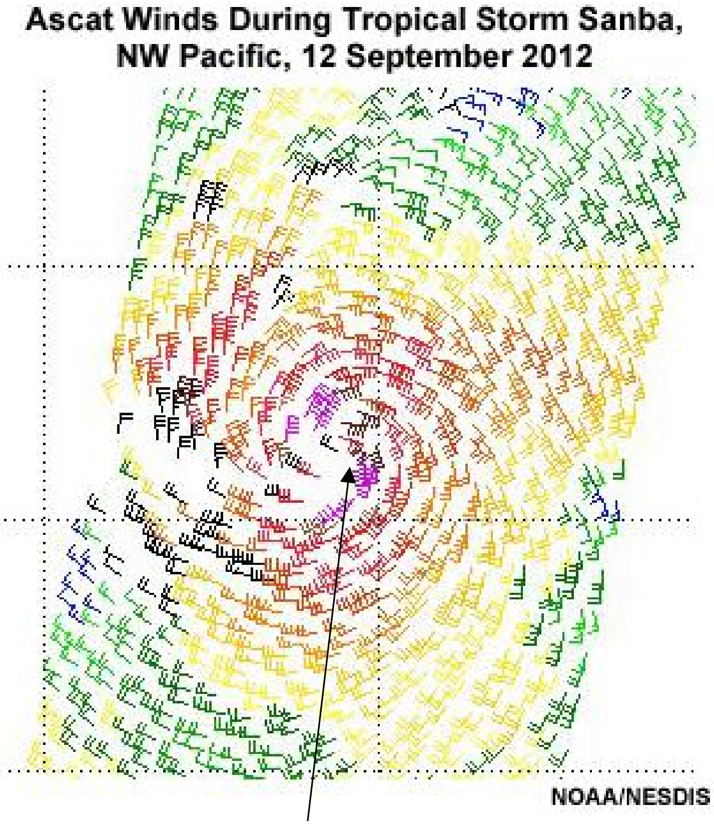

Typhoon positioning

Example of ASCAT Use
TC Center Fixing

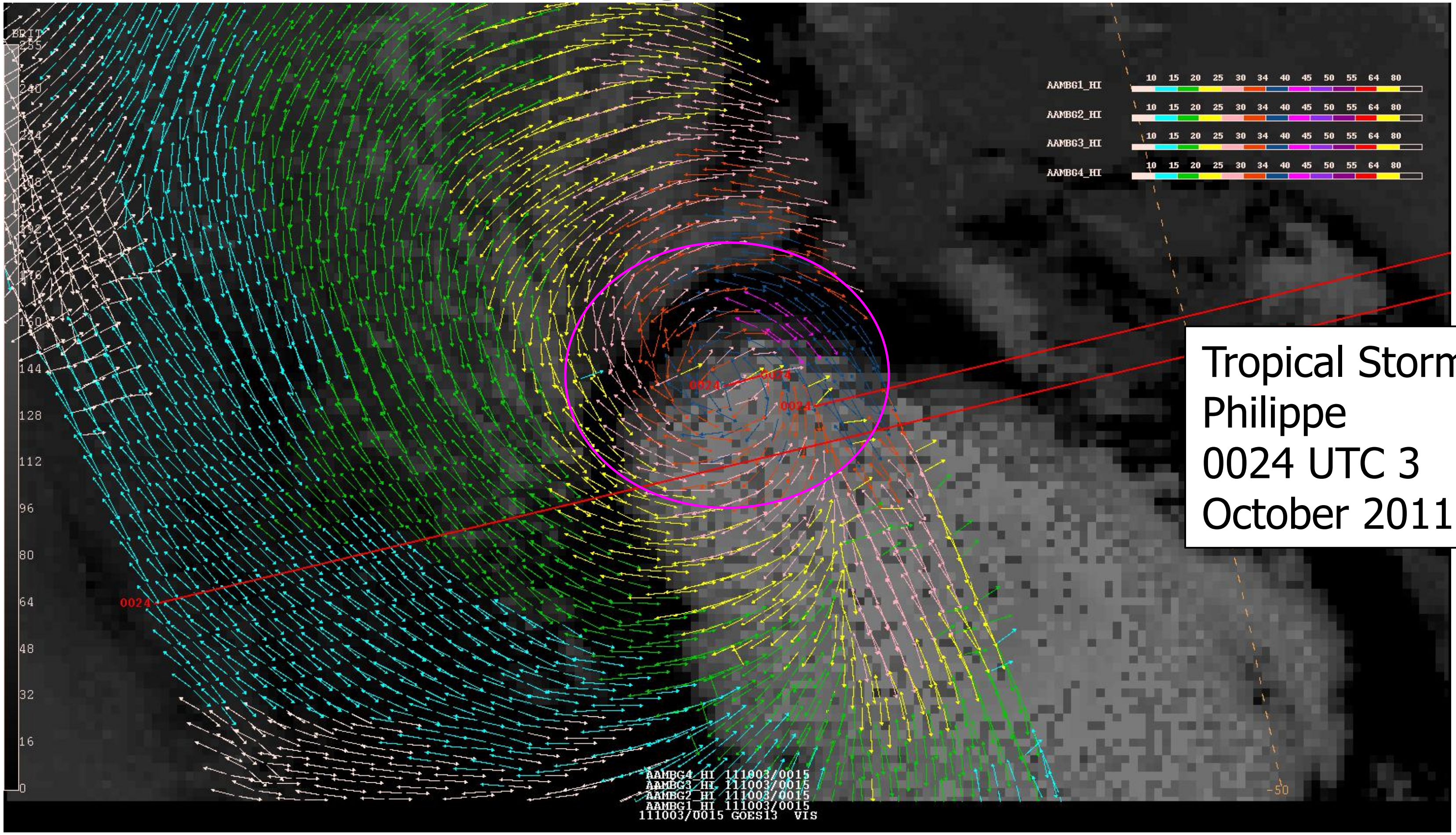

- Reduced rain contamination and prevalence of 3rd and 4th ambiguities in areas of low winds makes center fixing with ASCAT somewhat easier than with QuikSCAT if the pass samples the center location

Example of ASCAT Use

TC Intensity Analysis

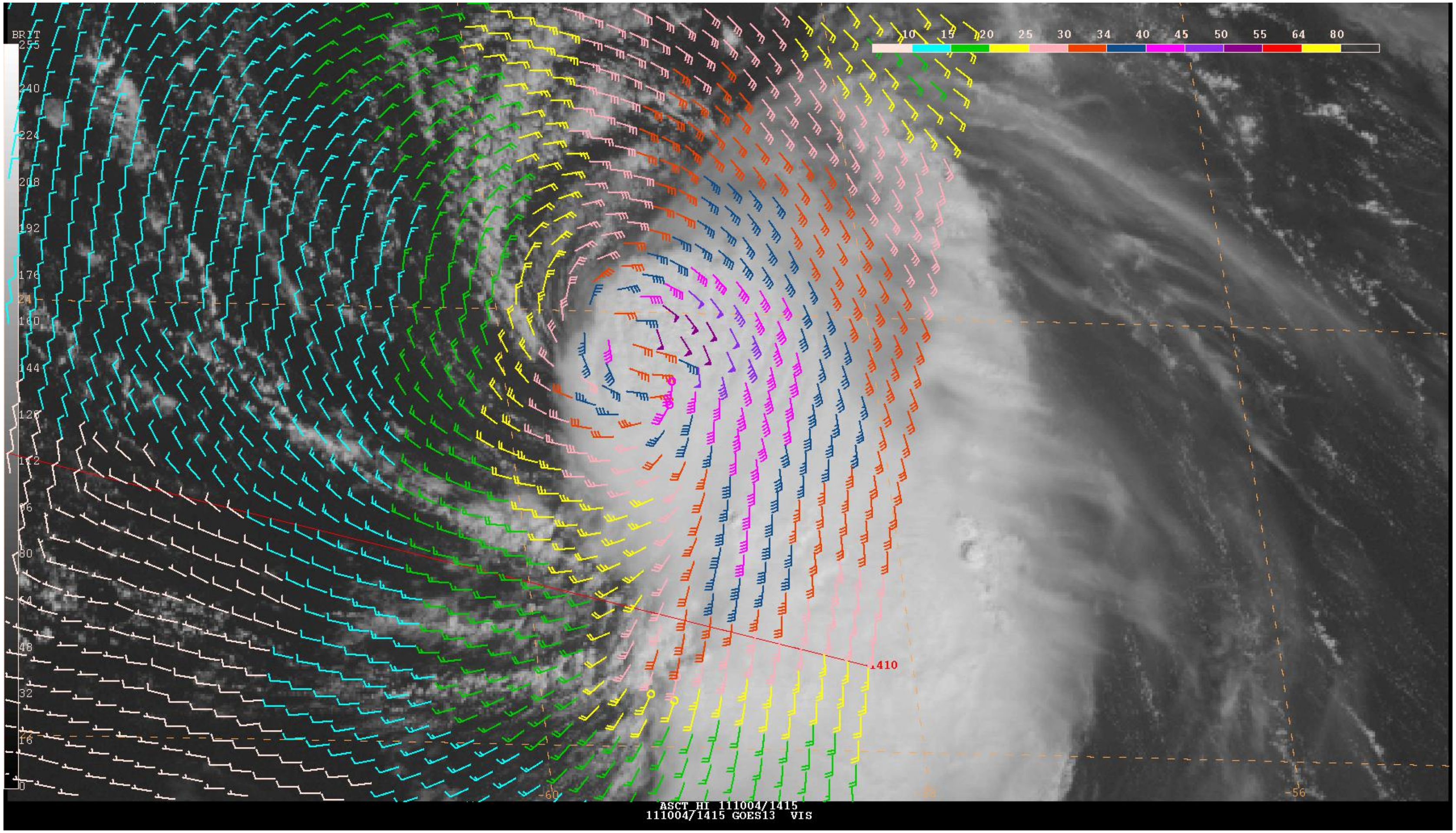

- ASCAT pass over Tropical Storm Philippe at 1410 UTC 4 October 2011 revealed the cyclone to be stronger (50-55 kt) than suggested by Dvorak satellite intensity estimates (45 kt)
- It is difficult to assess the peak intensity with ASCAT however due to spatial sampling considerations, especially in stronger TCs

Comparison of 12.5Km and 25Km resolution products in Offshore China

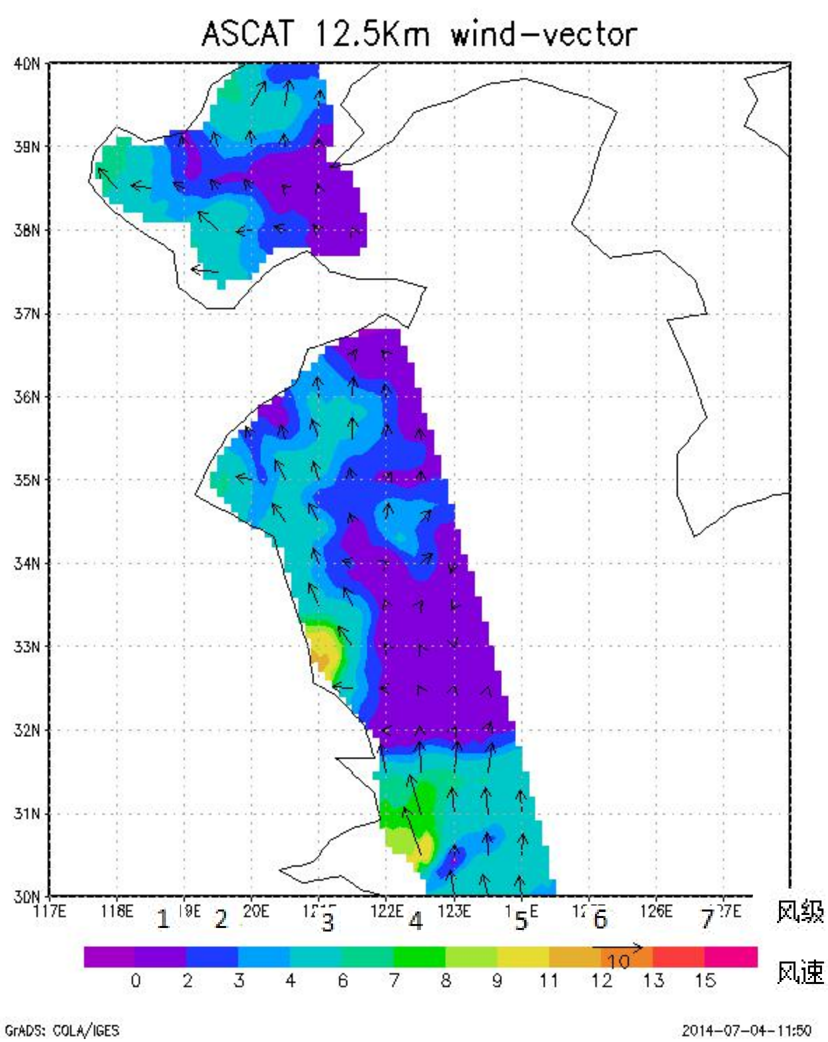

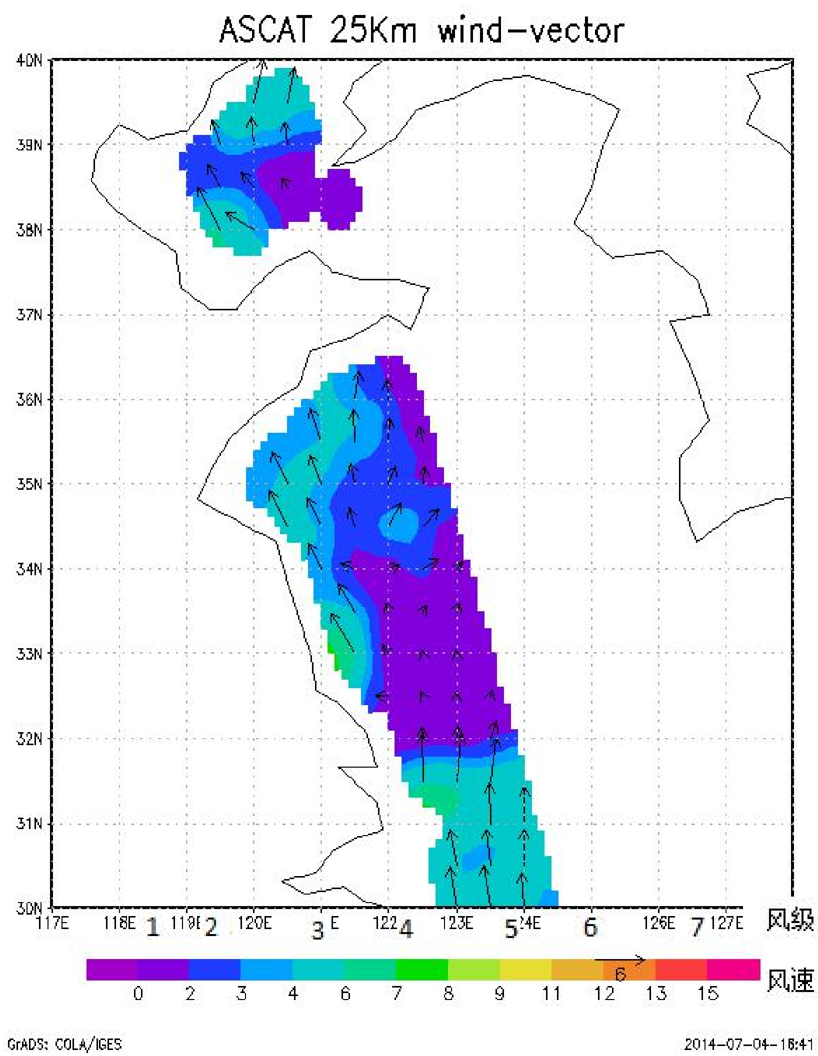

HY-2 satellite instruments

- **Radar altimeter**
  - Operating frequency: 13.58MHz, 5.25GHz
  - High precision: <4cm (under the star)
  - Sea and land observation function
- **Microwave scatterometer**
  - Operating frequency: 13.256GHz
  - Swath: H polarization > 1350km,

    V polarization > 1700km

    (much wider than Quickscat and ASCAT)

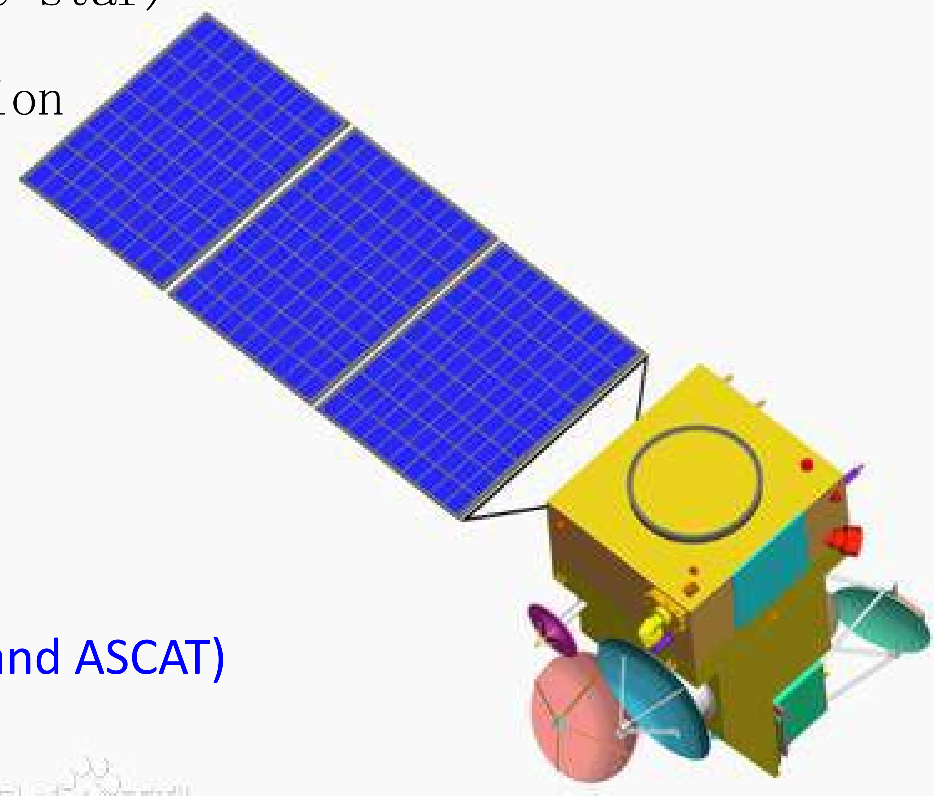

HY-2 satellite remote sensing product

Evaluation of accuracy of main parameters in data products

- **→Sea surface altitude**

  The sea surface altitude measurement accuracy is 6.3 cm; JASON-2 is 5.4 cm.

- **→Effective wave height**

  The accuracy is 29cm estimated using buoy; JASON-2 is 27cm.

- **→Sea surface wind field**

  The wind speed accuracy is better than 2m/s; the wind direction accuracy is better than 20 degrees that is equal to ASCAT.

Distribution of main ocean parameters from HY-2 satellite product

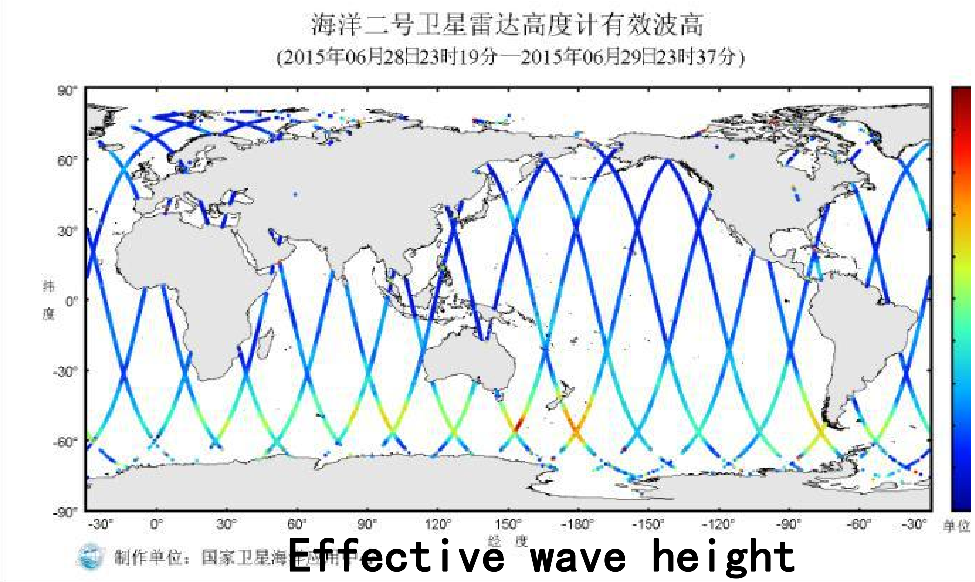

Effective wave height

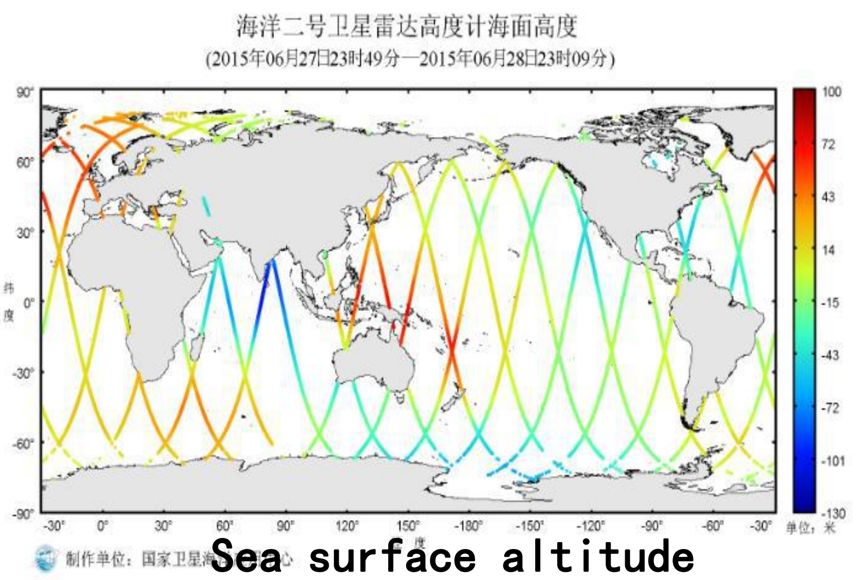

Sea surface altitude

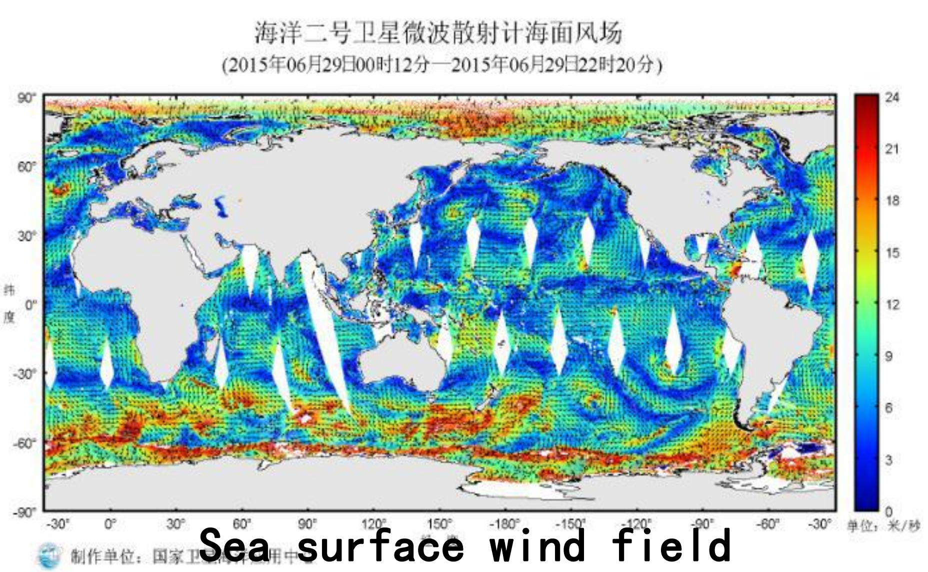

Sea surface wind field

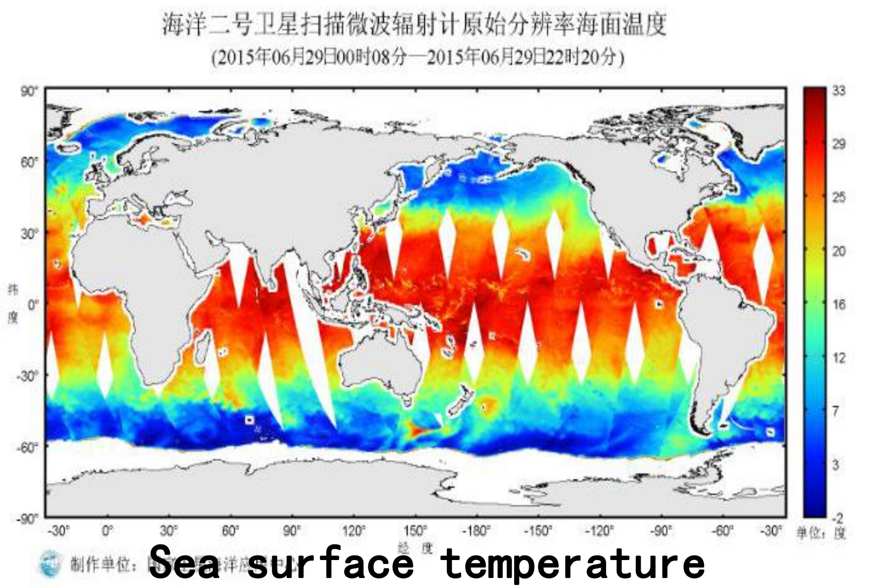

Sea surface temperature

- In July 2015, HY-2 satellite continuously monitored typhoon “Chan-hom” and “Nangka”, providing effective information for marine weather forecasting, disaster prevention and mitigation.

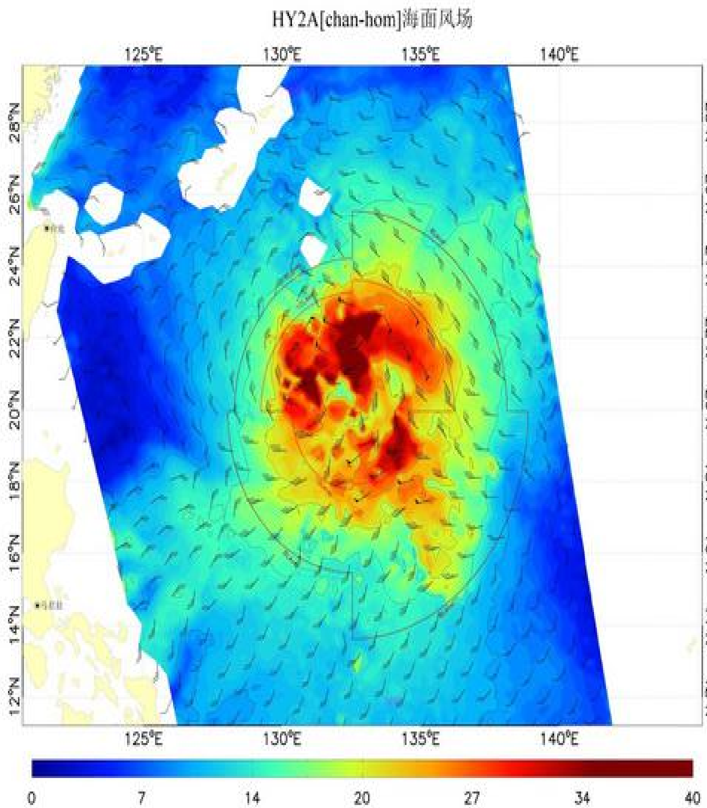

Typhoon ″Chan-hom″ landed in Zhoushan, Zhejiang Province around 16:40 on the 11th, becoming the strongest typhoon that landed in Zhejiang in July 1949.

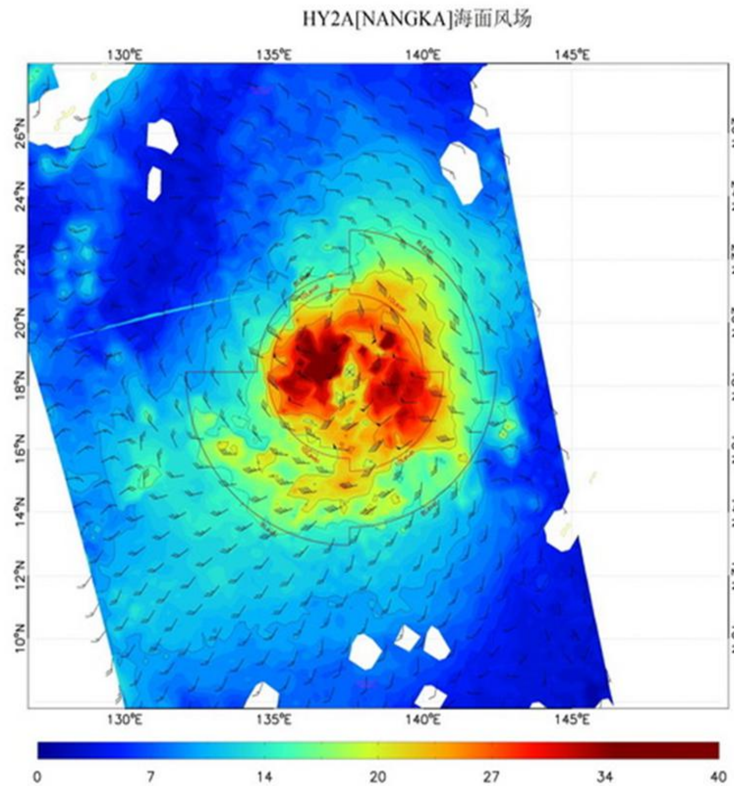

The typhoon Nangka is located at 18° north latitude and 137° east longitude at 09:00 on July 12, with a maximum wind speed of 38m/s.

TC monitoring examples from SWAP

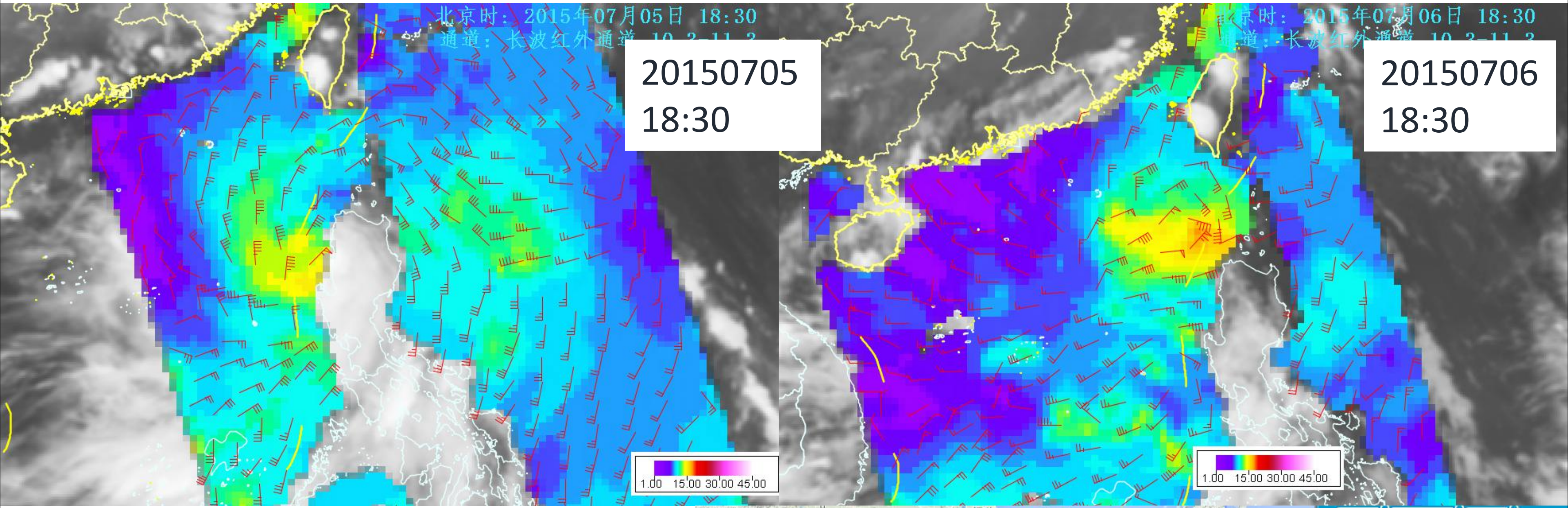

Monitoring of Severe Tropical Storm 'LINFA'(201510) by HY-2A

——from SWAP platform

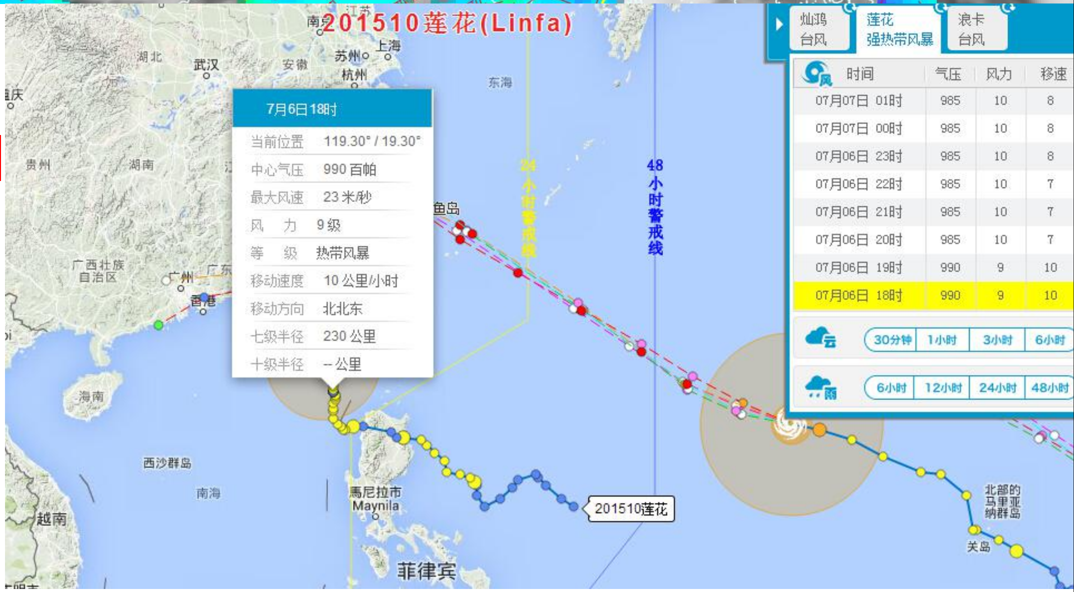

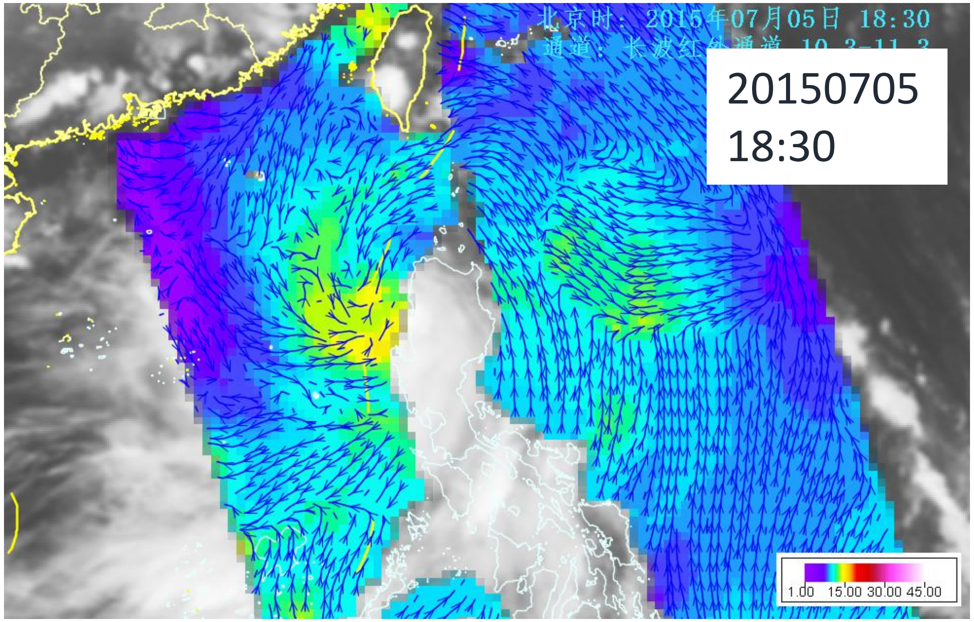

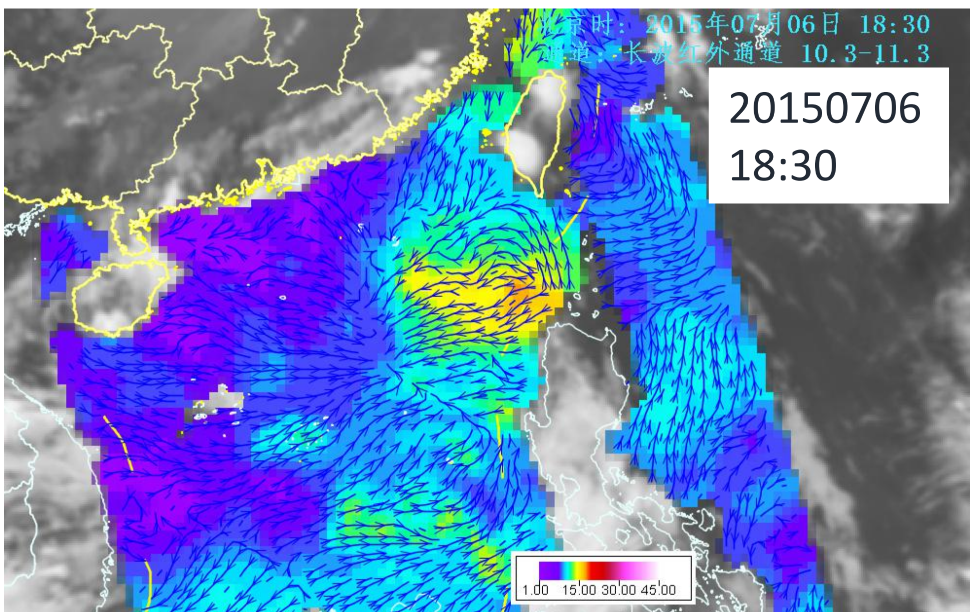

Monitoring of Severe Tropical Storm 'LINFA'(201510) by HY-2A

Flow field analysis

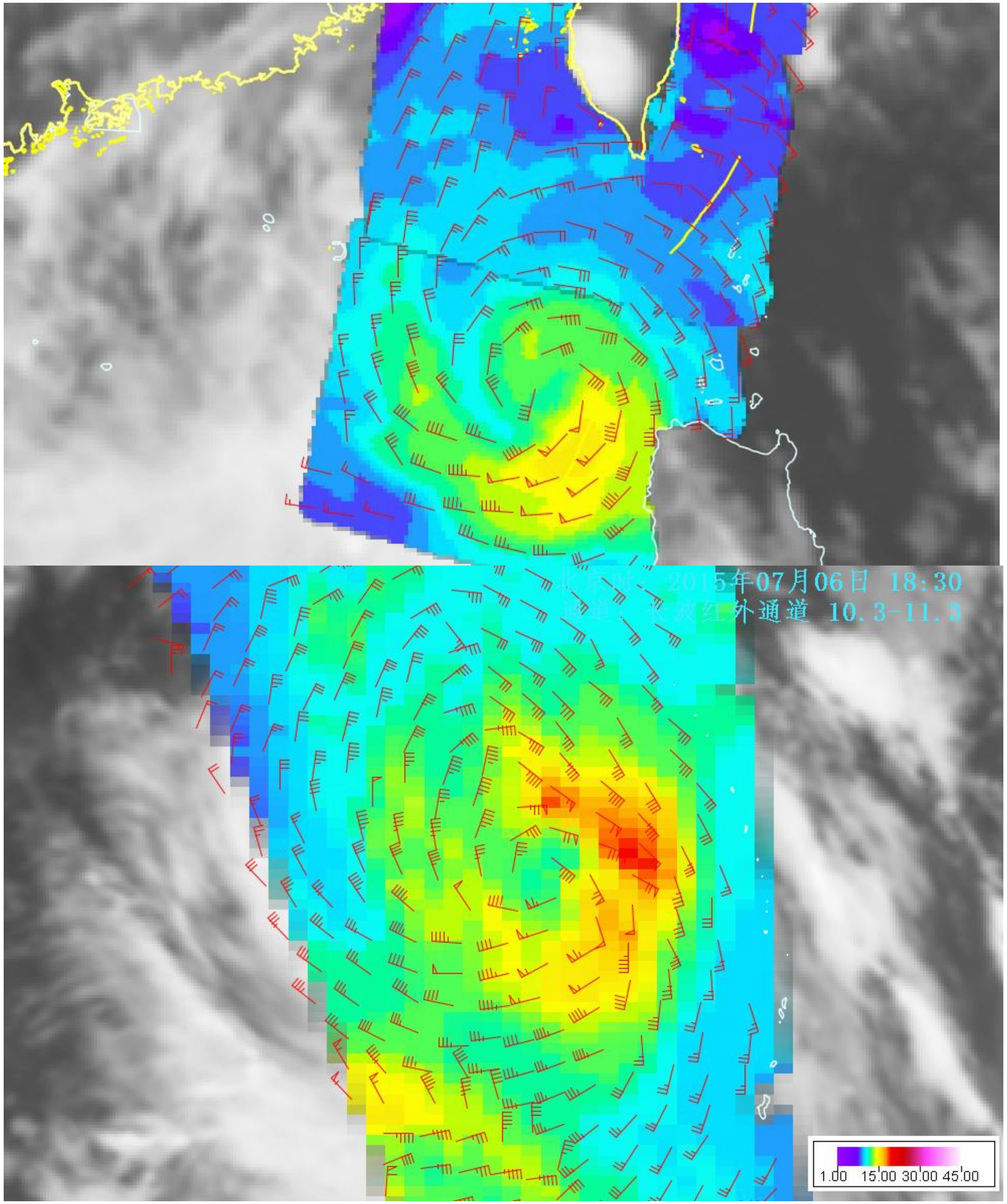

Monitoring of Severe Tropical Storm ‘LINFA’(201510) and Typhoon ’CHAN-HOM’(201509) by ASCAT onboard MetOp from SWAP platform

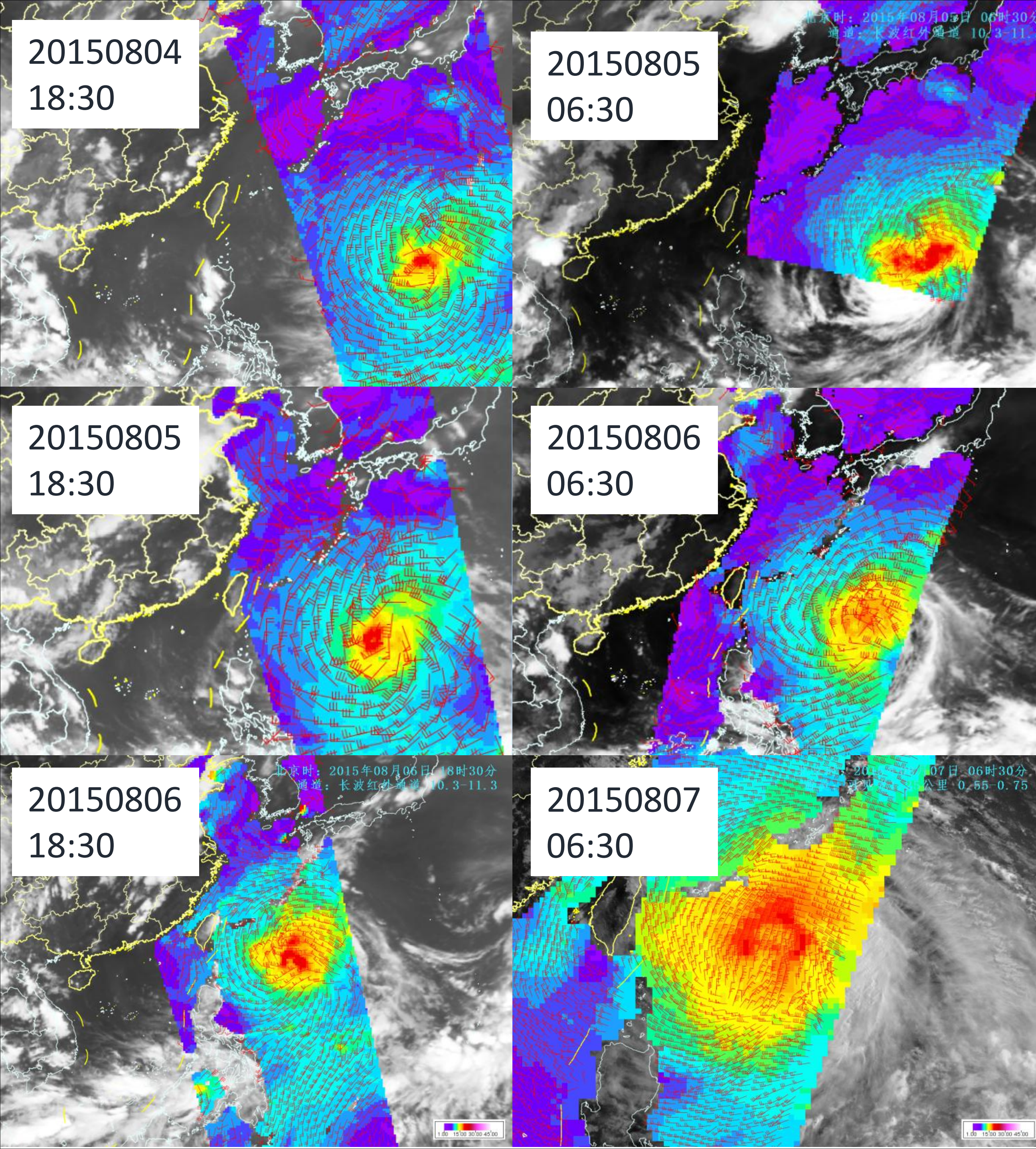

Continuous monitoring of Typhoon 'Soudelor'(2015 13) by HY-2

October 28~30, 2012, the "Sandy" hurricane swept across the eastern coast of the United States. The HY-2A satellite successfully observed the hurricane and its moving direction on the 27th, which provided an early warning of landing on the 28th. . The HY-2A satellite was the only satellite in the world to obtain information on wind and waves during the hurricane.

Changes in wind field and wave height during Hurricane Sandy
(Left: wind field from Microwave scatterometer. Right: effective wave height from radar altimeter)

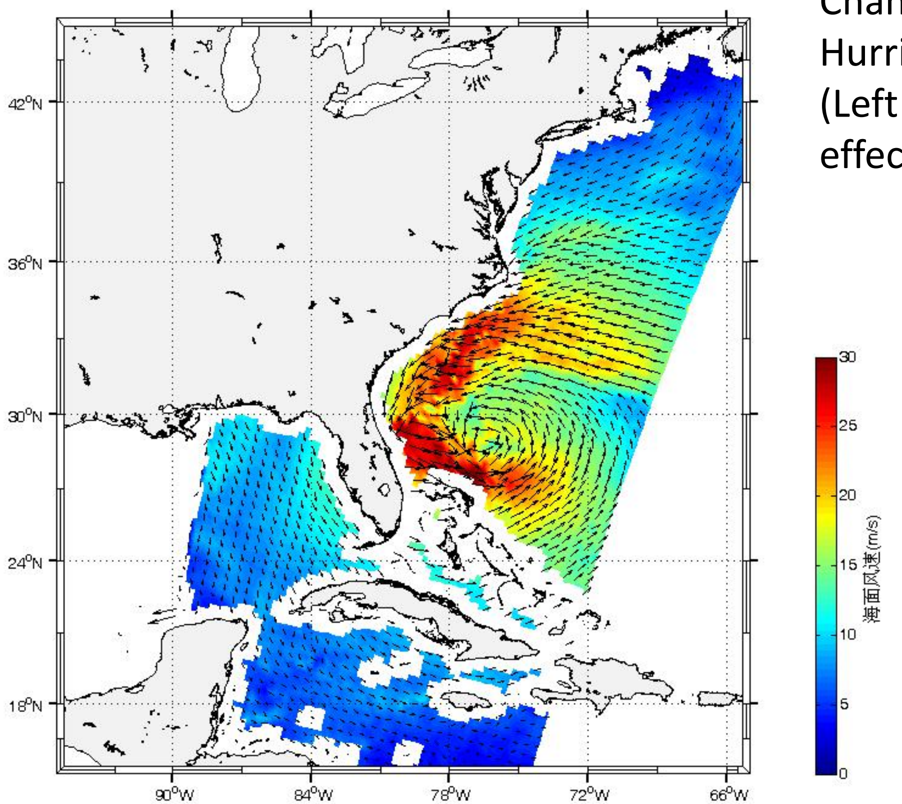

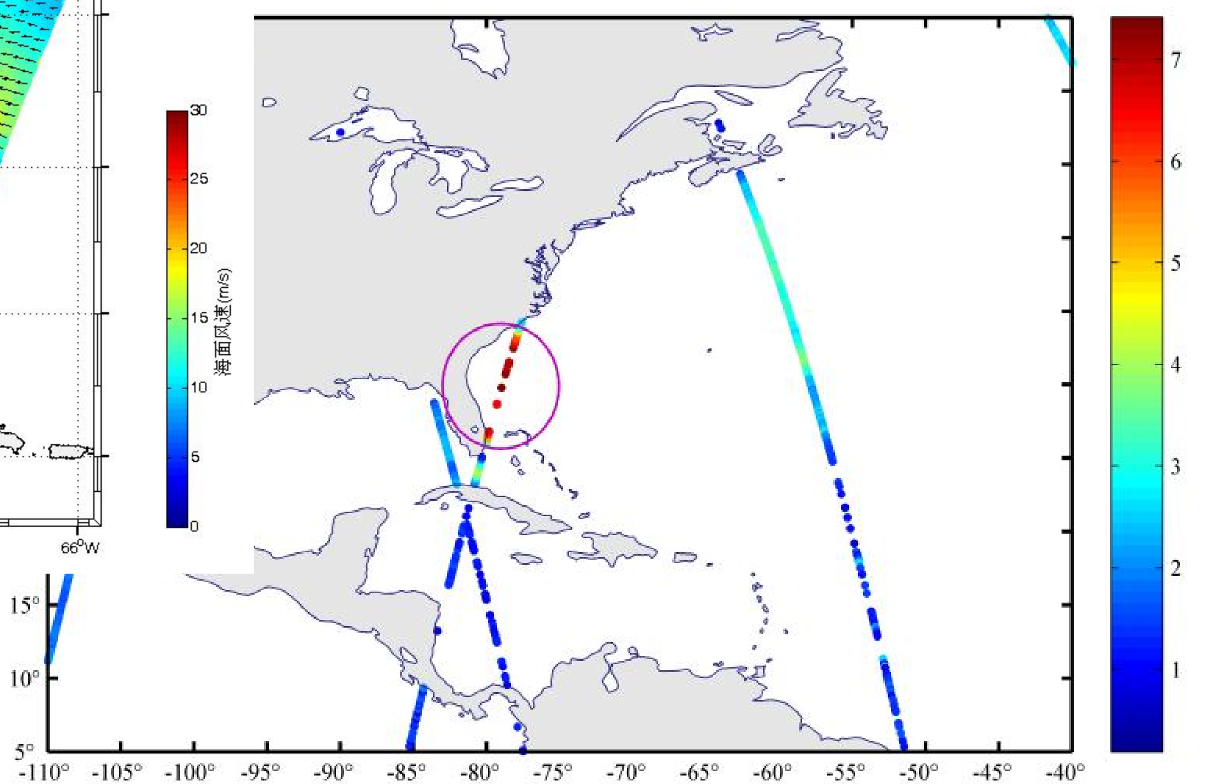

Joint application of wind field products by multi-sensor

Metop/ASCAT

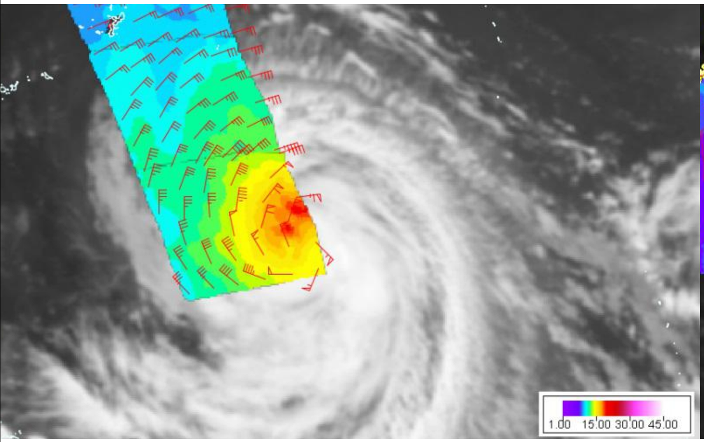

Metop/ASCAT

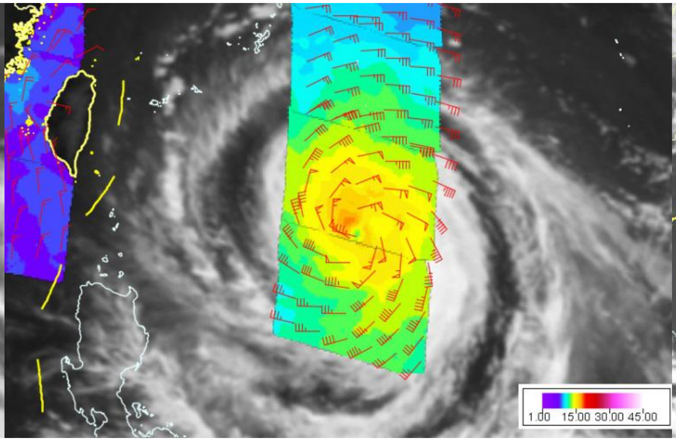

HY-2

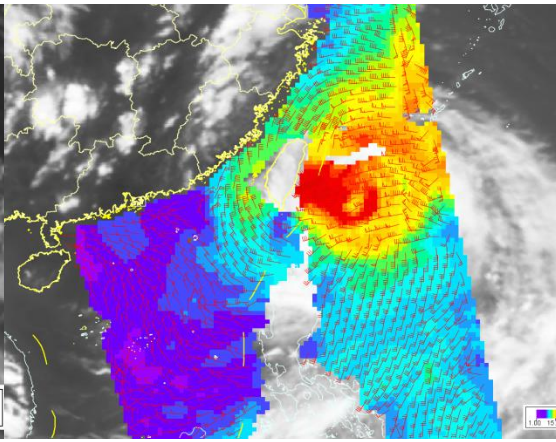

Sea surface wind speed product retrieved by FY-3 microwave imager

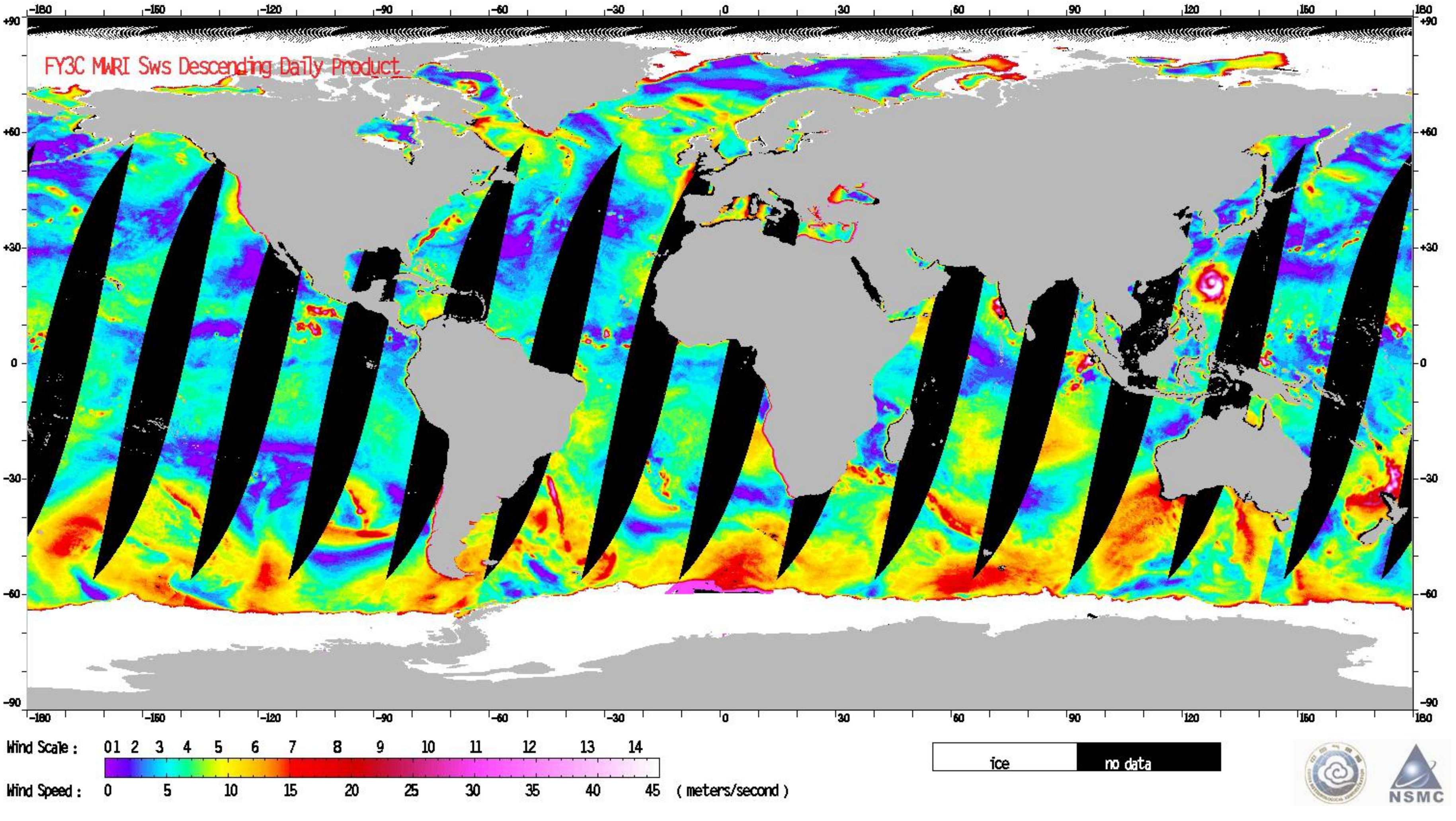

Sea surface wind speed product retrieved by FY-3 microwave imager

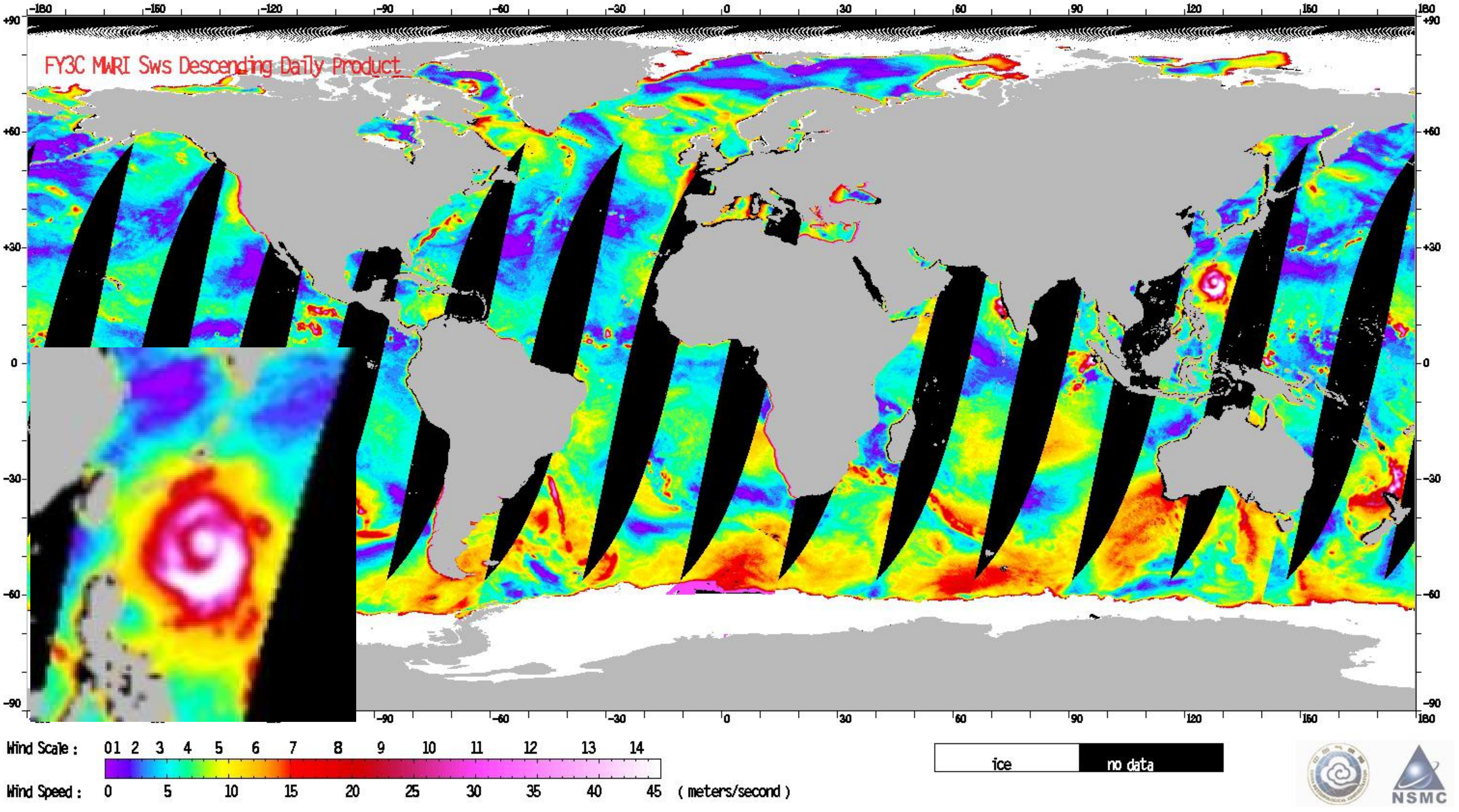

Scatterometer / radiometer

	"NEOGURI" 7.7	"RAMMASUN" 7.18	"MATMO" 7.22
ASCAT	25m/s	25m/s	25m/s
FY3-WMRI	45m/s	45m/s	45m/s
Ture	55m/s	52m/s	40m/s

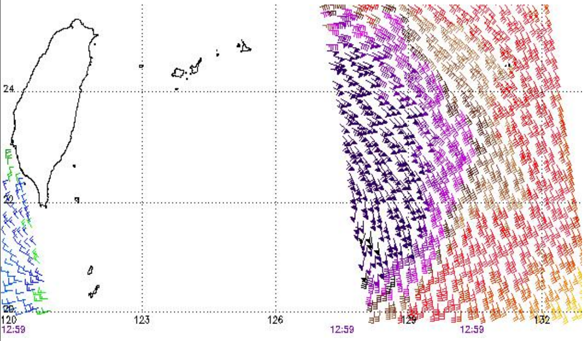

"Neoguri" 7.7

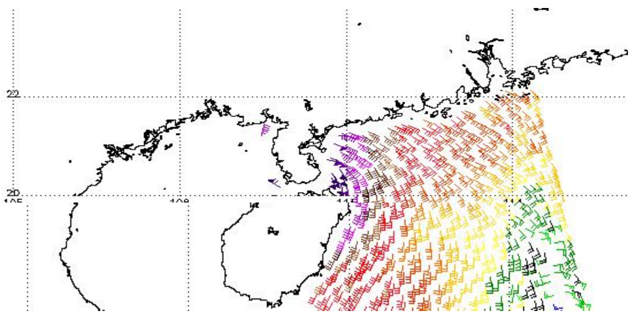

"Rammasun" 7.18

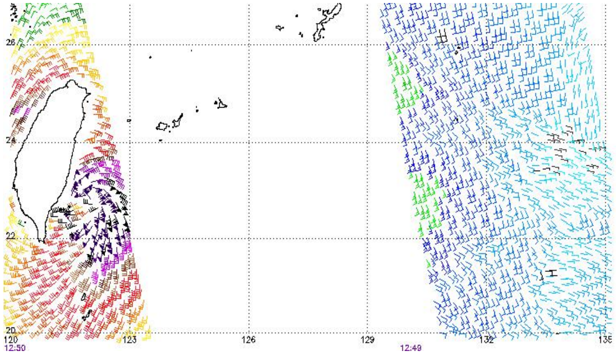

"Matmo" 7.22

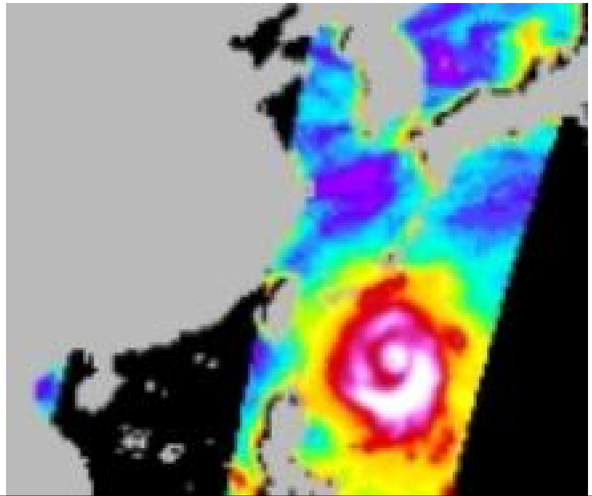

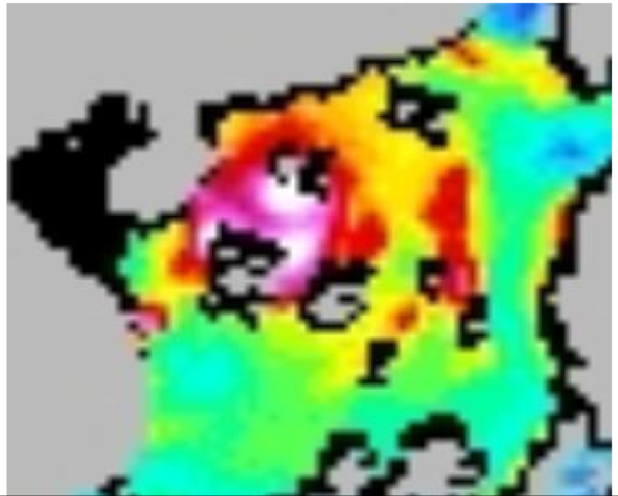

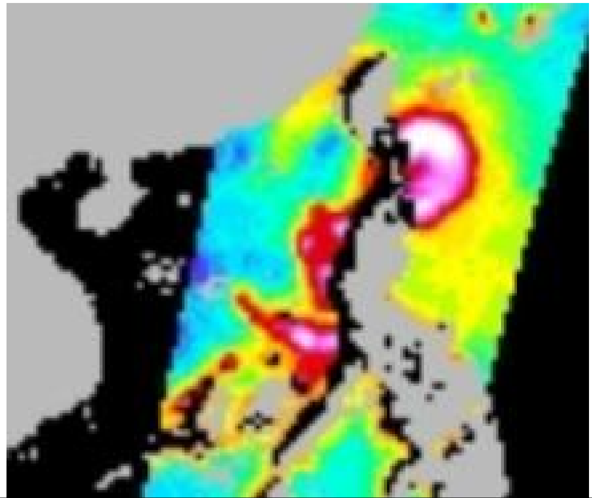

GF-3 typhoon wind field retrieval

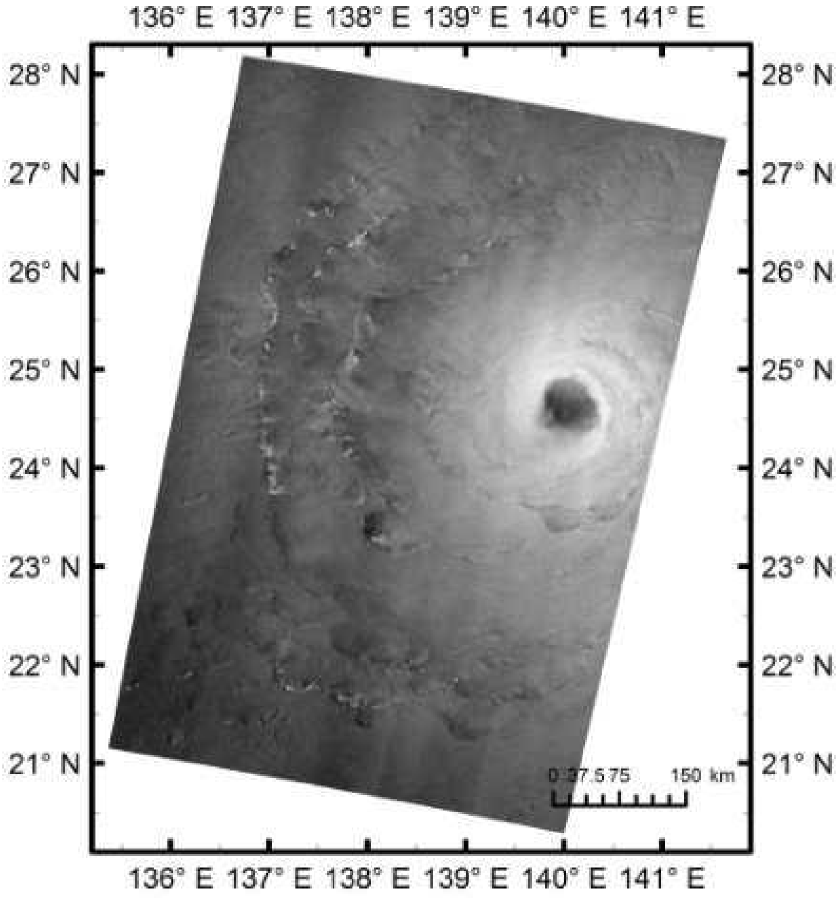

Shooting typhoon

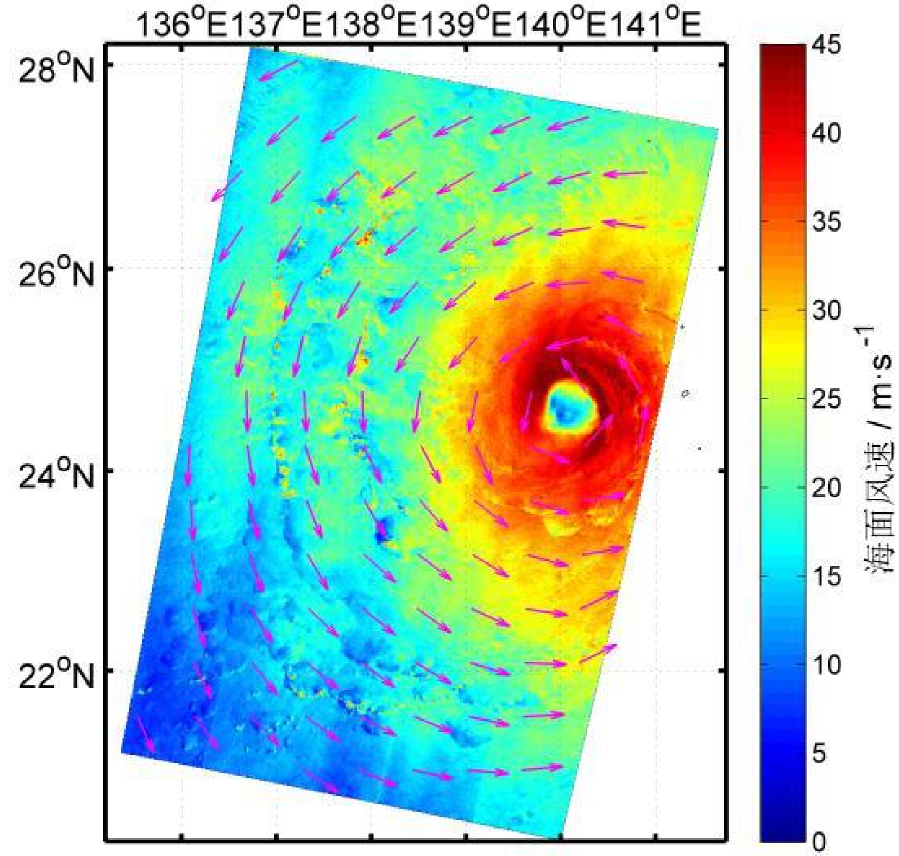

Retrieval of typhoon

- The GF-3 satellite retrieved (24.64N, 140.01E) typhoon wind speed and direction on August 18, 2018 with a resolution of 500 meters and a range of 300x600km; Eye, sea wind, wind direction and spiral Rain belt was shown.

GF-3 High resolution sea wind product

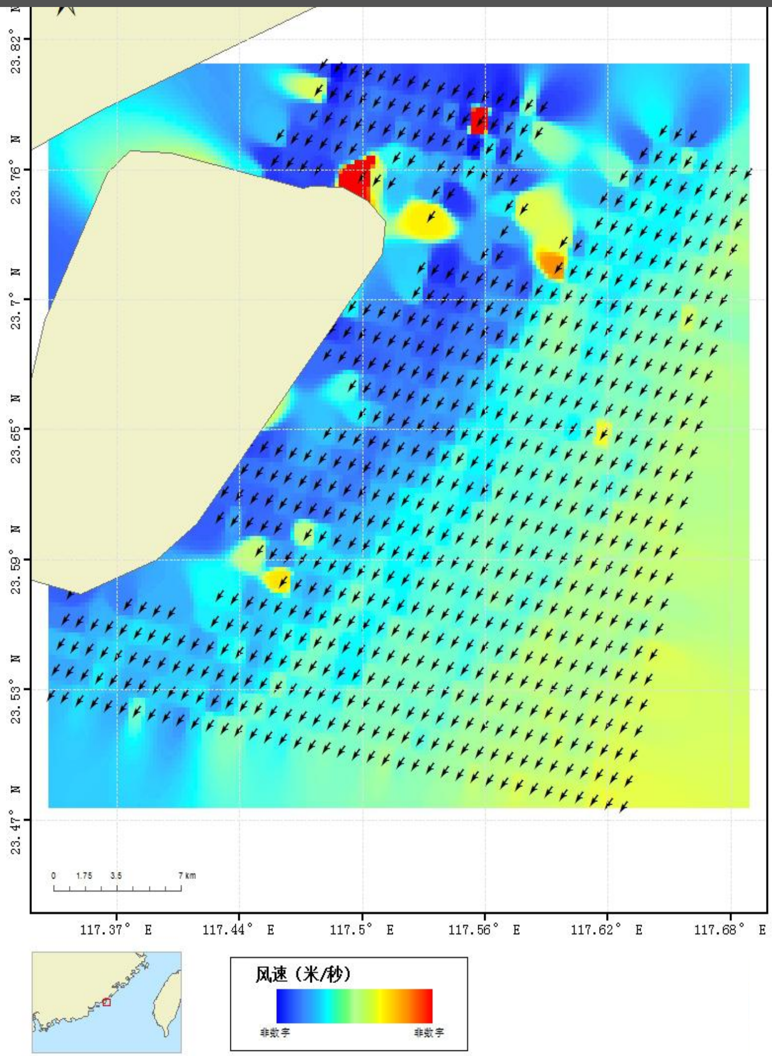

- On January 12, 2017, the GF-3 captured and retrieved the sea surface wind speed and direction in Dongshan County, Fujian Province, with a resolution of 8 meters and a range of 30*30km. It can be seen that there are large wind vortexes in the northern sea and low wind speed in the east of the island, high wind speed in open sea. The high-resolution sea wind products can contribute offshore meteorological security and marine traffic safety.

Some problems in sea surface wind analysis

There are still some problems in the ocean surface wind data, mainly:

(1) When the tropical cyclone is strong, there are some deviations in the wind direction and speed. For weaker TC, this deviations are not obvious.

(2) The error will increase when surface wind speed exceeds 30 m/s. The wind speed is much underestimated for strong TC.

TRMM (Tropical Rainfall Measuring Mission)

- US-Japan joint mission to observe tropical precipitation.
- Equipped with the first-ever spaceborne precipitation (PR) at Ku-band to perform 3D precipitation measurements.
- Lanched on Nov. 28 1997 and re-entered the Earth's atmosphere on June 15, 2015, at 11:55 p.m.

US-Japan joint mission

Japan: PR, launch

US: satellite, TMI, VIRS, CERES, LIS, operation

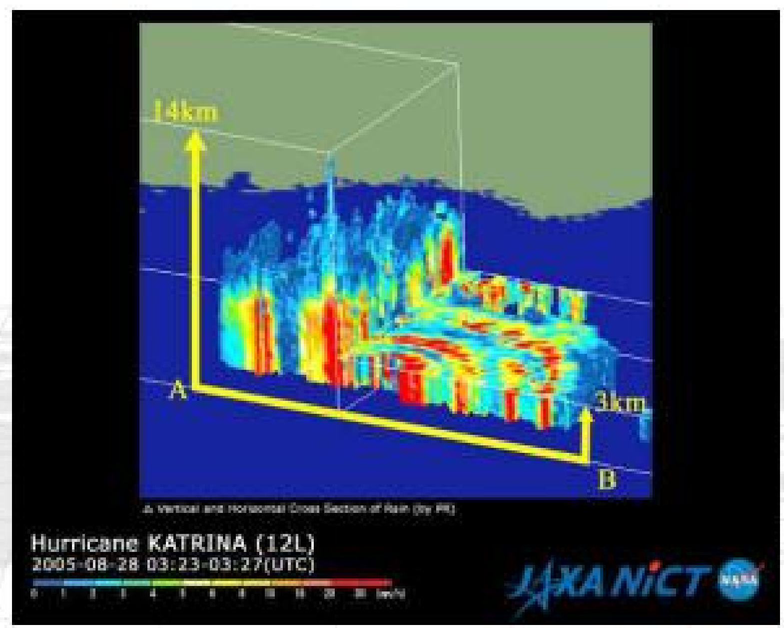

GPM: Global Precipitation Measurement Mission

Core Observatory:
Ku/Ka-band Dual-frequency Precipitation Radar (DPR)
multi-channel.GPM Microwave Imager (GMI)

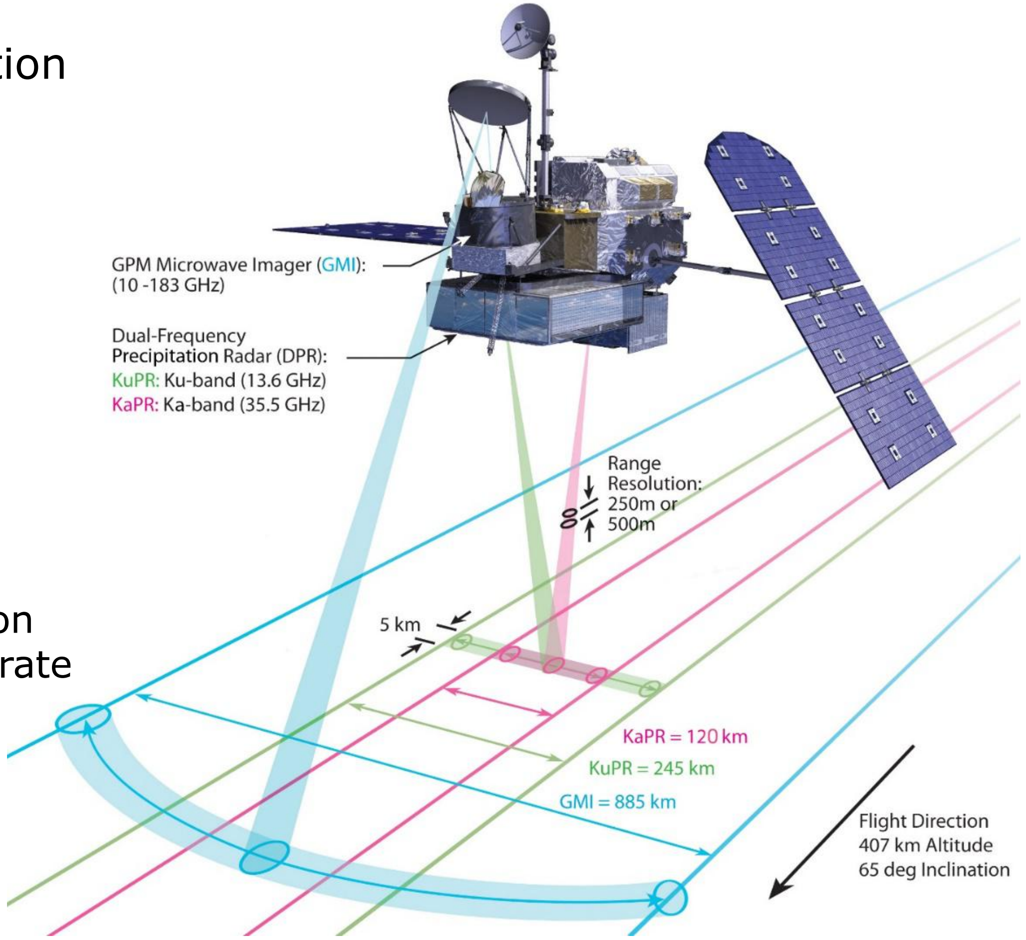

Relative to the TRMM precipitation radar, the DPR is more sensitive to light rain rates and snowfall. In addition, simultaneous measurements by the overlapping of Ka/Ku-bands of the DPR can provide new information on particle drop size distributions over moderate precipitation intensities.

Instruments of GPM

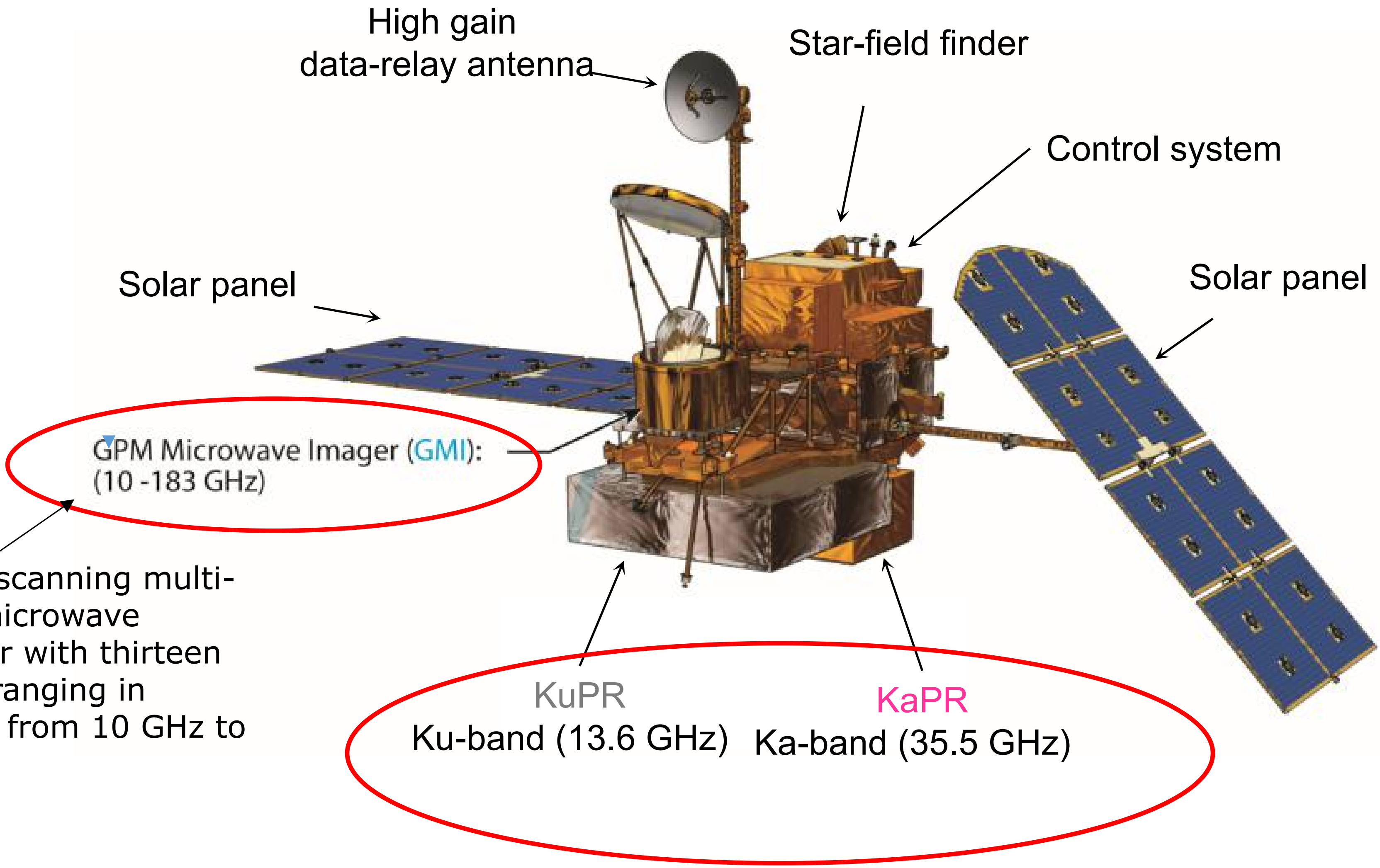

A conical-scanning multi-channel microwave radiometer with thirteen channels ranging in frequency from 10 GHz to 183 GHz.

The first space-borne Ku/Ka-band Dual-frequency Precipitation Radar (DPR)

Monitoring Typhoon Precipitation

The GPM core observatory satellite passed above the Philippine Sea on Oct. 29, 2018 at 0212 UTC (Oct. 28 at 10:12 p.m. EDT).

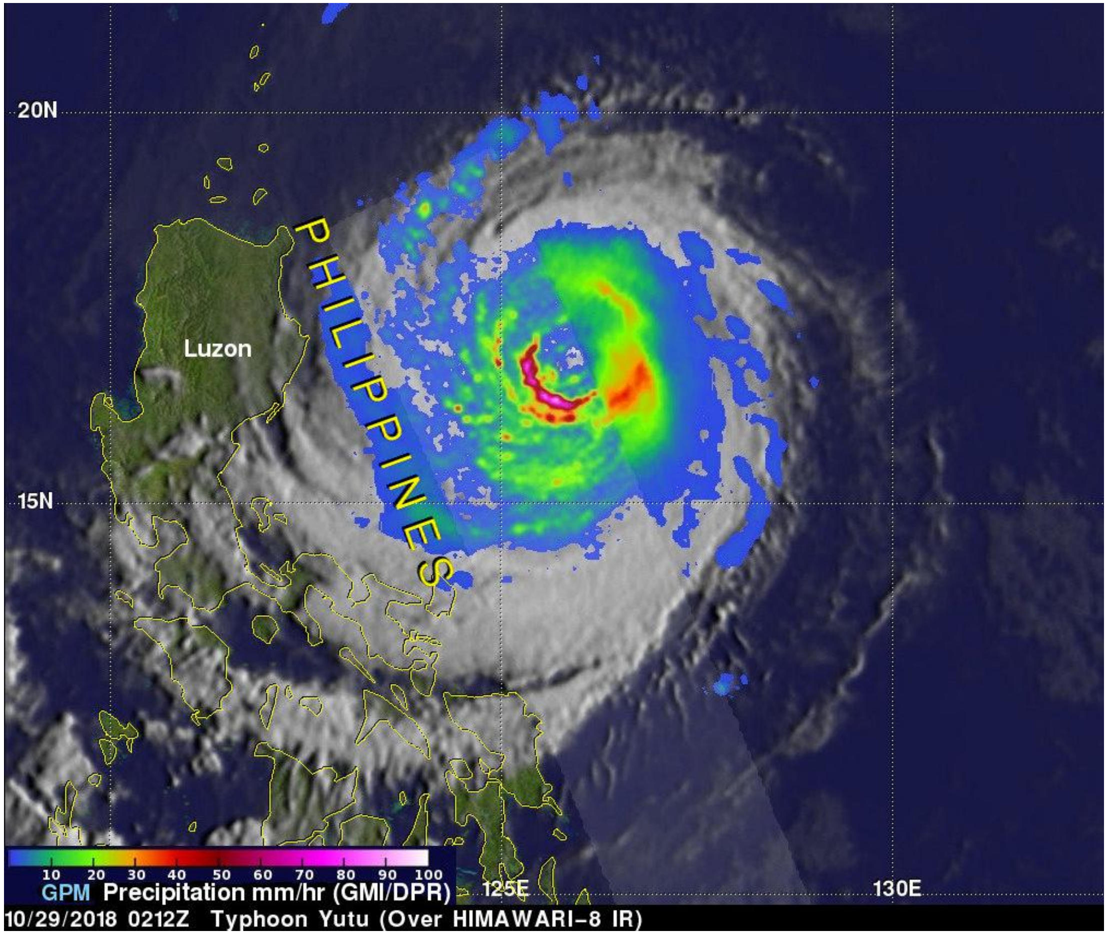

Those GPM data revealed that heavy rainfall within the typhoon covered an area the size of Luzon. Extreme precipitation falling at a rate of over 178 mm (7 inches) per hour was also revealed by GPM's radar (DPR Ku Band) within powerful storms in Yutu's southwestern eye wall.

Monitoring Typhoon Precipitation

Typhoon: JELAWAT on March 28, 2018

Gray: FY4A AGRI T12
Color: GPM gridded product.

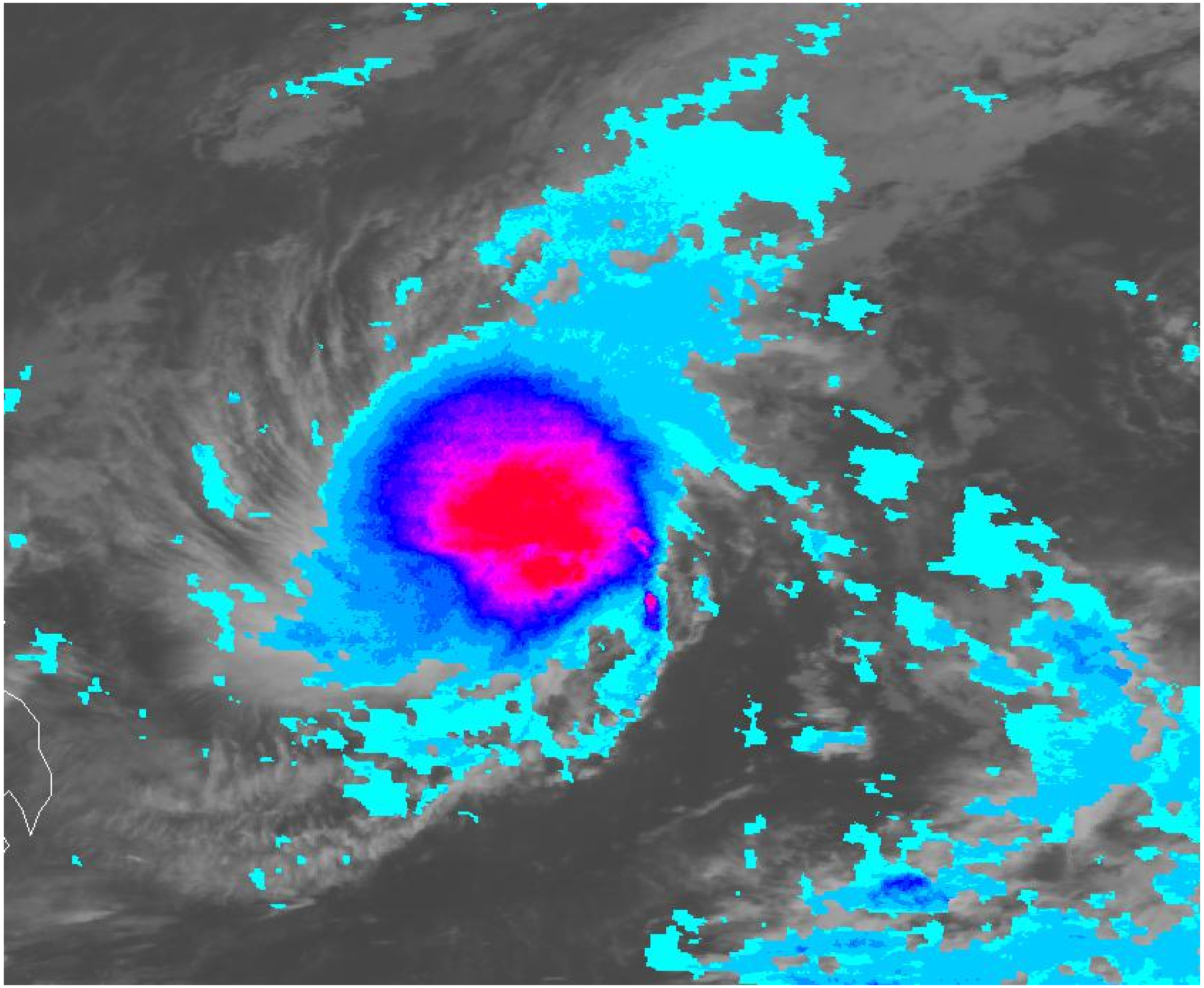

Monitoring Typhoon Precipitation

The GPM core satellite flew over **Trami** on Sept. 24, 2018, at 8:03 a.m. and found **extremely heavy rainfall in the super typhoon's well** defined circular eye.
Rain was also falling at a rate of over 120 mm (4.7 inches) per hour within intense storms in a strong feeder band well southwest of Trami's eye.

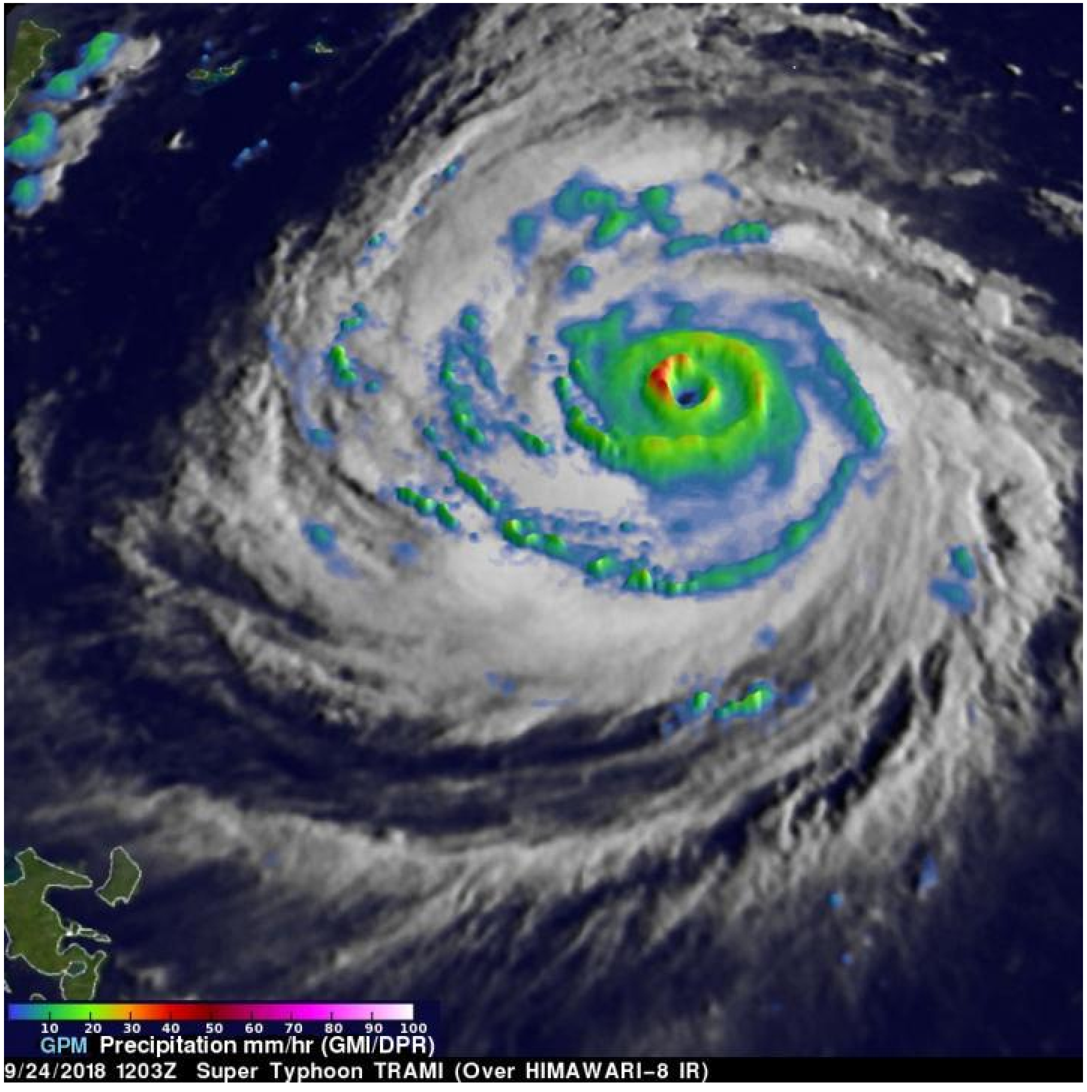

An example of observed Ze before the QC procedures and superobbed Ze that passed the QC procedures for KuNS Ze.

Observed Ze before QC procedures and (c),(d) super obbed Ze after QC procedures for KuNS around Typhoon Halong at 1200 UTC 31 Jul 2014.

Observed Ze before QC procedures and (c),(d) super obbed Ze after QC procedures for KuNS around Typhoon Halong at 1200 UTC 31 Jul 2014.

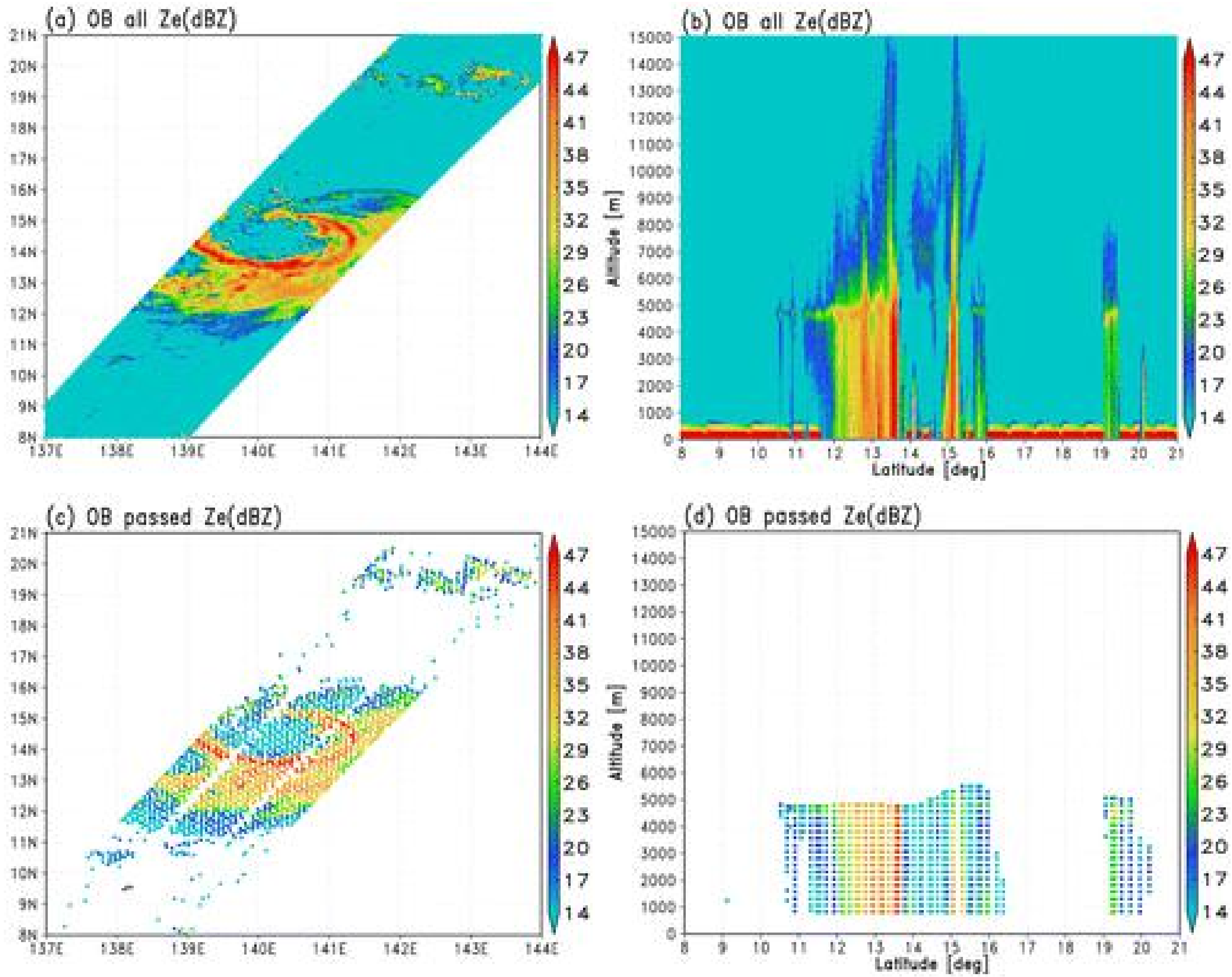

GPM 3D Views Powerful Typhoon Yutu

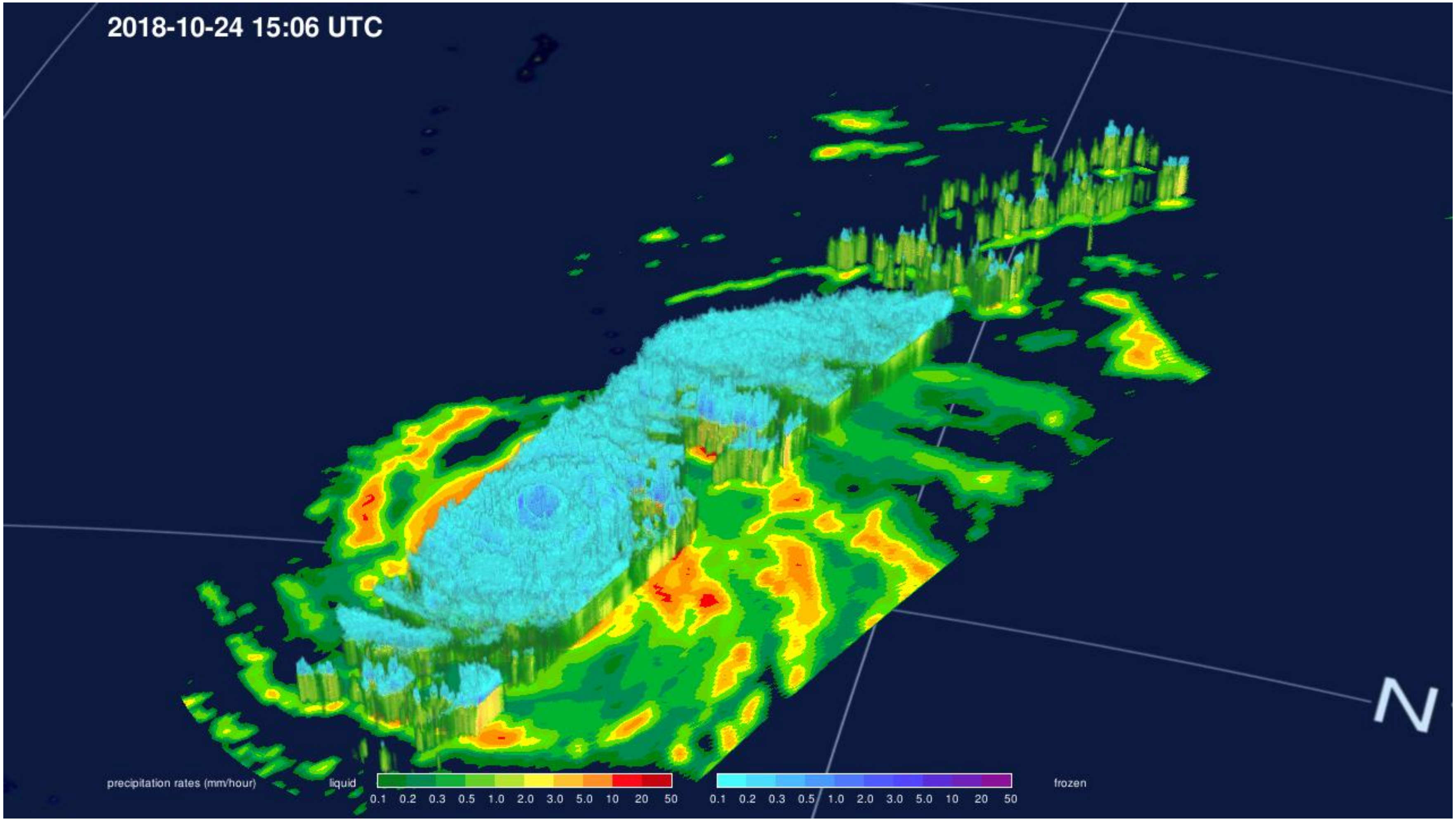

GPM 3D Views Powerful Typhoon Yutu

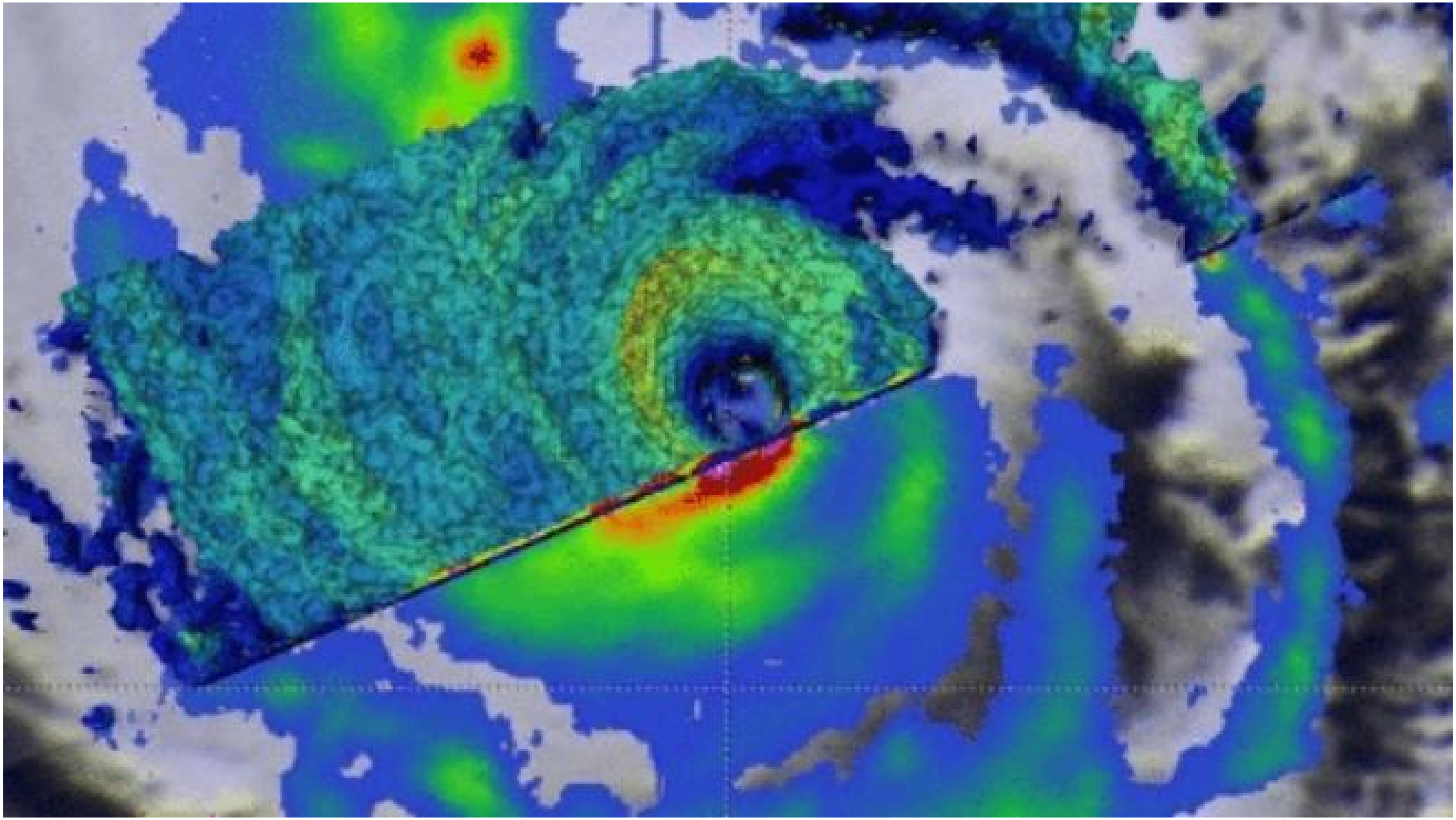

GPM 3D Views Powerful Typhoon Simon

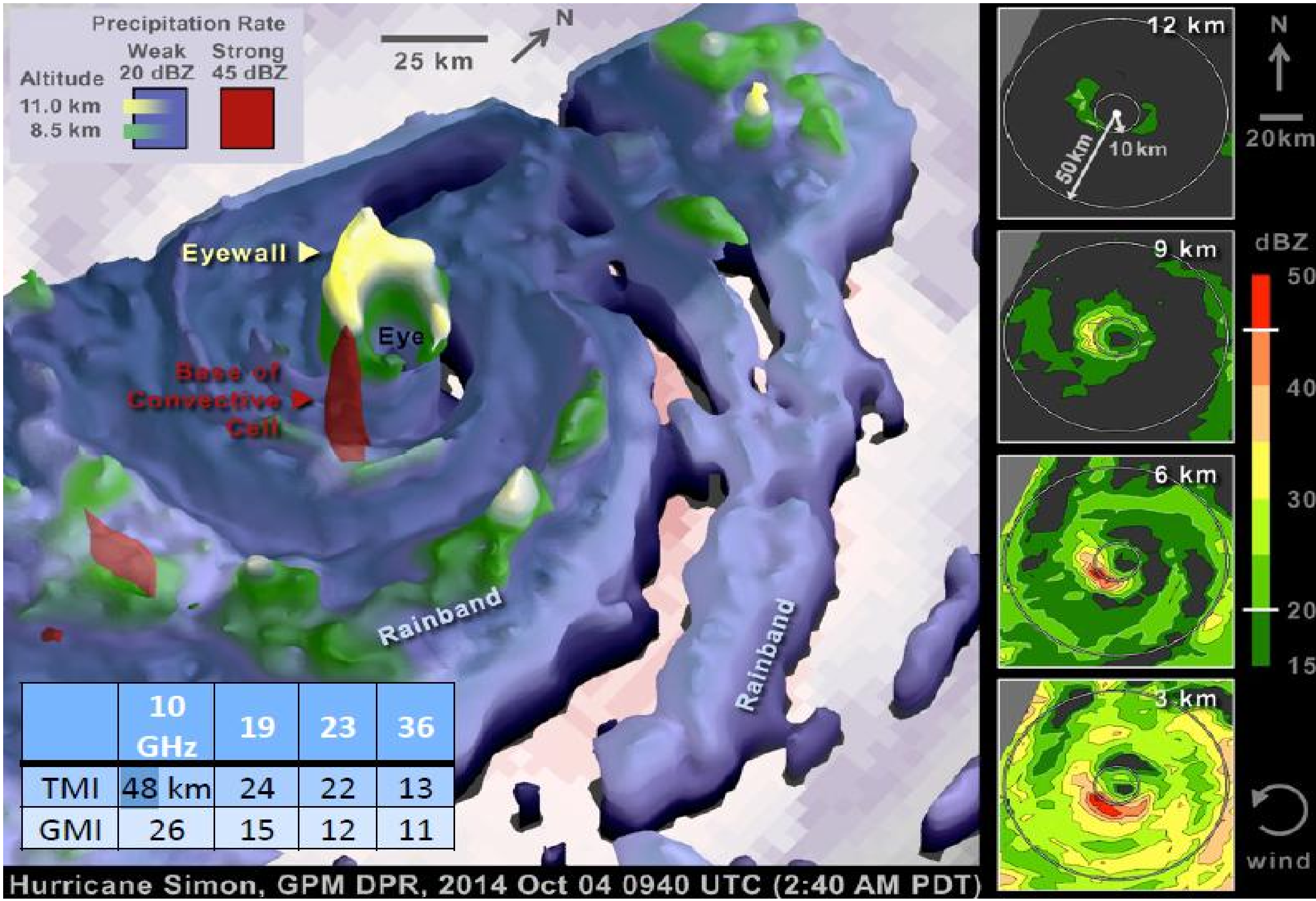

	10 GHz	19	23	36
TMI	48 km	24	22	13
GMI	26	15	12	11

GPM 3D Views Powerful weather system

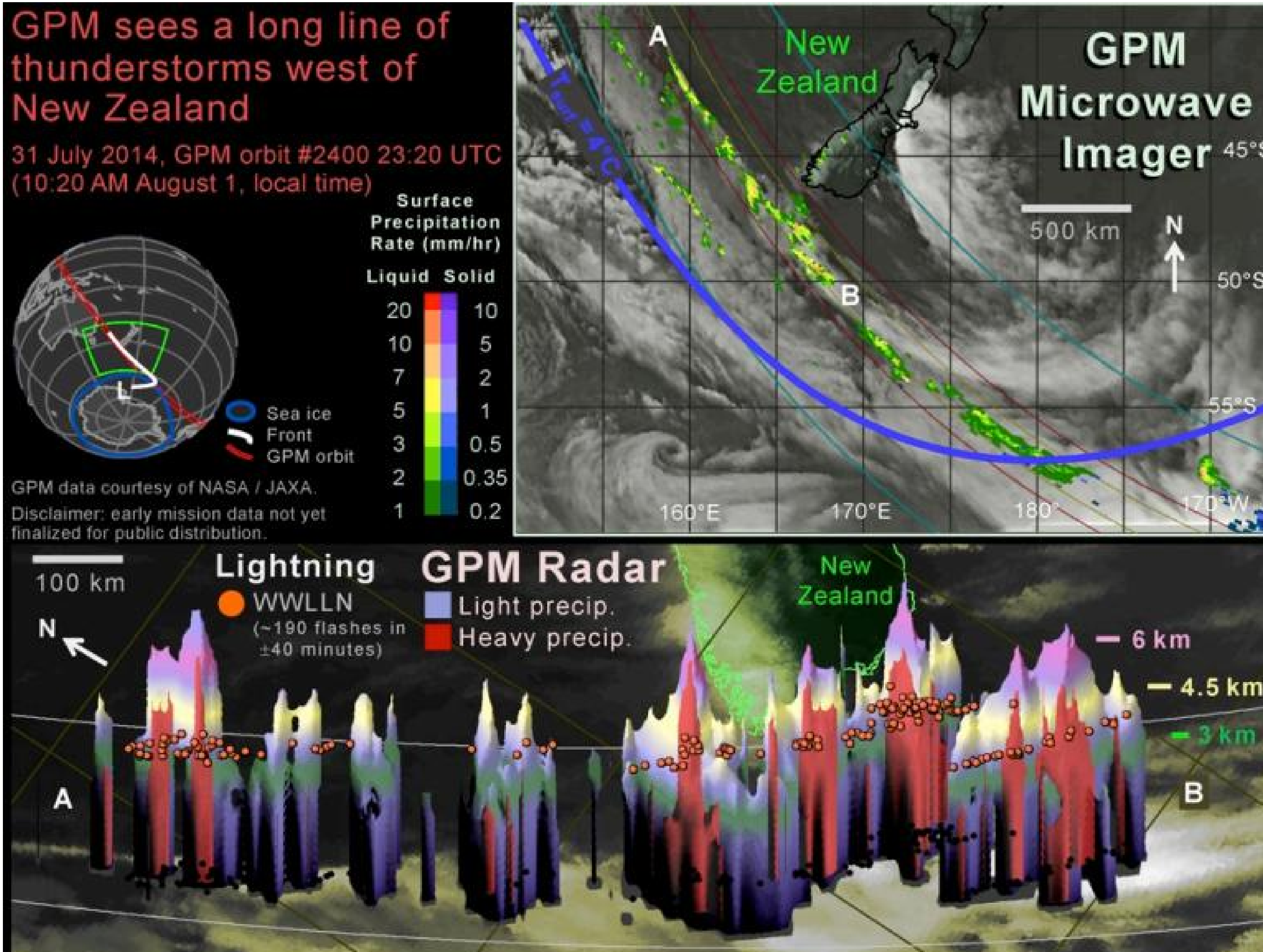

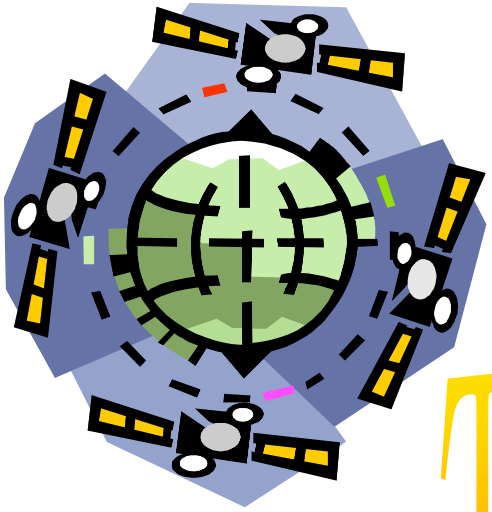

…… Stop Here

Thank you!

GPS/BD Radio Occultation

Basic measurement principle:

Deduce atmospheric properties based on precise measurement of phase delay and amplitude.

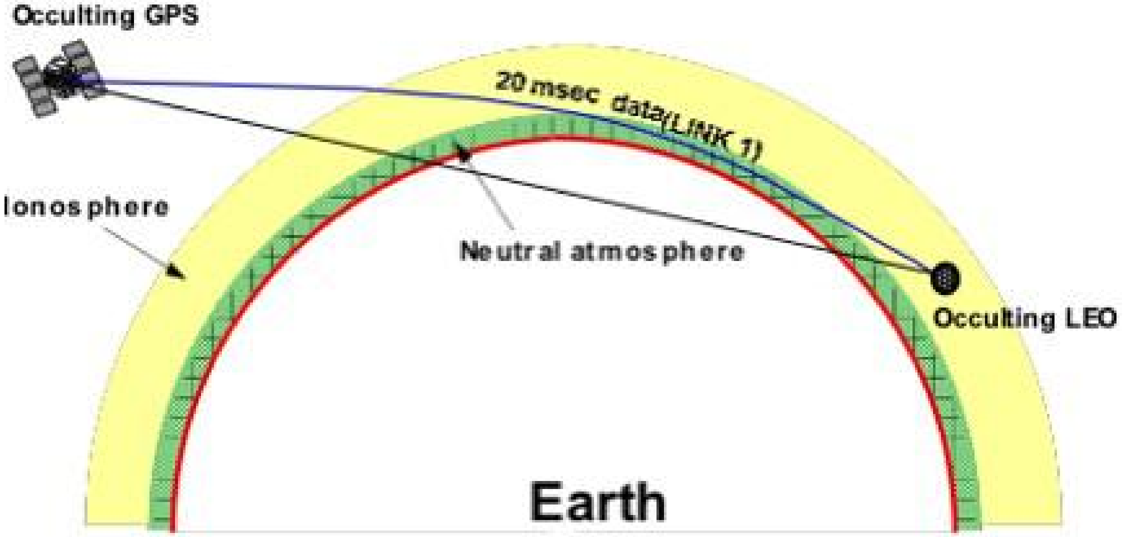

GPS RO missions

COSMIC (Constellation Observing System for Meteorology, Ionosphere and Climate)

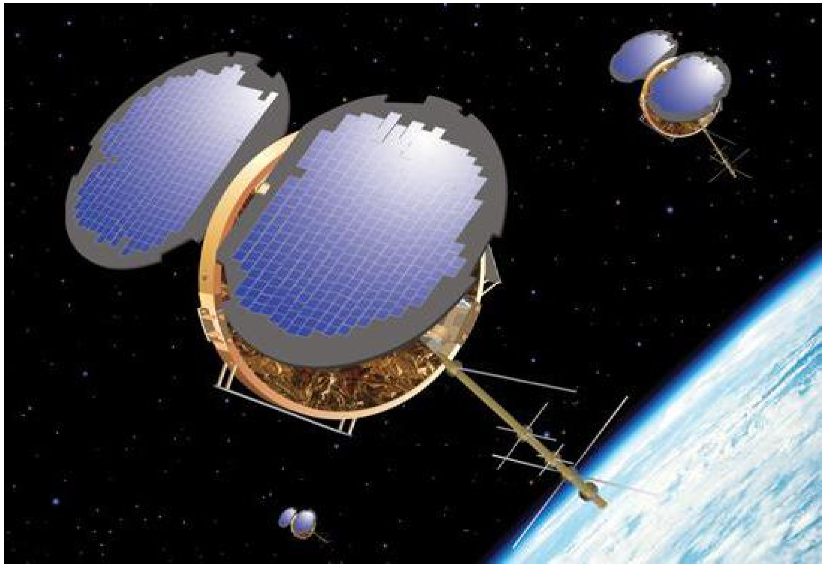

- 6 Satellites launched in April 15 2006
- Three instruments:
  GPS receiver, TIP, Tri-band beacon
- Demonstrate quasi-operationa GPS limb sounding with globa coverage in near-real time
- Climate Monitoring

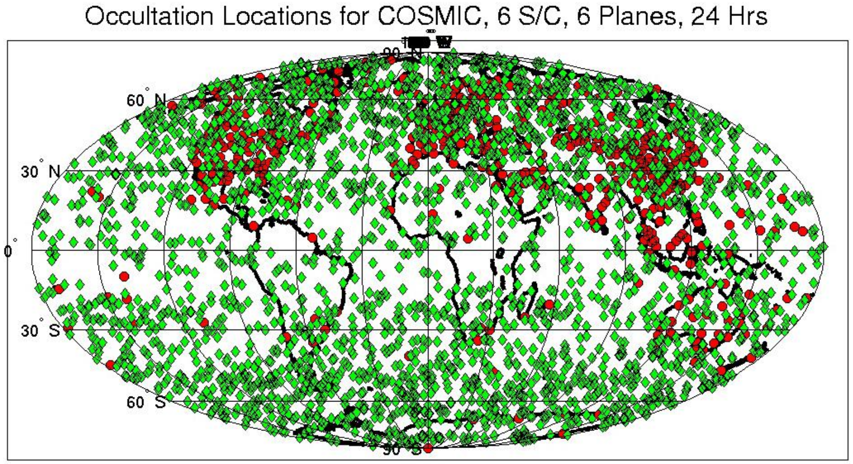

GPS/BD RO missions

FY-3 C/D

FY-3D BDS RO.location(16days)

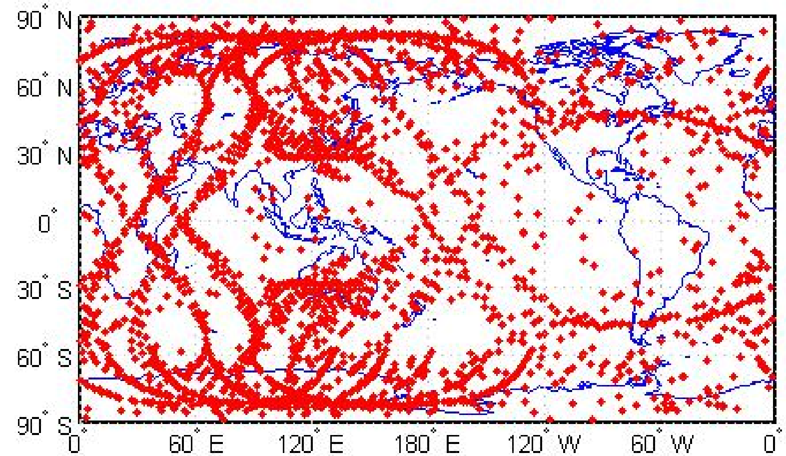

FY-3D GPS RO.location(16days)

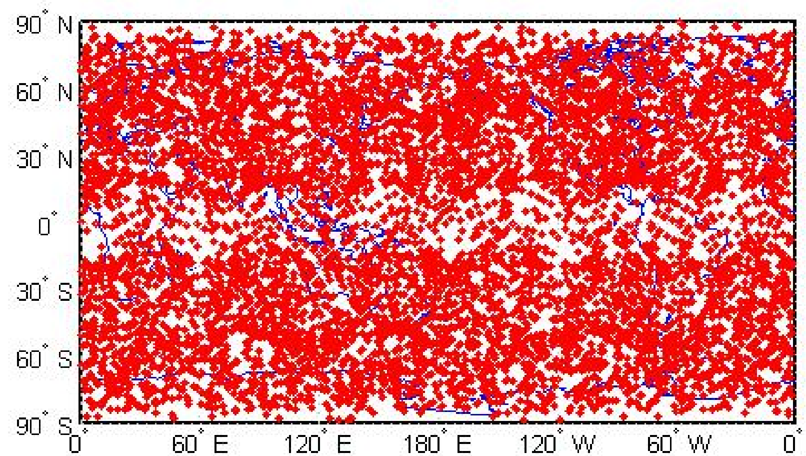

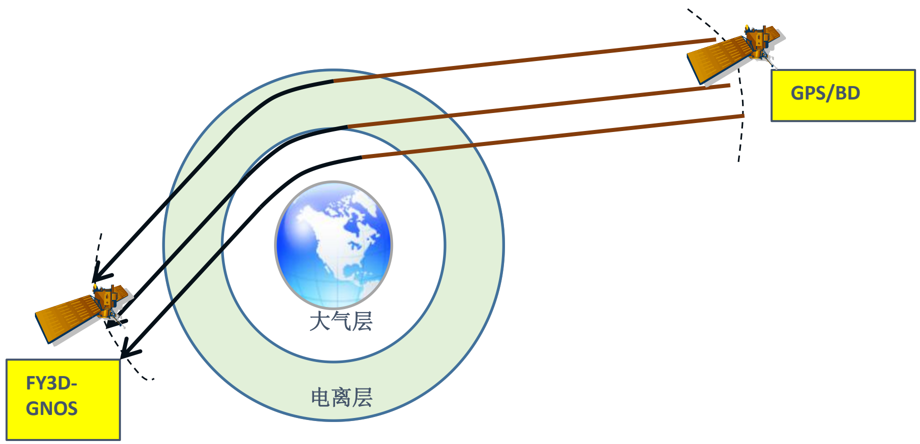

GPS radio occultation measurements & processing

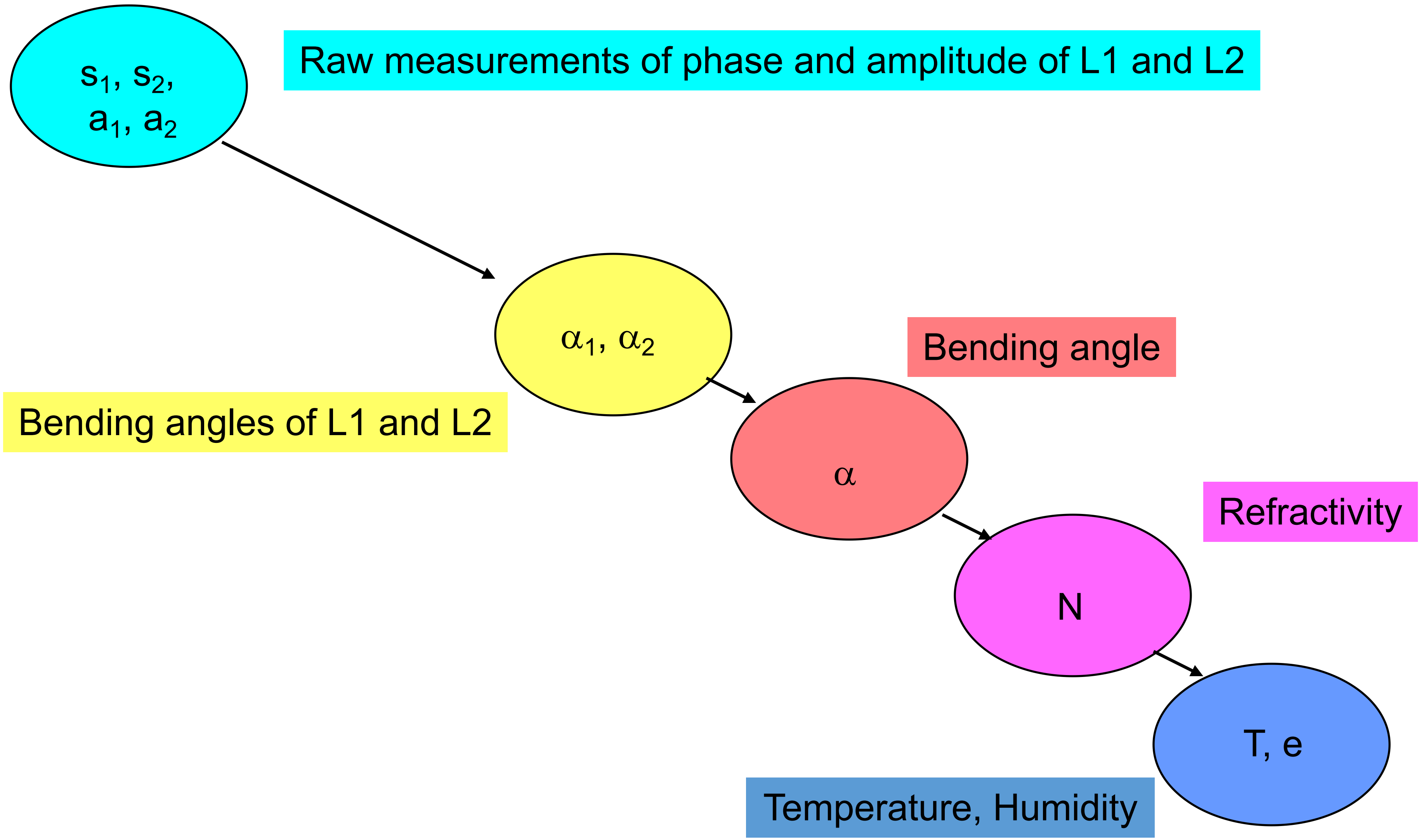

GPS RO data used in data assimilation in typhoon prediction

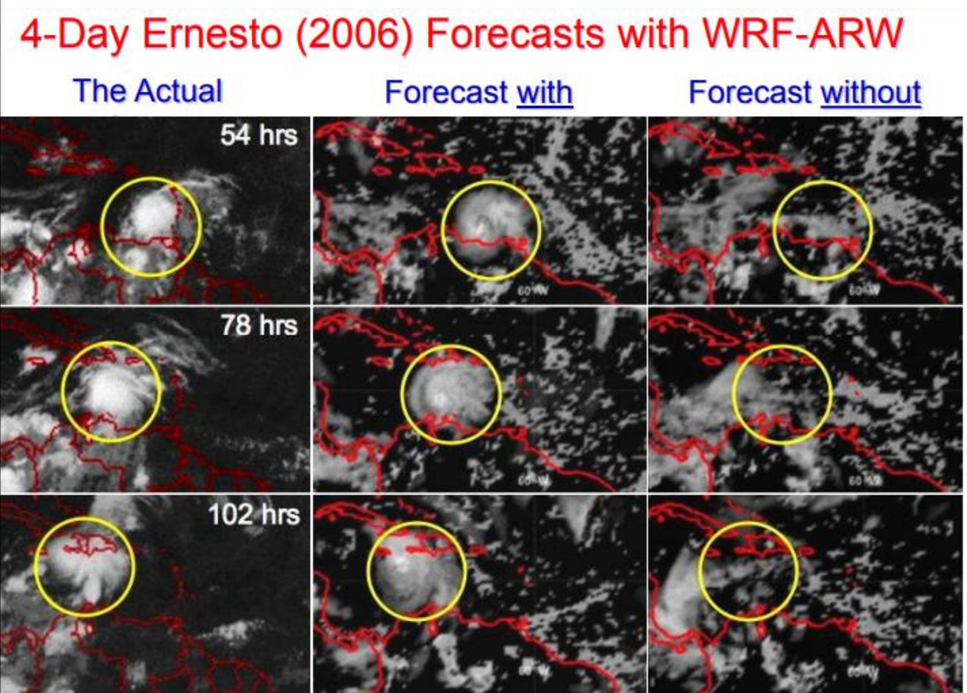

Liu et al. (2012, MWR)

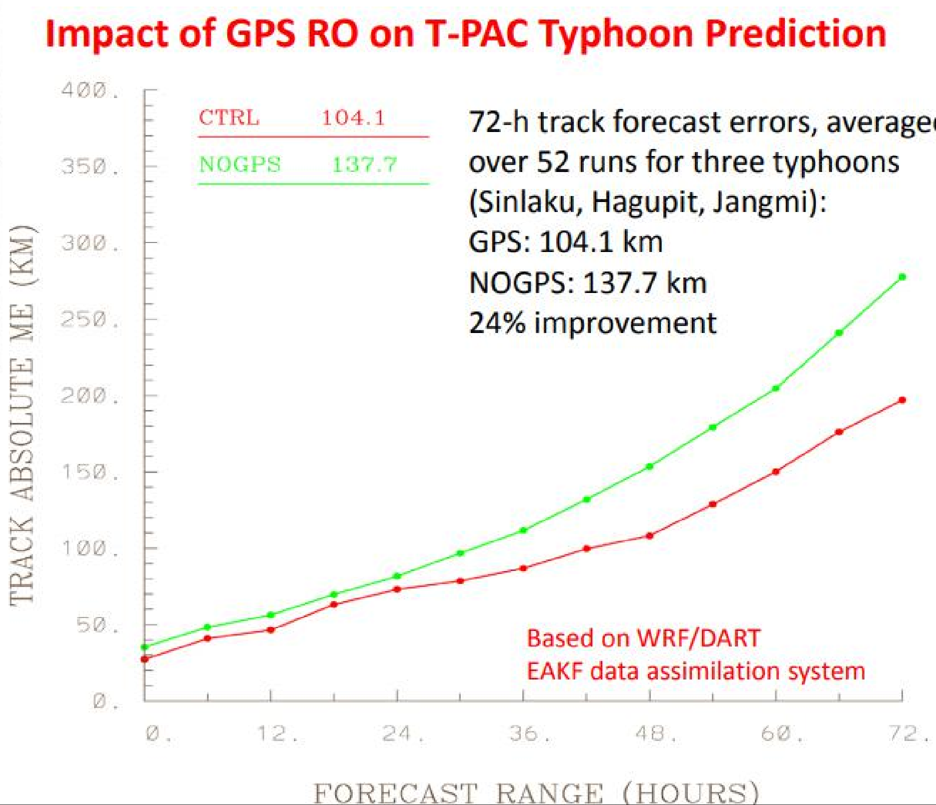

Determining the tropical cyclone center using ocean wind data

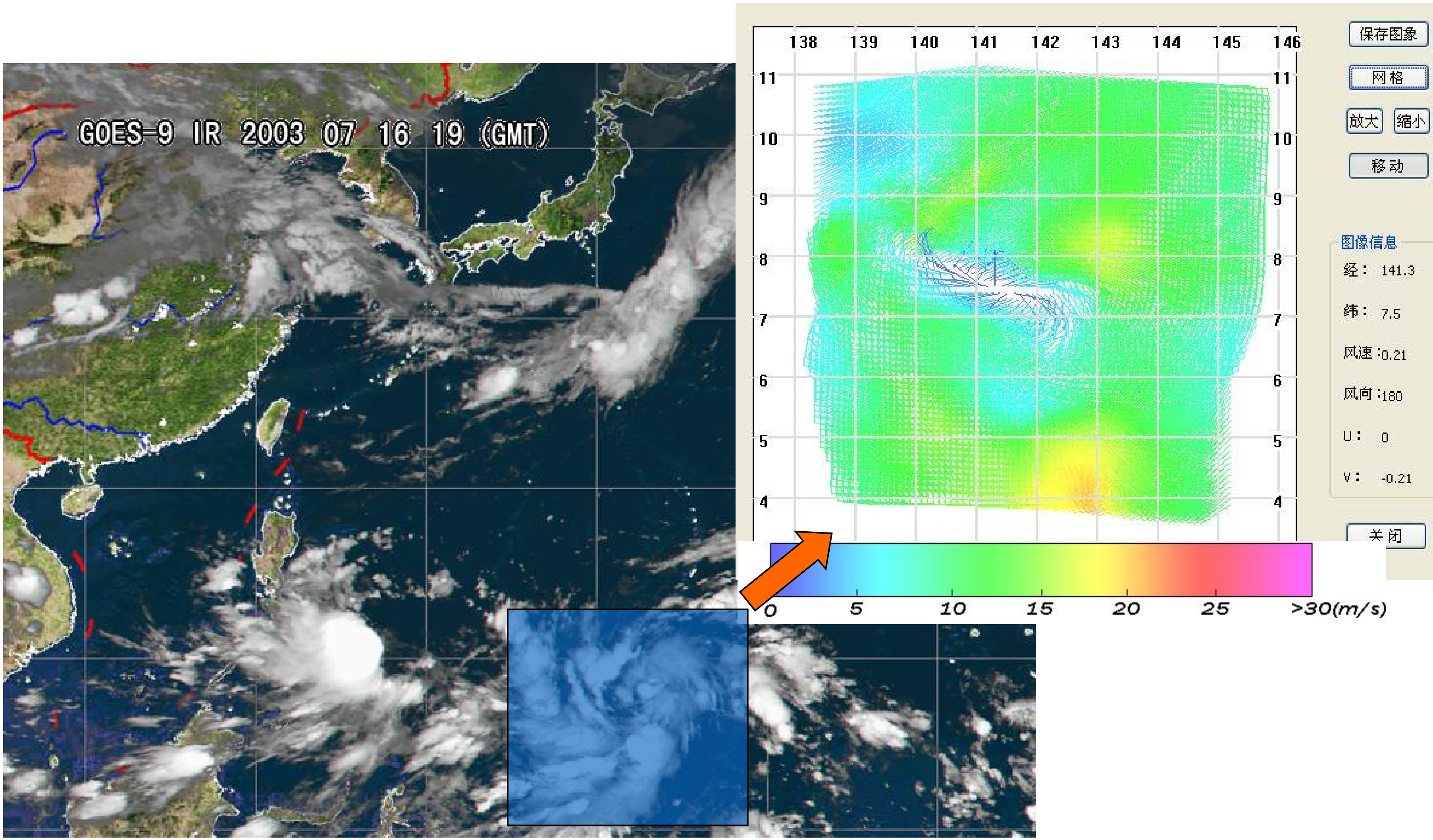

Determining the tropical cyclone center using QuikScat ocean wind data

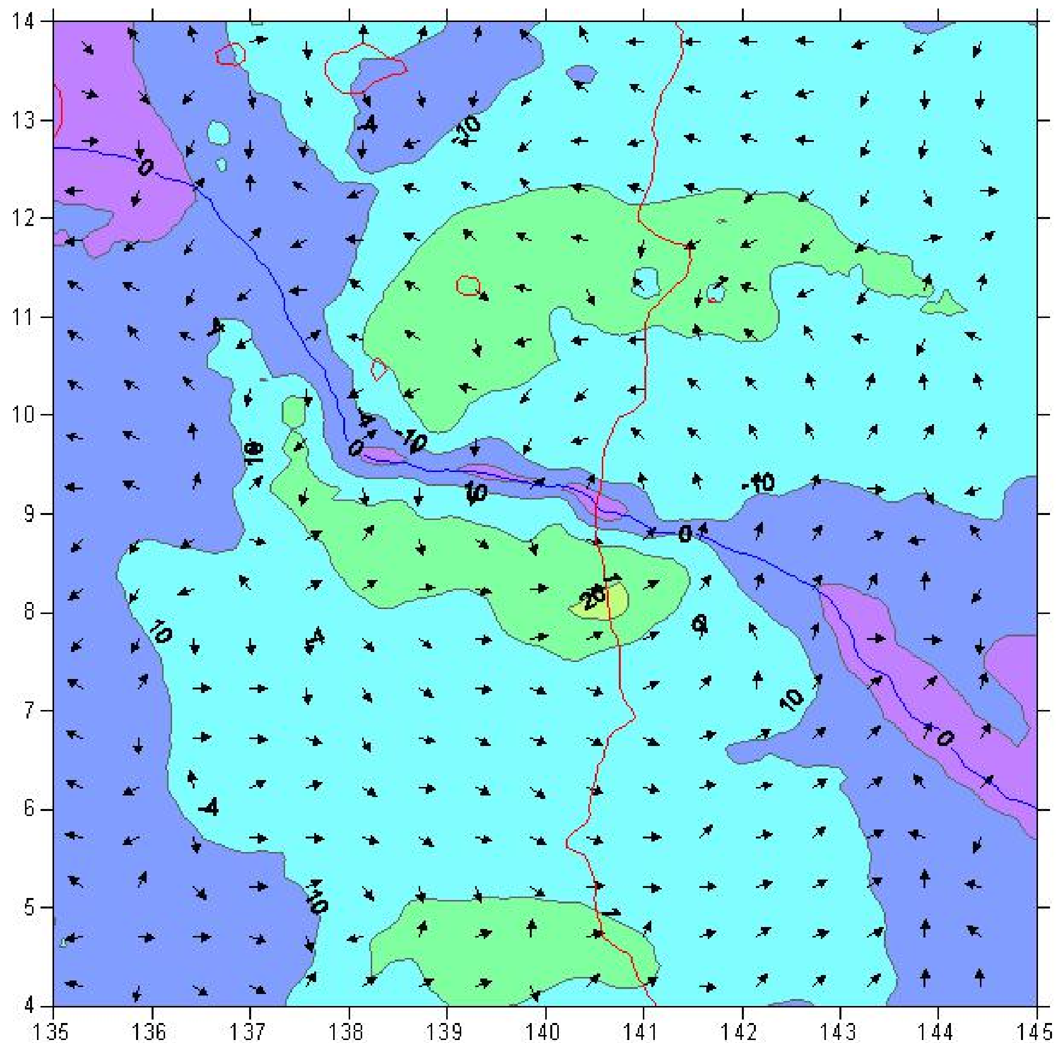

2003-07-16 Ocean surface wind field

- ✓ Wind speed, wind direction
- ✓ Meridional component zero value line (blue line)
- ✓ Zonal component zero value line (red line)

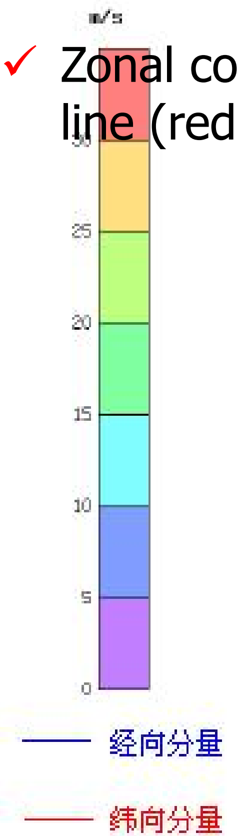

Determining the tropical cyclone center using QuikScat ocean wind data

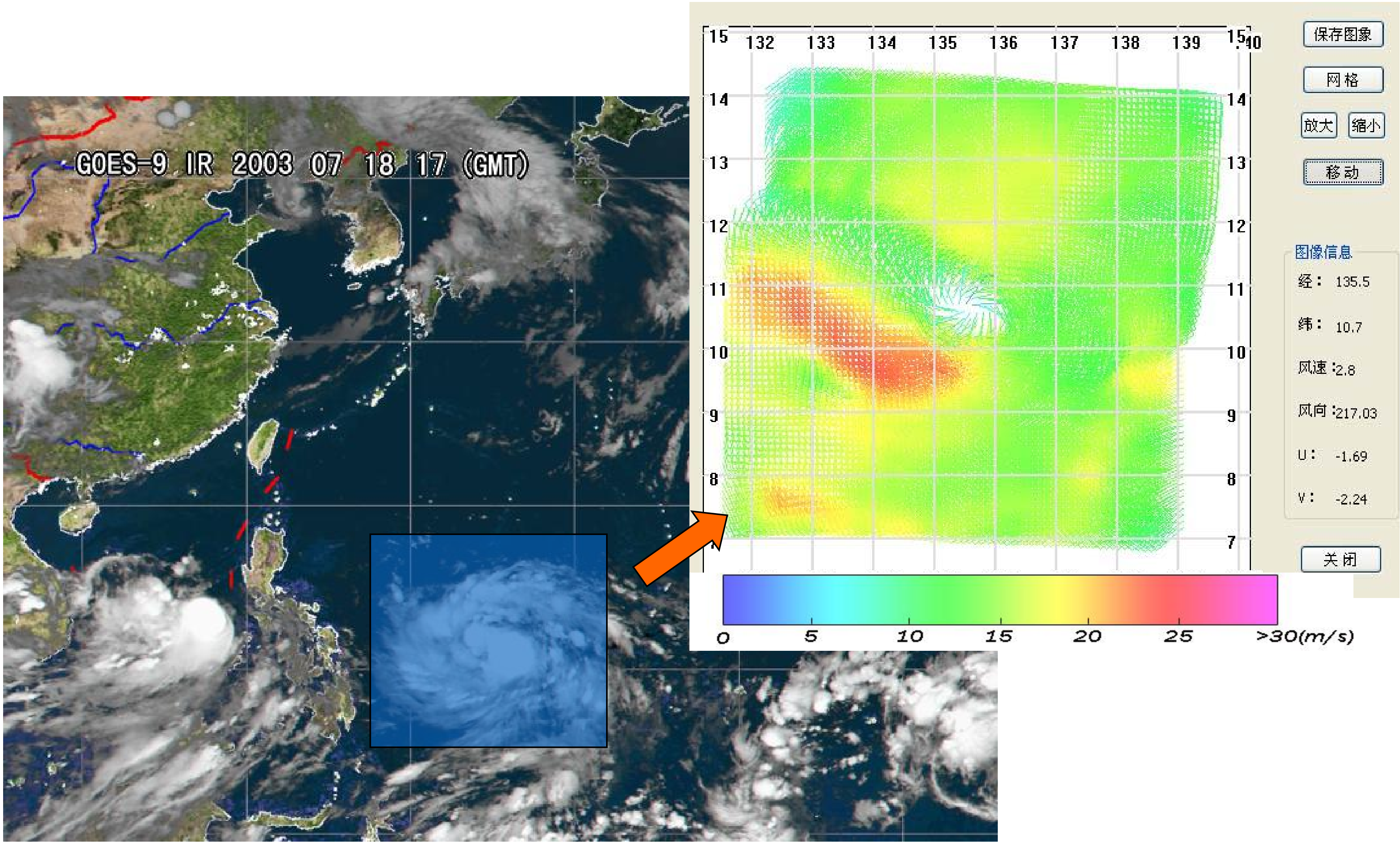

QuikSCAT application example ------ tropical cyclone monitoring

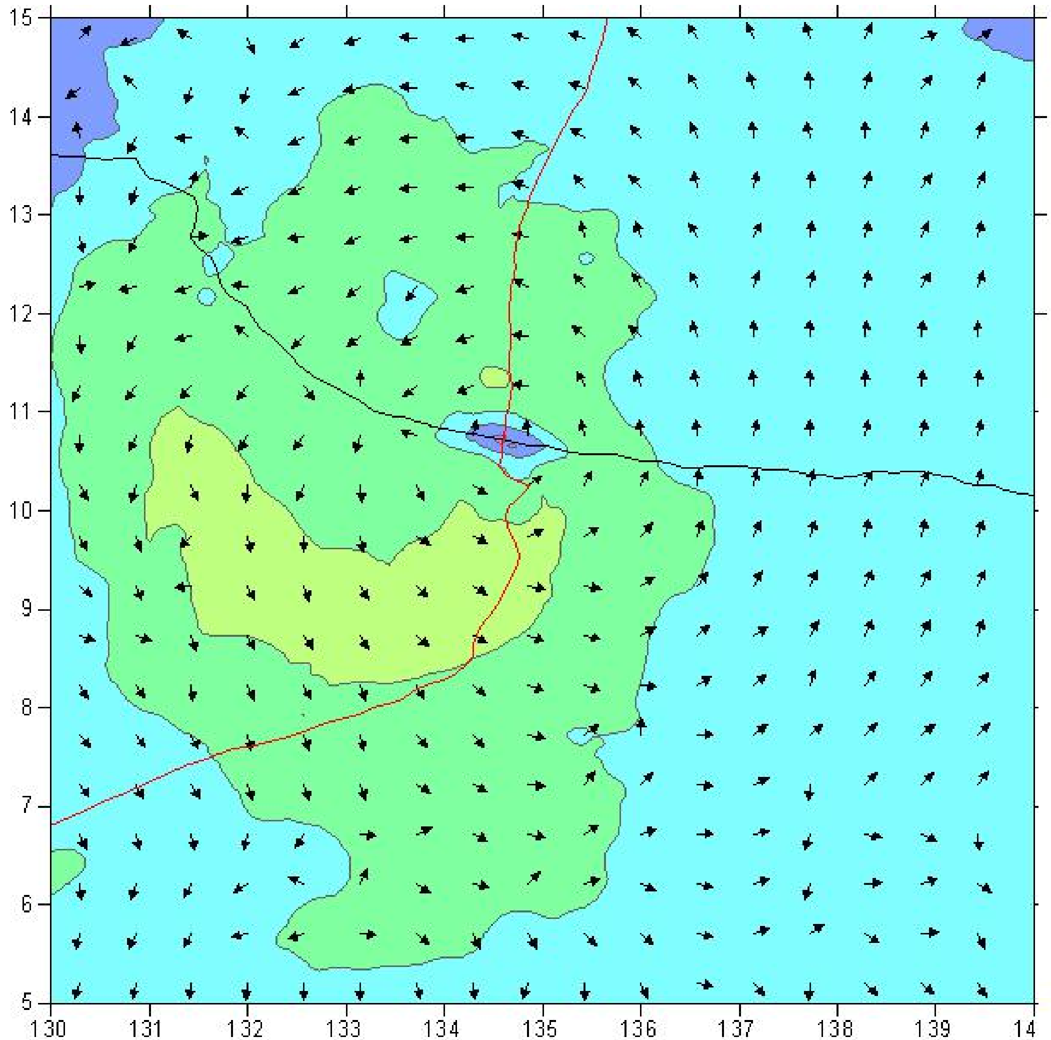

2003-07-18 Ocean surface wind field

- ✓ Wind speed, wind direction
- ✓ Meridional component zero value line (blue line)
- ✓ Zonal component zero value line (red line)

Determining the tropical cyclone center using QuikScat ocean wind data

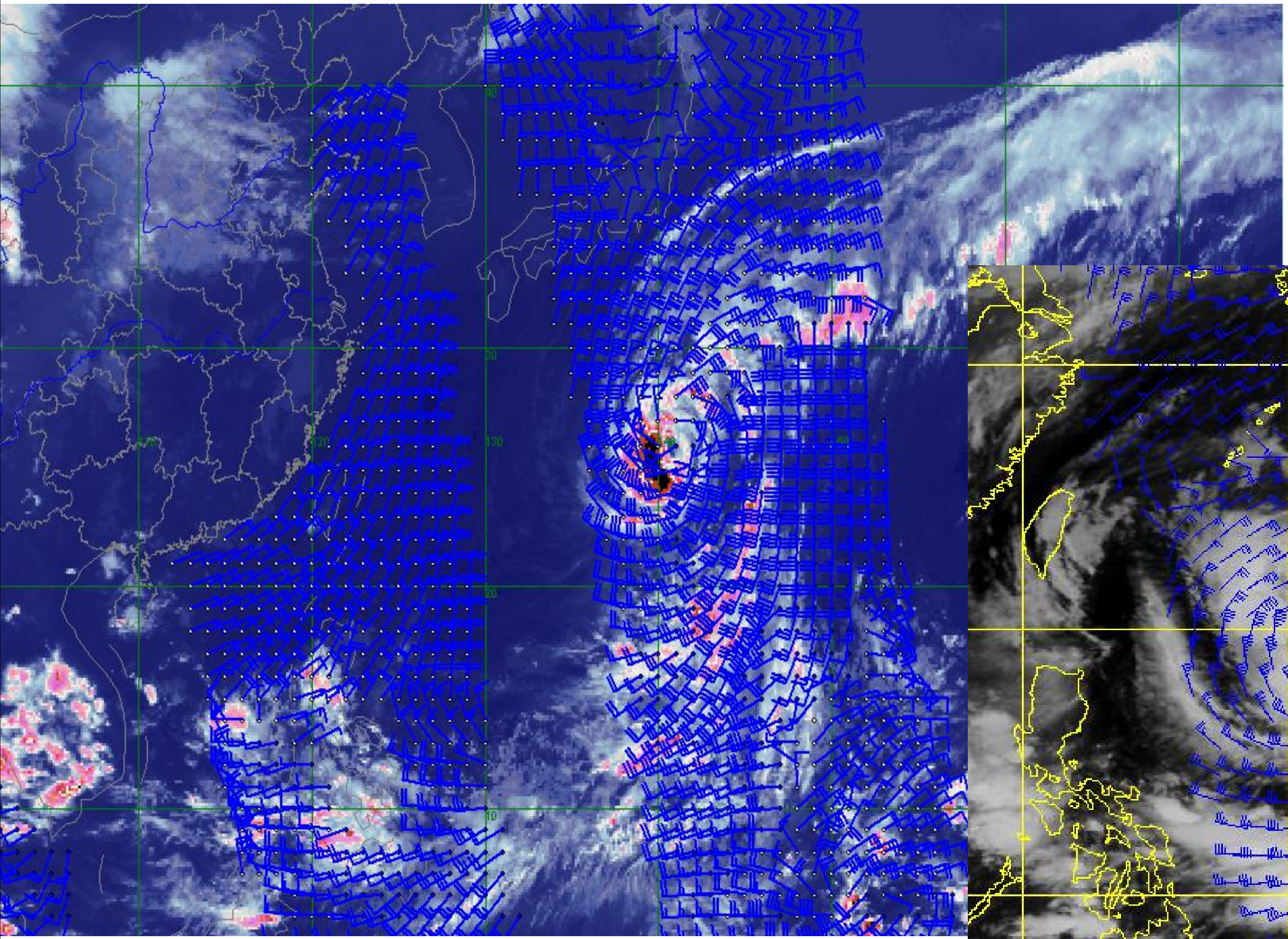

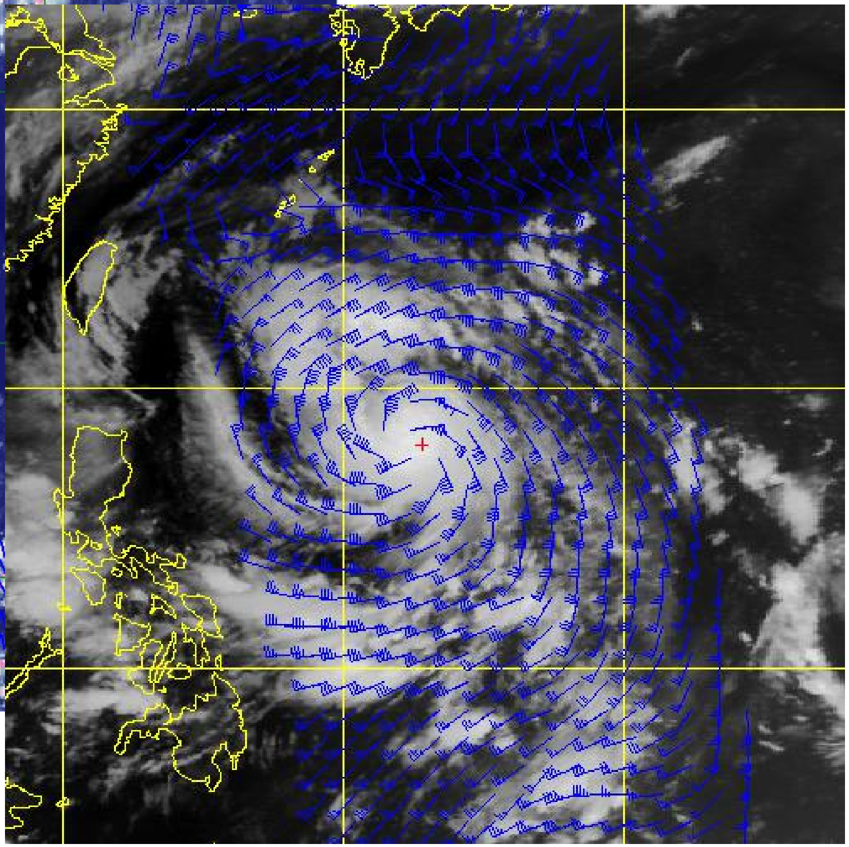

Determination of range of tropical cyclone winds by QuickScat

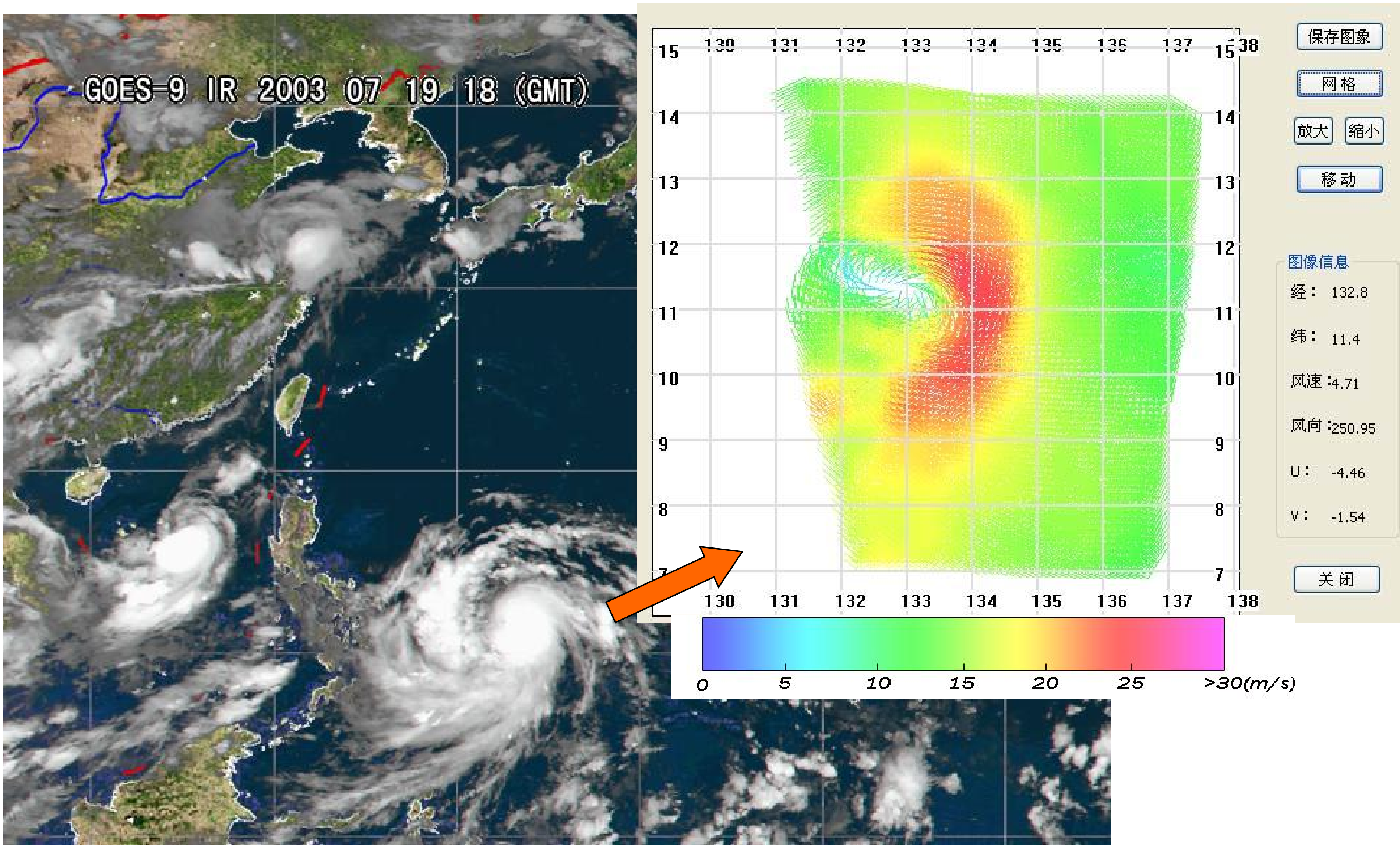

Determination of range of tropical cyclone winds by QuickSCAT

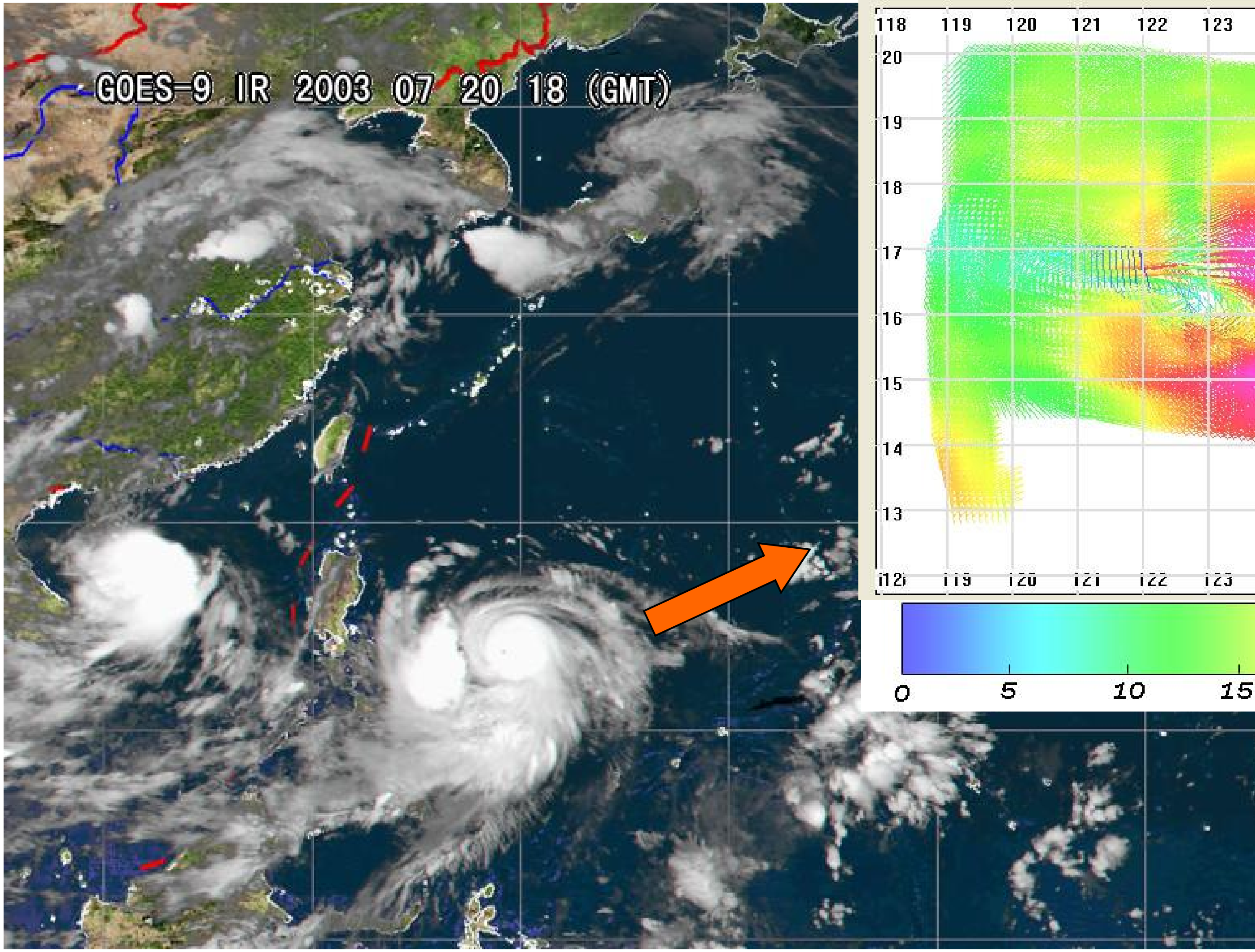

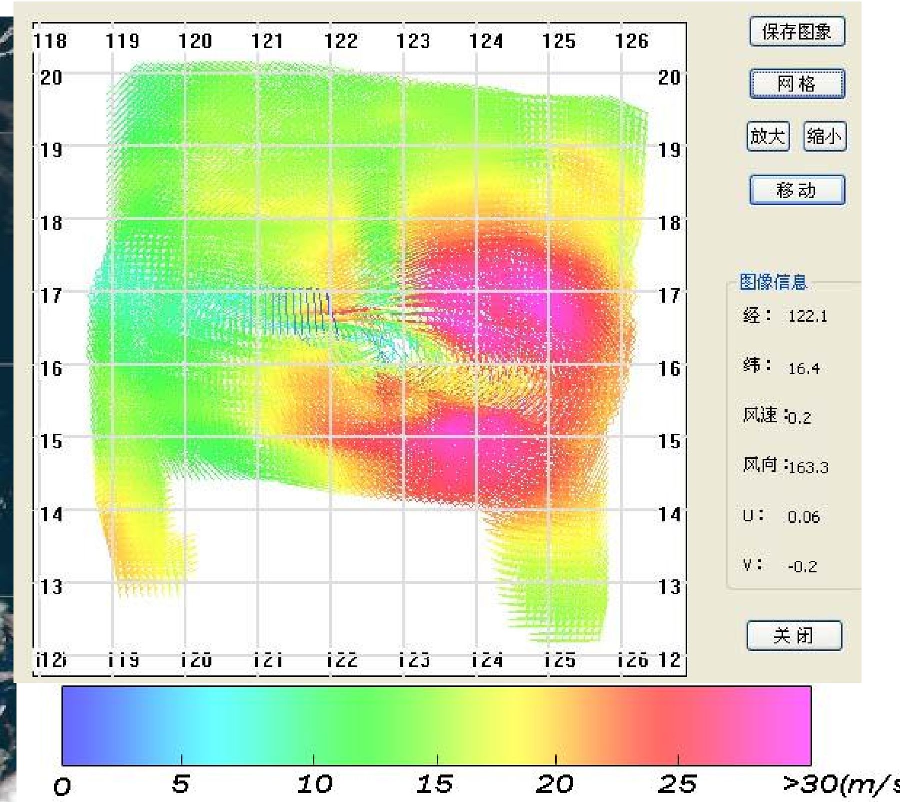

The windy area further expanded on second day.

Determination of typhoon intensity of QuikSCAT surface wind

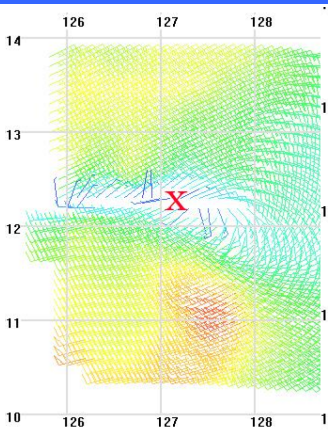

June 14th, 06:00

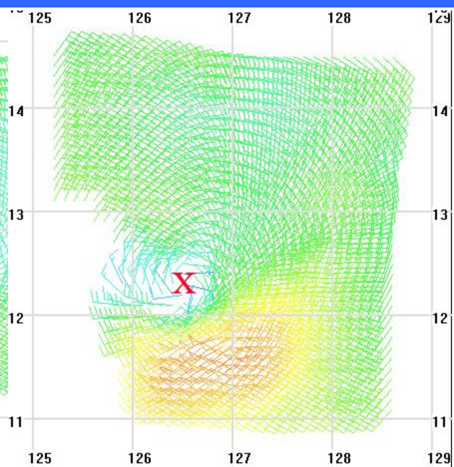

June 14th, 17:00

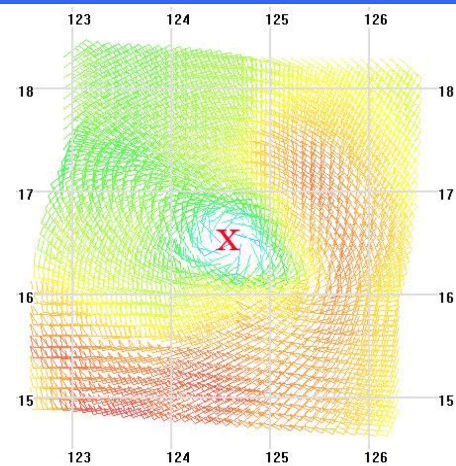

June 16th, 06:00

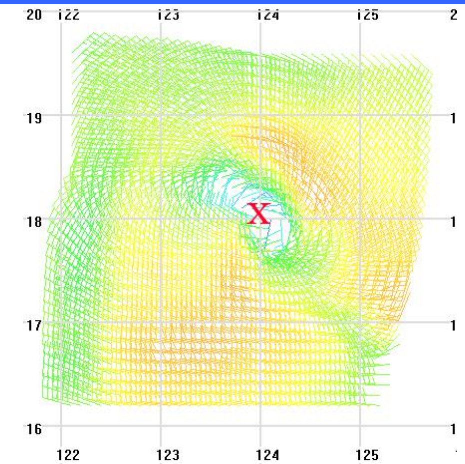

June 16th, 17:00

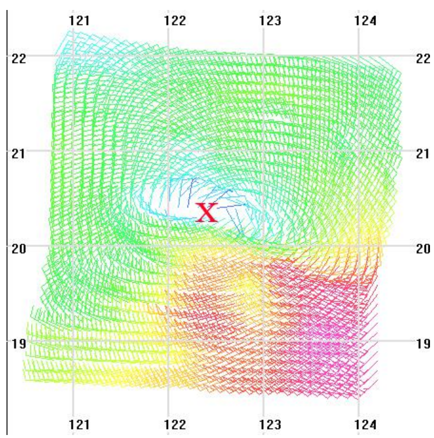

June 17th, 06:00

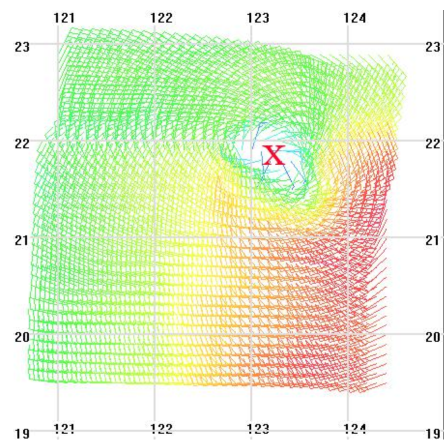

June 17th, 17:00

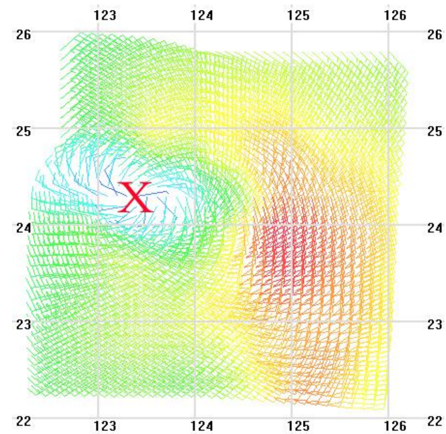

June 18th, 05:00

0306# typhoon

According quickly dissipation of strong convection near the eye wall from the ocean surface wind data, the stage of weakening or denaturation of tropical cyclone was judged.